INFORMATION TO USERS

This manuscript has been reproduced from the microfilm master. UMI films the text directly from the original or copy submitted. Thus, some thesis and dissertation copies are in typewriter face, while others may be from any type of computer printer.

The quality of this reproduction is dependent upon the quality of the copy submitted. Broken or indistinct print, colored or poor quality illustrations and photographs, print bleedthrough, substandard margins, and improper alignment can adversely affect reproduction.

In the unlikely event that the author did not send UMI a complete manuscript and there are missing pages, these will be noted. Also, if unauthorized copyright material had to be removed, a note will indicate the deletion.

Oversize materials (e.g., maps, drawings, charts) are reproduced by sectioning the original, beginning at the upper left-hand corner and continuing from left to right in equal sections with small overlaps.

ProQuest Information and Learning
300 North Zeeb Road, Ann Arbor, MI 48106-1346 USA
800-521-0600

DISSERTATION

PROTEOMIC ANALYSIS OF *PSEUDOMONAS PUTIDA* F1 DURING GROWTH ON TOLUENE-PHENOL MIXTURES

Submitted by

Kee-Hong Kim

Department of Chemical Engineering

In partial fulfillment of the requirements

For the Degree of Doctor of Philosophy

Colorado State University

Fort Collins, Colorado

Summer 2002

COLORADO STATE UNIVERSITY

April 15, 2002

WE HEREBY RECOMMEND THAT THE DISSERTATION PREPARED UNDER OUR SUPERVISION BY KEE-HONG KIM ENTITLED

PROTEOMIC ANALYSIS OF *PSEUDOMONAS PUTIDA* F1 DURING GROWTH ON TOLUENE-PHENOL MIXTURES

BE ACCEPTED AS FULFILLING IN PART THE REQUIREMENTS FOR THE DEGREE OF DOCTOR OF PHILOSOPHY

Committee on Graduate Work

Advisor

Department Head

ABSTRACT OF THESIS

PROTEOMIC ANALYSIS OF *PSEUDOMONAS PUTIDA* F1 DURING GROWTH ON TOLUENE-PHENOL MIXTURES

In both natural and engineered environments, microorganisms grow on mixtures of organics. However, little is known about microbial growth on mixtures, especially in the context of biodegradation. For example, previous research showed that the biodegradation kinetics of *Pseudomonas putida* F1 growing on mixtures of toluene and phenol were difficult to predict, despite the fact that the metabolic pathway for these substrates is the same.

To investigate the physiological effects of the toluene-phenol mixtures on the growth of *P. putida* F1, a proteomics approach was utilized. An optimal proteome analysis procedure was developed and the proteomes of *Pseudomonas putida* F1 grown on either a single substrate (toluene or phenol) or a toluene-phenol mixture were analyzed by two-dimensional polyacrylamide gel electrophoresis. Three groups of proteins (Group T, P, and M), which were differentially produced when the bacterium grew on toluene, phenol, or the toluene-phenol mixture, respectively, were categorized by two strict criteria: reproducibility and uniqueness.

Based on the proteome analysis, selected Group T, P, and M proteins were subjected to N-terminal sequencing, and mass spectrometry, and results of these analyses were used in searches of the protein identities. Two different mass spectrometers were utilized: a matrix-assisted laser desorption/ionization time-of-flight mass spectrometer for mass fingerprinting and a tandem mass spectrometer (electrospray ionization mass spectrometer) for *de novo* peptide sequencing.

Two proteins were identified: acyl carrier protein (ACP) and β-ketoadipate:succinyl CoA transferase. The function of ACP, an essential protein in the biosynthesis of fatty acids, triggered the investigation of the compositional changes in the phospholipid fatty acids of the cellular membrane. The phospholipid fatty acid composition was found to dramatically change depending on the growth substrate(s). These membrane compositional changes during the biodegradation of the toluene-phenol mixture were used to form the hypothesis that the presence of toluene altered the structure of cellular membrane in favor of toluene transport and inhibited the transport of phenol into the cell. Once the cell consumed toluene, the membrane structure changed to be favorable to phenol transport across the cell membrane. The production of β-ketoadipate:succinyl CoA transferase during the biodegradation of phenol might suggest either incidental gene induction or a basal level of phenol metabolism via the β-ketoadipate pathway metabolism.

To consider more diverse contaminant mixtures, the growth of *P. putida* F1 on mixtures of toluene-phenol and two different heavy metals was also examined. The bacterium

displayed better tolerance to cadmium than to chromate during growth on toluene, phenol, and their mixture. The metal tolerance of the bacterium remained at a similar level regardless of the substrate. Heavy metals substantially inhibited the cell growth rate on all substrates and the inhibitory effect was also reflected in decreased cell growth yields. Transmission electron microscopy was utilized to observe any alterations in the cellular membrane integrity. The microscopy images suggested that the presence of chromate, even at a low concentration (1.0 ppm), severely disturbed the cellular membrane and resulted in a loss of cell integrity.

This research provides (1) physiological observations of *Pseudomonas putida* F1 in the biodegradation of toluene-phenol mixtures with proteomic analysis, (2) some fundamental evidence to better understand the relationships between biodegradation and the transmembrane transport of toluene-phenol mixtures, and (3) the effects of heavy metals on the biodegradation of toluene-phenol mixtures by *P. putida* F1.

Kee-Hong Kim

Department of Chemical Engineering

Colorado State University

Fort Collins, CO 80521

Summer 2002

Acknowledgements

Many wonderful people have helped me to finish this dissertation. Prof. Kenneth F. Reardon has guided, helped, and mentored me as the advisor. He has not been only a mentor to me, but also a wonderful friend. My committee members, Professors Vincent Murphy, James Linden, John Belisle, and Herbert Schweizer, have provided excellent service for this dissertation.

Many other people also significantly helped me during my research with various ways: Dr. Brian Batt and Mr. William Lauderdale for technical assistance, Prof. Katheryn Resing for tandem mass spectrum interpretation, Dr. Phillip Ryan for MALDI-MS spectrum acquisition and interpretation, Ms. Kimberly Davison for TEM imaging, and Dr. Paul Harris in the Novozymes Biotech, Inc. for being a wonderful boss during my first postdoctoral period.

Many friends in the laboratory helped me to survive in the Reardon Group with their friendship and helps: Derek Campbel, Dale Brown, Jeremy Porter, Shelley Allen, Christopher Breifogel, Jessica Lyle, Mike Fredrickson, Jennifer Po, Dr. Julio Zimbron, Dr. Julia Bull-Rogers, Dr. William Wangard III, and Dr. Paul Olson. Many other people were there for me and I deeply appreciate all their assistance.

During all those years, my parents, in-law parents, all my brothers and sisters have always believed and loved me. I deeply appreciate their support and love.

My greatest appreciation goes to my lovely and dedicated wife, soon-to-be Dr. Dong-Soon Bae and my lovely little daughter, Soo-Gyeong. They have always been the greatest supporter of me and the most important people in my life.

I appreciate you all!

To my mother in heaven.....

Table of Contents

List of Figures

List of Tables

CHAPTER I INTRODUCTION

I.1 Biodegradation of Aromatic Hydrocarbon Mixtures

Biodegradation could be defined as the transformation of chemicals by microorganism(s) in various media such as water and/or soils. In other words, microorganisms play the key role in a biodegradation process. Contamination of soil and/or water often occurs with chemical mixtures. Pollutant mixtures may contain organic chemicals, inorganics, heavy metals, or radionuclides, and these materials substantially influence to the biodegradation of other chemicals by microorganism (7, 17, 24). Mixed pollutants may interact among those chemicals, and these interactions could cause unexpected inhibition by removal of one chemical by microorganism(s) (22). Our research group has studied the biodegradation of chemical mixtures in the changes of kinetics. Mathematical modeling of the kinetics could be an excellent starting point to investigate the kinetic correlation of degradation of chemical mixtures by a microorganism. However, the kinetic study relies on phenotypical observation in the correlation of the microbial growth with biodegradation of chemical mixtures. With this approach, no biological and physiological information would be discovered during the biodegradation of chemical mixtures by a certain microorganism. Without more detailed biological information than the kinetic characteristics (e.g. specific growth rate, substrate coefficients, mass transfer limitation, degradation rates, etc), complete and effective understand of the biodegradation phenomena of the chemical mixtures would be difficult. To meet this demand in this study, an effective and powerful technology is employed to explore more

deeply the biological responses to the existence of organic chemical mixtures in the growth of a microorganism.

In addition to the biodegradation investigation of organic chemical mixtures, co-contamination of various media often occurs. Even if microbes require metals for their biological activities and metals are present in soils and waters, metals also could be toxic to microbes when their concentration reaches a certain level (9, 15). Because of the highly toxic effect of heavy metals to human beings and other species, the Environmental Protection Agency (EPA) strictly controls the contamination of soils and waters by heavy metals. The co-contamination of soils and waters by hydrocarbon and heavy metals occurred during recent decades all around the USA. Once co-contamination occurs in soils or water, the existence of heavy metals significantly inhibits the biodegradation of hydrocarbons by inhibiting the growth or biological activities of the indigenous microbial community (18, 23). This results in a prolonged threat to the public health by toxic contaminants in soils and water.

To develop and enhance the biodegradation process for hydrocarbons in the presence of high concentrations of heavy metals in soils and water, utilization of proper microbes that are tolerant to heavy metals would be essential. When the co-contamination is due to mixtures of heavy metals and hydrocarbons, the biodegradation mechanism is much more complicated. Based on the study of biodegradation of hydrocarbon mixtures by a model microbe, the effects of heavy metals on the biodegradation of hydrocarbon mixtures

could provide important fundamental data for further studies in biodegradation of co-contamination.

I.2 Genomics and Proteomics

Genomics can be defined as the study of DNA and it lead great success of life science. Genomic sequence data of many prokaryotic and eukaryotic cells has been catalogued in online databases and open to the life science community. By the collaboration of life science with computer science, genomic sequence databases in online from help researchers to analyze their DNA and protein sequence information biologically and statistically. Since the advent of the real-time polymerase chain reaction (RT-PCR), the expression level of mRNA can be monitored in real time, and the effort to connect the DNA sequence information and its mRNA expression level has been made and achieved some success (14). However, biological functions of those DNA sequences are not always enough to explain what their functions in a cell are by correlating the expression of mRNA (2, 12).

If a genome is considered as a blueprint of a house, proteins can be thought of the construction materials such as bricks, wallpapers, tiles, pipes, and so on. In others words, proteins represent the phenotypic outlet. Proteomics is the complementary term of "Genomics" (27). Various definitions of proteomics are available, but I would prefer to use the original concept proposed by Dr. Wilkins in 1995: thus, the concept of the proteome is "fundamentally different from that of the genome: while the genome is

virtually static and can be well-defined for an organism. the proteome continually changes in response to external and internal events"(27). In the view point of dynamic change of proteome in a cell with the response to extra- and intra-stimuli. proteomics can be defined as the study of proteome with state-of-art modern technologies such as mass spectrometry. laser science. nanotechnology. high pressure liquid chromatography. etc. Most proteomic research falls into three general categories(1. 3. 4. 6. 8. 13. 16. 21. 28): (I) differential protein production in terms of the changes in quantity: (II) identification of proteins involved in the special biological events and characterization of identified proteins including post-translational modification such as phosphorylation. glycosylation. and so on: (III) protein-protein interactions including the changes in functional activities.

Proteomics has been applied to discover new drugs. to investigate the effects of a newly developed drug on animal cells. and to elucidate the pathways of infection by viruses or bacteria (28). Recently. the applications of proteomics have been expanded widely due to the rapid development of technologies for proteomics and the Internet. Researchers can readily access the equipment for the separation of the total proteome of a target organism more easily than ever before. and the results can be also easily compared and interpreted through the Internet (4).

The development of technologies for a proteomic study is categorized into two important groups: for the first. the purification of several thousands of proteins in one gel. which is called two-dimensional polyacrylamide gel electrophoresis (2-D PAGE) (5. 10. 11). It consists of two parts. isoelectricfocusing (IEF) and SDS-PAGE. The second aspect of

technological improvements comes from mass spectrometry and development of databases. Various types of mass spectrometry for macrobiomolecules and genome databases on the Internet make it possible for the researchers to quickly identify the proteins from the 2-D PAGE gels (19, 20, 25, 26). Combining both technologies expedites the whole proteomic research and generates high data throughput.

A large volume of research has been carried out in the biotechnology, biochemistry, and molecular biology areas with proteomics, but not many attempts have been made to apply it to environmental biotechnology. One of the goals for this dissertation project is to adapt these powerful proteomics concepts and techniques to study environmental biotechnology.

I.3 Reference

1. **Abbott, A.** 1999. A post-genomic challenge: learning to read patterns of protein synthesis. Nature **402:**715 - 720.

2. **Anderson, L., and J. Seilhamer.** 1997. A comparison of selected mRNA and protein abundences in human liver. Electrophoresis **18:**533-537.

3. **Blackstock, W. P., and P. W. Malcolm.** 1999. Proteomics: quantitative and physical mapping of cellular proteins [Review]. Trends Biotechnol **17:**121-127.

4. **Dunn, M. J.** 2000. From genome to proteome : advances in the practice and application of proteomics. Wiley-VCH. Weinheim : New York.

5. **Dunn, M. J., and A. Gorg.** 2001. Two-dimensional polyacrylamide gel electrophoresis for proteome analysis. p. 43-60. *In* P. S.R. and M. J. Dunn (ed.). Proteomics. Springer-Verlag New York Inc., Trowbridge, UK.

6. **Dutt, M. J., and K. H. Lee.** 2000. Proteomic analysis. Current Opinion in Biotechnol. **11:**176-179.

7. **Egli, T.** 1995. The ecological and physiological significance of the growth of heterotrophic microorganisms with mixtures of substrates. p. 305-386. *In* J.G.Jones (ed.). Advances in Microbial Ecology. vol. 14. Plenum Press. New York.

8. **Gabor Miklos, G. L., and R. Maleszka.** 2001. Integrating molecular medicine with functional proteomics: Realities and expectations. Proteomics **1:**30-41.

9. **Gadd, G. M.** 1992. Microbial control of heavy metal pollution.. p. 59-87. *In* J. C. Fry. Gadd, G.M., Herbert, R.A., Jones, C.W., and Watson-Craik, I.A. (ed.). Microbial control of pollution. Cambridge University Press. Cambridge, United Kingdom.

10. **Görg, A., W. Postel, and S. Gunther.** 1988. Two-dimensional electrophoresis. Electrophoresis **9:**531-546.

11. **Görg, A., W. Postel, and S. Gunter.** 1988. The current state of two-dimensional electrophoresis with immobilized pH gradients. Electrophoresis **9:**531-546.

12. **Gygi, S. P., Y. Rochon, B. R. Franza, and R. Aebersold.** 1999. Correlation between Protein and mRNA Abundance in Yeast. Mol. Cell. Biol. **19:**1720-1730.

13. **Hatzimanikatis, V., L. H. Choe, and K. H. Lee.** 1999. Proteomics: Theoretical and experimental considerations. Biotechnol. Prog. **15:**312-318.

14. **Hatzimanikatis, V., and K. H. Lee.** 1999. Dynamical analysis of gene networks requires both mRNA and protein expression information. Metabolic Engineering **1:**E1-E7.

15. **Ietswaart, G. J. H., and W. A. J. Ernst.** 1992. Seasonality of VAM infection in three populations of *Agrostis capillaris* (Gramineae) on soil with or without heavy metal enrichment. Plant. Soil. **139:**67-73.

16. **Kellner, R.** 2000. Proteomics: Concepts and perspectives. Fresenius J. Anal. Chem. **366:**517-524.

17. **Klecka, G. M., and W. J. Maier.** 1988. Kinetics of microbial growth on mixtures of pentachlorophenol and chlorinated aromatic compounds. Biotech. Bioeng. **31:**328-335.

18. **Kuo, C., and B.R. S. Genthner.** 1996. Effects of added heavy metal ions on biotransformation and biodegradation of 2-chlorophenol and 3-chlorobenzoate in anaerobic bacteria consortia. Appl. Environ. Microbiol. **62:**2317-2323.

19. **Mann, M.** 1994. Sequence database searching by mass spectrometric data. p. 223-245. *In* R. Kellner, F. Lottspeich., H.E. Meyer. (ed.). Microcharacterization of proteins. VCH. Weinheim.

20. **Mann, M., and M. Wilm.** 1994. Error-tolerant database identification of peptides in sequence databses by peptide sequence tag. Anal. Chem. **66:**4390-4399.

21. **Peng, J., and S. P. Gygi.** 2001. Proteomics: the move to mixtures. J. Mass. spectrom. **36:**1083-1091.

22. **Reardon, K. F., D. C. Mosteller, and J. D. Rogers.** 2000. Biodegradation kinetics of benzene, toluene, and phenol as single and mixed substrates for *Pseudomonas putida* F1. Biotechnol. Bioeng. **69:**385-400.

23. **Reber, H.** 1992. Simultaneous estimates of the diversity and the degradative capability of heavy-metal-affected soil bacterial communities. Biol. Fert. Soils. **13:**181-186.

24. **Saez, P. B., and B. E. Rittmann.** 1993. Biodegradation kinetics of a mixture containing a primary substrate(phenol) and an inhibitory co-metabolite (4-chlorophenol). Biodegradation **4:**3-21.

25. **Shevchenko, A., A. Loboda, A. Shevchenko, W. Ens, and K. G. Standing.** 2000. MALDI Quadrupole Time-of-Flight Mass Spectrometry: A Powerful Tool for Proteomic Research. Anal. Chem. **72:**2132-2141.

26. **Shukla, A. K., and J. H. Futrell.** 2000. Tandem mass spectrometry: dissociation of ions by collisional activation. J. Mass Spectrom. **35:**1069-1090.

27. **Willkins, M. R., J.C.. Sanchez, A.A. Gooley, R.D. Appel, I. Humphery-Smith.** 1995. Thinking big proteome studies in a post-genome era. Biotechnol. Gene. Eng. Rev. **13:**19-50.

28. **Wilson, J. F.** 2001. New technology spurs on proteomics. The Scientist **15:**12-13.

CHAPTER II BACKGROUND

II.1 Biodegradation of Aromatic Hydrocarbon Mixtures by *Pseudomonas putida* F1

Large amounts of mono-aromatic compounds have been produced around the world as starting materials for the production of plastics, synthetic fibers, and pesticides, and also used in fuels as solvents (9). Through spills, leakage from tanks, and other releases, mono-aromatics have become prevalent environmental contaminants, usually in mixtures. Many pure and mixed cultures capable of growth on mono-aromatics such as toluene (2, 10), benzene (28) and phenol (39, 60), have been isolated and studied. Although microorganisms also biodegrade mixtures of aromatics (20, 47, 55, 75), little is known about the physiological changes that occur during this mixed-substrate growth.

Of the bacteria known to biodegrade aromatic hydrocarbons, *Pseudomonas putida* F1 has been well characterized. This organism can use toluene, benzene, ethylbenzene, phenol, and other aromatics as sole carbon and energy sources (29). The biodegradation of all of these compounds by *P. putida* F1 is initiated by toluene dioxygenase (TDO) (85), a three-component, NADH-dependent, soluble enzyme that adds oxygen to the aromatic ring (23, 29, 102). Using specific mutants of *P. putida* F1, Spain and (85), demonstrated that the toluene dioxygenase (TDO) enzyme system was responsible for the hydroxylation of phenol. Other enzymes encoded by the *tod* operon catalyze the sequential transformation of the toluene dioxygenase products to tricarboxylic cycle intermediates (104).

In a recent study of the biodegradation of benzene, toluene, and phenol by *P. putida* F1, we observed that the presence of toluene or benzene substantially inhibited the consumption of phenol (73). In fact, phenol degradation did not begin until the medium was nearly depleted of toluene. Since the metabolism of each of these compounds follows the same metabolic pathway, this was not a case of diauxic growth (induction of new catabolic enzymes). Moreover, the kinetics were not well described by a purely competitive inhibition model, which would have been expected if both substrates completed for the same enzyme(s).

II.2 Proteomics

In 1992, Willkins (a professor at the University of Geneva, Switzerland) and Hochstrasser (a professor at the Geneva University Hospital, Swiss) asked a question to biochemistry society: "If we cannot understand how the proteins in life's simplest organisms operate, how can we ever hope to understand how the more than 700,000 proteins are working in the human body?" They came up with the new term "Proteome" that is the PROTEin complement expressed by a genome of tissue. (http://www.abrf.org/ABRFNews/1996/December1996/Proteome.html) (94). "Proteomics" or "Proteomic analysis" is an attempt to describe the molecular basis of (patho) physiological processes (45). Proteome analysis was originally a protein characterization method, but its application to identification of proteins that are differentially produced in response to a cellular activity becomes more powerful when it is combined with genomics, which can be defined as the study of *genes* and their function. Kellner described the synergistic effect of the combination of genomics and proteomics (45). How genomics and proteomics are synergistic is depicted in Figure II-1. Biological information flows from DNA to protein via RNA. Understanding the function of genomic data depends on understanding the production pattern of proteins in response to cellular activity. When genomics and proteomics are combined with each other, better and more complete understanding of biological activity is possible.

Type of Information	Biological Carrier	Field of Application
Gene Sequence data ↓ Gene Expression data	DNA RNA	GENOMICS
↓ **Gene Product data** ↓ **Protein Function data**	**Protein**	**PROTEOMICS**

Figure II-1 Genomics and proteomics are synergistic (45).

Since protein production is dynamical in response to external and internal events, pursuing differential production and understanding co-regulation at the level of protein production are difficult. However, the exciting increase in the amount of genomic sequence data, combined with mass spectrometry technologies, allows a researcher to identify hundreds of proteins within a week (1). Although this impressive rate of protein identification and understanding is still highly dependent on the availability of genomic data for a particular organism and the relevant technologies are still under development, proteomics is the best tool to answer the question raised by Willinks and Hochstrasser.

II.2.1 PROTEOME ANALYSIS

II.2.1.1 Two Dimensional Polyacrylamide Gel Electrophoresis

Two-dimensional PAGE consists of isoelectric focusing (IEF) and sodium dodecylsulfate-polyacrylamide gel electrophoresis (SDS-PAGE). Since the first 2-D PAGE procedure reported by O'Farrell (59) and Klose (48) in 1975, it has been a standard technique for the separation of complex mixtures of proteins. The typical method of 2-D PAGE can often separate up to several thousands of proteins from whole cell and specific tissue homogenates, and the capacity of protein separation goes upto 10,000 proteins on a gel when large format gel is utilized (17, 18, 33). Two-dimensional gel electrophoresis is able to separate proteins of either acidic or basic pI is suitable for virtually all kinds of protein samples from bacteria to human cells. This method has also been employed to elucidate physiological changes in *Pseudomonas putida* and other microbial cells (6, 30, 46, 51, 73).

II.2.1.1.1 Isoelectric focusing

Each protein has an unique primary structure that is determined by the composition of polar and non-polar side chains of amino acids. Because of the different composition of amino acids in a polypeptide, every single protein has its own isoelectric point (pI). The net charge of a protein is the sum of all the negative and positive charges of its amino

acid side chains and the amino- and carboxyl-termini. The isoelectric point is the specific pH where the net charge of the protein is zero. If two proteins that have different pI points are added to a pH gradient and subjected to the influence of electric field, these two proteins will migrate to the position in the gradient at which the net charge of each protein is zero, and will be separated from each other regardless of their molecular weight. Isoelectric focusing (IEF) is the technique that uses this simple but specific characteristic of proteins. For successful separation of protein mixtures by IEF, three important parameters should be taken into account in the separation process: pH gradient, denaturing proteins (in other word, solublized proteins), and matrix. IEF is operated under denaturing conditions for the highest resolution. The degree of denaturation and solubilization of a polypeptide is the most important factor to achieve successful separation of protein mixtures. Protein solubilization and denaturations carried out with a mixture of urea and detergents ensures that each protein is only in its primary structure and minimizes aggregation or interaction among proteins (18, 19, 32, 33). The pH gradient is formed either by carrier ampholyte in a tube gel matrix (48, 59) or with an Immobiline system (7, 33, 34). Due to the endosmosis effect to the cathode and difficult reproducibility, the use of carrier ampholytes is now obsolete. Instead, Immobiline pH gradient (IPG) replaced carrier ampholytes beginning in 1982. An IPG is created by covalently incorporating a gradient of acidic and basic buffering groups (acrylamido buffer) into a polyacrylamide gel when it is cast (7). IEF with IPG is more reproducible because the covalently attached gradient cannot drift. The development of the IPG technique significantly improved the feasibility of IEF and protein separation (32-35).

II.2.1.1.2 Sodiumdodecyl sulfate Polyacrylamide Gel Electrophoresis

SDS-PAGE separates proteins in mixtures with respect to their molecular weights. Proteins are reacted with excessive amounts of SDS to give them entirely negative charge of proteins so that their different net charge cannot affect the migration of proteins in a ployacrylamide gel within an electric field. The mass ratio of SDS to protein is approximately 1.4. The SDS also helps to denature polypeptides by disrupting hydrogen bonds, blocking hydrophobic interactions, and partially unfolding the protein molecules, thereby minimizing differences in molecular form by eliminating the secondary and tertiary structure of proteins (76). To obtain complete protein unfolding, either dithiothreitol (DTT) or β-mercaptoethanol is added to reduce all cysteine residues and it results in the breaking all disulfide bonds in the tertiary peptide structure. When proteins are treated with both SDS and a reducing reagent, exclusive separations of protein mixtures by molecular weight are possible (49, 76, 91).

II.2.1.2 Protein Detection

For subsequent analysis, proteins separated by 2-D PAGE on a gel should be detected by a suitable staining method. Protein detection methods can be divided into three categories: fluorescent, non-fluorescent, and isotopic. Since the isotopic method is useful to analyze the proteome itself but is not generally suitable for subsequent protein identification methods, it is not discussed here. Several excellent reviews are available (70-72, 77, 88, 89).

For non-fluorescent protein detection in a gel. Coomassie blue organic dye has been widely used since its introduction in the early 1960s (56). Coomassie blue dye is able to detect as little as 30-100 ng of a protein. but it is considerably less sensitive than silver staining or fluorescent detection (8). However. Coomassie blue has two considerable advantages in proteomics research. The first is that it is completely compatible with the subsequent protein analyses. which are Edman degradation N-terminal sequencing after visualization of proteins on polyvinylidene difluoride (PVDF) membrane (41. 93) and mass spectrometry (43).

Silver staining was first introduced by Switzer *et al* (88) for staining proteins in polyacrylamide gels. It was at least 100 times more sensitive than Coomassie blue staining and opened the era of detecting nanogram levels of proteins instead of the microgram range provided by Coomassie blue staining. More than 100 silver staining procedures are available (70-72). The biggest disadvantage of any silver-staining procedure. however. is that it differentially stains protein depending on the degree and types of protein modifications. Thus. the quality of staining is poor when proteins are glycosylated or bound with calcium (77. 98). Some silver stains are also compatible with both a nanoflow tandem mass spectrometry and MALDI-TOF MS (27. 81). and a typical ESI-MS after being electroblotted onto either nitrocellulose or PVDF membrane (89).

Typical fluorescent chemicals for protein staining in a polyacrylamide gel are non-covalently bound fluorophores. Fluorescent stains can be an excellent choice. especially for a large scale of proteomics research. because it usually yields a superior linear

dynamic range of detection compared to colorimetric stains. Recently, the SYPRO Orange and Red dyes have become popular (5, 86, 87). They are virtually not fluorescent in aqueous solution, but become fluorescent in non-polar solvents or upon association with SDS-protein complexes. The sensitivity of SYPRO Ruby is as good as a silver stain (86, 87). Both SYPRO dyes are compatible with mass spectrometric analysis of peptides including MALDI-TOF MS and ESI-MS(/MS) (5).

II.2.2 PROTEIN IDENTIFICATION

The description of biological information flow is that the genetic information stored in genetic sequence of DNA is translated to proteins via the transcription of mRNA. Based on this fact, many researches have been made to interpret the relationship between the expression level of mRNA and their protein production to describe the state of biological system (3, 36, 37). However, the alteration of biological information of a cell in response to harsh environment (e.g. the existence of toluene-phenol mixtures in the growth medium) or other disturbances could not be adequately explained or predicted by a simple correlation between mRNA transcription and protein translation (3, 36). Because biological activities in a cell are generally controlled by the production of proteins and their subsequent modifications, stimulate or inhibit their enzymatic activity. For these reasons, identifying proteins that are differentially produced is critical to understand the adaptation of a cell to the state of environments. Protein identification can be achieved by combining two important technologies (14, 43): peptide analysis and bioinformatics.

Peptide sequence analysis has been performed by the traditional N-terminal de novo sequencing by Edman degradation or the state-of-the-art tandem mass spectrometry. Since it requires greater amount of purified peptide samples than that of mass spectrometric approach (93), it becomes obsolete for high throughput proteomic analysis based on two-dimensional protein separation. Despite this critical disadvantage for the modern proteomics, it has regained attention due to the advent of new equipment that is able to sequence amino acids at the femtomole level of peptide sample (14). However, even this new machine has another crucial disadvantage in that it needs a much longer time of analysis per peptide sample than that of mass spectrometry. However, the new machine can significantly contribute to protein identification by verifying amino acid sequences obtained by tandem mass spectrometric analysis (4).

Mass spectrometry has become a key tool in correlating proteins to their genes (14, 15, 17) and has benefited from the advances in genomic sequence analysis. It requires extremely low level of peptides, as low as an attomole of peptide (61), and very short sample analysis time. Furthermore, identifying proteins via mass spectrometry can be easily automated by combining two-dimensional analysis, peptide preparation, and database searching (42, 50, 62, 82). Rapid de novo sequencing of proteins can also be achieved partially or fully by a tandem mass spectrometer. However, since identification of proteins by a mass spectrometry is solely dependent on the size analysis of peptides, careful interpretation of mass spectra based on solid backgrounds in chemistry and biology and practical experience are essential (82). To avoid the misinterpretation of mass spectra and resulting false protein identification, several computer software

packages have been developed to calculate and determine ion fragments from a parent ion (27, 38, 64).

II.2.2.1 Principle of mass spectrometry for biomolecules

The principal purpose of mass spectrometry is to measure the molecular weight of a macromolecule without destruction of its original structure. To measure the molecular weight of proteins and peptides by a mass spectrometer, they should be gas-phase ions (25). Ionization of macromolecules is defined as a process that produces an ion from a neutral atom or molecule. Ionization of proteins or peptides can be achieved by either surface ionization or electron ionization (25). Electron ionization is defined as ionization of any species by electrons and it is described by the following (63)

$$M + e^- \rightarrow M^{+\bullet} + 2e^- \quad \text{for atoms and molecules.}$$

and

$$M^{\bullet} + e^- \rightarrow M^+ + 2e^- \quad \text{for radicals.}$$

With respect to ionization methods, mass spectrometers for protein identification fall into two unique types. Matrix-assisted laser desorption/ionization (MALDI) uses laser power for surface ionization, while electrospray ionization (ESI) performs electron ionization of proteins or peptides.

Three unique mass analyzers are utilized and Figure II-2 provides a schematic description of each type (101). For triple quadrupole mass spectrometer, ions are selected with the

first mass spectrometer (MS-1) and passed into a collision cell (MS-2) for activation. Fragment ions are then separated in the last mass analyzer (MS-3). In quadrupole ion trap mass spectrometer, ions are injected into the ion trap from an external ion source. Ejecting from the trap volume all other ions isolates a precursor ion. By applying a resonance voltage across the end-caps, the motion of the selected precursor ion is increased, causing multiple low-energy collisions. The resulting fragment ions are then scanned in turn from the ion trap into a detector using a mass-selective instability scan. For reflectron time-of-flight mass spectrometer, ions are accelerated from the ion source into the field-free region. A particular m/z value is selected by timing the arrival of ions at an electronic gate. The collection of metastable decomposition products enters the reflectron. Ions are separated on the basis of kinetic energy with the lighter fragment ions exiting earlier.

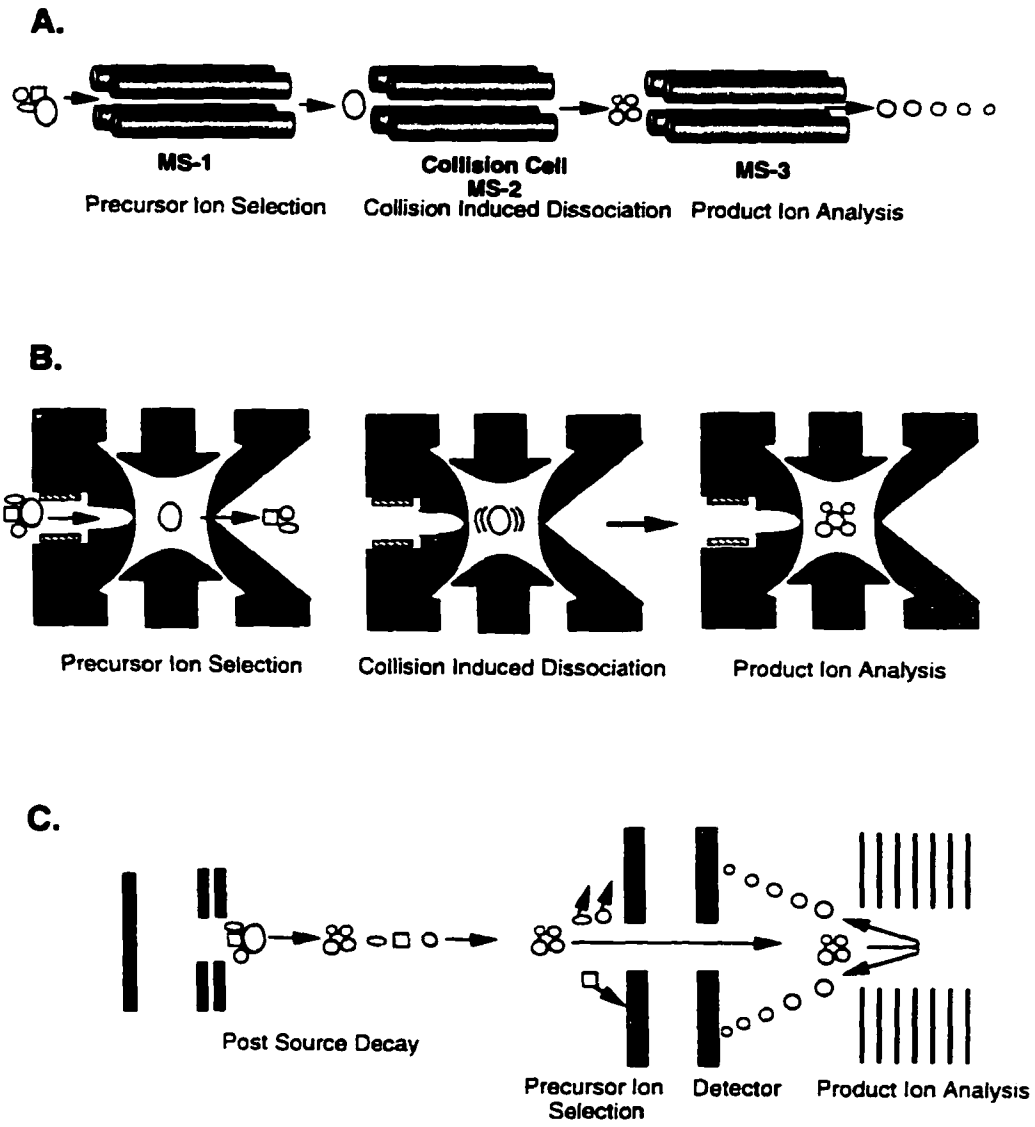

Figure II-2 Three instruments used to perform tandem mass spectrometry (101) (A) Triple quadrupole mass spectrometer. (B) Quadrupole ion trap mass spectrometer. (C) Reflectron time-of-flight mass spectrometer.

II.2.2.2 Electrospray mass spectrometer

ESI is a continuous ionization method that creates molecular ions by a potential difference between a capillary and the inlet to the mass spectrometer. Charged droplets are generated by the electric field in the form of mist (25). The important advantage of ESI is the ability to form highly charged ions without further fragmentation. It lowers the mass-to-charge (*m/z*) values to a range easily measured by various types of mass analyzers. Mann *et al* (52) described algorithms for interpretation of multiply charged ions. From this simple division of a measured mass with its true charge status, the calculation of the true molecular masses of molecular ions is simple. Even though the ESI procedure has been known to tolerate the salts and detergents found in buffer systems, it is recommended to remove these chemicals from a peptide mixture prior to injection, because they may cause ambiguous molecular determination or suppress the formation of analyte ions. An ESI mass spectrometer is always connected to a high-pressure liquid chromatography (HPLC) with a microbore or capillary C_{18} column (the choice varies with the nature of the samples) for separation of peptides proteolyzed by modified or non-modified Trypsin (82). If ESI uses only one mass analyzer, it is called ESI-MS. When it employs two mass analyzers and one collision-induced dissociation (CID) device between the two mass analyzers, it is called ESI-MS/MS or a tandem mass spectrometer. ESI-MS(/MS) is always connected to a liquid chromatography unit, so LC ESI-MS/MS is another name.

II.2.2.3 MALDI-TOF

MALDI utilizes nitrogen lasers for the ionization of biomolecules. The bottleneck of the use of lasers for mass spectrometry was to keep the intact molecular structure of a biomolecule following laser treatment. However, Karas and Hillenkemp found that incorporation of an analyte into the crystalline structure of small UV-absorbing molecules provided a safe vehicle for ions to be created from polar or charged biomolecules (44). Ever since then, MALDI Time-of-Flight (MALDI-TOF) has become the most feasible and accurate tool to obtain the mass fingerprint of a peptide mixture due to its ability to analyze femtomole amounts of peptides in a short time (53, 79, 100). Mass fingerprint information can be matched with protein and genomic databases to obtain protein identification and the analysis of post-translational modification. The implementation of MALDI-TOF MS peptide analysis in current proteomics research requires high sample throughput combined with high detection sensitivity and mass accuracy (11, 31, 80, 84, 90). These demands place requirements on sample purification, enrichment, and preparation for MALDI-TOF MS, which should be reproducible, cost-effective, and yielding MALDI samples suitable for the automation of whole processes.

II.2.2.4 Databases and search engines

The protein identification process requires not only the facilities for obtaining mass fingerprints but also the protein and genomic databases of an organism. More than 30 prokaryotic and some eukaryotic organisms' genomic sequences are available (81, 82, 99, 101). Several excellent search engines have been developed to perform searches against

those genome databases in several different formats (21, 22). The types of databases and search engines for the mass spectra from either MALDI-TOF or LC ESI-MS(/MS) is described in Table II-1. Since MALDI requires much shorter time and smaller protein samples for analysis than LC-ESI-MS(/MS), MALDI-TOF becomes the standard in industries and academic proteomics researches for high throughput process (84).

Table II-1 (A) Proteomics research related World Wide Web sites. (B) File Transfer Protocol (FTP) sites for proteomic research. More resources in the Internet are well described by Murray (58). Using the mass spectra from simple mass fingerprints and sequences obtained by Edman degradation or tandem mass spectrometer, identification of interested proteins is feasible with these databases and tools.

World Wide Web sites	
Genome	
GenBank	http: www.ncbi.nlm.nih.gov Genbank GenbankSearch.html
EMBL	http: www.ebi.ac.uk
GDB	http: gdbwww.gdb.org
GSDB	http: www.ncgr.org gsdb gsdb.html
TIGR	http: www.tigr.org
Proteome	
SWISS-PROT	http: www.expasy.ch sprot sprot-top.html
OWL	http: www.bis.med.jhmi.edu Dan proteins owl.html
NRL3D	http: www-nbrf.georgetown.edu pirwww dbinfo nrl3d.html
PDB	http: www.rcsb.org pdb
Prosite	http: www.expasy.ch prosite
Enzyme	http: www.expasy.ch enzyme
SW-2D	http: www.expasy.ch ch2d ch2d-top.html
NCBInr	http: www.ncbi.nlm.nih.gov
dbEST	http: www.ncbi.nlm.nih.gov dbEST index.html
Database correlation programs	
BLAST	http: www.ncbi.nlm.nih.gov BLAST
ExPASy	http: www.expasy.ch tools
PROWL	http: www.proteometrics.com
UCSF	http: donatello.ucsf.edu
MASCOT	http: www.matrixscience.com
SEQUEST	http: fields.scripps.edu sequest index.html

(A)

File Transfer Protocol Sites
Protein databases
ftp: ncbi.nlm.nih.gov genbank genpept.fsa.Z
ftp: ncbi.nlm.nih.gov genbank README.genbank ***
ftp: ncbi.nlm.nih.gov blast db nr.Z
ftp: ncbi.nlm.nih.gov blast db README
ftp: ncbi.nlm.nih.gov repository OWL owl.fasta.Z

ftp: ncbi.nlm.nih.gov repository OWL README
ftp: ftp.ncifcrf.gov pub nonredun protein.nrdb.Z ***
ftp: ftp.ncifcrf.gov pub nonredun NRP.readme
EST sequences
ftp: ncbi.nlm.nih.gov repository dbEST README
ftp: ncbi.nlm.nih.gov repository unigene Hs.seq.uniq.Z
ftp: ncbi.nlm.nih.gov repository unigene README
ftp: ncbi.nlm.nih.gov repository unigene Hs.info
ftp://ncbi.nlm.nih.gov/repository/dbEST/dbEST.weekly.FASTA.mmddyy.Z (mmddyy=date)
Yeast sequence database
ftp: genome-ftp.stanford.edu pub yeast yeast_protein yeast_nrpep.fasta.Z
ftp: genome-ftp.stanford.edu pub yeast yeast_ORFs orf_trans.fasta.Z
ftp: genome-ftp.stanford.edu pub yeast yeast_protein README

*** Non-redundant (nr) databases from genbank and protein.nrdb from ncicrf are updated daily.

(B)

II.2.2.5 Amino acid sequencing

Conventional protein sequencing using Edman degradation has been used as a strategy to identify proteins (14, 41, 43, 74). Edman sequencing can also be combined with mass spectrometry for protein identification (14, 41, 43). The peptide sequences acquired by internal (93) or external Edman sequencing were run against genomic sequence databases for protein identification (14, 41). Due to the demand of high throughput analysis of protein samples separated by 2-D PAGE, mass spectrometric methods are the best choice to obtain partial or full amino acid sequences.

Brilliant advances of both MALDI and ESI-MS technology has expedited the speed of protein sequencing from significantly smaller amounts of protein samples. Peptide sequencing techniques based on MALDI have been evolved to MALDI tandem ion trap mass spectrometry (MALDI-ITMS) (66-69) and MALDI quadrupole time-of-flight mass spectrometry (MALDI- QTOF) (80, 82, 90). However, even if MALDI-based peptide sequencing is relatively simple, fast, and needs smaller amount of protein samples than

ESI-based methods, it is likely to generate a false identification when of more than one protein is present in the gel spot or in the case that the protein of interest is heavily modified by post-translational modification (21, 54, 79, 99).

Since Hunt and *et al* (38) demonstrated the use of nano-electrospray tandem MS to determine amino acid sequences of proteins, tandem ESI-MS has been considered one of the important techniques for protein sequencing (16, 21, 26, 38, 57, 78, 83, 95, 96). With the development of special software package, SEQUEST, that can perform database search shortly after acquiring tandem mass spectra by ESI-MS/MS, rapid identification of proteins by de novo peptide sequencing is possible (16, 21). However, peptide sequences are deduced automatically or manually by the interpretation of tandem mass spectra so that erratic interpretation was a concern when the tandem mass spectra were not clear enough for unambiguous interpretation (65, 78, 95). To overcome this ambiguousness in sequencing, a viable alternative method was developed by labeling ^{18}O to the carbon terminus of peptide fragments before analysis on an ion trap tandem mass spectrometer (65) or nano-electrospray quadrupole/time-of-flight mass spectrometer (78). The oxygen isotope (^{18}O) specifically binds to the C-terminal of each peptide fragments, leading to an increase of its molecular weight (+18) on tandem mass spectrogram. This method significantly improved the confidence of amino acid sequence of proteins and made rapid and confident identification of proteins based on de novo amino acid sequence acquired by a tandem mass spectrometer.

II.2.2.6 Strategy of protein identification

Since the efficiency and degree of complexity for protein identification depends highly on whether or not the complete genomic sequence for a target organism is available, a strategy should be carefully designed prior to the start of proteomics research. Besides the availability of genomic sequences, there are several more important rate-limiting steps during the protein identification process. When genomic sequences are available, a simple mass fingerprint can be obtained by either MALDI-TOF (Qin, 1997 #137; Henzel, 1993 #37; Parker,1998 #105) or LC-ESI-MS (13, 100), and searching for identification against appropriate protein or genomic databases can be performed with peptide mass search engines. However, if neither complete nor partial genomic sequences for the target organism are available, partial or complete de novo amino acid sequencing is essential. Two methods of sequencing procedures have been developed: (A) N-terminal sequencing by Edman degradation (41, 43, 74, 93) after protein separation with 2-D PAGE and (B) in-gel digestion with trypsin (12, 74) followed by HPLC separation and subsequent database search with BLAST (Basic Local Alignment Search Tool. http://www.ncbi.nlm.nih.gov/BLAST/). The integration of Edman and mass spectrometric data is also an excellent approach (14, 43). Several excellent reviews for the protein identification strategy based on the combination of ESI-MS/MS and subsequent database search are available (15, 25, 40).

Without complete genomic sequences, the combination of rapid de novo sequences of proteins or peptides and PCR-based gene cloning system is necessary for the effective identification and further characterization of proteins. Shevchenko *et al* (82) recently

proposed a strategy for identifying homologous proteins by a combination of MALDI-QTOF MS and a modified BLAST search protocol.

II.2.3 EMERGING NEW TECHNOLOGIES IN PROTEOMICS

Since the genomes of both prokaryotic and eukaryotic cells are being sequenced, researchers in industry, academia, and government have turned their attention to sequence proteins. In large-scale proteomics projects, automation of proteome analysis, peptide sample preparation, and identification procedures must be accomplished to reach the goal. Many biotechnological and mechanical companies are diligently working to provide novel tools to identify more quickly and precisely the thousands of proteins produced by all kinds of life forms (97). This recent tide of emerging new technologies falls into two big categories: protein separation and mass spectrometry.

Conventional protein separation techniques, like 2-D PAGE, are highly labor-intensive and do not always provide reliable quantitative information. In addition to these, it is difficult to identify certain classes of proteins like membrane bound, highly acidic or basic, and extremely low abundant proteins (18, 24, 92). Gao *et al* (Jiang, 20001 #179; Gao, 2001 #178) reported an integrated on-line platform that is able to digest polypeptides, to separate peptide fragments, and to obtain identification with ESI-MS. This microfluidic system enables one to save a considerable amount of time for the

identification process with less than nanogram of proteins and to connect identification process with upstream protein separation through an on-line interface.

Based on the idea that MALDI and nanoflow tandem mass spectrometer need less than a picomole of proteins in the identification process, nanotechnology is also playing a critical role in the development of automatic protein separation and identification. A capillary electrophoresis (CE) unit is the most suitable technique to handle an extremely small amount of protein solution. Zhang *et al* (103) designed a capillary electrophoresis/electrospray mass spectrometry system that is able to automatically sample from a microwell plate. This new micro device integrates a sub-atmospheric ESI interface with injection directly from microwell plates that hold peptide samples. Okerberg *et al* developed another application based on capillary electrophoresis (61). Their system can analyze an ultra low concentration of peptides, as low as an attomole, within a 1.5 μm capillary channel after tryptic digestion. By using the intrinsic fluorescence of peptide fragments through excitation of aromatic amino acid residues, they can detect as little as 0.7 attomole of tryptophan. Lazar *et al* (50) reports the application of a "chip" to digest and analyze proteins using a hybrid microchip nanoelectrospray device and time-of-flight mass spectrometry detection. This system can digest proteins and analyze their mass fingerprint through a NanoESI tip while the whole process is monitored on-line. The protein requirement for the identification process was in the range of low femtomole or even attomole quantities of analyte/spectrum.

The boom of new technologies in proteomics is just at the beginning. It is obvious that tremendous numbers of new technologies will be revealed in a few years and they will lead to save huge amount of time and effort. Maybe one or half a day will be sufficient soon to identify more than 5000 proteins from unknown genome sequence organism with minimum involvement of proteomist.

II.3 References

1. **Abbott, A.** 1999. A post-genomic challenge: learning to read patterns of protein synthesis. Nature **402:**715 - 720.

2. **Alvarez, P. J., and T. M. Vogel.** 1991. Substrate interactions of benzene, toluene, and para-xylene during microbial degradation by pure cultures and mixed culture aquifer slurries. Appl. Environ. Microbiol. **57:**2981-2985.

3. **Anderson, L., and J. Seilhamer.** 1997. A comparison of selected mRNA and protein abundences in human liver. Electrophoresis **18:**533-537.

4. **AppliedBiosystems.** http://www.appliedbiosystems.com/pa/347607/347607.html.

5. **Berggren, K. N., E. Chernokalskaya, M. F. Lopez, J. M. Beechem, and W. F. Patton.** 2001. Comparison of three different fluorscent visualization strategies for detecting *Escherichia coli* ATP synthase subunits after sodium dodecyl sulfate-polyacrylamide gel electrophoresis. Proteomics **1:**54-65.

6. **Birnbaum, S., and J. Bailey.** 1991. Plasmid presence changes the relative levels of many host cell proteins and ribosome components in recombinant *Escherichia coli*. Biotechnol. and Bioeng. **37:**736-745.

7. **Bjellqvist, B., K. Ek, P. G. Righetti, E. Gianazza, A. Görg, R. Westermeirer, and W. Postel.** 1982. Isoelectric focusing in immobilized pH gradients: principle, methodology, and some application. J. Biochem. Biophys Methods **6:**317-339.

8. **Brush, M.** 1998. Dye hard: protein gel staining products. Scientist **12:**16-22.

9. **Budavari, S., Ed.** 1996. The Merck Index : an Encyclopedia of Chemicals, Drugs, and Biologicals. Merck, Whitehouse Station, NJ.

10. **Chang, M.-K., T. C. Voice, and C. S. Criddle.** 1993. Kinetics of competitive inhibition and cometabolism in the biodegradation of benzene, toluene, and *p*-xylene by two *Pseudomonas* isolates. Biotechnol. Bioeng. **41**:1057-1065.

11. **Chapman, J. R.** 2000. Mass spectrometry of proteins and peptides. Humana Press, Totowa, NJ.

12. **Cohen, S. L. a. B. T. C.** 1997. Mass spectrometry of whole proteins eluted from sodium dodecyl sulfate-polyacrylamide gel electrophoresis gels. Anal. Biochem. **247**:257-267.

13. **Davis, M. T., Lee, T. D.** 1998. Rapid protein identification using a micro scale electrospray LC/MS system on an ion trap mass spectrometer. J. Am. Soc. Mass Spectrom. **9**:194-201.

14. **Di Maro, A., Pasquale Ferranti, Mariarosaria Mastronicola, Letizia Polito, Andrea Bolognesi, Fiorenzo Stirpe, Antonio Malorni, Augusto Parente.** 2001. Reliable sequence determination of ribosome- inactivating proteins by combining electrospray mass spectrometry and Edman degradation. J. Mass Spectrom. **36**:38-46.

15. **Dongre, A. R., J. K. Eng and J.R. Yates III.** 1997. Emerging tandem-mass-spectrometry techniques for the rapid identification of proteins. Trends Biotechnol. **15**:418-425.

16. **Ducret, A., Van Oostveen, I., Eng, J., Yates, J.R., Aebersold, R.** 1998. High throughput protein characterization by automated reverse-phase chromatography/electrospray tandem mass spectrometry. Protein Sci. **7**:706-719.

17. **Dunn, M. J.** 2000. From genome to proteome : advances in the practice and application of proteomics. Wiley-VCH, Weinheim : New York.

18. **Dunn, M. J., and A. Gorg.** 2001. Two-dimensional polyacrylamide gel electrophoresis for proteome analysis. p. 43-60. *In* P. S.R. and M. J. Dunn (ed.). Proteomics. Springer-Verlag New York Inc., Trowbridge, UK.

19. **Dutt, M. J., and K. H. Lee.** 2000. Proteomic analysis. Current Opinion in Biotechnol. **11:**176-179.

20. **Egli, T.** 1995. The ecological and physiological significance of the growth of heterotrophic microorganisms with mixtures of substrates. p. 305-386. *In* J.G.Jones (ed.). Advances in Microbial Ecology, vol. 14. Plenum Press, New York.

21. **Eng, J. K., McCormack, A.L., Yates, J.R., III.** 1994. An Approach to Correlate Tandem Mass Spectral Data of Peptides with Amino Acid Sequences in a Protein Database. J. Am. Soc. Mass Spectrom **5:**976-989.

22. **Fernandez-de-Cossio, J., and Y. S. Javier Gonzalez, Takaki Shima, Nobuaki Okumura, Vladimir Besada, Lazaro Betancourt, Gabriel Padron, Yasutsugu Shimonishi, Toshifumi Takao.** 2000. Automated interpretation of low-energy collision-induced dissociation spectra by SeqMS, a software aid for de novo sequencing by tandem mass spectrometry. Electrophoresis **21:**1694-1699.

23. **Finette, B. A., V. Subramanian, and D. T. Gibson.** 1984. Isolation and characterization of *Pseudomonas putida* PpF1 mutants defective in the toluene dioxygenase enzyme system. J. Bacteriol. **160:**1003-1009.

24. **Gabor Miklos, G. L., and R. Maleszka.** 2001. Integrating molecular medicine with functional proteomics: Realities and expectations. Proteomics **1:**30-41.

25. **Gaskell, S. J.** 1997. Electrospray: Principles and Practice. J. Mass Spectrom. **32:**677-688.

26. **Gatlin, C. L., J. K. Eng, S. T. Cross, J. C. Detter, and J. R. Yates III.** 2000. Automated Identification of Amino Acid Sequence Variations in Proteins by HPLC/Microspray Tandem Mass Spectrometry. Anal. Chem. **72:**757-763.

27. **Gatlin, C. L., G. R. Kleemann, L. G. Hays, A. J. Link, and J. R. Yates III.** 1998. Protein Identification at the Low Femtomole Level from Silver-Stained Gels Using a New Fritless Electrospray Interface for Liquid Chromatography-Microspray and Nanospray Mass Spectrometry. Anal Biochem **263:**93-101.

28. **Gibson, D. T., J. R. Koch, and R. E. Kallio.** 1968a. Oxidative degradation of aromatic hydrocarbons by microorganisms. I. Enzymatic formation of catechol from benzene. Biochemistry 7:2653-2662.

29. **Gibson, D. T., G. J. Zylstra, and S. Chauhan.** 1990. Biotransformations catalyzed by toluene dioxygenase from *Pseudomonas putida* F1. p. 121-132. *In* I. S. Silver. A. M. Chakrabarty. B. Iglewski. and S. Kaplan (ed.). Pseudomonas: Biotransformations. Pathogenesis. and Evolving Biotechnology. American Society for Microbiology. Washington D.C.

30. **Givskov, M., L. Eberl, and S. Molin.** 1994. Responses to nutrient starvation in *Pseudomonas putida* KT2442: two-dimensional electrophoretic analysis of starvation- and stress-induced proteins. J. Bacteriol. **176:**4816-4824.

31. **Gobom, J., M. Schuerenberg, M. Mueller, D. Thesis, H. Lehrach, and E. Nordhoff.** 2001. a-cyano-4-hydroxycinnamic acid affinity sample preparation. A protocol for MALDI-MS peptide analysis in proteomics. Anal. Chem. **73:**434-438.

32. **Görg, A., W. Postel, C. Friedrich, R. Kuick, J. R. Strahler, and S. M. Hanash.** 1991. Temperature-dependent spot positional variability in two-dimensional polypeptide patterns. Electrophoresis **12:**653-658.

33. **Görg, A., W. Postel, and S. Gunther.** 1988. Two-dimensional electrophoresis. Electrophoresis **9:**531-546.

34. **Görg, A., W, S. Postel, and J. W. Gunter.** 1985. Improved horizontal two-dimensional electrophoresis with hybrid isoelectric focusing in immobilized pH gradients in the first dimension and laying-on transfer to the second dimension. Electrophoresis **6:**599-604.

35. **Görg, A., W. Postel, and S. Gunter.** 1988. The current state of two-dimensional electrophoresis with immobilized pH gradients. Electrophoresis **9:**531-546.

36. **Gygi, S. P., Y. Rochon, B. R. Franza, and R. Aebersold.** 1999. Correlation between Protein and mRNA Abundance in Yeast. Mol. Cell. Biol. **19:**1720-1730.

37. **Hatzimanikatis, V., and K. H. Lee.** 1999. Dynamical analysis of gene networks requires both mRNA and protein expression information. Metabolic Engineering **1:**E1-E7.

38. **Hunt, D. F., J.R. Yates III, J. Shabanowitz, S. Winton, and C.R. Hauer.** 1986. Protein sequencing by tandem mass spectrometry. Proc. Natl. Acad. Sci. **83:**6233-6237.

39. **Hutchinson, D. H., and C. W. Robinson.** 1988. Kinetics of the simultaneous batch degradation of *p*-cresol and phenol by *Pseudomonas putida*. Appl. Microbiol. Biotechnol. **29:**599-604.

40. **Jensen, O. N., M. R. Larsen, and P. Roepstorff.** 1998. Mass spectrometric identification and microcharacterization of proteins from electrophoretic gels: Strategies and applications. Proteins: Structure, Function, and Genetics **Suppl. 2:**74-89.

41. **Jensen, O. N., O. Vorm, and M. Mann.** 1996. Sequence patterns produced by incomplete enzymatic digestions or one-step Edman degradation of peptide mixtures as probes for protein database searches. Electrophoresis **17:**938-944.

42. **Jiang, Y., P.C. Wang, L. E. Locascio, and C. S. Lee.** 2001. Integrated plastic microfluidicm devices with ESI-MS for drug screening and residue analysis. Anal Chem **73:**2048-2053.

43. **Johnson, R. S., and K. A. Walsh.** 1992. Sequence analysis of peptide mixtures by automated integration of Edman and mass spectrometric data. Protein Sci. **1:**1083-1091.

44. **Karas, M., and F. Hillenkamp.** 1988. Laser desorption ionization of proteins with molecular masses exceeding 10.000 daltons. Anal. Chem. **60:**2299-301.

45. **Kellner, R.** 2000. Proteomics: Concepts and perspectives. Fresenius J. Anal. Chem. **366:**517-524.

46. **Kertesz, M. A., T. Leisinger, and A. M. Cook.** 1993. Proteins induced by sulfate limitation in *Escherichia coli*, *Pseudomonas putida*, or *Staphylococcus aureus*. J. Bacteriol. **175:**1187-1190.

47. **Klecka, G. M., and W. J. Maier.** 1988. Kinetics of microbial growth on mixtures of pentachlorophenol and chlorinated aromatic compounds. Biotech. Bioeng. **31:**328-335.

48. **Klose, J.** 1975. Protein mapping by combined isoelectric focusing and electrophoresis of mouse tissues. A novel approach to testing for induced point mutation in mammals. Humangenetik **26:**231-234.

49. **Laemmli, U. K.** 1970. Cleavage of structural proteins during the assembly of the head of bacteriophage T4. Nature **227:**680-685.

50. **Lazar, I. M., R. S. Ramsey, and J. M. Ramsey.** 2001. On-Chip Proteolytic Digestion and Analysis Using "Wrong-Way-Round" Electrospray Time-of-Flight Mass Spectrometry. Anal. Chem. **73:**1733 -1739.

51. **Lupi, C. G., T. Colangelo, and C. A. Mason.** 1995. Two-dimensional gel electrophoresis analysis of the response of *Pseudomonas putida* KT2442 to 2-chlorophenol. Appl. Environ. Microbiol. **61:**2863-2872.

52. **Mann, M., C. K. Meng, and J. B. Fenn.** 1989. Interpreting mass spectra of multiple charged ions. Anal. Chem. **61:**1702-1708.

53. **Mann, M., Lamond, A.** 1997. Cell biology and the genome projects-A concerted strategy for charterizing multiprotein complexes using mass spectrometry. Trends Cell Biol. **7:**139-142.

54. **Mann, M., and M. Wilm.** 1994. Error-tolerant database identification of peptides in sequence databses by peptide sequence tag. Anal. Chem. **66:**4390-4399.

55. **Meyer, J. S., M. D. Marcus, and H.L. Bergman.** 1984. Inhibitory interactions of aromatic organics during microbial degradation. Environ. Toxicol. Chem. **3:**583-587.

56. **Meyer, T., and B. Lambert.** 1965. Use of Coomassie brilliant blue R250 for the electrophoresis of microgram quantitiea of paratoid saliva proteins on acrylamide-gel strips. Biochim. Biophys. Acta. **107:**144-145.

57. **Morris, H. R., T.Paxton, and A. Dell.** 1996. High sensitivity collisionally activated decomposition tandem mass spectrometry on a novel quadrupole/orthogonal accerleration TOF mass spectrometer. Rapid Commun. Mass Spectrom. **10:**889-896.

58. **Murray, K. K.** 1999. Internet resources for mass spectrometry. J. Mass Spectrom. **34:**1-9.

59. **O'Farrell, P. H.** 1975. High resolution two-dimensional-electrophoresis of proteins. J. Biol. Chem. **250:**4007-4021.

60. **Okaygun, M. S., L. A. Green, and A. Akgerman.** 1992. Effects of consecutive pulsing of an inhibitory substrate on biodegradation kinetics. Environ. Sci. Technol. **26:**1746-1752.

61. **Okerberg, E., and J. B. Shear.** 2001. Attomole-level protein fingerprinting based on intrinsic peptide fluorescence. Anal. Chem. **73:**1610 -1613.

62. **Pevzner, P. A., Z. Mulyukov, V. Dancik, and C. L. Tang.** 2001. Efficiency of Database Search for Identification of Mutated and Modified Proteins via Mass Spectrometry. Genome Res **11:**290-299.

63. **Price, P.** 1991. Standard definitions of terms relating to mass spectrometry. J. Am. Soc. Mass Spectrom **2:**336-348.

64. **Qian, M. G., and D. M. Lubman.** 1996. Procedures for Tandem Mass Spectrometry on an Ion Trap Storage/Reflectron Time-of-flight Mass Spectrometer. Rapid Communications in Mass Spectrometry **10:**1911-1920.

65. **Qin, J., C.J. Herring., and X. Zhang.** 1998. De novo peptide sequencing in an ion trap mass spectrometer with O18 labeling. Rapid Commun. Mass Spectrom. **12:**209-216.

66. **Qin, J., and B. T. Chait.** 1996. Matrix-Assisted Laser Desorption Ion Trap Mass Spectrometry: Efficient Isolation and Effective Fragmentation of Peptide Ions. Anal. Chem. **68:**2108-2112.

67. **Qin, J., and B. T. Chait.** 1996. Matrix-Assisted Laser Desorption Ion Trap Mass Spectrometry: Efficient Trapping and Ejection of Ions. Anal. Chem. **68:**2102-2107.

68. **Qin, J., D. Fenyö, Y. Zhao, W. W. Hall, D. M. Chao, C. J. Wilson, R. A. Young, and B. T. Chait.** 1997. A Strategy for Rapid, High-Confidence Protein Identification. Anal. Chem. **69:**3995-4001.

69. **Qin, J., J. J. Ruud, M. Steenvoorden, and B. T. Chait.** 1996. A Practical Ion Trap Mass Spectrometer for the Analysis of Peptides by Matrix-Assisted Laser Desorption/Ionization. Anal. Chem. **68:**1784-1791.

70. **Rabilloud, T.** 1992. A comparison between low background silver diamine and silver nitrate protein stains. Electrophoresis **13:**429-439.

71. **Rabilloud, T.** 1990. Mechanisms of protein silver staining in polyacrylamide gel: a 10-year synthesis. Electrophoresis **11:**785-794.

72. **Rabilloud, T.** 1999. Silver staining of 2-D electrophoresis gels. p. 297-305. *In* A. Link (ed.), 2-D Proteome Analysis Protocol, vol. 112. Humana Press, Totowa, NJ.

73. **Reardon, K. F., D. C. Mosteller, and J. D. Rogers.** 2000. Biodegradation kinetics of benzene, toluene, and phenol as single and mixed substrates for *Pseudomonas putida* F1. Biotechnol. Bioeng. **69:**385-400.

74. **Rosenfeld, J., J. Capdevielle, J.C. Guillemot, and P. Ferrara.** 1992. In-gel digestion of proteins for internal sequence analysis after one- or two-dimensional gel electrophoresis. Anal. Biochem. **203:**173-179.

75. **Saez, P. B., and B. E. Rittmann.** 1993. Biodegradation kinetics of a mixture containing a primary substrate(phenol) and an inhibitory co-metabolite (4-chlorophenol). Biodegradation **4:**3-21.

76. **Schagger, H., and G. von Jagow.** 1987. Tricine-sodium dodecyl sulfate-polyacrylamide gel electrophoresis for the separation of proteins in the range from 1 to 100 kDa. Anal. Biochem. **166:**368-379.

77. **Schleicher, M., and D. Watterson.** 1983. Analysis of differences between Coomassie blue stain and silver stain procedures in polyacrylamide gels: conditions for the detection of calmodulin and troponin C. Anal Biochem **131:**312-317.

78. **Shevchenko, A., I. Chernuchevich, and W. Ens.** 1997. Rapid de novo peptide sequencing by a combination of nanoelectrospray. isotope labeling and a quarrupole/time-of-flight mass spectrometer. Rapid Commun. Mass Spectrom. **11:**1015-1024.

79. **Shevchenko, A., O. N. Jensen, A. V. Podtelejnikov, F. Sagliocco, M. Wilm, O. Vorm, P. Mortensen, A. Shevchenko, H. Boucherie, and M. Mann.** 1996. Linking genome and proteome by mass spectrometry: Large-scale identification of yeast proteins from two dimensional gels. PNAS **93:**14440-14445.

80. **Shevchenko, A., A. Loboda, A. Shevchenko, W. Ens, and K. G. Standing.** 2000. MALDI Quadrupole Time-of-Flight Mass Spectrometry: A Powerful Tool for Proteomic Research. Anal. Chem. **72:**2132-2141.

81. **Shevchenko, A., M. Wilm, O. Vorm, and M. Mann.** 1996. Mass spectrometric sequencing of proteins from silver-stained polyacrylamide gels. Anal Chem **68:**850-858.

82. **Shevchenko, A., S. Sunyaev, A. Loboda, A. Shevchenko, P. Bork, W. Ens, K. G. Standing.** 2001. Charting the proteomes of organisms woth unsequenced genomes by MALDI-quadrupole time-of-flight mass spectrometry and BLAST homology searching. Anal. Chem. **ASAP Web Release.**

83. **Shevchenko, A., M. Wilm, and M. Mann.** 1997. Peptide sequencing by mass spectrometry for homology searches and cloning of genes. J. Protein Chem. **16:**481-490.

84. **Sinclair, B.** 1999. MALDI-TOF goes mainstream. The Scientist **13:**18-20.

85. **Spain, J. C., G. J. Zylstra, C. K. Blake, and D. T. Gibson.** 1989. Monohydroxylation of phenol and 2,5-dichlorophenol by toluene dioxygenase in *Pseudomonas putida* F1. Appl. Environ. Microbiol. **55:**2648-2652.

86. **Steinberg, T. H., R. P. Haugland, and V. L. Singer.** 1996. Applications of SYPRO Orange and SYPRO Red Protein Gel Stains. Anal. Biochem. **239:**238-245.

87. **Steinberg, T. H., L. J. Jones, R. P. Haugland, and V. L. Singer.** 1996. SYPRO Orange and SYPRO Red Protein Gel Stains: One-Step Fluorescent Staining of Denaturing Gels for Detection of Nanogram Levels of Protein. Anal. Biochem. **239:**223-237.

88. **Switzer, R., C. Merril, and S. Shifrin.** 1979. A highly sensitive silver stain for detecting proteins and peptides in polyacrylamide gels. Anal. Biohem. **98:**231-237.

89. **van Oostveen, I., A. Ducret, and R. Abersold.** 1997. Collidal silver staining of electroblotted proteins for high sensitivity peptide mapping by liquid chromatography-electrospray ionization tandem mass spectrometry. Anal Biochem **247**.

90. **Verhaert, P., S. Uttenweiler-Joseph, M. d. Vries, A. Loboda, W. R. Ens, and K. G. Standing.** 2001. Matrix-assisted laser desorption/ionization quadrupole Time-of-Flight Mass Spectrometry: An elegant tool for peptidomics. Proteomics **1:**118-131.

91. **Westermeier, R.** 1997. Electrophoresis in practice. 2nd ed. VCH-Verlag. Weinheim.

92. **Wilkinson.** 2000. Pursuing proteomes. The Scientist **14:**28-30.

93. **Williams, K., U. Hellman, R. Kobayashi, W. Lane, S. Mische, and D. Speicher.** 1997. Internal protein sequencing of SDS PAGE-separated proteins: A collaborative ABRF study. p. 99-109. Techniques in Protein Chemistry. vol. VIII. The Association of Biomolecular Resource Facilities. ABRF. Academic Press.

94. **Willkins, M. R., J.C.. Sanchez, A.A. Gooley, R.D. Appel, I. Humphery-Smith.** 1995. Thinking big proteome studies in a post-genome era. Biotechnol. Gene. Eng. Rev. **13:**19-50.

95. **Wilm, M., A. Shevchenko, T, Houthaeve, S. Breit, L. Schweigerer, T. Fotsis, and M. Mann.** 1996. Femtomole sequencing of proteins from polyacrylamide gels by nano-electrospray mass spectrometry. Nature **379:**466-469.

96. **Wilm, M., G. Neubauer, and M. Mann.** 1996. Parent Ion Scans of Unseparated Peptide Mixtures. Anal. Chem. **68:**527-533.

97. **Wilson, J. F.** 2001. New technology spurs on proteomics. The Scientist **15:**12-13.

98. **Wirth, P., and A. Romano.** 1995. Staining methods in gel elctrophoresis. including the use of multiple detection methods. J. Chromatogr. **698:**123-143.

99. **Yates, I., J. R., J.K. Eng, A.L. McCormack, D. Schieltz.** 1995. A method to correlate tandem mass spectra of modified peptides to amino acid sequences in the protein database. Anal. Chem. **67:**1426-1436.

100. **Yates, J., S. Speicher, P. R. Griffin, and T. Hunkapiller.** 1993. Peptide mass maps: A highly informative approach to protein identification. Analytical Biochemistry **214:**397-408.

101. **Yates, J. R. I.** 1998. Mass spectrometry and the age of the proteome. **33:**1-19.

102. **Yeh, W. K., D. T. Gibson, and T. N. Liu.** 1977. Toluene dioxygenase: A multicomponent enzyme system. Biochem. Biophy. Res. Comm. **78:**401-410.

103. **Zhang, B., F. Foret, and B.L. Karger.** 2001. High-throughput microfabricated CE/ESI-MS: automated sampling from microwell plate. Anal Chem **EST 6.5**.

104. **Zylstra, G. J., L. P. Wackett, and D. T. Gibson.** 1989. Trichloroethylene degradation by *Escherichia coli* containing the cloned *Pseudomonas putida* F1 toluene dioxygenase genes. Appl. Environ. Microbiol. **55:**3162-3166.

CHAPTER III MATERIALS AND METHODS

III.1 Chemicals, Microorganism and Media

All chemicals used for the studies were purchased from various sources, but the grade of them was the highest purity or HPLC compatible unless noted.

Pseudomonas putida F1 (*P. putida* F1 or PpF1) was used for all studies and was obtained from Dr. David Gibson at the University of Iowa, USA. *Pseudomonas putida* F1 was maintained two different methods. For longer than an year of storage, cells were lyophilized and kept in a –80 °C freezer. For less than a few months of storage, cells were frozen and kept in a –20 °C until used.

Two different growth media for cultivation of PpF1 were used during the studies. For the proteomic analysis, *P. putida* F1 was cultivated in Mineral Salt Base (MSB) with toluene or phenol as the carbon source (10). Modified PIPES (11) medium was used to study the effects of heavy metals on each substrate because MSB contains metal chelating chemicals and it could artificially change the availability of amended metals to *P. putida* F1. The pH for both media was adjusted to the same value (6.8) by concentrated HCl for MSB or by concentrated KCl for PIPES medium. The ingredients of each medium are introduced in Table III-1 and Table III-2, respectively. Since no metal chelating reagent was included in PIPES medium, the trace metal solutions should be carefully added after addition of all salt solutions to water. Once salt solutions were mixed in 600 ml of

NanoPure water. the trace metals were slowly added into the 600 ml of NanoPure water and salt on a stirring plate. The PIPES medium solution should be kept with no color or visible particles in it. The pH of PIPES medium was adjusted by slowly adding 0.5 M KCl. The medium was continuously stirred during the whole medium preparation process.

Table III-1 Mineral Salt Base Medium (10)

Solution A	
Chemical	Mass, g/L
Na_2HPO_4	141.2
KH_2PO_4	136
Solution B	
Chemical	Mass, g/L
Nitrilotriacetic acid	10
$MgSO_4$	14.45
$CaCl_2\ 2H_2O$	3.33
$(NH_4)6Mo_7O_{24}\ 4H_2O$	9.25
$FeSO_4 \cdot 7H_2O$	0.099
Metals 44	50 mL
Solution C	
Chemical	Mass, g/L
$(NH_4)_2SO_4$	200 g

Composition of MSB
Soln A:B:C = 40:20:5 mL/L

Table III-2 Modified PIPES Medium

Chemical	Mass, g/L
PIPES ($C_8H_{16}N_2O_6S_2Na_2$)	17.315
NaCl	4.68
KCl	1.49
NH_4Cl	1.07
Na_2SO_4	0.43
$MgCl_2\ 6H_2O$	0.2
$CaCl_2\ 2H_2O$	0.03
$Na_2HPO_4\ 7H_2O$	0.172
$FeSO_4\ 12H_2O$	0.005

III.2 Analytical Methods

III.2.1 CELL CONCENTRATION

The concentration of *P. putida* F1 in bioreactors was determined by spectrophotometry (DU640, Beckman). The linearity of the calibration curve for MSB and PIPES media between optical density at 600 nm and the actual cell dry mass was examined and shown in Figure III-1. The cells were harvested from a bioreactor at the middle of exponential growth and the dry cell weight (DCW) was determined by measuring the actual dry weight of cells after drying the harvested cells in a drying oven. The harvested cells were differentially diluted with the corresponding medium and measured their dry weights.

Since the cell concentration growing in PIPES medium was lower than in MSB, no dilution was necessary to measure the cell concentration in PIPES medium.

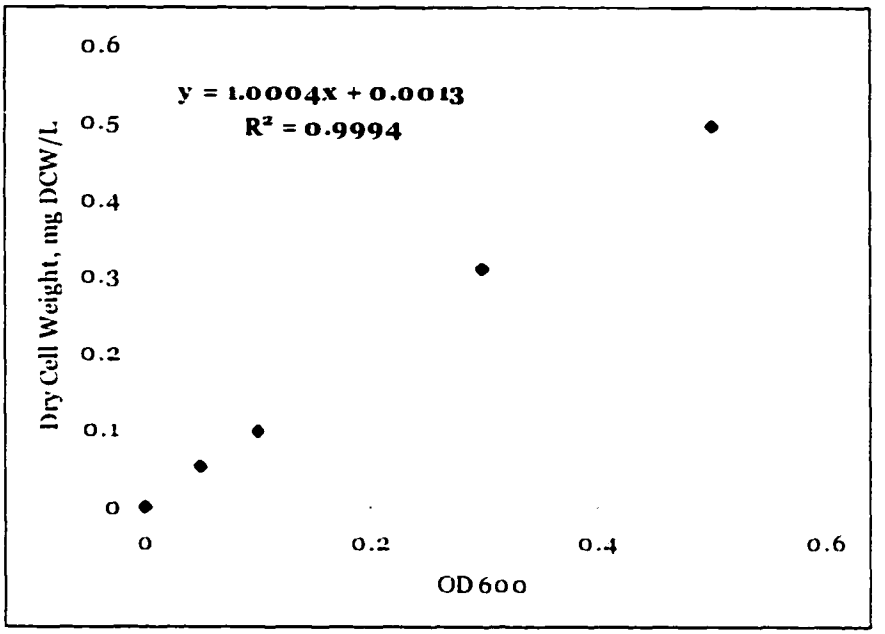

A

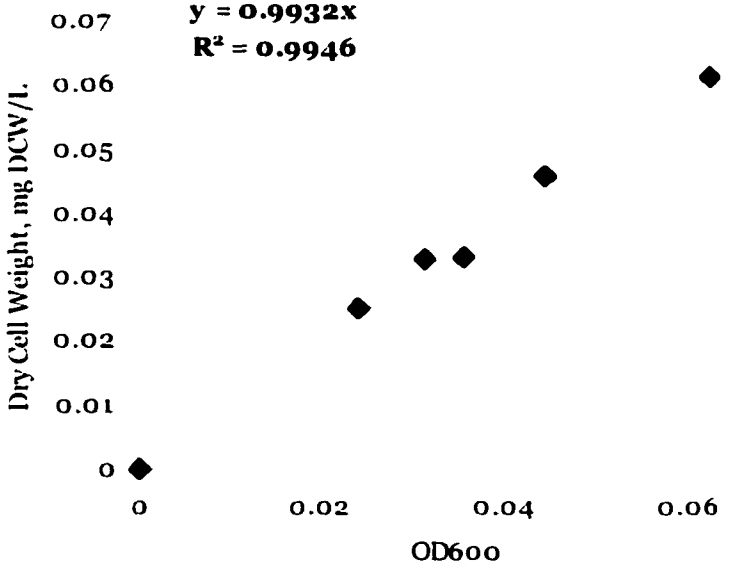

B

Figure III-1 A calibration curve for optical density (OD_{600}) and mg dry cell weight per liter (mg DCW/L) for MSB (A) and PIPES (1) medium.

III.2.2 SUBSTRATE CONCENTRATION

Toluene, phenol, and their mixtures were utilized for the growth of *P. putida* F1 as the sole carbon and energy source for all studies in this dissertation.

III.2.2.1 Standards

To translate the integrated peak areas from a gas chromatography-mass spectroscopy (GC-MS) into the concentration of substrates, toluene or phenol standards were used. Highly concentrated solutions of toluene and phenol in methanol were used as the aqueous standards. These solutions were then diluted to the desired concentrations with either MSB or PIPES medium.

The toluene or phenol standards (Sigma) were prepared from commercially available aqueous standards, and their concentration was in range from 5 to 1000 μM. For the chloroform extraction method, 750 μl of each concentration of standard, diluted with the corresponding medium, was mixed with the same volume of chloroform in a clean GC vial. Then, it was vigorously mixed for 15 min on a vortexer (Genie II, Fisher) where held maximum 30 vials. The organic (bottom) phase was transferred to a new GC vial, and 5 μl of 10 mM *p*-xylene (internal standard) was added. Then the vial was capped, and placed in the autosampler.

Standards were examined before actual samples were measured and the standards were run after every 20 unknown samples. In this way, the minimum variability of GC-MS measurements between batches could be ensured.

III.2.2.2 Procedure

The concentration of toluene was only measured in the aqueous phase. Reardon, *et al* (14) experimentally proved that mass limitation was negligible for toluene when the initial substrate concentration was 0.5 mM and the impeller rotation was 500 rpm. With the initial concentration of toluene (0.42 mM) and 200 rpm of impeller rotation, the equilibrium of toluene between aqueous and gaseous phase was assumed.

To minimize the loss of toluene during the sampling process from a bioreactor, the liquid extraction process was begun as quickly as possible right after a sample was taken from a bioreactor. Toluene was immediately extracted from aqueous phase by mixing with the same volume of chloroform as aqueous sample, 750 μl, in a GC vial. Then an extraction solution in a GC vial was mounted on a vortexer, and vigorously mixed for at least 15 min at room temperature. The organic phase was separated, and transferred to a new GC vials. Before capping with a crimper, 5 μl of 10 mM *p*-xylene was added in each vial as an internal standard. Phenol was extracted and prepared for GC-MS analysis in the same way as toluene.

To detect and measure the concentration of toluene and phenol, gas chromatography-mass spectrometric detection (GC-MS) method was used. The crimped vials were placed onto the Hewlett-Packard model 7673 autosampler tray. The chloroform layer was removed and analyzed using an HP 5890 II gas chromatography equipped with a mass selective detector (HP 5971A). Compounds were separated on a 50 m, 0.2 mm HP-5 column. High purity helium flowed through the column at 1.9 ml/min at 45 psi (14). "KHKIM.m" method file for both toluene and phenol analysis was used to store and execute the detailed separation profile.

III.2.3 PROTEIN QUANTIFICATION

Handling with proteins needs great care and caution, because there are proteolytic enzymes and many other proteins on human hands. These proteins can easily contaminate the samples and lead to significant misinterpretation in proteomic analysis. One should always wear gloves in handling protein samples.

III.2.3.1 Chemicals

Several different methods for protein quantification are available, but BCA methods from Pierce were used for all studies. Two different methods can be used with the BCA protein assay kits from Pierce: Protein Assay and Microprotein Assay. The Microprotein assay method was used here. This assay can detect as low as 1 μg. It is consisted of three different solutions, which are Solution A, Solution B, and Solution C. To make 10

ml of working solution. 5 ml of Solution A. 4.8 ml of Solution B. and 0.2 ml of Solution C were mixed well in clean glassware. Water bath should be turn on and set at 60 °C during the preparation of working solution.

III.2.3.2 Standard

To translate the absorbance value at 522 nm into the concentration of protein in a liquid sample. a known concentration of standard protein. bovine serum albumin (BSA). was used. The concentration of commercially available BSA (Pierce) was 2 μg/μl. It was diluted with MSB or PIPES to the range of target protein concentration. and BSA was prepared 0 to 10 μg per 2 ml of total solution that was consisted of 1 ml working solution and 1 ml of corresponding medium. Standard proteins were heated in a 60 °C water bath along with the samples. An example of a standard curve is presented in Figure III-2. To ensure more conversions. a standard curve should be made fresh in every time.

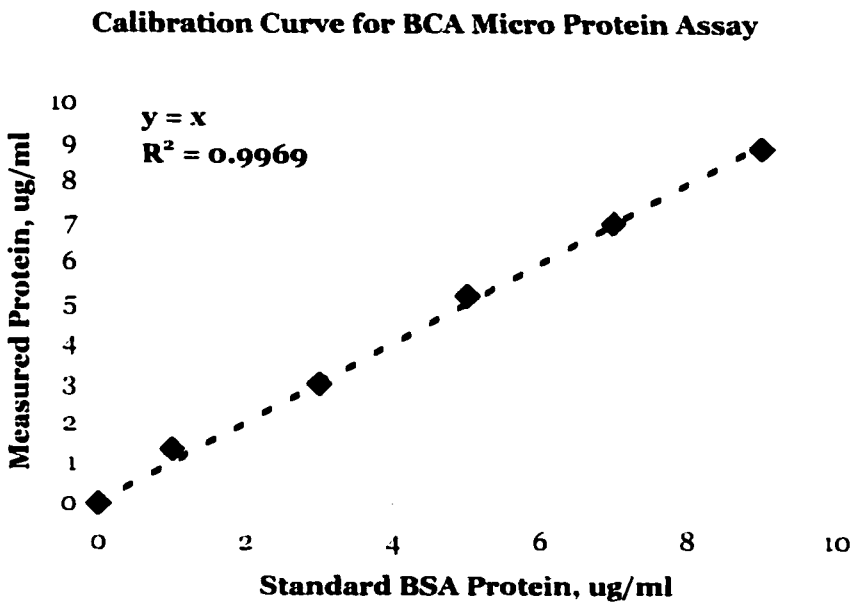

Figure III-2 An example standard curve between known concentration of standard proteins and their optical density values at 522 nm for microassay method of BCA from Pierce.

III.2.3.3 Assay

Since the working solution is two times concentrated (2x), it should be diluted with an equal volume (1 ml) of an appropriate medium. The final volume of a working solution per unknown sample was 2 ml. In addition, the protein samples were always highly concentrated, so it was necessary to dilute them to appropriate concentration (less than 10 μg/μl). All dilutions were performed with either MSB or PIPES, and 10 μl of diluted protein samples were added into the final working solution. The BSA standard and protein samples were placed in a 60 °C water bath for 1.0 h. The color of the working solutions including the protein sample turn violet and the intensity of color is

proportional to the concentration of protein. After heating, the working solution was cooled to room temperature, transferred to a spectrophotometer (DU640, Beckman), and their absorbances were measured at 522 nm by the pre-programmed method file, KH_BCA. The standard curve was prepared first with zero-intercept regression and then the protein samples were measured.

III.2.3.4 Storage

After finishing the protein assay, protein samples were appropriately labeled and stored until used. The storage method was determined by the duration of storage. For a few weeks of storage, protein samples were frozen at –20 °C. For storage up to a year, all protein samples were frozen at -80°C. For storage longer than a year, the protein samples were lyophilized and stored at –80 °C.

III.2.4 METAL DETECTION

III.2.4.1 Inductively Coupled Plasma Mass Spectrometry

Samples were diluted with NonoPure water to approximately 1.0 ppm of cadmium or chromium because all heavy metals were initially amended at known concentration and metal detection equipment was calibrated with two points of standard metal concentrations (0 and 2.0 ppm). Diluted samples were loaded on the autosampler of inductively coupled plasma mass spectrometer (ICP-MS, IRIS, Thermo Jarrell Ash).

Samples were analyzed with a method file name "KHKIM", and a standard curve file name "K_Cd_Cr". A two- point standard was used by the ICP-MS calibration and a 5-point standard curve for Cd and Cr was separately prepared to evaluate the performance of the ICP-MS (Figure III-3). Quality control (QC) was performed by analyzing a known concentration, which was 2.0 ppm Cd and Cr, after 20 samples. Most measured concentrations of samples were ranged between 10 and 1500 ppb.

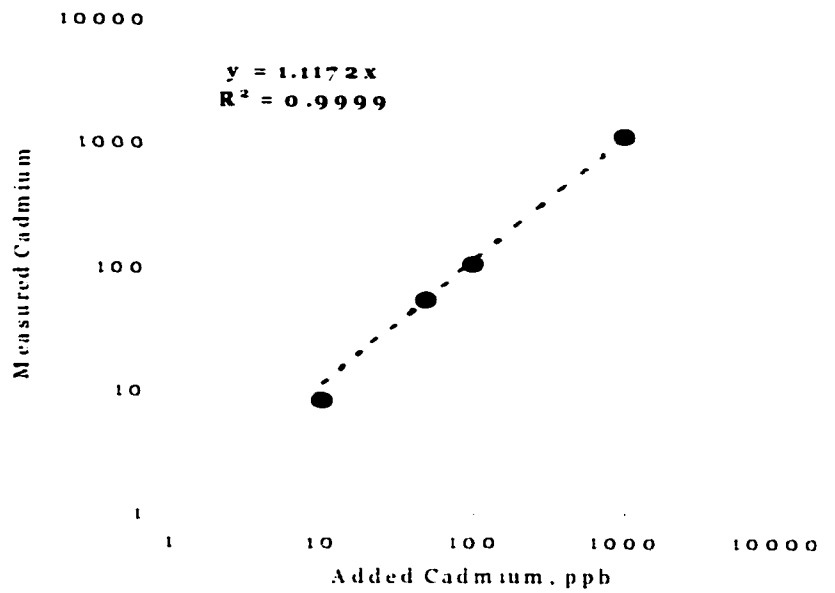

(A)

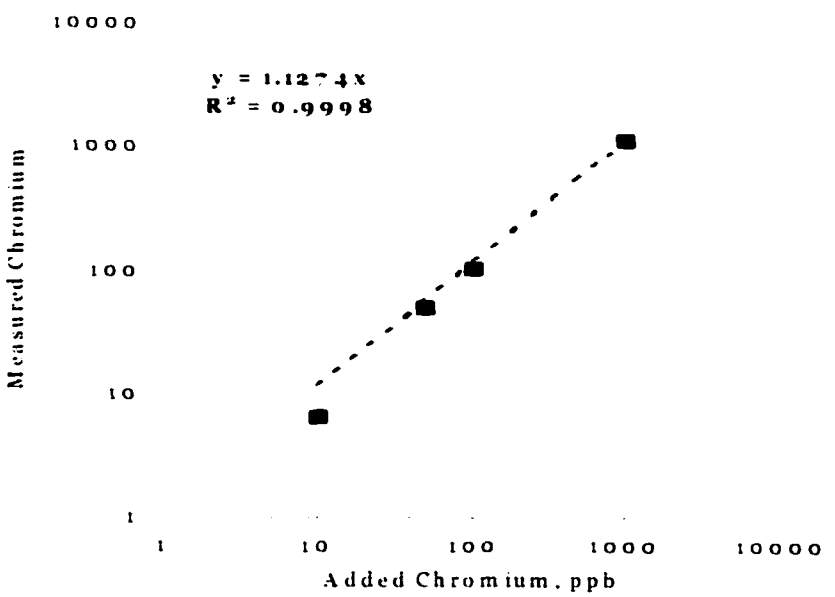

(B)

Figure III-3 Calibration curves for metals in ICP. The slopes of the lines for both cadmium (A) and chromium (1) are approximately equal to 1.

III.3 Batch Cultivations

The same conditions were need for the growth of PpF1 for both proteome analysis and the study of heavy metal effects.

III.3.1 Preparation for Inocula

Frozen *P. putida* F1 was thawed slowly in cold water and used for Petri dish cultures. Petri dishes were prepared with autoclaved Tryptic Soy Broth (TSB) and Bacto Agar medium. TSB Agar medium included 15 g/L of Tryptic Soy Broth, 15 g/L of Bacto Agar, and either MSB or PIPES medium. *P. putida* F1 on TSB agar were incubated at 30 °C for 24 h in the presence of toluene or phenol as an inducer. Toluene was introduced in the gas phase. Phenol, 0.5 mM, was included in TSB medium. A colony on a Petri dish was picked and transferred to 5 ml TSB medium in a test tube. The inoculated test tube was incubated in a shaking incubator at 30 °C with 200 rpm for at least 16 h. Once OD_{600} of the cells in a test-tube culture reached 1.5, inocula were ready to be inoculated.

III.3.2 Substrate Addition

Because of the volatility of toluene and phenol under autoclaving conditions (121 °C for 45 min), all substrates were added after autoclaving. A sterilized syringe was used to inject toluene into a reactor under the laminar hood. The concentration of toluene

substrate was 0.42 mM and 0.23 mM for single and mixed substrate growth of PpF1, respectively. Phenol was separately dissolved in sterilized water and injected into a bioreactor under the laminar hood. The concentration of phenol for single and mixed substrate batch cultivation of PpF1 was 0.5 and 0.25 mM, respectively. To ensure the equilibrium of the volatile substrate between liquid and gas phase, the bioreactor was stirred for 8 h before inoculation with cells.

III.3.3 INOCULATION

The working volume of either MSB or PIPES for a bioreactor was 1.0 L, and the size of *P. putida* F1 inoculum was 1.0 dry cell weight (DCW) mg/L. Each inoculation was prepared independently for a bioreactor to ensure random inoculation and injected into a bioreactor under the laminar hood.

III.3.4 SAMPLING

Each sample (2.0 ml) was taken from through a sampling tube through head plate to about 1 cm from the bottom of a batch reactor. Samples were divided into two parts. One part (1.0 ml) was filtered by a 0.2 μm syringe filter and used as a blank for optical density measurement at 600 nm and used to measure the concentration of substrates (toluene and/or phenol). Another part (1.0 ml) without filtration was used to measure the

concentration of cells. With respect to the cell growth patterns on different substrates. the frequency of sampling was decided differently. In general. one sample an hour was taken during the growth of PpF1 on toluene regardless of the medium (MSB or PIPES). For growth of the cells on phenol. one sample per two hours was taken during exponential growth phase. In all cases. the first sample was taken within10 min after inoculation and was considered as time-zero sample. Sampling frequency during the mixture growth experiments was hourly.

For the phospholipid fatty acid analysis. one sample per cultivation was taken from the middle of exponential phase of PpF1 growth on toluene or phenol. Three samples were taken from the toluene-phenol mixed growth. one sample from in the beginning. middle. and nearly end of exponential growth phase. Cells were separated from the medium by centrifuge at 8.000 × g (GS-3. Superspeed Centrifuge. Sorvall RC-5B) for 40 min. Precipitated cells were washed twice with 50 mM Tris-HCl. pH 7.0. and then freeze dried by a lyophilizer for 24 hours. Dried cells were stored in −20 °C until analyzed.

III.3.5 TOLUENE SPIKE EXPERIMENTS

A batch reactor was used for the study. The working volume was 1.0 L of MSB (pH 6.8) and a batch reactor was stirred at 200 rpm. To prevent the loss of volatile substrates. the batch reactor was operated in closed system and maintained the temperature of the MSB medium at 30 °C. The head space (1.0 L) of the bioreactor was reserved to provide

oxygen for the growth of aerobic cell (*P. putida* F1). A bioreactor was inoculated with 1.0 mg of PpF1 in 0.25 mM phenol. When the growth of PpF1 reached the beginning of exponential stage, 0.25 mM of toluene was spiked. The samples were taken from a reactor to monitor optical density and substrate concentration with the same as described in III.4.4. PLFA samples were taken immediately before the toluene spike from the middle of toluene degradation, and from the end of phenol degradation. PLFA samples were prepared as described in III.4.4.

III.3.6 EFFECTS OF HEAVY METALS

The same conditions for the preparation of inoculum, substrate addition and all other conditions as proteome study were applied for the study of heavy metal effects.

III.3.6.1 Metal Addition

Two different heavy metals were used, $CdCl_2$ and CrO_3. To avoid the precipitation of heavy metals by autoclaving condition (121 °C for 45 min), heavy metals were added into a medium after autoclave and cool-down. Concentrated metal salt stock solutions (100 mM) of $CdCl_2$ and CrO_3 were prepared with autoclaved Nanopure H_2O. Ten parts per million (ppm) of $CdCl_2$ was added to a bioreactor with 0.42 mM toluene or 0.5 mM phenol for the growth of PpF1 on single substrates or 0.25 mM Toluene and Phenol for mixed substrate experiments.

III.3.6.2 Sampling

The same frequency of sampling as described in III.4.4 was carried out. However, each sample was divided into three parts. The first and second parts were used to measure the optical density at 600 nm for biomass concentration and to monitor toluene and/or phenol concentration. The last part of each sample was used to measure the concentration of soluble metal ions by ICP-MS.

For PLFA analysis, one sample was taken from the middle of the exponential growth phase of each cultivation. Cells were prepared by the same method as described in III.4.4.

III.4 Serum Bottle Cultivation

To examine the tolerance of *P. putida* F1 in the presence of cadmium and chromium, serum bottle cultivation was used with various concentrations of heavy metals. The total volume of a serum bottle was 65 ml and the working volume was 20 ml. Toluene and/or phenol was used as sole energy and carbon source, and modified PIPES medium was used (Table III-2). During the cultivation, each serum bottle was sealed from environment and the air in the headspace provided oxygen for the growth of *P. putida* F1. The concentration of substrates was 0.5 mM phenol or 0.42 mM toluene for single substrate experiments and 0.22 mM of toluene and phenol for mixed substrate cultivation. Cadmium was added at 0, 10, 20, 30, and 50 ppm in 20 ml of PIPES, and chromate (VI) was added at 0, 0.2, 0.5, 1.0, 5, 10, and 20 ppm in 20 ml of medium.

Cell concentration was measured as colony forming units (CFU) per milliliter of growth medium in the presence of various concentrations of cadmium or chromate (VI). Each metal/organic combination was duplicated and the results were obtained by the average value of two CFU/ml values. Every day, 50 µl of medium was taken from each serum bottle, diluted properly with sterilized PIPES medium, and spread by a glass spreader on a sterilized TSB agar plate. This TSB agar medium did not contain heavy metals. After 24 hours of culture in a 30 °C fixed incubator, the colonies on a plate were counted under an illuminated magnifier. The period of culture was 7 days.

To monitor the heavy metal concentration from each serum bottle, 1.0 ml of culture medium was removed and filtered with a 0.2 µm syringe filter. The filtrates were properly labeled and stored at room temperature until measured. The concentration of metals was detected and quantified by Ion-Coupled Plasma Spectrophotometer described in analytical methods section.

III.5 Transmission Electron microscopy

All samples for transmission electron microscopy (TEM) were harvested in the beginning of the stationary phase of PpF1 cultivation. The cultivations that were sampled are presented in Table III-3.

Table III-3 Sample designation for transmission electron microscopic investigation. Toluene: 0.42 mM. Phenol: 0.5 mM. Cadmium: 10 ppm. Chromium: 1.0 ppm. Each sample had different growth period.

Description	Toluene	Phenol	Cadmium	Chromate (VI)	Growth Period, h*
Control	+	-	-	-	15
Tol + Cd	+	-	+	-	30
Tol + Cr	+	-	-	+	96**
Phe + Cd	-	+	+	-	60

* Batch bioreactor cultivation.
** Serum bottle cultivation

Cultivation broth was centrifuged at 10,400 x g for 30 min. For thin sectioning the cell pellets were gently washed twice in 0.1 M cacodylate buffer (pH 6.8) and resuspended in a fixative solution (2% glutaraldehyde in 0.1 M cacodylate). Samples were sitting overnight at 40 °C, then dehydrated in an ethanol series and embedded in Spurr resin. Sectioning was carried out with Potter Blum MT1 ultramicrotome at 150 nm thick. Slices were stained with lead citrate and uranyl acetate followed by mounted on formular coated copper grid. Preparations were examined with a JEOL 2000 EX electron microscope. Electron Density Scanning (EDS) was acquired by Kevex 8000 at 60 kV for 300 sec per spectrum.

III.6 Proteome Analysis

III.6.1 Cell Harvest and Disruption

To analyze the proteome over the growth of *P. putida* F1 on toluene or/and phenol, *P. putida* F1 cells were harvested and analyzed by 2-D PAGE. The complete growth profiles of *P. putida* F1 on each single substrate and toluene-phenol mixtures were first obtained without cell harvesting. Based on these growth profiles, *P. putida* F1 was harvested in a subsequent experiment from the middle of exponential growth phase for single substrate growth. Four different cell-sampling events were carried out for the growth of *P. putida* F1 on toluene-phenol mixtures. In order to ensure the consistent growth of *P. putida* F1 without any effect of culture volume, four independent batches of *P. putida* F1 growth on toluene-phenol mixtures were conducted to harvest from four different growth points.

Cells were separated by centrifugation at 10,400 × g for 40 min (4 °C). The cell pellet was washed, centrifuged twice, and resuspended with sonication buffer (50 mM Tris-HCl, pH 7.2, 10% glycerol). Cells were dispensed and transferred into cryogenic tubes, and stored at -70 °C until use. Each 1 mL of cell suspension was sonicated (SONICATOR XL, Heat Systems) using a microtip at full power for 10 min (2 seconds on/2 seconds off) in an ice-water bath. The cell debris and membrane was removed by ultracentrifuge (L7 Ultracentrifuge, Rotor Type 70Ti, Beckman) at 220,000 × g at 4 °C for 60 min.

III.6.2 PROTEIN EXTRACTION, CONCENTRATION, AND WASHING

Since no detergent was used to extract proteins from *P. putida* F1 and cell membranes were discarded after ultracentrifugation (100.000 x g for 1 h at 4 °C), the supernatant protein solution was considered as soluble proteins. It is possible for this soluble protein sample to include some membrane bound proteins, but I assume the proportion of them is negligible. The protein solution was further concentrated with a centrifugal concentrator (10 kD cut-off size, Microsep, Pall Filtron), and washed several times with low salt buffer (10 mM Tris-HCl, pH 7.2) until the total concentration of buffer salt reached lower than 10 mM by adding twice volume of fresh low salt buffer and the final protein concentration reached 6 ~ 8 μg/μl. Prior to 2-D PAGE analysis, protein concentrations were determined by the bicinchoninic acid (BCA) micro-assay method (Pierce), following the instructions provided as described in III.3.3. After determination of the protein concentration, the protein solution was stored at –20 °C for a short period of storage or –80 °C for long-term storage until used.

III.6.3 TWO-DIMENSIONAL POLYACRYLAMIDE GEL ELECTROPHORESIS

Proteins were separated by the method of O'Farrell (12)with minor modifications. All chemicals used for 2-D PAGE analysis were of electrophoresis grade from Sigma or Bio-

Rad unless otherwise noted. To avoid contamination during both IEF and SDS-PAGE processes, gloves were worn all the time.

III.6.3.1 Isoelectricfocusing, IEF

III.6.3.1.1 Protein Solubilization

For analytical gels, twelve micrograms of proteins from each sample were mixed with 130-µL isoelectric focusing (IEF) sample buffer. For a preparative gel, 300 to 400 micrograms of protein were mixed with 250-µL of IEF buffer for a 13-cm long IPG strip. IEF sample buffer contained 9.5 M urea, 4% (wt/v) 3-[(3-cholamidopropyl) dimethyl-ammonio]-1-propanesulfonate (CHAPS), 5% (v/v) pH 4-7 and 0.5% (v/v) pH 3-10 Phymalytes (Amersham-Pharmacia Biotech), 5% (v/v) ß-mercaptoethanol, and 0.005% bromophenol blue in deionized water (NANOpure system with ultrafilter, Barnsted Model D4751). The resulting mixtures were placed on a rotating wheel overnight at room temperature to obtain extensive solubilization. Through all the protein solubilization process, no heating step was included at all and all processes were carried out at less than 25 °C (room temperature).

III.6.3.1.2 Preparation of Immobilized pH Gradient Strips and Protein Loading

For the first-dimension isoelectric focusing (IEF), 7-cm long immobilized pH gradient (IPG) gels (pH 4 to 7, Amersham-Pharmacia) for analytical size separation and 13-cm

long IPG gels (pH 4 to 7) for preparative size gels were used. IPG strips were rehydrated for at least 10 h at room temperature with IEF sample buffer/protein mixtures in a rehydration tray from Amersham-Pharmacia Biotech.

III.6.3.1.3 Running Conditions

To avoid re-crystallization of urea during the IEF process for both sizes of IPG strips, the temperature of cooling bed was maintained at 20 °C. Once IEF was finished, all IPG strips were separately wrapped in clean and sterilized aluminum foil. Each wrapped IPG strips was stored –20 °C until used.

III.6.3.1.3.1 Analytical Gel

IEF was performed with the Multiphor electrophoresis unit (Amersham-Pharmacia) using a voltage program that first increased linearly from 0 to 300 V for 0.01 h and then maintained 300 V for 4.5 h for pre-focusing of proteins. After this, the voltage increased linearly from 300 to 2000 V over 5.0 h, and remained at 2000 V for 6.5 h. Focusing was conducted for a total of 20100 V·h.

III.6.3.1.3.2 Preparative Gel

Since protein loading on a 13-cm long IPG strip was much higher than that on 7-cm IPG strips, the separation conditions were different from that of analytical gel. Preparative gel

separation was carried out by the step-increase voltage method. The voltage was initially applied at 35 V for 12 hours. 500 V for 1 hour. 1000 V for 1 hour. 2000 V for 1 hour. and finally increased to 3500 V for 19 hours.

III.6.3.2 SDS-PAGE

SDS-PAGE was performed in 12% slab gels for both sizes of IPG strips.

III.6.3.2.1 Pre-Equilibrium of IPG Strips

After IEF separation was completed. the IPG gel was subsequently exposed for 10 min to 3 ml of equilibration solution containing 62.5 mM Tris HCl (pH 6.8). 2.3% (w/v) sodium dodecylsulface (SDS). 5.0% (v/v) β-mercaptoethanol. 10% (v/v) glycerin. and 0.005% (v/v) bromophenol blue solution.

III.6.3.2.2 Running Condition

For the second-dimension analysis (SDS-PAGE). the equilibrated strip was placed on the top of a 12% slab gel (70 × 90 × 1.0 mm) for an analytical gel and of a 12% slab gel (160 × 200 × 1.0 mm) for a preparative size gel. and embedded in 0.5% agarose preheated to 70°C. SDS-PAGE was carried out in a Mini-PROTEAN II cell (2) with 8 mA constant current for an analytical gel until the bromophenol blue dye reached 5 mm from the

bottom of the gel. Electrophoresis for a preparative gel was conducted at a constant current of 20 mA per gel in a PROTEAN II xi cell (2).

III.6.3.3 Protein Detection

Protein detection was performed by several different methods to obtain the maximum detection level for each size of SDS-PAGE gels. The analytical gel was stained by a silver nitrate kit (SilverXpress, NOVEX) using the instructions provided. Proteins on preparative gels were visualized by either Coomassie Blue R-250 (CBR) from Bio-Rad or SYPRO Ruby reagent (Molecular Probes).

CBR staining was performed as follows: a gel was removed from a gel casting in PROTEAN xi II. Then the gel was transferred and soaked in 1% CBR stock solution for 2 hours and placed on a rocking shaker at room temperature. CBR stock solution contained 1% (w/v) CBR, 40% methanol (v/v), 10% (v/v) acetic acid, and NanoPure (NP) water. After this staining process, CBR solution was slowly drained and the gel was washed twice by adequate amount of NP water. For destaining background, the gel was soaked again in a Destaining Solution I, compose of 40% methanol (v/v), 10% (v/v) acetic acid, and NanoPure (NP) water. This solution was replaced with enough volume of fresh solution to cover the gel several times. Destaining Solution I was replaced by Destaining Solution II after the background blue color in the gel disappeared. The whole destaining process was conducted on the rocking shaker and it lasted about 10 hours.

For SYPRO Ruby staining, a gel was rinsed twice with 40% methanol (v/v), 10% (v/v) acetic acid, and NanoPure (NP) water for 30 min each before SYPRO Ruby stock solution was added. SYPRO Ruby stock solution was added without dilution and it was good for about 10 uses for the preparative size gels. SYPRO Ruby solution was added on to cover the whole gel surface. A gel was stained with gentle agitation either for 3 hours for maximal sensitivity or it could be left in the stain solution overnight (16-18 hours) without overstaining. The gel was rinsed in 10% methanol, 7% acetic acid for 30 to 60 min to decrease background fluorescence. Protein spots on the SYPRO Ruby stained gel were viewed on a UV transilluminator (Fisher) that has two excitation peaks of 300 nm and 480 nm, and an emission maxima was centered at 618 nm.

III.6.3.4 Storage of 2-DE Gels

Two different methods were used for storage of a gel. For a short-term storage, the gel was safely stored in NP water for several months without losing any staining. However, when it was necessary to store a gel for longer than a few months, the gel was dried in a gel dryer. The gels were dried by a homemade drying kit and drying film (NOVEX).

Before the gel was applied between two sheets of drying films, it was soaked in drying solution (10% (v/v) glycerol and NP water) and gently agitated for 2 h. Two sheets of drying film were soaked in the drying solution until all wrinkles in the film were

disappeared. A soaked drying film was placed on a drying frame, covered with the SDS-PAGE gel, and then the second soaked drying film was placed on top of the gel surface carefully and slowly. All air bubbles between the gel and soaked drying film were removed before the clamps were applied so that air bubbles did not break the gel during the air-drying process. To remove air bubbles, a clean glass test tube was gently and slowly rolled over the surface of the upper film. Once all air bubbles were removed and another drying frame was placed on top of the gel sandwich, each side of a frame set was clamped with two strong clamps. The drying frame was placed on a bench under room temperature for 24 hours. A completely dried gel could be stored for many years without any distortion of its image.

III.6.3.5 Image Acquisition and Analysis

Air-dried gels were scanned with a Scanview 3000 (Umax) to acquire digital images, and the spot pattern was analyzed using Phoretix 2D (Total Lab) software.

III.7 Protein Identifications

III.7.1 N-TERMINAL SEQUENCING

III.7.1.1 External Sequencing

The electrotransfer method was conducted by the Burnette (4) and Bolt (3). The Mini Trans-Blot modules from Bio-Rad were used to perform the electrotransfer (Figure III-4), and a detail schematic diagram for the preparation of the module is shown in Figure III-5.

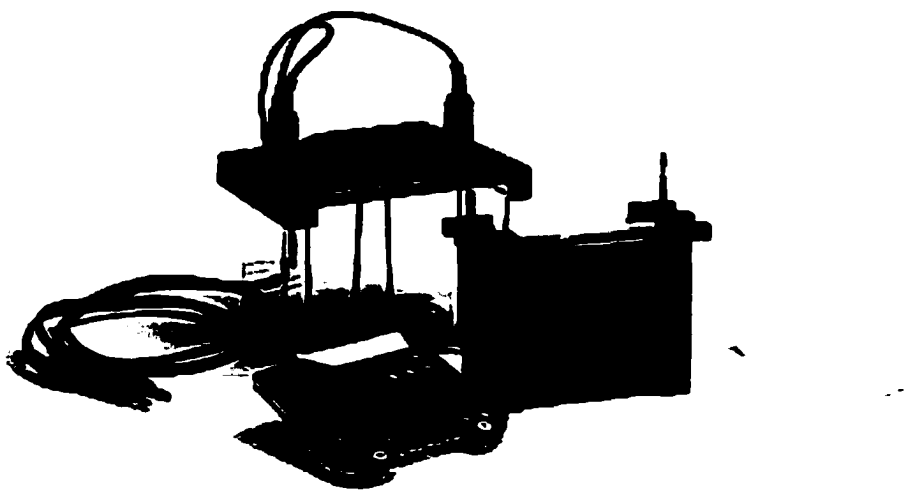

Figure III-4 The Mini Trans-Blot module. It consisted of a buffer tank, two gel holder cassettes, 4 fiber pads, electrode assembly, a cooling unit, and a lid with cable.

While the proteins were being separated via SDS-PAGE, the Trans-Blot module was prepared for operation. Six pieces of Whatman filter papers were cut and soaked in one liter of the transfer buffer, composed of 39 mM glycine, 48 mM Tris base (pH 8.3), 0.037% (v/v) SDS, and 20% (v/v) methanol. A piece of hydrophillic polyvinylidene

fluoride (PVDF) membrane from Bio-Rad was also soaked in the transfer buffer for 1 h. The size of both filter paper and PVDF membrane was equal to the size of the slab gel and it was important to wear gloves for module preparation. Oils and secretions from the skin could prevent the transfer of proteins from the gel to the PVDF membrane. The porous pads and a gel holder were also soaked in the transfer buffer, and all air bubbles trapped within the porous pads were removed by rolling a clean glass test tube over the pads.

Once SDS-PAGE was finished, the gel was carefully removed and transferred onto the PVDF membrane. The sequence of stacking in the Trans-Blot module is described in Figure III-5. The electrotransfer was conducted under constant voltage mode (150 V) for a period of 5 h. The temperature of the transfer buffer was kept at 4 °C and a magnetic stir bar was used during the whole transfer process. To prevent overheating, transfer was carried out at 4 °C. Removing all air bubbles between gel holders was important to attain homogeneous protein transfer.

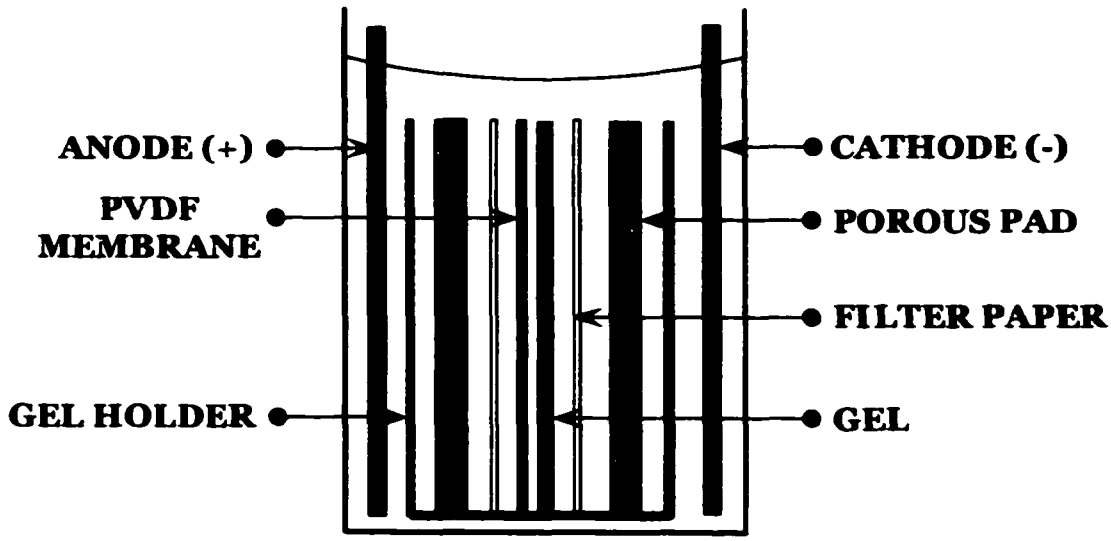

Figure III-5 Sequence of placement of the gel and PVDF membrane.

After protein transfers, the PVDF membrane was stained with the staining solution, 1 % (w/v) Coomassie Blue R-250, 40% Methanol, 10% Acetic acid, for 30 min, and the background was consecutively destained by Destaining Solutions I and II until the protein spots appeared.

The destained PVDF membrane was dried with air and the protein spots were excised with a pair of clean and sterilized scissors. The pieces of PVDF membranes that hold protein spots were separated and held in clean Eppendorf tubes. The PVDF membranes were properly labeled and shipped to Sandy Kielland (Victoria Protein Microchemistry Centre, Department of Biochemistry and Microbiology, University of Victoria, Victoria B.C. CANADA, phone: (250) 7218884, FAX (250) 7218855, Email: Kielland@UVic.ca Webpage http://www.proteincentre.com).

III.7.2 INTERNAL SEQUENCING

III.7.2.1 In-Gel Digestion

A protein spot in a 2-DE gel was digested by trypsin (Sequencing Grade Modified Trypsin, Promega). Peptide fragments were extracted and introduced either microbore HPLC for further separation or to a MALDI-TOF mass spectrometer.

In-gel digestion procedure with trypsin was optimized by the combination of three known methods (15-17). The procedure consisted of two parts: digestion and recovery. All 500 µl thin-wall PCR tubes were pretreated with 0.1% trifluoroacetic acid (TFA) and 50% acetonitrile (ACN) for 24 hours and dried in a clean hood before used. HPLC grade of water was used during in-gel digestion.

For the digestion of a protein in a gel, a target protein spot was first excised from a gel with a clean, sterile, 1.0 mm diameter Acu•Punch (Acuderm inc.), and gel pieces were transferred into a 500 µl thin-wall PCR tube. Gel excision was carried out in a laminar hood to avoid contamination by dust. Coomassie Blue R-250 (CBR) attached on protein must be completely removed by destaining solution I (10% acetic acid, 50% methanol, and water) before digestion with trypsin.

Once CBR was completely removed, Destaining Solution I was removed from the thin-wall PCR tube. The gel slices were mixed with 150 µl of reduction buffer (100 mM

NH_4HCO_3 pH 8.0 and 10 µl of 45 mM DTT), and rotated at 60 °C, 60 rpm for 30 min. The tube was subsequently added with 10 µl of alkylation buffer (100 mM iodoacetamide), and the tube was left in dark rack at room temperature for 30 min. Reduction and alkylation buffers were then carefully removed. The gel slices were covered with 500 µl of 100 mM NH_4HCO_3, pH 8.0 and rotated at 28 °C, 60 rpm for 20 min. This buffer was then removed and discarded. The gel slices were next covered in 500 µl of 50% acetonitrile (ACN) in 100 mM of NH_4HCO_3, pH 8.0 and rotated at 28 °C, 60 rpm for 20 min with a rocking shaker. The acetonitrile buffer was removed and the gel slices were cut into finer pieces on a clean piece of plastic wrap while using a sterile, fresh razor blade for each slice. The gel pieces were transferred into a second thin-wall PCR tube. The gel pieces were shrunk by adding 50 µl of 100% ACN and left in a laminar-flow hood at room temperature for 15 min. ACN solvent was removed from gel slices by completely drying them in a Speed Vac Plus (SC 110A, SAVANT) for 20 min. While the gel slices were dried, the trypsin solution was prepared.

Lyophilized trypsin (Promega) in a glass vial was added and resuspended in 20 µl of resuspension buffer (50 mM acetic acid) to make 1 µg /µl stock. To resuspend lyophilized trypsin, acetic acid buffer was pipetted up and down at least 20 times until all particles on the sides of vial were suspended. The vial was incubated at 30 °C for 15 min to activate the trypsin. Different amounts of trypsin were added into each PCR tube according to the staining intensity of each protein spot. For lighter staining spots, 100 ng of trypsin was added after further dilution of the 1 µg /µl trypsin stock with resuspension buffer. For very dark spots, 400 ng/µl trypsin was applied.

Completely dehydrated gel slices looked like a white pellet in the bottom of the PCR tube. The gel slice was reswelled with 10 µl of trypsin digestion stock by slowly and carefully adding solution directly onto the gel pieces. and the reswelling took 10 to 15 min in the laminar-flow hood at room temperature. Reswelled pellets with trypsin were covered by 20 to 40 µl of 25 mM NH_4HCO_3, pH 8.0 until all gels were fully covered by at least 1 mm of buffer. This increment was carried out very slowly to avoid disturbing the trypsin layer. It took about 30 min to add the buffer increment. Then the tubes were transferred to a shaking incubator at 37 °C at 60 rpm for 10 to 18 hours. The digestion period was applied differently according to the purpose of digestion and the amount of proteins applied. Tryptic digestion for MALDI-TOF was 16 to 18 hours. For the purification of peptide fragments by a microbore/capillary HPLC column. it was 10 hours.

To extract peptide fragments. all PCR thin-wall tubes were pretreated with ACN/trifluoreactic acid (TFA) buffer (0.1% TFA. 50% ACN) for 24 hours. The supernatant solution of a tryptic digestion tube was transferred to another new clean tube after a spin-down. The remaining peptides in the gel slices were extracted by sonication of a tube in 50 µl of ACN/TFA buffer (0.1% TFA. 50% ACN) for 10 min in a sonicatior bath (K5. Kraintek). Then the tube was vigorously vortexed and centrifuged for 5 min (Centriguge 5410. Eppendorf). This extraction process was repeated three times and all supernatant solution combined in the same tube. Solutions in the tube were completely dried by Speed Vac Plus (SAVANT).

Dried peptide fragments were stored –20 °C until further analyzed.

III.7.2.2 High Pressure Liquid Chromatography

III.7.2.2.1 Peptide preparation and injection

Peptide fragments were retrieved by adding various volume of ACN/TFA buffer (0.1% TFA in NanoPure water) depending upon the peptide concentration before it was applied to a microbore HPLC column (MAGIC C18, Michrom BioResources, Inc) on MAGIC 2000 HPLC system (Michrom BioResources), shown in Figure III-6. Then, the peptide solution was directly injected into a sample injection port with a 20 µl sample loop. The volume of sample injection depended on the concentration of peptides in a sample, but it was always less than 20 µl.

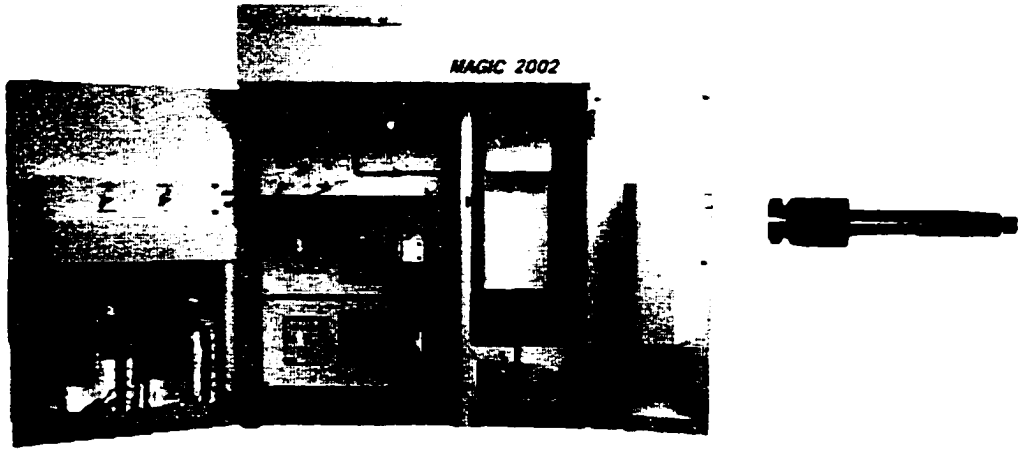

(A) (B)

Figure III-6 The MAGIC 2002™ (A) HPLC system and MAGIC C18 HPLC column (B).

III.7.2.2.2 Peptide separation

Two solvents were used to prepare and operate the HPLC system and a column. Solvent A contained 0.1% TFA in water purified by Milli-Q (Millipore), and Solvent B was 0.1% TFA in 100% ACN. The HPLC system was equilibrated with solvent A for 1 h at 50 µl/min. No air bubble was introduced in the HPLC system before connecting the C18 column to the HPLC. Once the C18 column was connected to the HPLC, Solvent A was introduced into the column to equilibrate it for 1 hour.

A method file, "me35minstd.met", was used to perform the peptide separation. The detailed elution program is shown in Table III-4.

Table III-4 HPLC operation program.

Time, min	Rate (µl/min)	% B	Volume, µl
0	50	5	0
2	50	5	100
22	50	65	1000
23	50	95	50
24	50	95	50
25	50	5	50
34	50	5	450
35	50	5	50

Each peak was manually collected with PCR thin wall tubes that were pretreated with 0.1% TFA and 50% ACN. The collection period was varied with the size of peak height and width. Since the volume of tubing between the UV detector cell and the flow rate (50 µl/min) of the HPLC pump was fixed, the time delay (t) was calculated by the following equation:

t = (tubing volume, μl)/(flow rate, μl/min)

The time delay for the HPLC system was less than 1.0 sec and it was implemented in collecting peaks.

III.7.2.2.3 Examine purity and size of peptide

Prior to applying a sample to the peptide sequencer, one microliter of sample from each peak fraction was applied to the MALDI-TOF MS to examine the purity and size of peptide. Sample preparation for the MALDI-TOF MS was discussed in section III.8.3.

III.7.2.3 Peptide Sequencing

Purified peptides in selected peak fractions from HPLC separation were transferred to a ProSorb™ Sample Preparation Cartridge (PERKIN ELMER) and adsorbed onto a PVDF membrane. If the sample volume was less than 100 μl, the sample was diluted with 100 μl of 0.1% TFA. A PVDF membrane was rewetted in the reservoir with 10 μl of methanol before use. Each peptide solution was washed with several aliquots of 0.1% TFA until the ACN concentration was reduced to below 15% prior to introduction into the ProSorb cartridge. Once the sorbant had sucked up all liquid from the sample reservoir through the PVDF membrane, the membrane was punched out a small round piece. To the dry the PVDF membrane, 15 μl of 0.1% TFA was added and wicked off the surface with filter paper after 15 seconds. Up to this point of the procedure, care was

taken to prevent drying of the PVDF membrane. PVDF membrane was soaked with 4 µl of methanol and allowed to dry thoroughly, and it was ready to be placed in the peptide sequencer (Procise, Applied Biosystems).

III.7.3 MASS SPECTROMETRY

III.7.3.1 MALDI-TOF MS

III.7.3.1.1 Sample Preparation

Dried peptide fragments were resuspended in 13 µl of sample preparation buffer (0.1% (v/v) trifluoroacetic acid (TFA), 50% ACN). A ZipTipC_{18} was used to desalt peptide fragment mixtures according to the vendor's instruction, Figure III-7. Peptide fragment mixtures were eluted from the ZipTip with elution solution (50% (v/v) acetonitrile (ACN), 0.1% TFA in NP water) into a clean PCR thin-wall tube. The final volume was about 10 µl and the samples were ready to use for either MALDI-TOF or ESI-MS/MS.

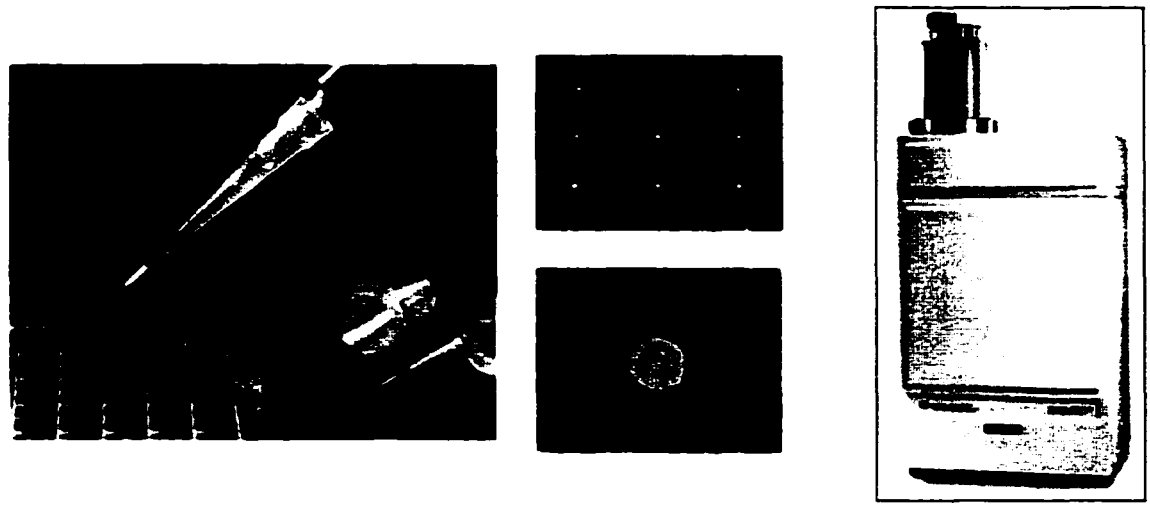

(A) (B) (C)

Figure III-7 Direct sample loading on a MALDI-TOF sample plate (http://home.appliedbiosystems.com/). (A) Sample spotting through the ZipTip™. (B)(1) Magnified image for a peptide sample and α–matrix on a stainless steel MALDI-TOF sample plate. (C) Voyager-DE MALDI-TOF from Applied Biosystems.

For MALDI-TOF MS, 0.8 μl of sample was spotted onto a MALDI-TOF stainless steel sample plate. On top of the sample, 0.8 μl of α-cyano-4-hydroxycinnamic acid matrix (α–matrix) (5, 7, 20) was added and the sample plate allowed to place at room temperature for 10 min until all liquid in the analyte-matrix crystallization was gone. The sample plate was inserted into the MALDI-TOF MS (Voyager-DE™ Pro, Applied Biosystems, MA), Figure III-7(B). The remaining peptide fragments were stored in a -20 °C freezer until further analyzed by a microbore HPLC for internal N-terminal sequencing or a tandem mass spectrometer (ESI-MS/MS).

III.7.3.1.2 MALDI Spectra Acquisition and Calibration

The generic software from the vendor was used to acquire MALDI spectra. All spectra were collected and recorded using delayed-extraction (DE) mode (18). To avoid the saturation of the detector with low-molecular-weight ions (< 400 Da) derived from matrix degradation, the low mass gate was used. The accelerating voltage was set to 25 kV. The nitrogen laser power was applied as low as possible within the power levels required, but the approximate range used was between 1650 and 2000 depending on the concentration of peptide mixtures. The laser was applied to at least 5 different spots on an analyte-matrix crystal spot to enhance the intensities of each spectrum.

In order to adjust the mass assignment of the acquired spectrum, a calibration series was conducted using both external and internal standards (9). The external standard was used to evaluate the signal to noise (S/N) ratio at a certain laser intensity and to identify the background impurities from the α-matrix (α-cyano-4-hydroxy-trans-cinamic acid, Hewlett Packard) before peptide samples were analyzed. Trypsin peptide fragments obtained by autolysis were used as an internal standard. Both the 842.50 Da (m/z) and the 2283.17 Da (m/z) monoisotopic peaks were always observed in MALDI spectra from peptide mixtures of samples that were cleaved by a modified porcine trypsin (Promega), and they are often used for internal mass calibration (13, 19).

III.7.3.2 Electrospray and Tandem Mass Spectrometry

III.7.3.2.1 Sample Preparation

The peptide fragment mixture resulting from digestion of a 2-D PAGE protein spot by trypsin was resuspended in 11 μl of HPLC buffer A (ACN/H_2O/acetic acid:5/95/0.1, v/v, %). The sample tube was sonicated in a sonication bath for 5 min and centrifuged at 15,000 rpm for 10 min with a microcentrifuge (Eppendorf). Ten micro litter of soluble sample was manually injected into the HPLC with a Hamilton syringe and an additional 20 μl of HPLC buffer A was injected immediately.

III.7.3.2.2 Micro HPLC and Tandem Mass Spectrometry

All LC-MS/MS analyses were performed using a PC-controlled micro capillary HPLC system (Eldex Micropro). The standard gradient was from 5% to 80% Buffer B over 30 min using acetonitrile (ACN) buffers in the presence of acetic acid (Buffer A: ACN/H_2O/Acetic acid = 5/95/0.1%, v/v; Buffer B: ACN/H_2O/Acetic acid = 80/20/0.1%, v/v) at an constant flow rate of 5.0 μl/min. The detailed operation program is presented in Table III-6. The system pressure reached about 1650 lb/in.^{2} (5.0 μl/min) for 300 sec when the protein sample was injected. The system pressure was decreased and maintained at ~1400 lb/in.^{2} while the peptide mixtures were separated by the HPLC program.

Table III-5 Detailed HPLC operation program.

Time, min	%B	%A
0	5	95
45	60	40
50	80	20
60	80	20
65	5	95
90	5	95

Peptide analyses were performed using a Thermo Finnigan LCQ ion trap mass spectrometer (ITMS) (Finnigan) equipped with atmospheric pressure ionization (8). The LCQ was operated under automatic control in the "Tune Plus" view with the automatic gain control (AGC) active unless stated otherwise. The AGC targets were: Full MS-5e + 008 and MS/MS-1e + 005. Spectra were acquired in automated MS/MS mode with collision-induced dissociation (CID) at 30 eV. During an automated run, a product ion spectrum was acquired if an ion was present in a scan above a specific threshold. The mass spectrometer continued to alternate between MS (3 μs scans per scan) and MS/MS mode (5 μs scans per scan) until the ion intensity dropped below the threshold. The scan range for MS mode was set at 200-2000 mass-to-charge (m/z). A parent ion default charge state of +2 is used to calculate the scan range for acquiring tandem mass spectra. Further details are described in Chapter V.

III.7.3.3 Spectra Analysis

The peptide masses and the resulting ions obtained by the first MS and second analyzer were transferred to the Xcalibur software (Finnigan). A search was performed the peptide masses from the first MS against the FASTA format of the non-redundant protein database in the National Center for Biotechnology Information (NCBInr) through the SEQUEST computer algorithm in the Xcalibur software package. SEQUEST-SNPs dynamically generates all possible single-nucleotide polymorphisms (SNPs) based on the NCBInr database, translates these sequences to peptides, and analyzes these peptides with an algorithm developed by Eng *et al* (6). The search and analyses were run on an Intel Pentium III 600 MHz and required 1 – 1200 sec depending on the size of database to search the identification. More details are also described in Chapter V.

III.8 References

1. **Abbott, A.** 1999. A post-genomic challenge: learning to read patterns of protein synthesis. Nature **402:**715 - 720.

2. **Bio-Rad.** 1996. 2-D SDS-PAGE Standards. Product instruction 600-0039 Ch.B:011688. Bio-Rad Laboratories.

3. **Bolt, M. W., and P. A. Mahoney.** 1997. High-Efficiency Blotting of Proteins of Diverse Sizes Following Sodium Dodecyl Sulfate-Polyacrylamide Gel Electrophoresis. Anal. Biochem. **247:**185-192.

4. **Burnette, W. N.** 1981. "Western Blotting": Electrophoretic transfer of proteins from sodium dodecyl sulfate-polyacrylamide gels to unmodified nitrocellulose and radiographic detection with antibody and radioiodinated protein A. Anal. Biochem. **112:**195.

5. **Cohen, S. L. a. B. T. C.** 1997. Mass spectrometry of whole proteins eluted from sodium dodecyl sulfate-polyacrylamide gel electrophoresis gels. Anal. Biochem. **247:**257-267.

6. **Eng, J. K., McCormack, A.L., Yates, J.R., III.** 1994. An Approach to Correlate Tandem Mass Spectral Data of Peptides with Amino Acid Sequences in a Protein Database. J. Am. Soc. Mass Spectrom **5:**976-989.

7. **Gobom, J., M. Schuerenberg, M. Mueller, D. Thesis, H. Lehrach, and E. Nordhoff.** 2001. a-cyano-4-hydroxycinnamic acid affinity sample preparation. A protocol for MALDI-MS peptide analysis in proteomics. Anal. Chem. **73:**434-438.

8. **Griffin, P. R., J. A. Coffman, L. E. Hood, and J. R. Yates, III.** 1991. Structural analysis of proteins by capillary HPLC electrospray tandem mass spectrometry. Int. J. Mass Spectrom. Ion Processes **111:**131-149.

9. **Juhasz, P. M., L. Vestal, and S. A. Martin.** 1997. On the initial velocity of ions generated by matrix-assisted laser desorption ionization and its effects on the calibration of delayed extraction time-of-flight mass spectra. J.Am.Soc.Mass.Spectrom. **8:**209-217.

10. **Mosteller, D. C.** 1995. Biodegradation of organic pollutant mixtures by *Pseudomonas putida* F1. Thesis for Master:32-62.

11. **Nies, D. H.** 1995. The cobalt, zinc, and cadmium efflux system CzcABC from Alcaligenes eutrophus functions as a cation-proton antiporter in Escherichia coli. J. Bacteriol. **177:**2702-2712.

12. **O'Farrell, P. H.** 1975. High resolution two-dimensional-electrophoresis of proteins. J. Biol. Chem. **250:**4007-4021.

13. **Parker, K. C., J. I. Garrels, W. Hines, E. M. Butler, A. H. McKee, D. Patterson, and S. Martin.** 1998. Identification of yeast proteins from two-dimensional gels: working out spot cross-contamination. Electrophoresis **19:**1920-1932.

14. **Reardon, K. F., D. C. Mosteller, and J. D. Rogers.** 2000. Biodegradation kinetics of benzene, toluene, and phenol as single and mixed substrates for *Pseudomonas putida* F1. Biotechnol. Bioeng. **69:**385-400.

15. **Resing, K. A.** 2000. In-Gel Digestion Procedure. Personal Communication. Chemistry and Biochemistry Department. Unversity of Colorado at Boulder.

16. **Rosenfeld, J., J. Capdevielle, J.C. Guillemot, and P. Ferrara.** 1992. In-gel digestion of proteins for internal sequence analysis after one- or two-dimensional gel electrophoresis. Anal. Biochem. **203:**173-179.

17. **Steven, L. C., and B. T. Chait.** 1997. Mass Spectrometry of Whole Proteins Eluted from Sodium Dodecyl Sulfate-Polyacrylamide Gel Electrophoresis Gels. Anal. Biochem. **247:**257-267.

18. **Vestal, M. L., P. Juhasz, and A. Martin.** 1995. Delayed extraction matrix-assisted laser desorption time-of-flight mass spectrometry. Rapid Commun. Mass Spectrom. **9:**1044-1050.

19. **Vestling, M. M., C. M. Murphy, and C. Fenselau.** 1990. Recognition of trypsin autolysis products by high-performance liquid chromatography and mass spectrometry. Anal Chem **62:**2391-2394.

20. **Volm, O., P. Roepstorff, and M. Mann.** 1994. Improved resolution and very high sensitivity in MALDI TOF of matrix surfaces made by fast evaporation. Anal. Chem. **66:**3281-3287.

CHAPTER IV PROTEOME ANALYSIS OF *P. PUTIDA* F1 DURING THE BIODEGRADATION OF TOLUENE-PHENOL MIXTURES

IV.1 Research Motivation and Goals

Biodegradation of toluene and phenol mixtures by *P. putida* F1 was not well predicted by standard mathematical models (25) even though both toluene and phenol are metabolized by the same set of enzymes in the cell (29, 30). To understand biological process in a specific organism at a certain time, proteome analysis has several advantages (4, 6, 8, 11, 12, 15, 36). Proteins represent biological and physiological activities in a cell responding to cellular events. Investigation of differential protein production would provide more practical and specific information to understand the physiology of *P. putida* F1 during its growth on toluene and phenol mixtures.

Differential protein production in the cells during growth on each single substrate was studied first by comparing the proteins profiles. Since differences were noted, protein profiles were also compared during the growth of *P. putida* F1 on toluene-phenol mixtures. This study evaluated only soluble proteins, those that can be extracted to the protein extraction solution from the cells without the use of surfactants. The soluble

protein might include some proteins from the cell membrane fraction, but it should be a very small portion because of the hydrophobic nature of membrane proteins.

In this portion of the study, proteome analysis procedures for the soluble proteins from *P. putida* F1 were first developed and optimized. Second, the soluble proteins produced by *P. putida* F1 during growth on toluene, phenol, and their mixtures were analyzed. Results served to evaluate the differences in protein production during growth on the single substrates and their mixture.

IV.1.1 EVALUATION OF PROTEOME ANALYSIS PROCEDURE

IV.1.1.1 Protein solubilization and separation

Protein solubilization is the most important step for successful protein separation by 2-DE (5). The term solubilization refers to disruption of the molecular forces that maintain an intact structure of polypeptides and to yield separate polypeptide chains (23). Since no universally applicable protein solubilization process for all protein mixtures is available, all protein samples should undergo a search for the optimum solubilization condition (23). In this study, several different chemicals were used to obtain the optimum solubilization for the soluble proteins from *P. putida* F1. These chemicals fall into two categories according to their target bonds in polypeptides: covalent and non-covalent bonds.

IV.1.1.1.1 Disruption of covalent interactions

The strongest and most important covalent bond in proteins is the disulfide bond between thiol groups of cysteine amino acid. To maintain all proteins in their fully reduced state and to break any disulfide bonds, 5% (w/v) β-mercaptoethanol was included in the solubilization solution. Because of its buffering power (26) and high concentration of inherited artifacts in β-mercaptoethanol reagents (19), the use of β-mercaptoethanol has not generally been recommended. However, advances in the purification technology in the manufacturing process can remove these artifacts and, furthermore, β-mercaptoethanol is better than dithiothreitol (DTT) for maintaining all cysteines in completely reduced state (26). Maintaining cysteine in a reduced state was also very important for the identification of proteins with mass spectrometry after proteome analysis (28).

IV.1.1.1.2 Distruption of non-covalent interactions

Besides disulfide bonds in a protein, three other important forces keep protein structures intact: hydophobicity, hydrogen bonds and van der Waals interactions (33). Two different chemicals were used to break these non-covalent interactions, a neutral chaotrope and a detergent. Urea solublizes and unfolds most proteins to their fully random conformation, with all ionizable groups exposed to solubilizing solution (5, 18,

21, 23). Two different concentrations (8.0 and 9.5 M) of urea were examined. Figure IV-1 clearly shows the difference in protein separation. The higher concentration of urea (e.g. 9.5 M urea (Figure IV-1 (A)) solublized proteins much better than 8.0 M urea. Figure IV-1 (B). The concentration of urea selected as the optimum condition in solubilizing the soluble proteins from *P. putida* F1 was 9.5 M.

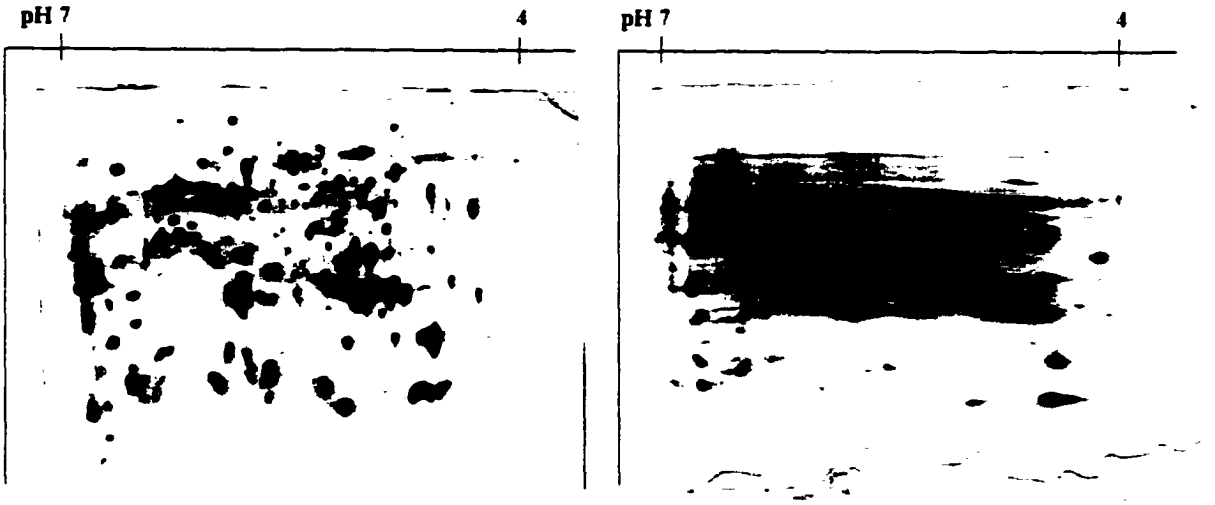

Figure IV-1 Effect of urea in protein solubilization in 2-D PAGE gels. (A) 9.5 M Urea. (B) 8.0 M Urea. Experimental conditions are described in III.6.3.

A detergent was always used to ensure complete sample solubilization and to prevent aggregation through hydrophobic interactions. Two different detergents were examined and the zwitterionic detergent CHAPS (3-([3-cholamidopropyl]dimethylammonio)-1-propanesulfonate) was selected it had better performance in solubilizing proteins. The non-ionic detergent (Triton X-100) was examined, but it could not effectively solublize

protein mixtures. Four percent (w/v) CHAPS in a solubilizing solution is often cited as the best concentration (22, 23). However, a couple of different concentrations were examined in this study. Four and eight percent (w/v) of CHAPS were independently examined and no significant difference was observed in 2-DE gels, so 4% CHAPS was used. The summary of the optimized protein solubilization reagents for the soluble protein of *P. putida* F1 is listed in Table IV-1.

Table IV-1 Components of the optimum protein solubilization for the soluble proteins from *P. putida* F1. The volume of water and proteins were varied according to the length of IPG strips. Grades of all chemicals were used electrophoresis grade or the highest purity.

9.5 M Urea
4% CHAPS
3% Phymalyte (pH 4-7)
5% β-mercaptoethanol
NanoPure Water
Proteins

IV.1.1.2 Separation of proteins

IV.1.1.2.1 Selection of IPG strips and sample loading

A wide range pH gradient IPG strip (pH 3-10) was used for the initial analysis of the protein in the first dimension (Figure IV-2 A). Most soluble proteins were focused between pI 4 and 7, but the resolution of proteins in the region pH 4-7 was poor because of the broad pH gradient. Use of a narrower range of pH, pH 4-7, allowed separation of most proteins with higher resolution (Figure IV-2 B). The proteins were well scattered around the entire gel area.

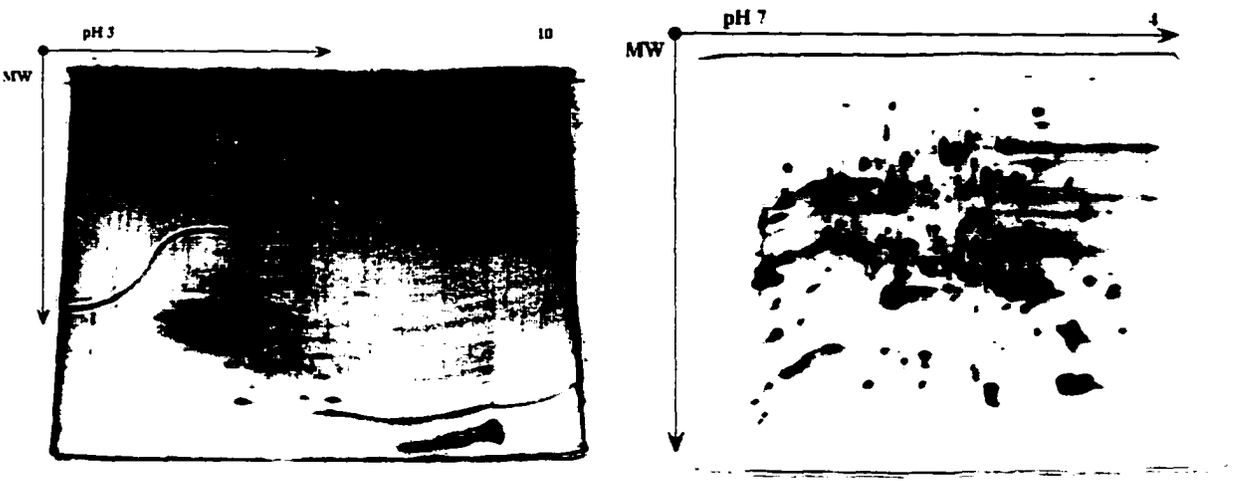

(A) (B)

Figure IV-2 A 2-DE separation of 12 µg of the soluble protein extracts from *P. putida* F1 grown on toluene single substrate. (A) A 7.0 cm linear pH 3-10 IPG strip was used in IEF step. (B) A 7.0 cm pH 4-7 linear gradient IPG strip was utilized for IEF. The second dimension was carried out by 12% SDS-PAGE gel in both cases. The proteins on both gels were visualized by silver staining (Silver Xpress, NOVEX).

Longer lengths of IPG strips (13 cm) were used for preparative protein separation for further protein identifications. Larger amounts of proteins could be separated in the longer IPG strips. Up to 400 μg of protein was applied to 13 cm IPG strips (pH 4-7).

Two different methods of introducing protein sample to IPG strips were examined, direct rehydration of IPG strips with the final solubilization solution including protein mixtures (Figure IV-3A) and loading protein mixtures via sample cups (Figure IV-3B). In the case of sample introduction with sample cups, IPG strips were fully rehydrated before the application of protein mixtures. With the direct application method, more protein could be loaded and separated. Advantage of sample application via sample cups is that the random proteolysis of protein mixtures can be minimized. However, the two sample application methods did not yield for the protein separation in this study, so the direct dehydration method was employed for this study.

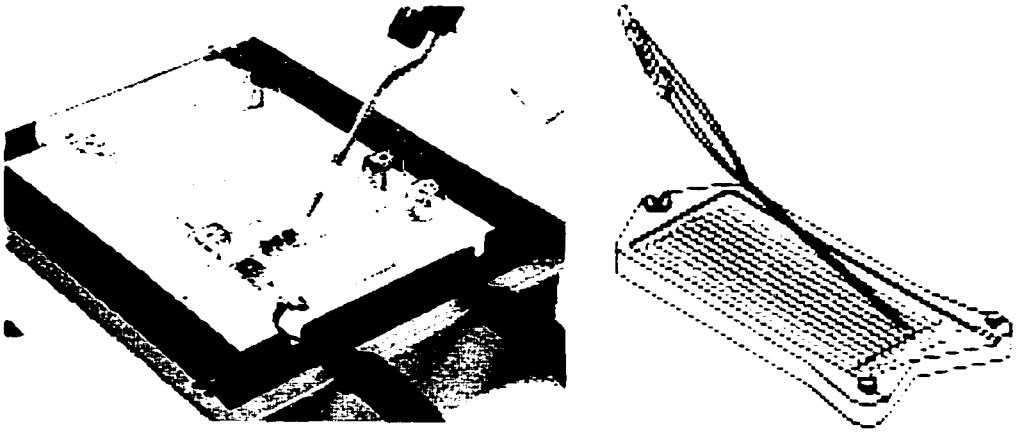

Figure IV-3 Introduction of protein samples to IPG strip. (A) Sample loading via sample cups. (B) Direct rehydration of an IPG strip with the protein solubilization solution.

IV.1.1.2.2 The first dimension: Isoelectric focusing

Completely solublized proteins were embedded in an Immobiline pH Gradient strip (IPG) in a reswelling tray. The Multiphore II separated the proteins in an IPG strip. During IEF, the temperature in the IPG strip was maintained at a constant temperature. Three temperatures, 4, 10, and 20 °C, were examined. The lower the temperature, the higher the rate of urea crystallization. Urea crystallization during IEF resulted in the partial disturbance of protein solubilization and generated irreproducible 2D gels (13). Thus, 20 °C was selected as the optimum temperature for IEF separation.

The period of total running time and the level of voltage applied to IPG strips were critical to good separation of protein mixtures and varied according to the amount of applied proteins. In the analytical size (10 – 20 μg proteins), the total focusing period was 20,100 V•h with a linear increment of voltage. A longer period of focusing time, 70,420 V•h, was applied for the preparative separation of proteins (up to 400 μg) with step increment of voltage.

IV.1.1.2.3 Equilibration of IPG strips between dimensions

After IEF separation, IPG strips were either immediately applied to SDS-PAGE or stored at – 20 °C until used. Whichever IPG strips were used, the strips were treated with equilibration solution (see Chapter III). During this step, excessive sodium dodecyl sulfate bound with polypeptides and made them completely negative charge, so that the proteins migrated properly during SDS-PAGE. However, longer than 10 – 15 min of equilibration could cause small proteins to diffuse out of IPG strips.

IV.1.1.2.4 The second dimension: SDS-PAGE

A gradient polyacrylamide gel (4 – 20%) for the second dimension separation of the proteins provided slightly better resolution in separating the smaller proteins, but a fixed percentage (12%) of the second dimension gel was used through all proteome separation. Since no steps to remove DNA and polysaccharides were incorporated in the entire

protein extraction, concentration, and washing processes, the final protein samples contained relatively high concentrations of nucleotides and polysaccharides. This could result in increased viscosity of the protein solubilization solution and then these molecules could clog the small pores of polyacrylamide gels used to separate the proteins (10, 11). Since the clogging of small pores in lower part of a slab gel could have resulted in generating irreproducible protein spots throughout a 2DE gel, a fixed percentage of slab gel system was selected for the study.

To avoid the distortion of protein separation by excessive heat generation during separation, cooling water was continuously introduced to the gel sandwich compartment and the temperature of coolant was maintained at 4.0 °C by a cooling unit.

IV.1.1.3 Protein visualization on a gel

One fluorescent (SYPRO Ruby) (32) and two non-fluorescent methods (Coomassie and silver) were examined to detect proteins on a 2-DE gel. Although the protein detection limit of Coomassie was much higher than two other methods, it is completely compatible with the subsequent protein identification by both N-terminal sequencing and mass spectrometry. It is also relatively simple method and more quantitative than silver staining. Coomassie Brilliant Blue R-250 was used to detect proteins either on a PVDF membrane after electrotransfer or preparative gels (Figure IV-4A).

SYPRO Ruby was claimed to yield detection limits as low as silver stain by the vendor (20) and previous studies (1, 31, 32, 34), but it was not able to visualize less than 1 μg of proteins (Figure IV-4B). In the presence of SDS in a gel, the maximum detection of proteins was carried out at 547 nm of wavelength for SYPRO Ruby. Otherwise, an emission maximum was centered at 631 nm (32). The gels stained with SYPRO Ruby were exposed on a UV illuminator that was fixed on 300 or 480 nm wavelengths, and these inappropriate wavelengths were probably responsible for such low detection of proteins (Figure IV-4B/C).

The silver stain method is popular for detection of proteins on an analytical gel. This method yielded reproducible detection of proteins and had an excellent detection limit (~ 1 ng) relative to the two other staining methods (Figure IV-4D).

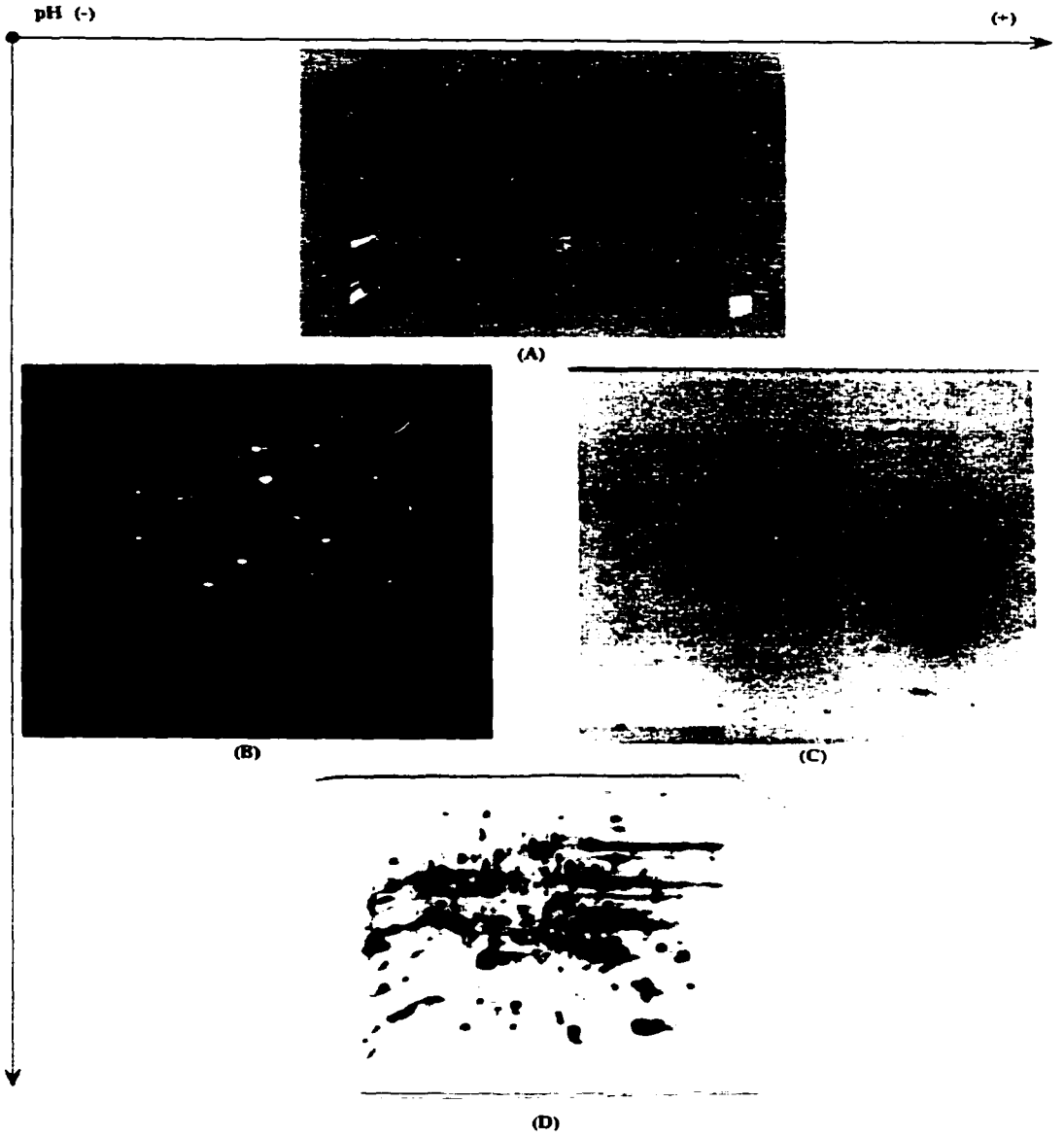

Figure IV-4 Protein detection with different staining methods. (A) Detection of toluene proteins (50 μg) with Coomassie Blue R-250 on a PVDF membrane. Three protein spots were excised and applied to N-terminal sequencer (See Chapter V for detail). (B) Detection of 50 μg of toluene proteins with SYPRO Red Protein Stain, photographed on a 300 nm of UV illuminator. (C) The inverted image of (B). (D) 12 μg of toluene proteins were visualized by silver stain.

IV.1.1.3.1 Calibration of 2-D PAGE gels

A set of standard proteins was used to calibrate 2-DE gels in pH gradient and molecular weight. The proteins were solublized by the pre-prepared standard solution from the vendor and separated by the developed condition in this study. The standard protein mixtures contained hen egg white conalbumin (76 kDa, pI 6.0, 6.3, 6.6), bovine serum albumin (BSA, 66.2 kDa, pI 5.4, 5.6), bovine muscle actin (43 kDa, pI 5.0, 5.1), rabbit muscle glyceraldehyde 3-phosphate dehydrogenase (GAPDH, 36 kDa, pI 8.3, 8.5), bovine carbonic anhydrase (31 kDa, pI 5.9, 6.0), soybean trypsin inhibitor (21.5 kDa, pI 4.5), and equine myoglobin (17.5 kDa, pI 7.0). Since more isozyme spots on both BSA and rabbit muscle actine (arrowheades) than the instruction from the vendor were detected, the silver staining method for the study was more sensitive than that of the vendor shown in Figure IV-5.

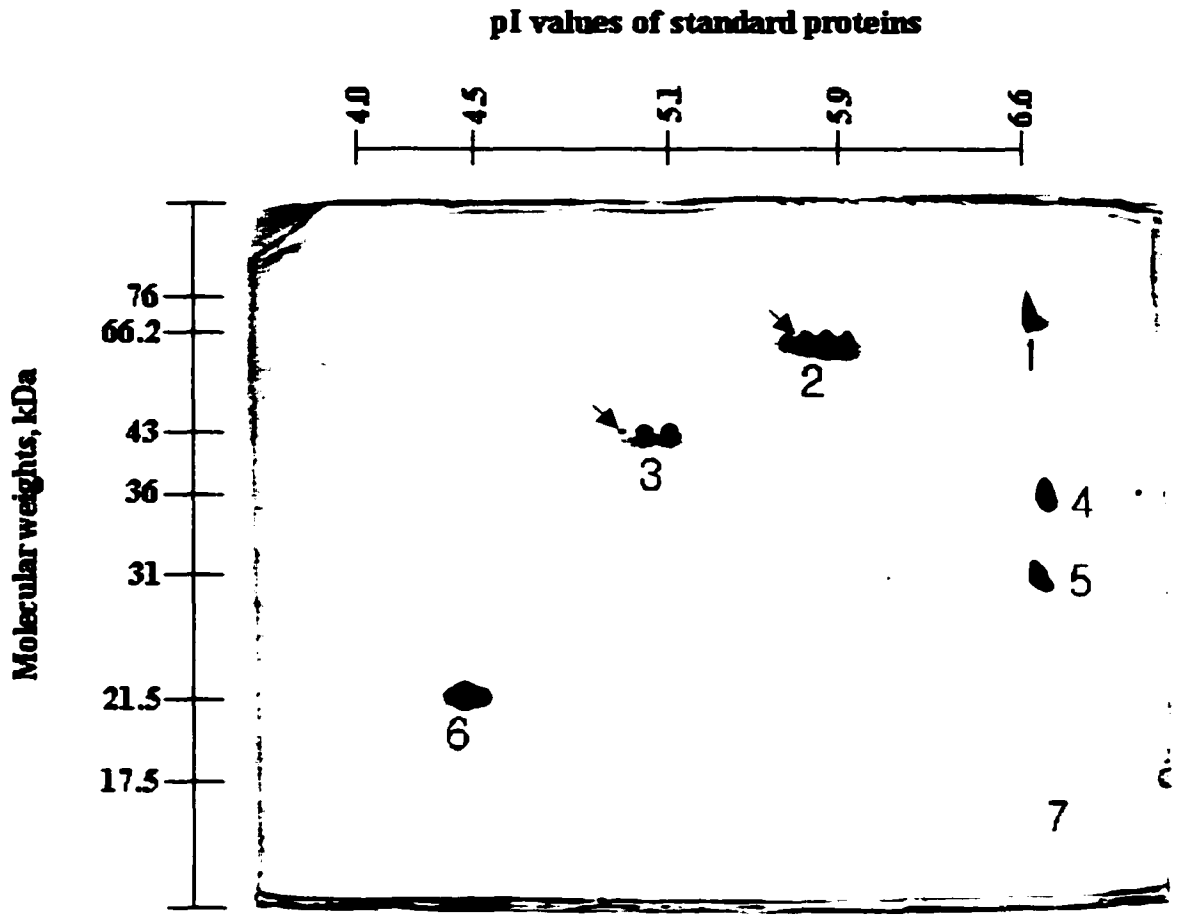

Figure IV-5 Two-dimensional electrophoresis pattern of 2-D SDS-PAGE Standards. One micro litter of the standard solution was run by the method developed for the study and silver stained. Arrows indicates the extra isozymes detected by the silver stain method for the study. The isoelectric points of BSA and muscle actin are altered by urea in the pre-prepared standard buffer (2). The running pI values of these proteins have been empirically determined. All other proteins migrate to their literature pI values. 1: hen egg white conalbumin (76 kDa, pI 6.0, 6.3, 6.6), 2: bovine serum albumin (66.2 kDa, pI 5.4, 5.6), 3: bovine muscle actin (43 kDa, pI 5.0, 5.1), 4: rabbit muscle glyceraldehydes 3-phosphate dehydrogenase (36 kDa, pI 8.3, 8.5), 5: bovine carbonic anhydrase (31 kDa, pI 5.9, 6.0), 6: soybean trypsin inhibitor (21.5 kDa, pI 4.5), and 7: equine myoglobin (17.5 kDa, pI 7.0)

IV.1.2 PROTEOME ANALYSIS OF GROWTH ON SINGLE SUBSTRATES

Concentration vs. time data for the growth of *P. putida* F1 on the individual substrates are shown in Figure. 1. The consumption of the initial concentration of toluene (0.42 mM in liquid) occurred in 15 h. including a 5-h lag time. Consumption of phenol was much slower: an initial concentration of 0.5 mM was depleted only after 90 h. including a 15-h lag time. Since the inocula for these cultures were grown with the appropriate carbon source (i.e., the toluene experiment was inoculated with a toluene-grown culture), these differing rates are intrinsic to this strain.

Samples for 2-D PAGE analyses were taken from each cultivation at the times indicated by the vertical lines in Figure IV-6. For the single-substrate experiments, these times corresponded to the mid-exponential growth phase (12 and 60 h for the toluene and phenol cultures, respectively). The 2-D PAGE results and a magnified portion of these gels for these samples are shown in Figure IV-7. On these gels, 281 proteins from toluene-grown cells and 288 proteins from phenol-grown cells are visible. Substantial differences between these soluble protein profiles are evident. It is notable that the pattern of spots on the toluene gel is similar to those reported by Vercellone-Smith and Herson using *P. putida* mt-2 grown on toluene (37).

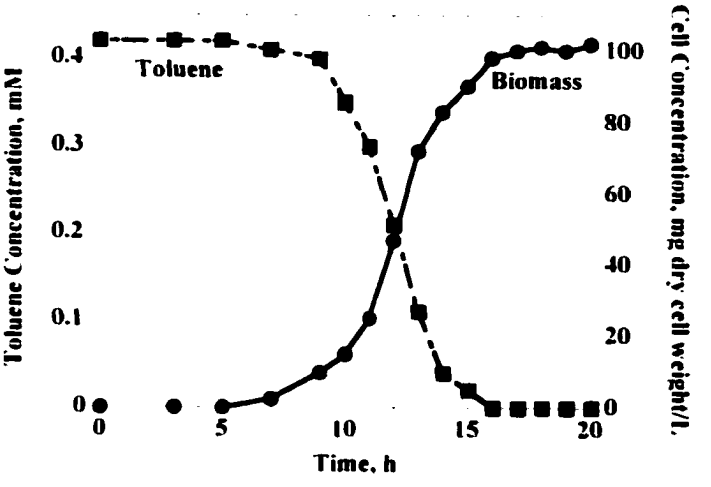

(A)

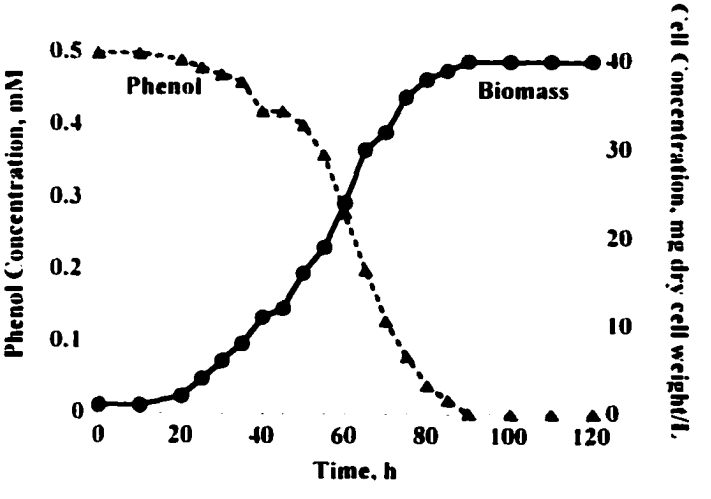

(B)

Figure IV-6 Data from single substrate cultivations of *P. putida* F1 on toluene (A) and phenol (B). Symbols indicate measurements of liquid-phase toluene (■), phenol (▲), and biomass (●) concentrations. Vertical lines denote times at which samples were removed for 2-D PAGE.

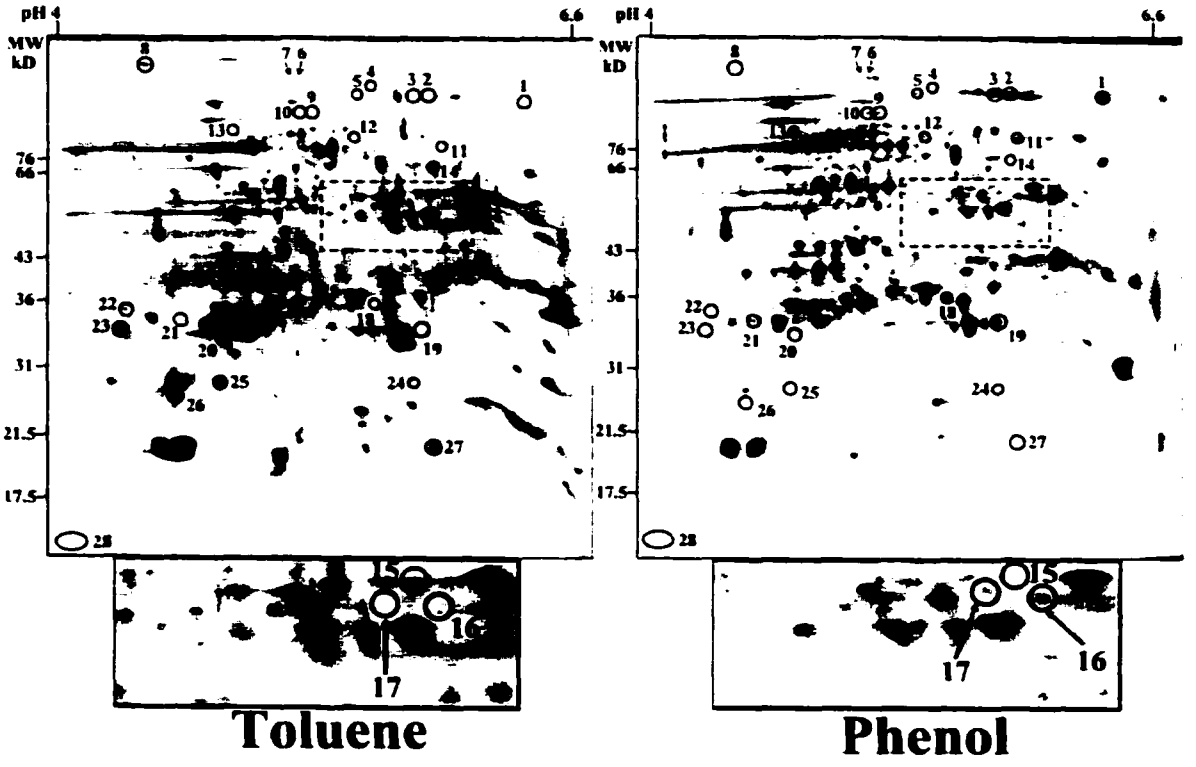

Figure IV-7 2-D PAGE gels of soluble proteins from *P. putida* F1 in mid-exponential growth on toluene (left panels) or phenol (right panels). Dotted boxes are enlarged below. Numbers indicate spots present in one gel but absent in the other: these proteins are listed in Table IV-2.

Proteins that were present on one of these gels but missing from the other are listed in Table IV-2. Other differences between the two samples (e.g., presence/absence of low-level proteins or variable levels of individual proteins) undoubtedly exist. The number of 2-D PAGE gel replicates was 5 to 10. Proteins were extracted from cells grown in three separate batch cultivations with the same culture conditions. The general protein pattern was well reproducible in all replicated gels, but some proteins, especially found in Phenol gels, displayed less reproducible than those in Toluene gels and those irreproducible proteins in Phenol gels were excluded in grouping. Proteins were categorized by two strict criteria: first, proteins in each group were reproducibly observed from at least five independent 2-D PAGE gels. Second, since we were only interested in the proteins that showed clear ON-OFF regulation, those proteins that changed their intensities were not classified. The number of 2-D PAGE gel replicates was 5 to 10. Proteins were extracted from cells grown in three separate batch cultivations with the same culture conditions. The general protein pattern was well reproducible in all replicated gels, but some proteins, especially found in Phenol gels, displayed less reproducible than those in Toluene gels and those irreproducible proteins in Phenol gels were excluded in grouping. Proteins were categorized by two strict criteria: first, proteins in each group were reproducibly observed from at least five independent 2-D PAGE gels. Second, since we were only interested in the proteins that showed clear ON-OFF regulation, those proteins that changed their intensities were not classified. However, we chose to apply strict criteria in compiling this table, focusing on those proteins that were clearly present or absent in our visual examination of the gels. We identified 10 proteins produced only in toluene-grown cells ("Group T") and 17 proteins that were found only in phenol-grown cells ("Group P"). These proteins were mainly focused between pH 4.0 and 6.5 and had molecular weights between 10 and 200 kD.

Table IV-2 Summary of protein production during growth on toluene, phenol, or their mixture: (+) indicates detection of a protein and (–) denotes no detect levels.

Protein No.	Substrate						Group Assignment
	Toluene	Phenol	Toluene-Phenol Mixture				
			A	B	C	D	
1	-	+	-	-	+	+	P
2	-	+	-	-	+	+	P
3	-	+	-	-	+	+	P
4	-	+	-	-	+	+	P
5	-	+	-	-	+	+	P
6	-	+	-	-	+	-	P
7	-	+	-	-	+	+	P
8	+	-	+	+	-	+	T
9	-	+	-	-	+	-	P
10	-	+	-	-	+	-	P
11	-	+	-	-	+	+	P
12	-	+	-	-	+	+	P
13	-	+	-	-	+	+	P
14	+	-	+	+	+	+	T
15	+	-	+	+	+	+	T
16	-	+	-	+	+	+	P
17	-	+	-	-	+	-	P
18	-	+	-	+	+	+	P
19	-	+	-	-	+	+	P
20	+	-	+	+	+	+	T
21	-	+	-	+	+	+	P
22	+	-	+	+	-	-	T
23	+	-	+	+	-	-	T
24	+	-	+	+	+	+	T
25	+	-	+	+	+	-	T
26	+	-	+	+	+	+	T
27	+	-	-	+	+	+	T
28	-	-	+	+	+	-	M
Total Protein	***281***	***288***	***295***	***284***	***252***	***300***	

IV.1.3 PROTEOME ANALYSIS OF GROWTH ON MIXED SUBSTRATES

Concentration vs. time data for the growth of *P. putida* F1 on the toluene-phenol mixture are shown in Figure IV-8. When both toluene and phenol were present, toluene consumption began first and was nearly completed before phenol concentrations decreased. The same observation has been made repeatedly in our laboratory (25).

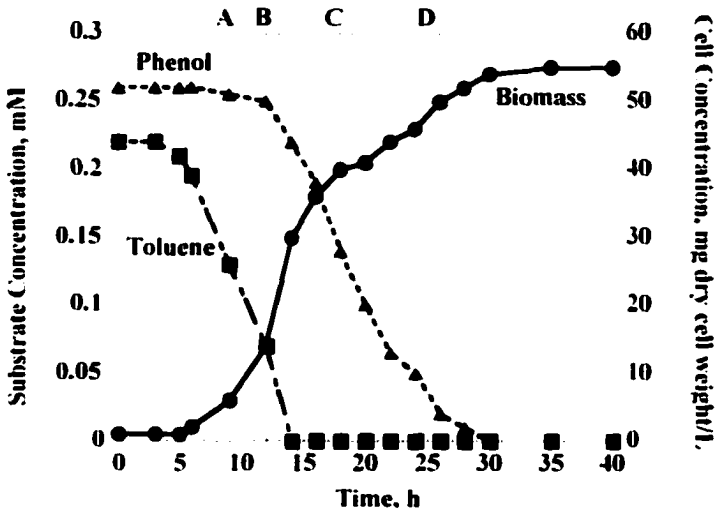

Figure IV-8 Data from a batch cultivation of *P. putida* F1 on a toluene-phenol mixture. Symbols indicate measurements of liquid-phase toluene (■), phenol (▲), and biomass (●) concentrations. Vertical lines denote times at which samples were removed for 2-D PAGE.

2-D PAGE samples were removed from the mixed-substrate experiment at four time points: (A) at 9 h, when only toluene was being consumed; (B) at 12 h, when toluene had just been depleted and shortly after phenol consumption had begun; (C) at 18 h, when about half of the phenol had been consumed; and (D) at 25 h, when the phenol

concentration was nearly zero. The 2-D PAGE results for these samples are shown in Figure IV-10. and an enlargement of the region within the dotted lines is shown in Figure IV-11. The changes in protein concentrations over the course of the mixture experiment are shown in Figure IV-12.

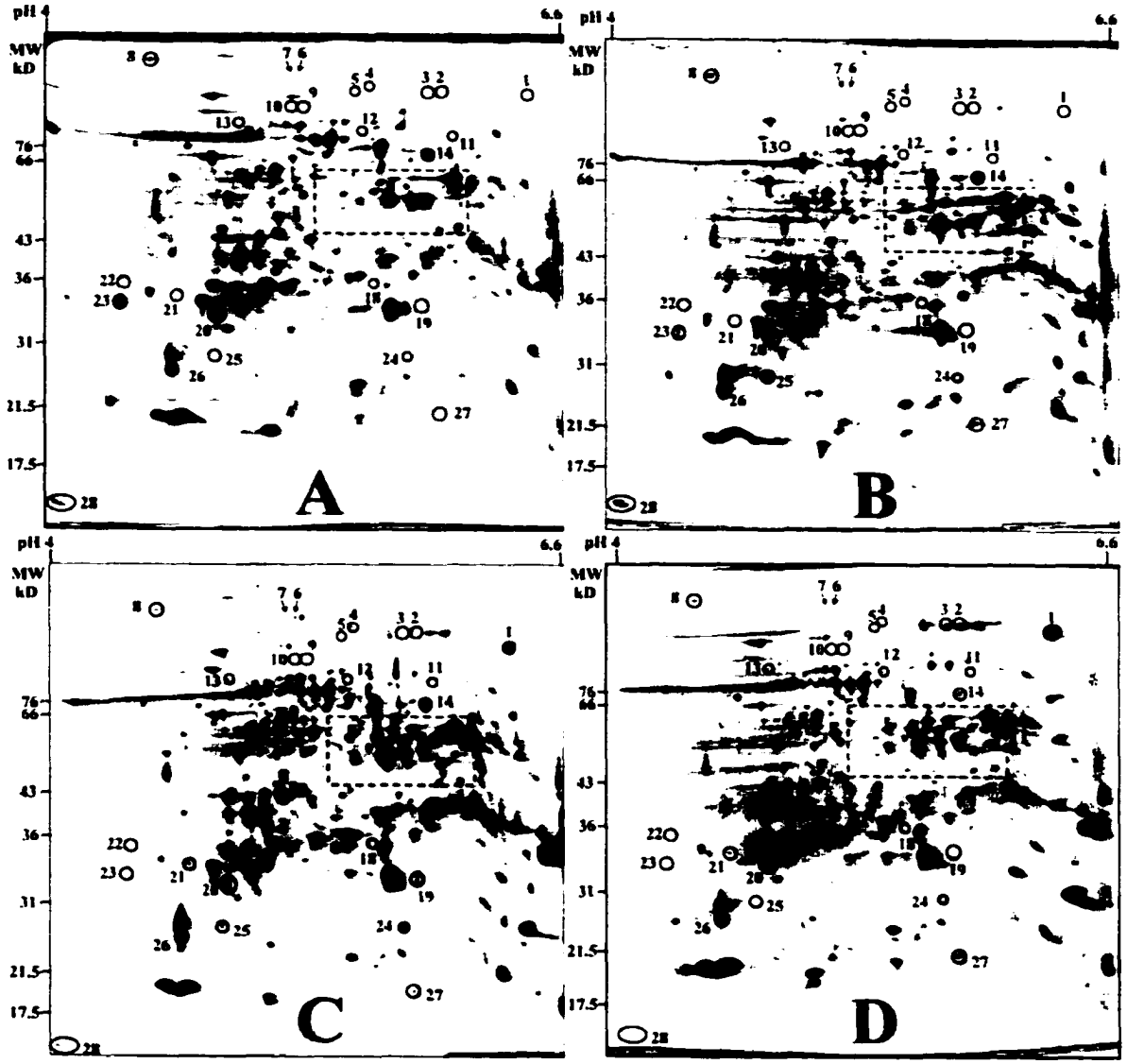

Figure IV-9 2-D PAGE gels of soluble proteins from *P. putida* F1 at the 4 different sampling points (A–D) of the toluene-phenol cultivation shown in Figure IV-8. Dotted boxes are regions that are enlarged in Figure IV-11. Numbers indicate proteins listed in Table IV-2.

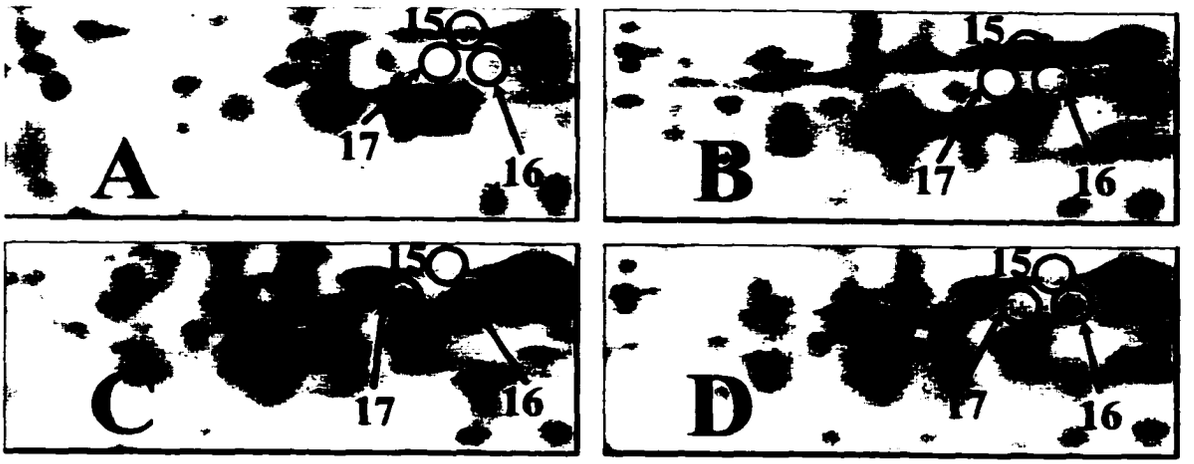

Figure IV-10 Enlarged images of the dotted boxes from 2-D PAGE gels shown in Figure IV-9. Numbers indicate proteins listed in Table IV-2.

All 10 of the Group T proteins and all 17 of the Group P proteins were detected at various times during the mixed substrate experiment (Figure IV-10, Table IV-2). In addition, another protein, labeled 28 in Figure IV-10, was detected in the mixture experiment and was assigned to Group M (Mixture). This protein was not detected on the single-substrate gels in Figure IV-7 (in which 12 μg of protein was loaded onto 70 × 90 mm gels); however, it was detected at very low levels in subsequent analyses when 250 μg of protein mixture was separated on a standard-sized (160 × 200 mm) gel. Protein #28 is relatively small (~10 kD) and has a pI near 4.

At Sampling Point A, the protein profile was essentially identical to that of the toluene-grown cells (Figure IV-10A). In particular, nine of the ten Group T proteins (#8, 14, 15, 20, 22, 23-26) were present; the exception was Protein #27. Low levels of the Group M protein (#28) were also detected in samples taken at this 9-h point. 2-D PAGE analysis

of other culture samples taken between 5 and 8 h of growth showed no evidence of Protein #28. No Group P proteins were detected at this sampling time.

At Sampling Point B. the cells had shifted from toluene to phenol as the primary substrate (Figure IV-9). All Group T proteins were still evident in these cells. although not all spot intensities were the same as those on the time A gels. While cellular levels of Proteins #8. 14. 22. 23 and 24 remained nearly the same at 12 h as at 9 h. the levels of Proteins #15. 25. 26 and 27 increased and the amount of Protein #20 decreased. Three of the Group P proteins (#12. 16 and 21) were detected at this time. and the intensity of the Group M protein spot (#28) was higher than that on the previous gel. It should be noted that the culture medium began to darken at this point. This color change. which continued for the duration of the cultivation. has been noted by others (9. 25) and has been attributed to autooxidation of catechol or other degradation intermediates.

The 2-D PAGE gel in Figure IV-10 C presents the protein profile of cells growing on phenol after toluene was completely depleted from the medium (Sampling Point C). Despite the absence of toluene from the medium for several hours. five Group T proteins #14. 20. 24. 26 and 26 were still present in the cells at levels similar to those at sampling point B. However. the levels of other Group T proteins (#8. 15. 23. 25. and 27) had clearly decreased. and one (#22) was no longer detected. Nearly all of the Group P proteins were evident in these cells at levels higher than in the 12-h sample. The Group M protein (#28) was present. but at lower levels than previously measured.

At the final sampling time, phenol concentrations were low. Seven of the Group T proteins (#8, 14, 15, 20, 24, 26 and 27) were still detected, although most were at lower levels than those at Sampling Time C. Higher levels of four Group P proteins (#1, 2, 3, and 13) were present at this time, and the concentrations of five others (#5, 6, 11, 12 and 21) were similar to those at the previous sampling time. In contrast, five Group P proteins (#4, 7, 9, 10 and 17) were no longer detected in the cells at this stage of the cultivation. The Group M protein (#28) also was not detected.

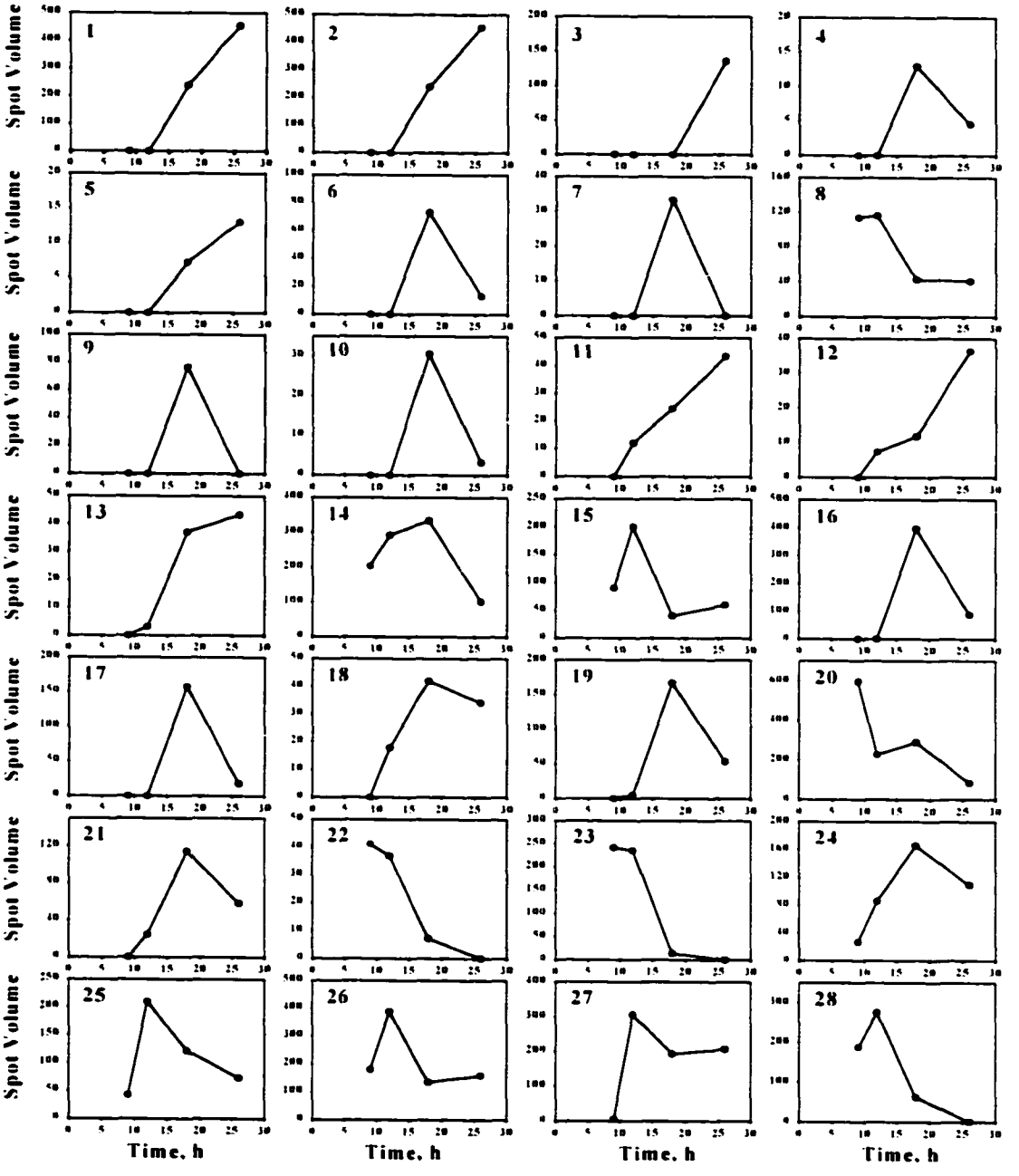

Figure IV-11 Time courses of intracellular concentrations of each of the Group T. P. and M proteins. Spot volumes were determined using Phoretix 2D software and reflect both spot size and intensity. Volume units are expressed on the same basis for all plots.

IV.2 Discussion

The results demonstrate that cells of *Pseudomonas putida* F1 synthesize different proteins when grown in batch culture on toluene alone, phenol alone, and mixtures of toluene and phenol. I grouped these differentially produced proteins according to the carbon and energy source(s) associated with their production. Thus, we detected (i) seventeen proteins synthesized during growth on phenol (Group P), (ii) ten proteins synthesized during growth on toluene (Group T), and (iii) one protein produced primarily during growth of *P. putida* F1 on the mixture of toluene and phenol (Group M). Since this information could increase our understanding of bacterial growth in mixed substrate environments, the identity and role of these proteins are of interest.

Cells grown on toluene alone did not produce Group P proteins, and those grown on phenol did not synthesize Group T proteins. Studies with *P. putida* F1 mutants have demonstrated that the initial reaction of both substrates is performed by toluene dioxygenase (30). Nearly identical metabolic intermediates (3-methyl catechol and catechol) result, and these are both cleaved by catechol 2,3-dioxygenase (13). Based on the high degree of similarity of enzymes and intermediates from the lower part of the *P. putida* F1 toluene catabolic pathway and those from the *P. pickettii* PKO1 phenol pathway (17).

Stress proteins are most generally defined as those that function to protect organisms from environmentally induced damage (27). Several studies have been performed in

which bacteria exposed to pollutants were observed to synthesize stress proteins (3, 7, 18, 35, 37). Often, the response to pollutant stress was found to overlap at least partially with responses to other stressors such as heat shock, oxidation, and SOS (3, 35, 37). Exposure of other *P. putida* strains to organic solvents has been observed to induce a variety of adaptation phenomena, including expression of a membrane-associated efflux system (16, 24), and alterations of the cell membrane (14, 24, 38). It is likely that at least some of the Group P and T proteins are associated with various stress responses to the presence of toluene and phenol. However, we also note that most of the stress response studies reported to date have involved sudden exposure of cells to levels of non-metabolizable chemicals that partially or totally inhibited growth. In contrast, *P. putida* F1 was grown on 50 (single substrate) or 25 (mixed substrate) mg/L toluene in our experiments, levels at which growth was not at all inhibited (25). The exposure to toluene and phenol in our experiments was not a sudden environmental perturbation; rather, inocula for the different cultivations were grown on the same substrate (or mixture) used in the primary experiment. And finally, strain F1 uses both pollutants as carbon and energy sources. It is thus possible that some of the Group T, P, and M proteins are associated with adaptation of *P. putida* F1 to the presence of phenol or toluene in their environment not for protection but rather to optimize cell growth.

The time sequence of results during the toluene-phenol mixture experiment sheds light on the transient nature of these responses. Of the Group T proteins, four (#8, 20, 22, and 23) decreased in concentration between Sampling Points A and D, while the other six increased and then decreased in concentration. Group P proteins showed analogous

temporal patterns, except that none were present at the first sampling point. Six of these proteins (#1, 2, 3, 5, 12, and 13) increased in concentration following the second sampling time, while the remaining Group P proteins reached a concentration maximum and declined to either low (#11, 16, 17, 18, 19, and 21) or nondetect (#4, 6, 7, 9, and 10) levels. Finally, the Group M protein was found to reach a concentration maximum near the time when the toluene concentration was very low and phenol consumption began. For the Group T and P proteins, then, there is a clear correlation between their presence in the cell and the identity of the substrate used for growth at that time in the cultivation.

Variations in the maintenance of these proteins were also noted, particularly among the Group T proteins. For example, the level of Group T protein #20 decreased through the mixture experiment but was retained at least 6 hours longer than other proteins with a decreasing pattern. Similarly, the levels of Group T proteins #14, 26, and 27 were found to increase from the first to the second sampling time, and then to remain at significant levels in the cells for the remainder of the experiment, long after toluene was depleted from the medium. Maintenance of intracellular levels of a protein is determined by interplay between synthesis and degradation that cannot be distinguished using 2-D PAGE. However, since these Group T proteins were not detected in the phenol-only cultivation, slower turnover of certain proteins is the more likely explanation for their longer maintenance times.

Although our focus was on the Group T, P, and M proteins, we note that the levels of proteins produced during growth on both substrates (i.e., all others not in Groups T, P, or

M) changed during the toluene-phenol mixture experiment. A prominent example of this is the protein above and to the right of #17 in Figure IV-11, the level of which increased and then decreased during the course of the mixed-substrate cultivation. Similar changes in other protein concentrations can also be noted in Figure IV-11.

In this work, we have clearly shown that cells growing on a mixture of substrates undergo significant physiological changes as reflected in their protein profiles. Furthermore, the production of particular proteins was related to the identity of the growth substrate, even when the same catabolic enzymes were used for both substrates. This connection between the patterns of protein production and substrate consumption suggests that further investigation of the identity and function of the Group T, P, and M proteins will lead to an explanation of the unusual mixed-substrate biodegradation kinetics observed previously in our laboratory (25). Although previous studies have examined the effects of toxic compounds on microorganisms, including those that also serve as growth substrates, ours appears to be the first report of microbial physiological responses to pollutant mixtures. This is an important issue, since most Superfund and other contaminated sites involve mixtures of hazardous chemicals. A complete understanding of bioremediation at these sites requires knowledge of the physiological responses of the responsible microorganisms to changes in their environment.

IV.3 References

1. **Berggren, K. N., E. Chernokalskaya, M. F. Lopez, J. M. Beechem, and W. F. Patton.** 2001. Comparison of three different fluorscent visualization strategies for detecting *Escherichia coli* ATP synthase subunits after sodium dodecyl sulfate-polyacrylamide gel electrophoresis. Proteomics **1**:54-65.
2. **Bio-Rad.** 1996. 2-D SDS-PAGE Standards. Product instruction 600-0039 Ch.B:011688. Bio-Rad Laboratories.
3. **Blom, A., W. Harder, and A. Matin.** 1992. Unique and overlapping pollutant stress proteins of *Escherichia coli*. Appl. Environ. Microbiol. **58**:331-334.
4. **Celis, J. E., Pavel Gromov.** 1999. 2D protein electrophoresis: can it be perfected? Current Opinion in Biotechnol. **10**:16-21.
5. **Dunn, M. J., and A. Gorg.** 2001. Two-dimensional polyacrylamide gel electrophoresis for proteome analysis. p. 43-60. *In* P. S.R. and M. J. Dunn (ed.). Proteomics. Springer-Verlag New York Inc., Trowbridge, UK.
6. **Dutt, M. J., and K. H. Lee.** 2000. Proteomic analysis. Current Opinion in Biotechnol. **11**:176-179.
7. **Faber F, T. E. a. W. H.** 1993. Transient repression of the synthesis of ompF and aspartate transcarbamoylase in *Escherichia coli* K12 as a response to pollutant stress. FEMS Microbiol. Lett. **111**:189-196.
8. **Gabor Miklos, G. L., and R. Maleszka.** 2001. Integrating molecular medicine with functional proteomics: Realities and expectations. Proteomics **1**:30-41.

9. **Gibson, D. T., G. J. Zylstra, and S. Chauhan.** 1990. Biotransformations catalyzed by toluene dioxygenase from *Pseudomonas putida* F1. p. 121-132. *In* I. S. Silver, A. M. Chakrabarty, B. Iglewski, and S. Kaplan (ed.), Pseudomonas: Biotransformations, Pathogenesis, and Evolving Biotechnology. American Society for Microbiology, Washington D.C.

10. **Gorg, A., W. Postel, and S. Gunther.** 1988. Two-dimensional electrophoresis. Electrophoresis **9:**531-546.

11. **Gorg, A., W. Postel, and S. Gunter.** 1988. The current state of two-dimensional electrophoresis with immobilized pH gradients. Electrophoresis **9:**531-546.

12. **Hatzimanikatis, V., L. H. Choe, and K. H. Lee.** 1999. Proteomics: Theoretical and experimental considerations. Biotechnol. Prog. **15:**312-318.

13. **Heald, S. C., and R. O. Jenkins.** 1996. Stability of toluene oxidation by *Pseudomonas putida* under nutrient deprivation. Appl. Microbiol. Biotechnol. **46:**388-392.

14. **Heipieper, F., and J. A. M. deBont.** 1994. Adaptation of *Pseudomonas putida* S12 to ethanol and toluene at the level of fatty acid composition of membranes. Appl. Environ. Microbiol. **60:**4440-4444.

15. **Kellner, R.** 2000. Proteomics: Concepts and perspectives. Fresenius J. Anal. Chem. **366:**517-524.

16. **Kieboom, J., J. J. Dennis, G. J. Zylstra, and J. A. M. de Bont.** 1998. Active efflux of organic solvents by *Pseudomonas putida* S12 is induced by solvents. J. Bacteriol. **180:**6769-6772.

17. **Kukor, J. J., and R. H. Olsen.** 1991. Genetic organization and rregulation of a meta cleavage pathway for catechols produced from catabolism of toluene, benzene, phenol, and cresols by *Pseudomonas pickettii* PKO1. J. Bacteriol. **173:**4587-4594.

18. **Lupi, C. G., T. Colangelo, and C. A. Mason.** 1995. Two-dimensional gel electrophoresis analysis of the response of *Pseudomonas putida* KT2442 to 2-chlorophenol. Appl. Environ. Microbiol. **61:**2863-2872.

19. **Marshall, T., and K. M. Williams.** 1984. Artifacts associated with 2-mercaptoethanol upon high-resolution two dimensional electrophoresis. Anal. Biochem. **139:**502-505.

20. **Molecular_Probes.** 1999. SYPRO Ruby Protein Gel Stain. Product Information MP 12000. Molecular Probes Inc.

21. **O'Farrell, P. H.** 1975. High resolution two-dimensional-electrophoresis of proteins. J. Biol. Chem. **250:**4007-4021.

22. **Perdew, G. H., H. W. Schaup, and D. P. Selivonchick.** 1983. The use of a zwitterionic detergent in two-dimensional gel electrophoresis of trout liver microsomes. Anal. Biochem. **135:**453-455.

23. **Rabilloud, T., and M. Chevallet.** 2000. Solubilization of proteins in two-dimensional electrophoresis. p. 9-29. *In* T. Rabilloud (ed.), Proteome Research: Two-dimensional gel electrophoresis and identification meyhods. Springer Verlag, Heidelberg, Germany.

24. **Ramos, J. L., E. Duque, J.-J. Rodriguez-Herva, P. Godoy, A. Haidour, F. Reyes, and A. Fernandez-Barrero.** 1997. Mechanisms for solvent tolerance in bacteria. J. Biol. Chem. **272:**3887-3890.

25. **Reardon, K. F., D. C. Mosteller, and J. D. Rogers.** 2000. Biodegradation kinetics of benzene, toluene, and phenol as single and mixed substrates for *Pseudomonas putida* F1. Biotechnol. Bioeng. **69:**385-400.

26. **Righetti, P. G., G. Tudor, and E. Ginnazza.** 1982. Effect of 2-mercaptoethanol on pH gradients in isoelectric focusing. J. Biochem. Biophys Methods **6:**219-227.

27. **Sanders, B. M.** 1993. Stress proteins in aquatic organisms: an environmental perspective. Crit. Rev. Toxicol. **23:**49-75.

28. **Sechi, S., and B. T. Chait.** 1998. Modification of cysteine residues by alkylation. A tool in peptide mapping and protein identification. Anal. Chem. **70:**5150-5158.

29. **Spain, J. C., and D. T. Gibson.** 1988. Oxidation of Substituted phenols by *Pseudomonas* putida F1 and *Pseudomonas* sp. strain JS6. Appl. Environ. Microbiol. **54:**1399-1404.

30. **Spain, J. C., G. J. Zylstra, C. K. Blake, and D. T. Gibson.** 1989. Monohydroxylation of phenol and 2,5-dichlorophenol by toluene dioxygenase in *Pseudomonas putida* F1. Appl. Environ. Microbiol. **55:**2648-2652.

31. **Steinberg, T. H., R. P. Haugland, and V. L. Singer.** 1996. Applications of SYPRO Orange and SYPRO Red Protein Gel Stains. Anal. Biochem. **239:**238-245.

32. **Steinberg, T. H., L. J. Jones, R. P. Haugland, and V. L. Singer.** 1996. SYPRO Orange and SYPRO Red Protein Gel Stains: One-Step Fluorescent Staining of

Denaturing Gels for Detection of Nanogram Levels of Protein. Anal. Biochem. **239:**223-237.

33. **Stryer, L.** 1996. Biochemistry. 4th ed. W.H. Freeman and Company. New York. USA.

34. **Valdes, I., and A. B. A. Pitarch, M. Llorente, C. Nombela, E. Mendez.** 2000. Novel procedure for the identification of proteins by mass fingerprinting combining two-dimensional electrophoresis with fluorscent SYPRO Red staining. J. Mass spectrom. **35:**672-682.

35. **VanBogelen, R. A., P. M. Kelley, and F. C. Neidhardt.** 1987. Differential induction of heat shock. SOS. and oxidation stress regulons and accumulation of nucleotides in *Escherichia coli*. J. Bacteriolol. **169:**26-32.

36. **VanBogelen, R. A., and F. C. Neidhardt.** 1990. Global systems approach to bacterial physiology: protein responders to stress and starvation. FEMS Microbiol. Ecology **74:**121-128.

37. **Vercellone-Smith, P., and D. Herson.** 1997. Toluene elicits a carbon starvation response in *Pseudomonas putida* mt-2 containing the TOL plasmid pWW0. Appl. Environ. Microbiol. **63:**1925-1932.

38. **Weber, F. J., S. Isken, and J A M de Bont.** 1994. *Cis/trans* isomerization of fatty acids as a defense mechanism of *Pseudomonas putida* strains to toxic concentrations of toluene. Microbiology **140:**2013-2017.

CHAPTER V IDENTIFICATION OF PROTEINS ASSOCIATED WITH THE BIODEGRADATION OF TOLUENE-PHENOL MIXTURE

V.1 Research Motivation and Goals

The proteome analysis in Chapter IV revealed that 10 Group T proteins, 17 Group P proteins and one Group M protein were differentially produced during the growth of *P. putida* F1 on toluene-phenol mixtures. The results from proteome analyses also demonstrated the power of 2-D PAGE to simultaneously separate and visualize several hundred proteins in a single gel. However, simply noting differences in spot patterns on gels provides little information about changes in cell physiology. To provide a more specific and particular understanding of the physiological changes of the cell in response to the presence of those chemical mixtures, both identification and characterization of important proteins are essential. This chapter presents the work that was done to identify the proteins corresponding to several spots, and characterization efforts are described in Chapter VI.

In order to analyze proteins at the subpicomol level from a 2-D PAGE gel, two unique and powerful tools were utilized: *de novo* N-terminal sequencing and mass spectrometry

followed by protein and genomic database searches. Protein identification through *de novo* sequencing was conducted via traditional N-terminal sequencing by Edman degradation from the external- and internal amino termini of proteins. Both matrix-aided laser desorption/ionization time-of-flight (MALDI-TOF) mass spectrometry and electrospray ionization tandem mass spectrometry (ESI-MS/MS) were employed to obtain mass spectra and peptide sequences. The combination of mass spectrometry and database searching makes it possible to obtain identifications of proteins faster and easier. However, the current procedures to acquire protein identifications are mostly based on those species that already had complete genomic sequences (42). Since the complete genomic sequence of *P. putida* F1 was not available, protein identification with conventional MS and database searching were examined by the all databases for previously sequenced genomes, from microorganisms to human.

In this chapter, results of protein identification obtained by several different technologies and the identification technologies themselves are evaluated based on their effectiveness and sensitivity.

V.2 Results

V.2.1 STRATEGY FOR OBTAINING PROTEIN IDENTIFICATION

The protein identification processes used in this work depended on the availability of facilities at the time. Protein samples from 2-D PAGE gels were subjected to in-gel digestion and subsequent protein extraction processes (Chapter III).

The following describes outline of each method for protein identifications. The detailed methods are described in the Chapter III and the corresponding sections are followed by the end of each paragraph.

A. Although Edman degradation N-terminal sequencing is an older technique, it could provide unambiguous peptide sequencing information from the amino terminus of a peptide (Chapter III.8.1).

B. Protein spots that could not be identified by the external Edman degradation method were trypsin digested and then separated in a microbore C_{18} HPLC column. Each peak fraction was manually collected. Trypsin digestion exposed the free amino termini of peptide fragments. The fractions that contained greater than 5 pmol of protein were transferred to PVDF membranes and subjected to the Edman degradation sequencing unit for internal N-terminal sequencing (Chapter III.8.2)

C. Protein spots that were not identified by either method of N-terminal sequencing were further examined by mass spectrometric technology. Protein spots from two 2-D PAGE gels were digested by a modified porcine trypsin and a ZipTip C_{18} microcolumn was used to remove salts from the peptide fragments solution. The desalted peptide fragments were analyzed by a MALDI-TOF mass spectrometer and the mass-to-charge information for each peptide peak was collected. The mass finger printing information acquired from MALDI-TOF was run against various protein and genomic databases through the Internet to identify the protein. (Chapter III.8.3.1).

D. Since Shevchenko *et al.* (39) reported that the amount of peptide was not sufficient to run MALDI-TOF Post Source Decay (PSD) if MALDI peptide mass mapping did not lead to direct protein identification. I did not use MALDI-TOF PSD even if the MALDI-TOF MS on the campus was capable of performing PSD operation. Instead. the remaining peptide samples after MALDI analysis and freshly prepared protein samples from gels were applied to an ion trap electrospray tandem mass spectrometer. Tandem mass spectra were interpreted manually for the peptide sequences. In this approach. peptides were separated by a capillary HPLC column and separated peptides were continuously injected into the ESI-MS/MS through a spray nozzle. Both the spectra acquired by the first and the second mass analyzer were recorded and searched against various protein

and genomic database with SEQUEST (6. 8. 27) and a peptide sequence tag algorithm (24. 28) (Chapter III.3.2).

V.2.1.1 Identification of the proteins by Edman degradation

V.2.1.1.1 External Sequencing

The proteins separated by 2-D PAGE were electrically transferred to PVDF membranes and detected by Coomassie blue stain. External Edman sequencing was performed by Ms. Sandy Kielland (Kielland *a* uvic.ca) of the University of Victoria, Canada. Five protein spots were excised from two membranes, shown in Table V-1. Three proteins (one from Group M and two from Group T) of interest were selected for the identification. Two protein spots (Figure V-1) were selected to evaluate the performance of Edman sequencing and detection limit.

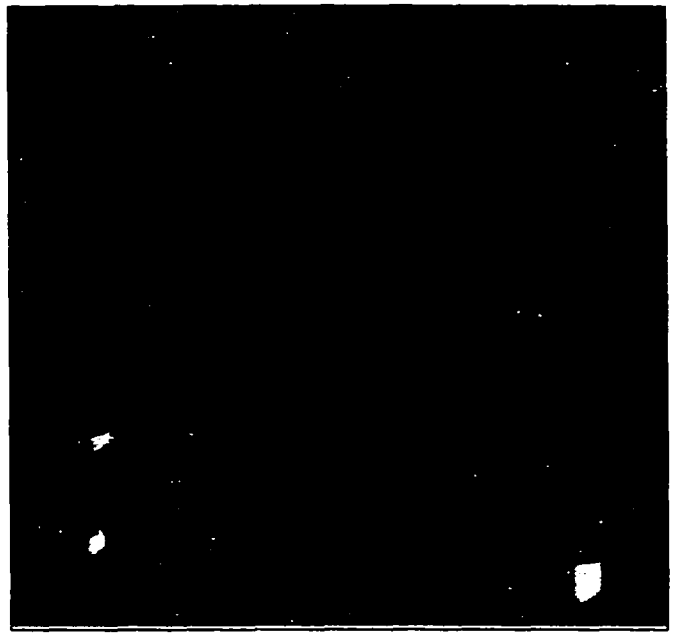

Figure V-1 **Protein separation from a PVDF membrane. Arrows in the left cornor indicate the protein spots for Test 1 (upper) and Test 2 (lower). The arrow in the bottom right cornor indicates #28 (Group M) protein. The two Group T proteins sent for analysis are not indicated here.**

Table V-1 **The list of samples that applied to Edman degradation for external amino acid sequencing. See Chapter III for the detail experimental condition.**

Protein Spot Number	Group	Starting amount of proteins pmol*
Test 1	-	90
Test 2	-	75
14	Group T	15
24	Group T	35
28	Group M	100

* Approximated visual estimate.

Only one protein was successfully sequenced from the amino terminus. Protein #28 was identified as Acyl Carrier Protein (ACP) by the fasta33_t search engine against SWALL (SWISS-PROT All library) protein database with 22 resulting amino acid sequences that were acquired by Edman sequencing. The N-terminal sequencer originally detected total 27 amino acid residues. but only 22 amino acid residues were used to search for an identity because the 23th to 27th amino acids had lower reliability in chromatogram analysis.

Table V-2 Identification of protein spot #28 by sequence identity comparison. Identification was searched by fasta3 search engine against SWALL database.

Species	5	10	15	20		z-score/ Probability	Ref.
Protein #28	- STIEE	RVKKI	VAEQL	GVKEE	EV	-	HERE
ACP_PSEAE	**M**STIEE	RVKKI	VAEQL	GVKEE	EV	246.6/5.0e-06	(21)
ACP_OCELI	- STIEE	RVKKI	V**S**EQL	GVKSE	E**I**	236/1.5e-05	(48)
ACP_Q9EZI1	**M**STIEE	RVKKI	V**V**EQL	GVKEE	EV	235.7/1.5e-05	(14)
ACP_PSESM	STIEE	RVKKI	VAEQL	GVKSE	EV	232.4/2.4e-05	(48)
ACP_ECOLI	STIEE	RVKKI	**IG**EQL	GVK**Q**E	EV	227.1/4.7e-05	(37. 45)

The other 4 proteins could not be sequenced either because of the blockage of their N-termini or due to an insufficient amount of protein samples on the PVDF membrane. The biggest problem in amino terminus sequencing is N-terminal blocked proteins: in this case. no free α–amino group is available for coupling with the Edman reagent. phenylisothiocyanate. and the chemical degradation process is blocked. N-terminal blockage is caused by either post-translational modification. e.g. acetylation of serine (S)

or threonine (T), or formylation of methionine (M), or by cyclization of glutamine (Q) when the N-terminal amino acid to pyroglutamic acid (22) and acetylation can happen because of prolonged exposure to acetic acid.

V.2.1.1.2 Internal Sequencing

The percentage of N-terminal blocked protein in prokaryotic cells is generally lower than in eukaryotic cells (18, 38). However, the proteins in *P. putida* F1 were observed to have a high level of amino terminus blockage because even with more than 50 pmol of both Test 1 (90 pmol) and 2 (75 pmol) sample proteins it was also impossible to read any sequences. When proteins have a high percentage of N-terminal blockage, the next alternative approach for protein identification could be either using internal N-terminal sequencing after proteolytic digestion of a protein and HPLC purification, or mass spectrometry (38, 53).

Two protein spots, #14 and 24, were subjected to a microbore HPLC column after in-gel digestion by modified porcine trypsin. The starting amount of protein was 60 pmol for #14 and 140 pmol for #24 collected from four standard slab gels stained by Coomassie blue.

Before running the N-terminal sequencer, all manually collected peak fractions were analyzed with MALDI-TOF to verify the existence of the peptide and to identify the trypsin autolysis products. Three typical sizes of trypsin peaks (label with "T" in Figure

V-2) were observed in MALDI spectra and they were excluded from N-terminal sequencing.

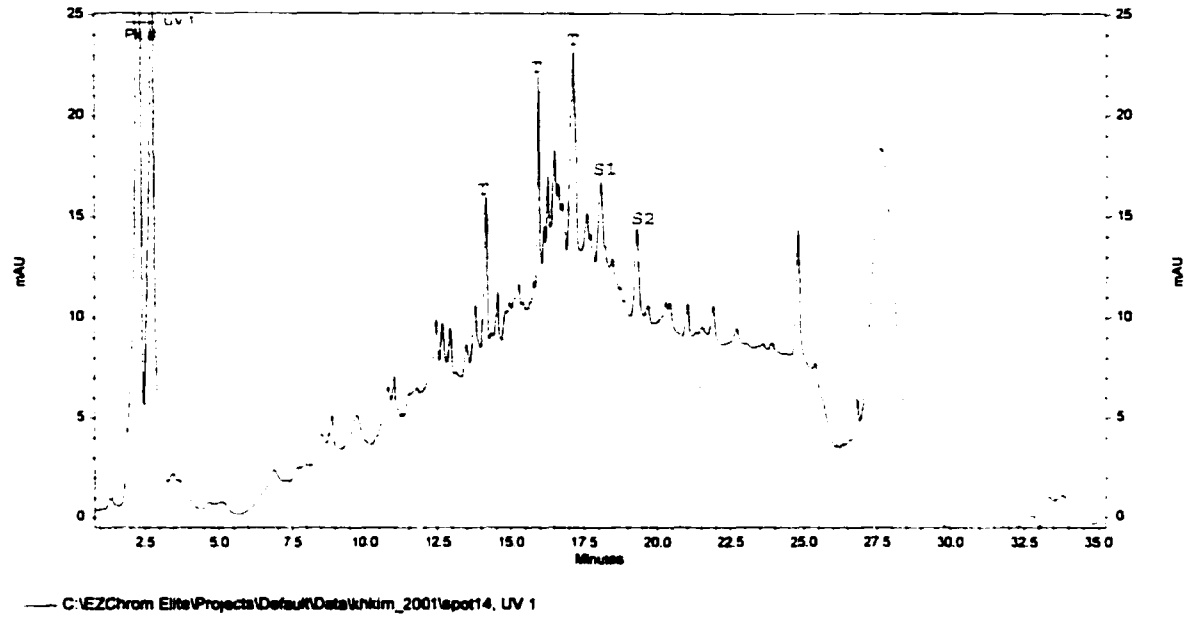

Figure V-2 HPLC chromatogram of Protein # 14 after trypsin digestion. Trypsin autolysis fragments are labeled with T. S1 and S2 denote the sample peaks that were subjected to Edman sequencing. One mass unit (mAU) is equivalent to 1 pmol. See Chapter III for the detailed operating conditions.

The concentrations of two significant peptide peaks from Protein #14, S1 and S2, were estimated a 5 pmol each. Both peptides were transferred to PVDF membranes individually and introduced to an N-terminal sequencer (Procise, Applied Biosystems) in the Macromolecular Resources Facility on the CSU campus (http://mmr.bmb.colostate.edu/).

Unfortunately, none of the peak fractions from Proteins # 14 and 24 were sequenced by the internal N-terminal peptide sequencing. Because the amount of peptides (~5 pmol)

was lower than the detection limit (10 pmol) of the N-terminal sequencer, the separation column for phenylthiohydantoin (PTH)-amino acid in the HPLC of the N-terminal sequencer could not detect a significant increase of any amino acid between separation cycles (Figure V-3).

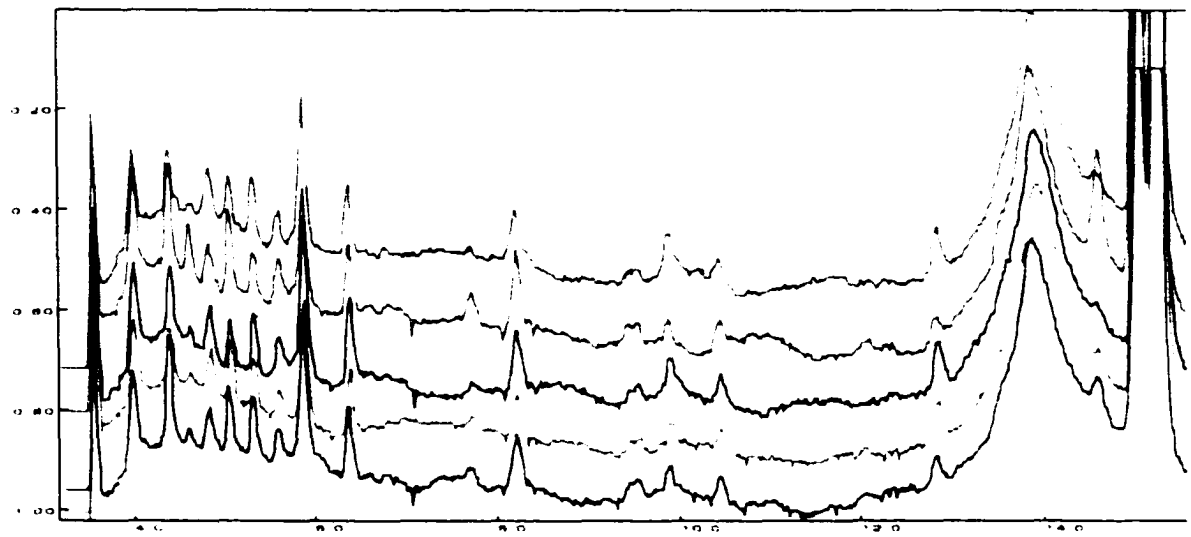

Figure V-3 Chromatogram of PTH-amino acid separation by HPLC in a N-terminal sequencer. This represents the combined chromatogram of five separate cycles of PTH-amino acid separation. Cycles are numbered from the bottom (cycle 1) to the top (cycle 5). By comparing previous and current chromatograms, peak that differs significantly from a previous trace represents a corresponding amino acid residue.

V.2.2 PROTEIN IDENTIFICATION BY MASS SPECTROMETRY

Some proteins of interest that could not be identified by Edman sequencing were identified by mass spectrometry. Protein identification by mass spectrometry is divided into two categories: mass analysis and amino acid sequencing (57). MALDI-TOF was employed to perform mass fingerprint analysis and an ion trap electrospray tandem mass spectrometer (LC-ESI-MS/MS) was utilized to obtain internal peptide sequences based on tandem mass spectra. Both mass analysis and sequencing data were analyzed with protein and genomic databases including various types of expressed sequence tag (EST) databases.

V.2.2.1 Selection of the proteins

At least 28 proteins were differentially produced during the biodegradation of toluene-phenol mixtures by *P. putida* F1. Since Protein # 28 was already identified as acyl carrier protein (ACP) by Edman sequencing, 27 proteins were candidates to be identified by mass spectrometry. Of those 27 proteins, six proteins were examined to obtain their identification by mass spectrometric analysis in this study. Three criteria were applied to the selection of proteins: First, target proteins should represent either Group P or Group T. To avoid cross contamination by adjacent protein spots, the second criterion was that target proteins should be isolated from neighboring proteins on the 2-D PAGE gels.

Third. target proteins should be able to be visualized by the Coomassie blue staining method to ensure as much starting protein mass as possible for in-gel tryptic digestion and consecutive mass spectrometric analysis. Table V-3 describes their starting mass. type of mass spectrometry. and group. The differential production profiles of the individually selected protein are presented in Figure V-4.

Table V-3 List of protein samples for mass spectrometric analysis. All protein samples were digested by trypsin in-gel digestion procedure. See Chapter III for more detail information.

Protein #	Group	Starting amount pmol*	Mass Spectrometer **
1	P	20	MALDI & ESI-MS/MS
8	T	23	MALDI & ESI-MS/MS
18	P	28	MALDI
19	P	30	MALDI
20	T	30	MALDI
24	T	35	MALDI

* Starting approximated amount is determined by visual estimation.

** Proteins # 1 and 8 were extracted from six 2-D PAGE gels for both MALDI and tandem mass spectrometry. Two 2-D PAGE gels were used to prepare the rest of the protein samples for MALDI-TOF alone. Proteins were separated by standard size 12% slab gels and detected by the Coomassie blue stain.

Protein #	2-D PAGE images during mixture experiment				Group
	A	B	C	D	
1		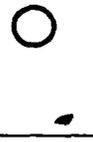			P
8					T
18	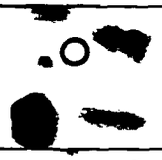				P
19				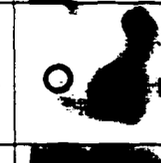	P
20		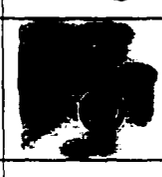	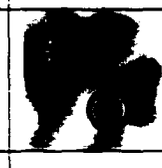	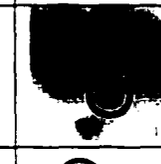	T
24					T

Figure V-4 Differential protein production of the proteins selected for mass spectrometric analysis during the growth of *P. putida* F1 on toluene-phenol mixtures. Proteins were selected by the three criteria discussed in the previous section.

V.2.2.2 Mass fingerprinting

For mass determination, the mass scale of a MALDI-TOF MS should be properly calibrated. The α-matrix contains its own mass spectrum. Since these generic mass spectra of the matrix may have greater ion densities than those of peptide molecular ions, they can lower the signal of real peptide masses in acquiring mass spectra. The generic spectra of the α-matrix are presented in Figure V-5A. However, since the small peptide fragments could often play an important role in protein identification and most of those generic spectra from the α-matrix were usually smaller than 750 (*m/z*), extra caution was practiced in collecting the peptide fragments smaller than 750 (*m/z*). The significant peaks (signal-to-noise (SN) ratio greater than 3) were collected and excluded from the sample peptide spectra.

For the calibration of the MALDI-TOF MS, two sets of mass standards were used (19). As an external mass standard, a mixture of angiotensin I (1296.7 Da), glucagon (3481.6 Da) and ubiquitin (8560.6 Da) were used. Ubiquitin is not shown in Figure V-5B because it falls outside the normal detection mass range (500 ~ 5000 Da). The external standard evaluates the quality of mass measurement for the sample peptide fragments. Both measured masses of angiotesin I (1296.68) and glucagons (3481.6) agreed with their reported masses with less than 25 ppm error. This agreement indicated the high accuracy of the MALDI measurements. The internal standard directly calibrates the mass measurements of sample peptide fragments within the sample peptide mixtures. Two particular products of autolysis trypsin peptides were employed as the internal standards

(842.56 and 2211.67 Da) as shown in Figure V-6 B-D. These two peptides are well known as internal standards (4, 12). The MALDI spectra of the α-matrix blank and autolysis trypsin peptides were excluded from a list of spectra that was used for the identification search. The threshold of signal to noise (S/N) in mass spectra was 3 to ensure unambiguous search results.

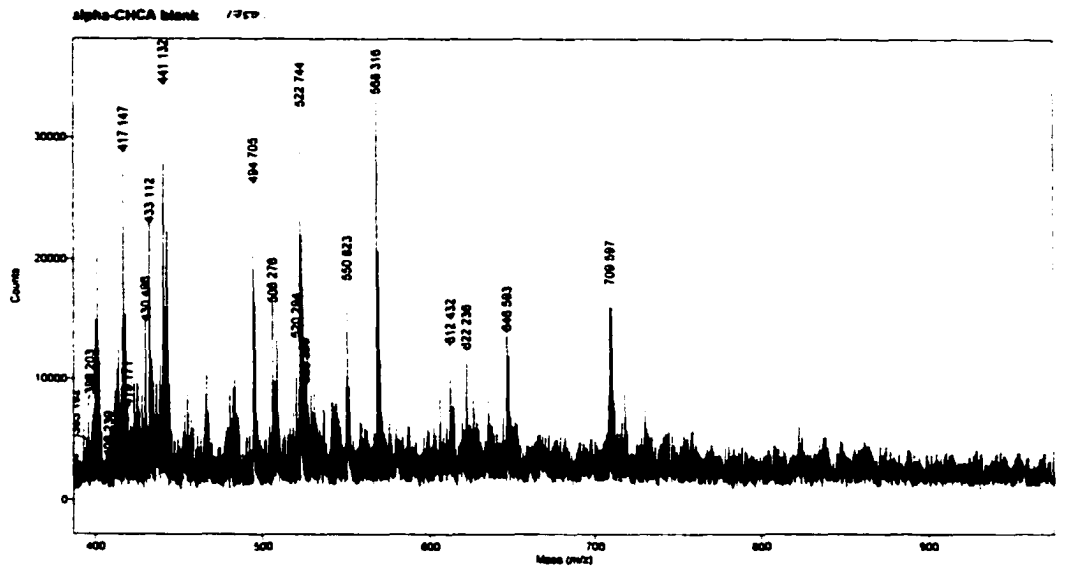

A

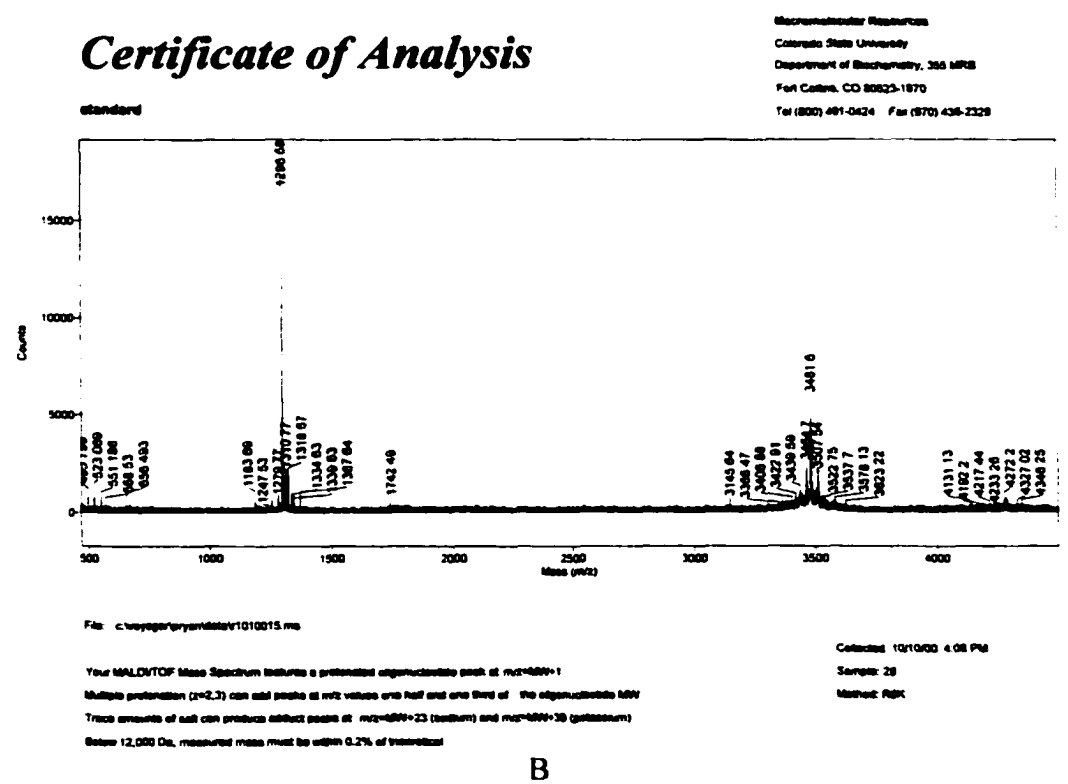

B

Figure V-5 **A: Generic mass spectra of α-matrix. B: Mass spectrum of the external standard peptides and impurities. angiotesin 1: 1296.7, glucagon: 3481.6, ubiquitin: 8560.6 (not shown). A laser intensity of 1750 was applied for both measurements.**

The MALDI spectra of Protein # 18 are shown in Figure V-6. The mass peaks outside the calibrated range (842.509 ~ 2283.22) were automatically extrapolated by the spectrum importing software (GRAMS32, Applied Biosystems). The mass spectra for Protein # 18 (Figure V-6A) had mass peaks ranging from 450 to 3500. Peptide fragments were sized between 450 and 3500 *m/z* and well-scattered peptide fragments indicated successful tryptic digestion. No peak greater than 3500 *m/z* was detected. Since this view of the mass spectrum is too wide to be analyzed, zoomed spectra were used to determine the mass of each peptide (Figure V-6B-E). The software performed individual mass assignment based on the manually selected threshold value. The threshold value was decided by signal-to-noise (SN) value of each protein sample and the applied laser intensity. Since higher laser intensities generated noisier peaks, a constant laser intensity was initially applied (1850), but it was varied up to 2000 when signals in a spectrum were too low because of the small amount of a peptide. Each peak represents monoisotopic ion in a spectrum. All detected peptide masses with a SN ratio greater than 3 were collected. Since this collection could include peaks generated by the α-matrix and autolysis trypsin fragments, sorting them out was necessary. After manual sorting, the final list of peptide mass was compiled in Table V-4.

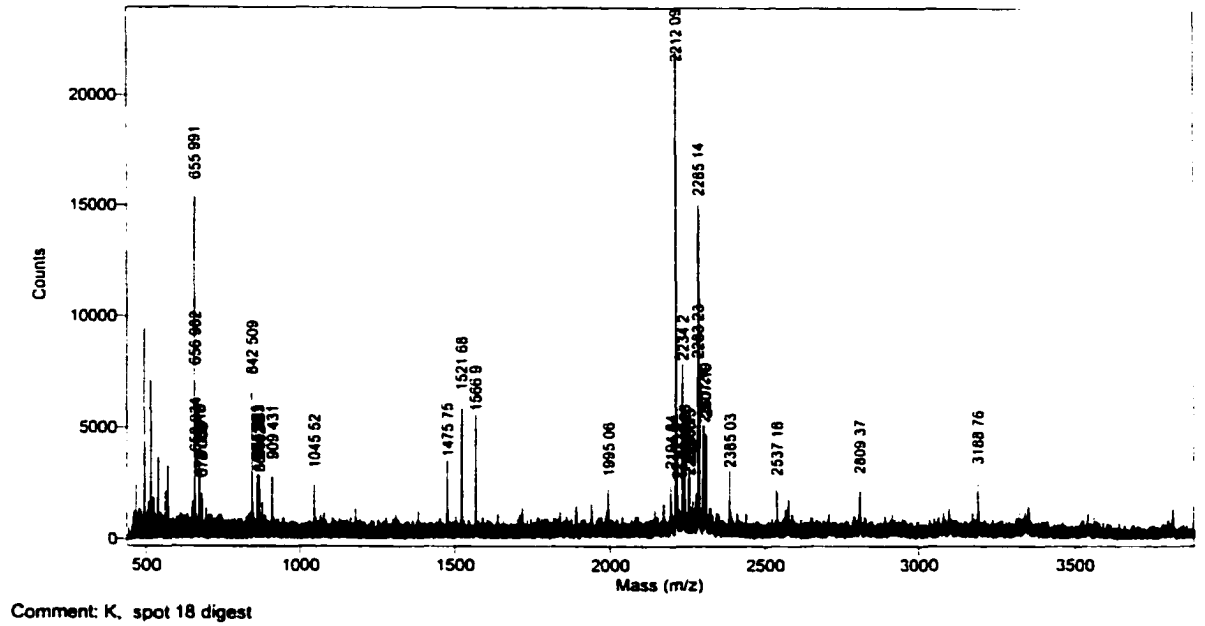

Comment: K, spot 18 digest

Method: R6K	Accelerating Voltage: 25000	Laser : 1700	Mirror Ratio: 1.100
Mode: Reflector	Grid Voltage. 75.000 %	Scans Averaged: 256	PSD Mirror Ratio: 1.0000
	Guide Wire Voltage: 0.050 %	Pressure: 4.44e-07	Timed Ion Selector: 382.2 OFF
	Delay: 350 ON	Low Mass Gate: 300.0	Negative Ions: OFF

A

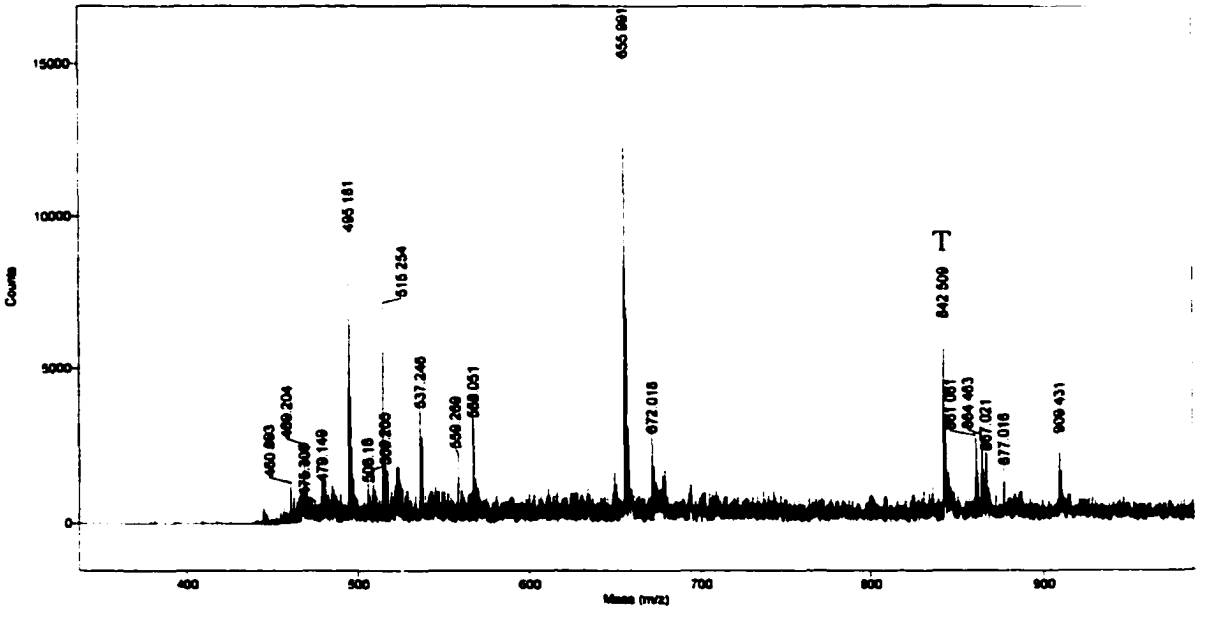

B

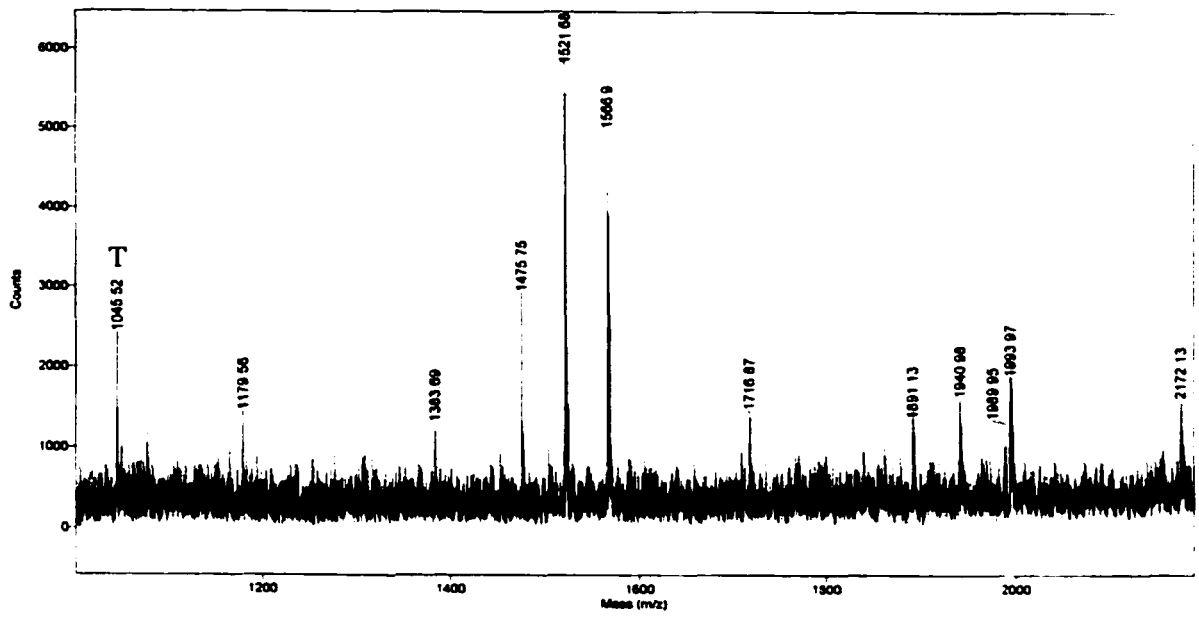

C

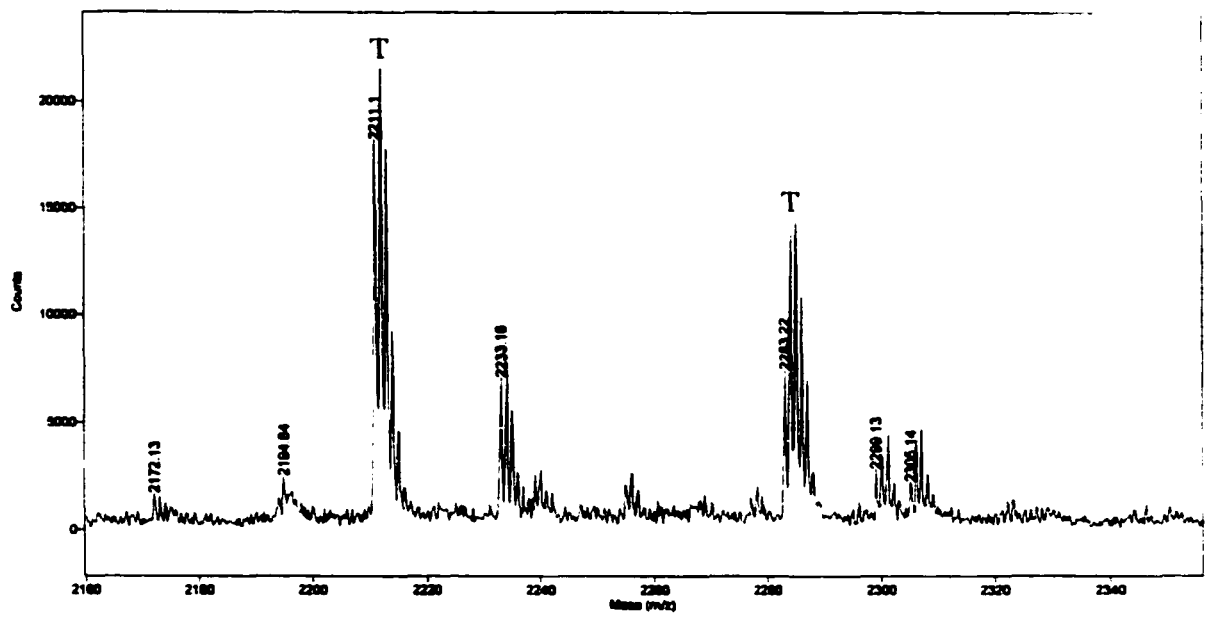

D

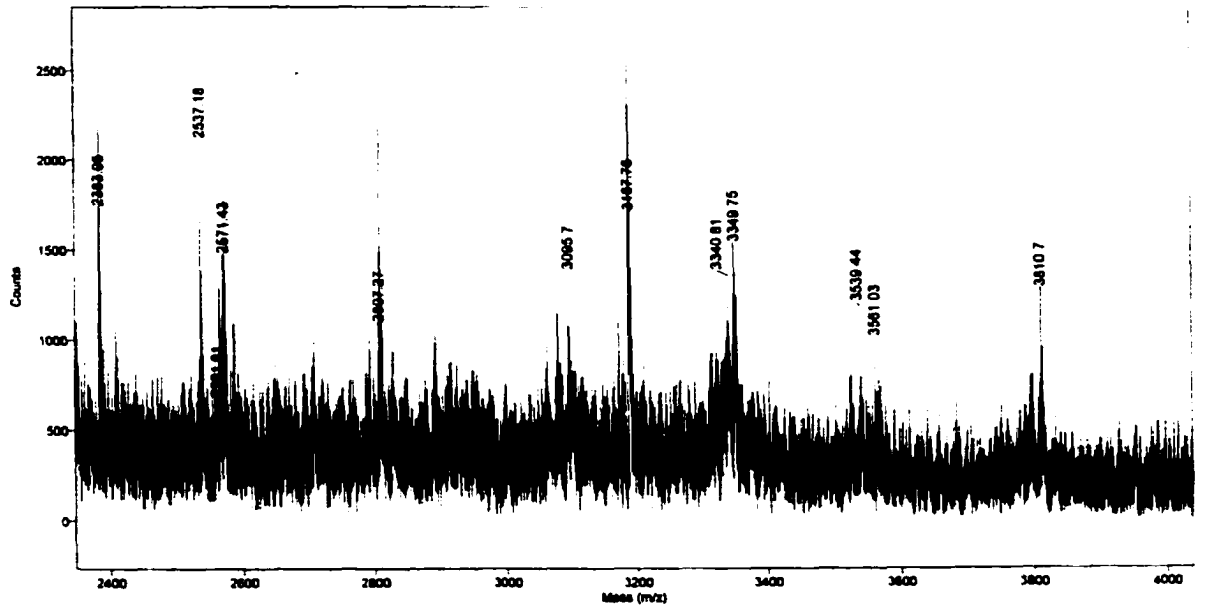

E

Figure V-6 **Mass spectra of Protein #18. A: Mass range 450 – 3500, B: Mass range 400 –1000, C: Mass range 1000 – 2200, D: Mass range 2150 – 2340, E: Mass range 2350 – 4000. All mass (*m/z*) values were obtained after calibration with the internal standard (842.509 and 2283.22). All detected trypsin fragments are labeled by "T".**

Table V-4 List of mass fingerprints of the target proteins. All possible trypsin and human keratin derived peaks were excluded.

Protein # 1	# 8	# 18	# 19	# 20	# 24
508.58	537.41	506.16	524.10	973.50	517.43
522.60	568.25	509.21	568.12	993.51	529.39
537.35	574.21	537.25	590.06	1036.53	537.45
550.69	635.44	559.27	656.01	1045.52	551.38
568.18	679.58	568.05	672.00	1090.50	559.38
656.06	684.40	655.99	1045.56	1107.52	566.55
672.02	689.44	672.02	1306.74	1118.48	635.42
1045.58	820.35	861.06	1336.72	1126.52	636.40
1067.59	864.47	864.46	1364.73	1165.55	668.42
2194.67	1045.42	867.02	1400.73	1193.61	679.62
2233.06	1126.34	877.02	1434.53	1201.63	684.44
2255.15	1307.34	909.43	1437.57	1234.68	689.43
2305.23	1365.36	1045.52	1543.86	1263.61	705.39
3310.57	1562.17	1521.68	1570.71	1277.66	843.51
3323.73	1607.22	1566.91	1700.84	1300.53	880.48
3338.57	1475.30	1716.88	1791.63	1307.64	1045.46
4489.50	1562.17	1891.13	1940.92	1320.56	1126.41
4728.88	1607.22	1940.98	2194.71	1329.60	1421.39
4747.16	1638.27	1989.95	2233.17	1365.64	1422.39
4760.48	1652.19	2172.13	2239.25	1373.60	1435.36
5560.75	1655.46	2194.84	2255.00	1390.64	1617.22
	1768.18	2233.16	2283.19	1427.78	1708.10
	1774.30	2299.13	2299.07	1458.76	1940.17
	1794.24	2305.14	2306.26	1561.76	1941.24
	1851.29	2537.18	2356.13	1575.77	1994.34

	1910.13	2561.81	2407.06	1638.83	2193.87
	1922.15	2571.44	2535.18	1699.74	2238.22
	1940.17	2807.27	2659.30	1707.77	2239.23
	1962.14	3095.70	2675.31	1791.75	2266.52
	1970.25	3187.76	2807.40	1838.90	2282.19
	1986.25	3340.81	3339.77	1851.95	2299.13
	2082.12	3349.75		1924.35	2406.85
	2144.03	3539.44		1940.87	2407.98
	2150.14	3561.03		2150.03	2410.00
	2193.89	3810.70		2194.59	2535.04
	2213.40			2234.04	2535.98
	2220.11			2239.05	2563.97
	2232.12			2261.22	2791.80
	2238.10			2297.08	2805.87
	2247.53			2367.23	2806.92
	2265.03			2408.68	2824.87
	2284.13			2502.22	2920.83
	2298.11			2537.61	3076.84
	2304.06			2566.24	3094.87
	2406.95			2585.05	3310.81
	2419.06			2706.05	3332.61
	2534.96			2792.18	3348.69
	2562.91			2808.30	3809.49
	2704.69			2826.77	
	2778.31			2873.95	
	2790.78			2933.42	
	2805.79			3050.19	
	2822.88			3079.19	
	2913.89			3079.79	
	2932.24			3097.25	
	3077.67			3350.04	
	3093.88				
	3310.26				
	3329.81				
	3337.09				
	3348.54				
	3393.11				
	3412.69				
	3807.35				
21 peaks	**74 peaks**	**35 peaks**	**31 peaks**	**56 peaks**	**48 peaks**

V.2.2.3 Database search

The National Center for Biotechnology Information (NCBI) provides a number of different bioinformatics databases and search engines for proteomics and genomics research (52). The protein identity search of this study used the nonredundant protein database of NCBInr through two different search engines, ProFound (58) and MS-Fit (30, 56). Since both search engines use different algorithms searching the same databases

(NCBInr and SWISS PROT), the identification could give higher confidence if the identification results agree with each other. MS-Fit determines protein identifications by the number of sample peptide matches with masses calculated for theoretically possible enzymatic cleavage (trypsin in this study) products for every sequence in a protein/DNA sequence database. The degree of matches is calculated by a scoring system based on the observed frequency of peptides from all proteins in a database in a given molecular weight range (called the "MOWSE" score) (30). Zhang *et al* (58) designed a new protein search engine in 2000, which utilized a Bayesian algorithm. The Bayesian algorithm calculates the rank of protein identity candidates by employing individual properties of a protein in the database as well as other information relevant to the peptide mapping experiments. Individual peptide mass information of the proteins # 1, 8, 18, 19, 20, and 24 were applied to both search engines independently and their identifications were searched against the same protein database. NCBInr protein database.

A number of parameters pertaining to sample peptide preparation was varied. Typical search parameters were as follow:

1. Cystein was completely alkylated by iodoacetamide (*S*-carbamidomethylcystein) to improve mass discrimination resulting to improved resolution during the equilibration process between IEF and SDS-PAGE.
2. Maximum peptide mass error allowed was 50 ppm or 0.5 Da.
3. More than 4 measured peptide masses should be matched with the theoretically produced peptide masses derived from the databases (NCBInr) to be considered as an identification candidate.

4. Up to two missed cleavages per peptide were considered.
5. No restriction was placed on the isoelectric point of the proteins, and the allowed protein mass range was 0 to 300 kDa unless otherwise noted.

A more detailed list of parameters is listed in Table V-5.

Table V-5 List of constraints for identification search.

Parameter	ProFound	Ms-Fit
Date [1]	May 9, 2001	May 9, 2001
Database [2]	5/7/2001 NCBInr	5/7/2001 NCBInr
Taxonomy Category	All	All
Mass Range [3]	All	All
pI Range [4]	0 - 14	0 – 14
Search for	Single protein	Identity
Digest by	Trypsin	Trypsin
Max. missed cut [5]	0 - 2	0 – 2
Modifications [6]	$+C_2H_3OH$@C -OH@M	$+C_2H_3OH$@C -OH@M
Charge State @ N-terminus	+MH	Protonated (+MH)
Mass Tolerance [5]	< 0.5 Da	< 100 ppm
DNA Frame Translation [7]	-	3
Min. # peptides required to match [7]	-	4
Pfactor [7]		0.4
Peptide masses are	Monoisotopic	Monoisotopic
Instrument [7]	-	MALDI-TOF

1. The lastest date of identity search.
2. NCBInr incorporates SWISS-PROTnr (52).
3. Fixed unless otherwise noted.
4. No variation at all.
5. Varied to find the highest z-score (ProFound) or MOWSE (MS-Fit).
6. Complete alkylation at cystein by the iodoacetamide. Neglect the possible alkylation by lysine residuals. Oxidation at methionine.
7. Parameters only for MS-Fit and used default values. Six frame translations could be better, but it was not available at the time.

V.2.2.4 Identifications

Great care was practiced during the tryptic digestion, peptide extraction, and spotting sample onto a MALDI sample plate, but some human keratin peptides were detected in the MALDI spectra. This indicates the outstanding sensitivity of MALDI-TOF MS technology. Before conducting an identification search of the sample proteins, human keratin peptides were sorted out from the collection of the sample peptide masses. The peptides from human keratin were 515.25, 1179.56, 1383.70, 1475.74, 1993.96, and 2383.94 Da. These peptides were detected from all six sample proteins, although the frequency and variety of appearance were varied among the samples. The information for keratin peptides was obtained from the Proteometrics web site (http://www.proteometrics.com/).

The results of a protein database search for Protein #18 are presented in Figure V-7. Since the NCBInr database has been updated regularly, the latest search results are presented here (May 9, 2001). However, the identification of Protein # 18 has been consistent since April, 2000 and the estimated z-score has not changed. The ProFound search engine ranked "3-oxoadipate CoA-transferase subunit A (β-ketoadipate-succinyl-CoA transferase" first, shown in Figure V7-A with a box. The probability of the ID candidate was 1.0, indicating a perfect match. The estimated z-score (2.28) is greater than 1.60, demonstrating that the ID does not include any random matches between the submitted peptide masses and the theoretically possible peptide masses in the entire NCBInr database (58). More detailed information of the ID is shown in Figure V7-B.

The total coverage of matched peptides is 37%, shows a ladder-type coverage that indicates no overlap, and there were zero missed cuts. The error range for six matched peptides is less than ± 0.2 Da, which is equivalent to 8.2 ppm. The theoretical pI value (5.3) of the first ranked ID candidate shows good agreement with apparent pI value (5.4) obtained from 2-D PAGE images. However, theoretical molecular weight (24.27 kDa) does not agree with the apparent molecular weight (37 kDa).

The same peptide mass information was introduced into another search engine, MS-Fit. The summary of the results by MS-Fit is presented in Figure V-7C. MS-Fit produced the same identification as ProFound. The same number and sizes of peptides were matched by the MS-Fit search engine (Figure V-7D). Based on this identification, the full protein sequence of ketoadipate-succinyl-CoA transferase was derived from the NCBInr protein database (Figure V-7E).

ProFound - Search Result Summary

1	1.0e+000	2.28	gi|1172040|sp|Q01103|PCAI_PSEPU 3-OXOADIPATE COA-TRANSFERASE SUBUNIT A (BETA-KETOADIPATE:SUCCINYL-COA TRANSFERASE)	37	5.3	24.27	
2	2.4e-009	-	gi|1151053|pir||G82581 probable binding protein component of ABC dipeptide transporter PA5317 [imported] - Pseudomonas aeruginosa (strain PAO1)	11	6.5	58.09	
3	1.8e-009	-	gi|9278613|emb|CAB97302.1| (AL160493) possible y50d7a.g protein [Leishmania major]	16	5.8	33.42	
+4	2.3e-010	-	gi|4741934|gb|AAD28763.1|AF130859_2 (AF130859) sialic acid lyase [Clostridium perfringens]	24	4.9	32.56	
5	8.4e-011	-	gi|3513641|gb|AAC71754.1| (AF071302) gag protein [Human immunodeficiency virus type 1]	26	6.4	27.22	
6	4.8e-011	-	gi|7471886|pir||B75597 first mannosyl transferase - Deinococcus radiodurans (strain R1)	18	6.8	40.88	
+7	4.6e-011	-	gi|7708187|emb|CAB90037.1| (AJ236425) ATP synthase beta subunit [Cerallia brachiata]	11	4.9	51.01	
+8	4.4e-011	-	gi|8050573|gb|AAF03257.1|AF071895_1 (AF071895) glucosamine 6-phosphate isomerase [Giardia intestinalis]	20	6.5	30.15	
9	4.1e-011	-	gi|11356003|pir||D82063 probable thiamin ABC transporter, permease protein VC2538 [imported] - Vibrio cholerae (group O1 strain N16961)	10	10.4	59.37	
10	2.3e-011	-	gi|6572105|emb|CAB63090.1| (AJ132928) riboflavin-specific deaminase / reductase [Bartonella henselae]	12	9.6	40.13	

A

ProFound - Search Result Details

Details:

gi|1172040|sp|Q01103|PCAI_PSEPU 3-OXOADIPATE COA-TRANSFERASE SUBUNIT A (BETA-KETOADIPATE:SUCCINYL-COA TRANSFERASE)

gi|281564|pir||A42985 3-oxoadipate CoA-transferase (EC 2.8.3.6) alpha chain - Pseudomonas putida

gi|551938|gb|AAA25922.1| (M88763) beta-ketoadipate succinyl-CoA transferase [Pseudomonas putida]

Sample ID : [Pass:0]
Measured peptides : 95
Matched peptides : 6
Min. sequence coverage: 37%

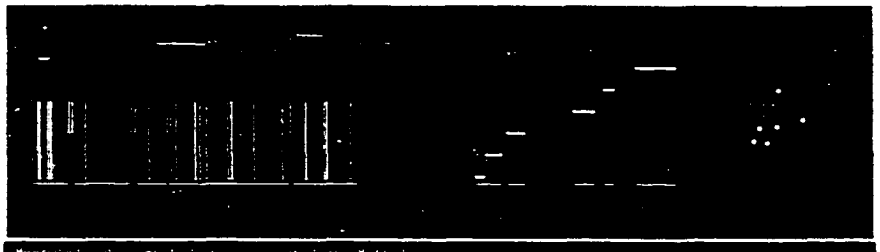

883.456	M	883.492	0.024	74	80	0	VVCSFPR
908.423	M	908.450	-0.027	165	171	0	[illegible]TYR
1520.869	M	1520.878	-0.009	81	92	0	GSDSYVFDELYR
1585.888	M	1585.840	0.057	98	109	0	IELEWVPGMLAER
1869.127	M	1869.976	0.149	149	158	0	MYVLEMPLHKDFALIK
3186.753	M	3186.881	0.092	187	215	0	TAIAQVSQWVELSELDPEHIITPSIFVQR

B

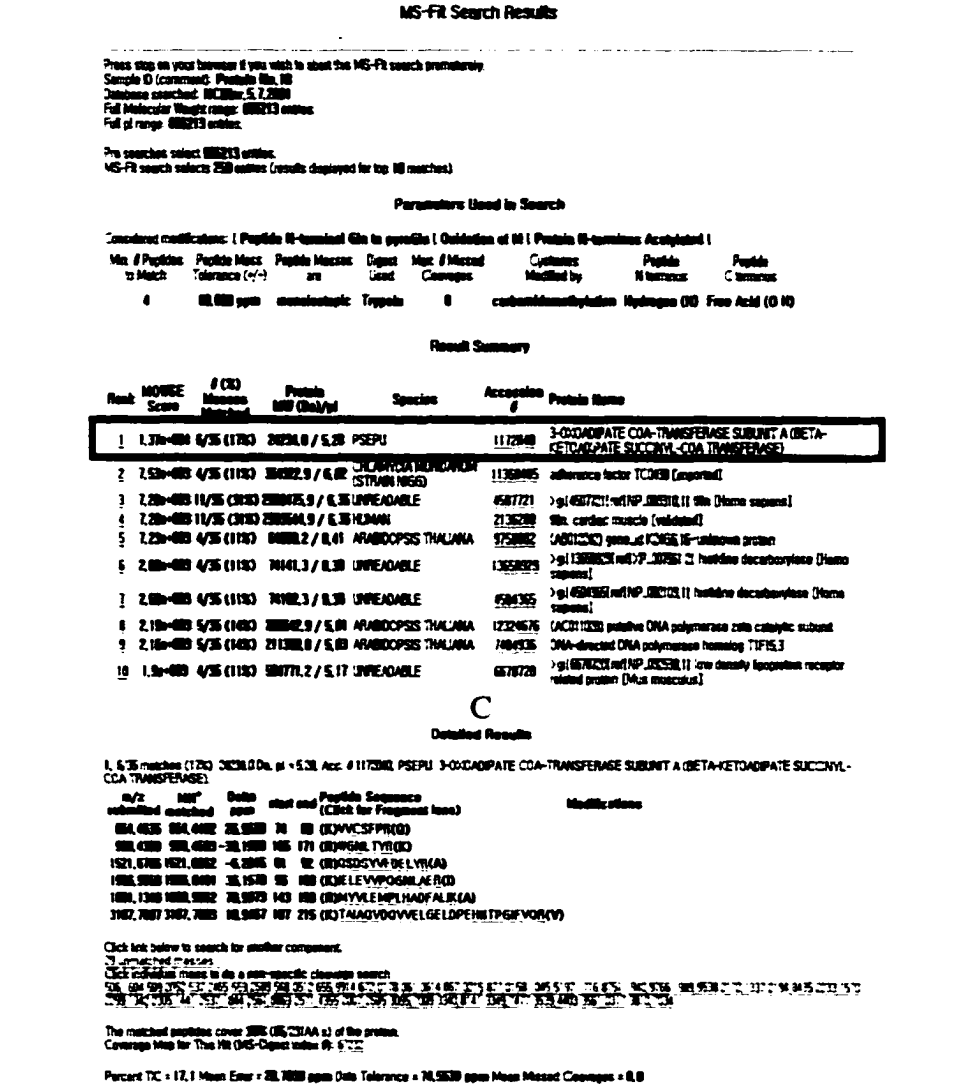

Figure V-7 Peptide mass fingerprint of the tryptic digest of Protein # 18 with the corresponding database (5/7/2001, NCBInr) search result using ProFound (version 4.10.8). A: ProFound search result summary B: Detailed search result of ProFound presents the peptide coverage and error map, detailed mass difference between measured and calculated peptide mass, and corresponding amino acid sequences of peptides. C: MS-Fit search result summary. D: Detailed results of protein at rank 1. E: Full protein sequence for Protein #18. Bold K and R represent the specific cleavage sites for trypsin. The box indicates the first ranked identification.

The same procedure for the identifications of other proteins (Protein # 1, 8, 19, 20, 24) was conducted, but no statistically significant identification was searched against the entire protein database in any case. For further identification search, an ion trap tandem mass spectrometer (ESI-MS/MS) was employed to obtain *de novo* peptide sequences.

V.2.2.5 *De novo* peptide sequencing by tandem mass spectrometry and search for protein identification

The performance of the capillary HPLC column separation and electrospray was examined with a standard peptides provided by the vendor (Michrom BioResources, Inc). The peptide standards consisted of 5 synthesized peptides (Table V-6). Their spectra are shown in Figure V-9. The separation of standard peptides indicates good separation in a capillary column and electrospray in ESI-MS. Tandem mass spectra were not acquired.

Table V-6 Five synthesized peptide standards.

Pepide Sequence	Molecular Weight, Da
RVTVHPI	883
RVTVHPF	917
RVTIHPF	931
DRVTVHPFHL	1282
DRVTIHPFHL	1296

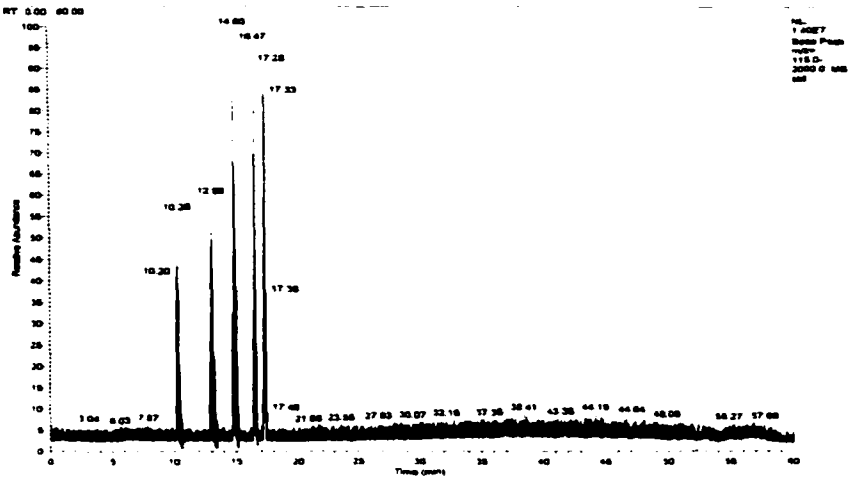

Figure V-8 Separation of peptide standards in a capillary HPLC column and detection after ionization by an electron spray ionization source.

Protein identification based on mass fingerprinting and relevant database searches has been successfully established in several previous reports (16, 40, 46, 56, 57). However, as presented in the previous section, it was not possible to obtain proper and unambiguous identification with the mass fingerprint method alone unless the complete genomic sequence of *P. putida* F1 was available. Because of this, the direct peptide sequencing approach was chosen to obtain protein identification.

Since Hunt et al. (15) first reported a method of peptide sequencing based on tandem mass spectra that were obtained by a triple quadrupole mass spectrometer, tandem mass spectrometers have been used as an important tool for sequencing peptides proteolyzed proteins extracted from a 2D PAGE gel (31, 36) or chemical lysis (15) of polypeptides. There are three reasons for using trypsin to obtain peptide fragments. First, trypsin usually produces peptides with less than 3000 Da, which is a feasible size for a collision-

induced dissociation (CID) process (50). Another benefit of using trypsin is to place basic residues at the C-terminus of a proteolysed peptide, e.g., arginine (13, 36). Trypsin has two specific cleavage sites on the C-terminus of arginine (Arg, R) and lysine (Lys, K). Thus, placing the basic residues on the C-termial side could be more predictable in producing peptide fragments because the presence of basic residues (especially arginine) in the middle of peptide sometimes results in the absence of fragmentation at contiguous peptide bonds neighboring with the basic residues (50). The last advantage of tryptic proteolysis for a tandem mass spectrometer is the practicability of DNA primer synthesis: thus, *de novo* peptide sequencing by a tandem mass spectrometer can be used not only for obtaining protein identification, but also for cloning genes with the polymerase chain reaction (PCR) (43). Arginine, leucine, and serine have six possible codons in microorganisms. Therefore, it is recommended to eliminate one of them from peptide fragments with trypsin prior to analysis in a tandem mass spectrometer and to increase the probability of gene isolation by a degenerative gene cloning method.

Proteolytic peptide mixtures were directly applied to a capillary HPLC column equipped with UV detector and micro buffer mixer. Each peptide, which was desalted, separated, and concentrated by a capillary HPLC column, was transferred on-line to an electrospray ionization source with nebulizing gas (nitrogen). An electrospray ion trap mass spectrometer (LCQ, Finnigan) was operated in a 'threshold-operation' mode in which the MS detects the intensity of the ions in the *m/z* range of 400 to 2000, and switches to the collision-induced dissociation (CID) mode when the intensities of the parent ions are greater than a preset threshold to obtain a CID spectrum on the most intense ion during

HPLC operation. Since no zoom scan mode was available, all CID spectra were acquired in the normal scan mode. The ion trap was operated with the automatic gain control (AGC) value at MS/MS: $1e + 005$ to better use the ion current for CID. The energy for collision was chosen at 40 eV. All mass spectrum data was acquired in the profile mode even though the centroid mode used less data storage space than the profile mode because the profile mode was the better choice to maintain all information including the raw signal-to-noise ratio, tune-up and operating parameters for future analysis. For manual sequence determination after mass spectrum acquisition, the spectrum was adjusted to centroid to reduce the signal-to-noise ratio, although peak shape information was lost.

V.2.2.5.1 Nomenclature of fragment ions

Any charged peptide ion that was present in amounts greater than the pre-set threshold value in AGC was fragmented by a neutral dissociation gas (argon for this study) in an ion trap. Several different types of fragment ions can be produced. A few different ways of designating these ions have been introduced (1, 2), e.g. ions involving cleavage of the peptide backbone. The identification of the proper fragment ions is important to extract the correct peptide sequence based on the CID mass spectrum. Three possible cleavage points of a peptide backbone have been identified (Figure V-9). They are designated as a, b, and c when the charge is retained at the N-terminal fragment of the peptide. The letters of x, y, and z are used when the charge is located at the C-terminus of a fragment ion. The number (1,2,3.....n) represents which peptide bond is cleaved counting from the

N- and C-terminus respectively and the number of amino acid residues in the fragment ions.

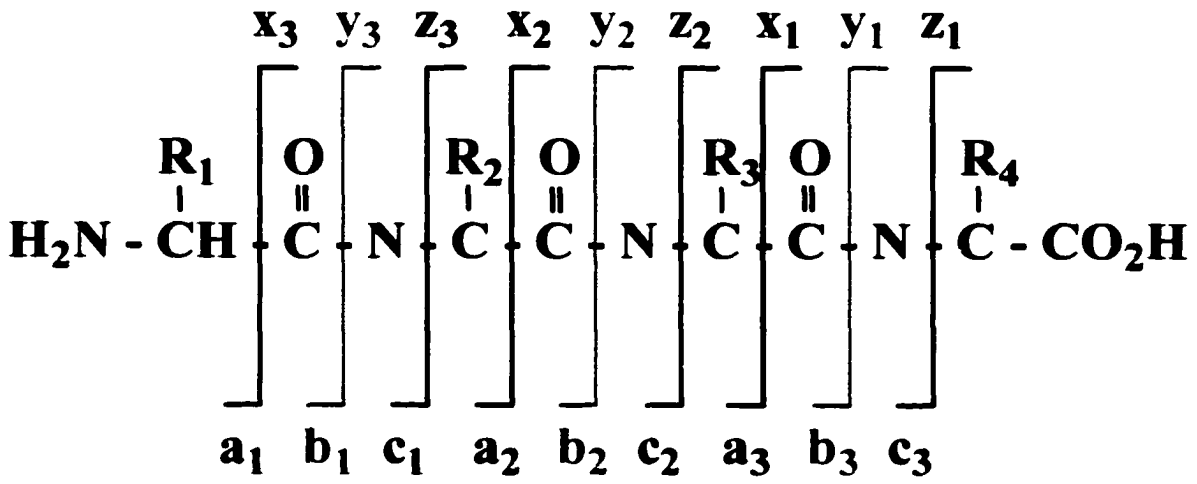

Figure V-9 Notations of fragment ions (1). Dominant ion fragments observed after low energy collision induced decomposition are the b and y series fragments, reflecting splitting in the middle of the peptide bond. Both b and y series fragments are used for deducing the primary sequence of an analyzed peptide fragment.

V.2.2.5.2 Principle of peptide sequencing

Collision of peptides with low energy CID results in a limited number of fragment ions (Figure V-10A). Of these fragment ions, both y-type and b-type ions are much more abundant than other ions (a-, c-, x-, and z-type ions) and are the key sequence-specific fragment ions. For the proposed mechanisms of ion fragmentations, see the review papers (15, 47, 51). The simplified scheme for peptide sequencing by tandem mass spectroscopy is described in Figure V-10B-C. Since the sum of the *m/z* values of b- and

y-type ions should be equal to the *m/z* value of the parent ions (Figure V-10A). the identification of both complementary fragment ions can be carried out in a straightforward manner (Figure V-10B). These peptide fragment ions then are measured by a MS analyzer and displayed in their *m/z* values shown in Figure V-10C. The difference between the sizes of two adjacent y- or b-type ions corresponds a monoisotopic mass of an amino acid residue (Table V-7) and peptide sequence is extended to the next residue by the same deduction manner between two other neighboring fragment ions. This string of amino acids results in the peptide sequences in opposite directions with b- and y-type ions: thus. if the peptide sequences are derived by the consecutive differences from the y-type ions. the read-out sequence begin at C-terminus toward N-terminus ($HOOC\text{-}R_4\text{-}R_3\text{-}R_2\text{-}R_1\text{-}NH_2$). If the sequences started to derive with b-ions. the read out is from N-terminus to C-terminus ($H_2N\text{-}R_1\text{-}R_2\text{-}R_3\text{-}R_4\text{-}COOH$). Since the sum of b- and y-ions to the *m/z* value of the parent ion can play a key role in assuring the quality and accuracy of peptide sequencing based on tandem mass spectrum. the ability to observe both b- and y-ions at the same time on a tandem mass spectrum is critical (35).

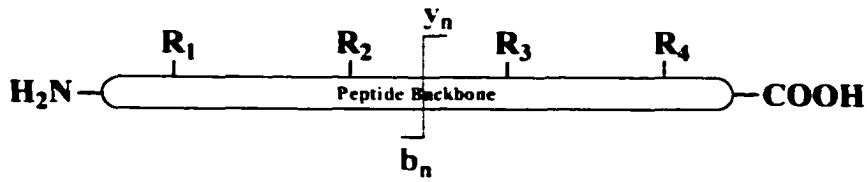

(A)

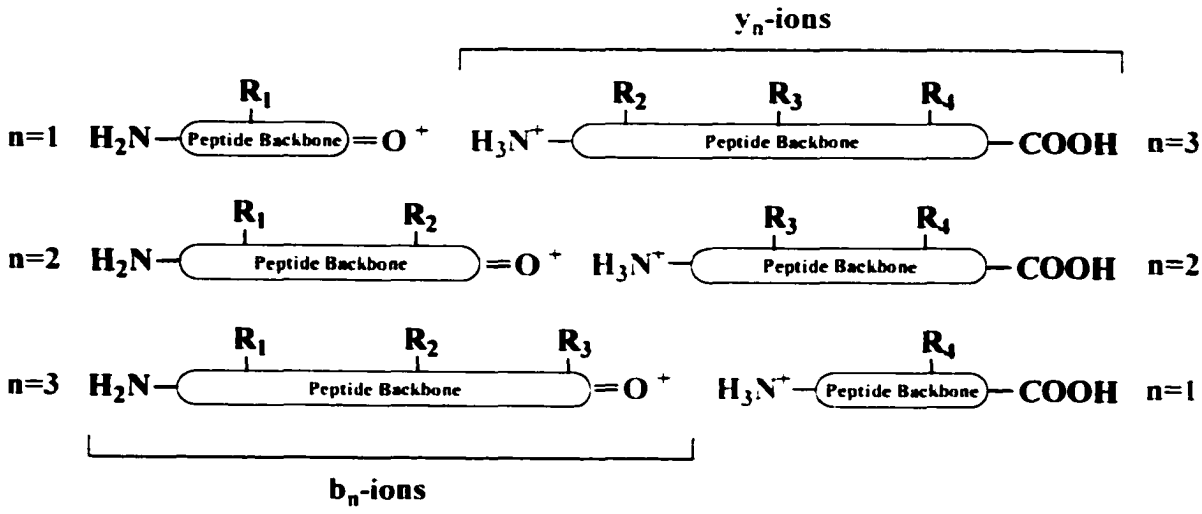

(B)

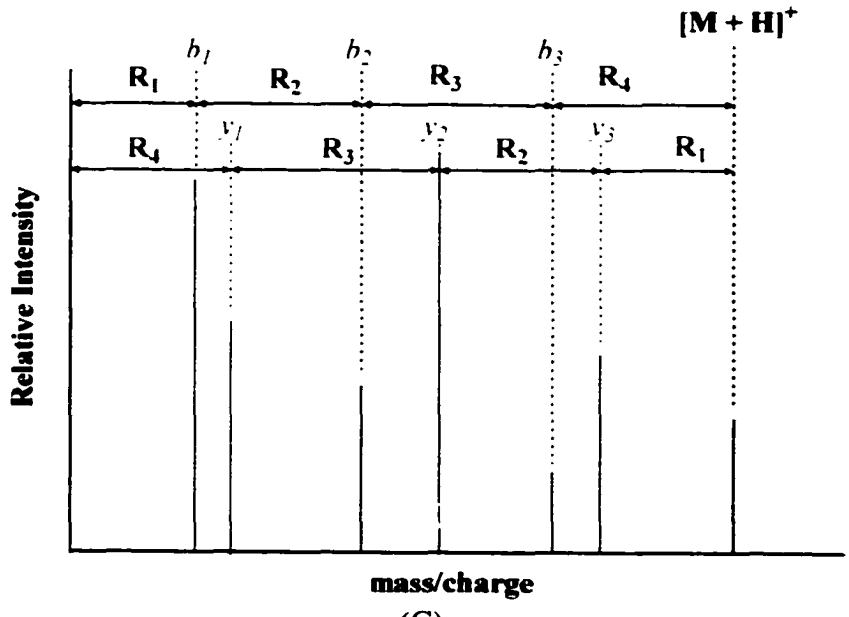

(C)

Figure V-10 Simplified scheme of peptide sequence determination based on tabdem mass spectrum. (A) description of precursor peptide, (B) types of predominant daughter ions in CID, (C) arrangement of tandem mass spectrum after CID fragmentation. The letter 'n' denotes the number of residues remaining in a daughter peptide fragment.

V.2.2.5.3 Peptide sequencing by tandem mass spectrum

The chromatogram of Protein #1 is presented in Figure V-11A. Of these peaks, the peptide sequences of only three peaks (retention time 13.48, 13.84, and 14.40 min, Figure V-11B) were successfully determined. Although many peaks were detected in the chromatogram and fragmented for CID operation, most of the tandem mass spectra from MS peaks were determined to be either trypsin or human keratin fragments by manual sequencing and identification search.

First of all, the molecular weight of a selected peptide fragment (a parent ion) should be deconvoluted to a monoisotopic *m/z* value and designated as $[M + xH]^{x+}$, where x represents the number of charges. Depending on the number of applied charges on the peptide, the displayed value of *m/z* on a MS mode spectrum can be varied. However, since it is known fact that an ESI MS dominantly produces doubly charged (+2) peptide fragments (15, 44), only the doubly charged peptides were sequenced in this study. The calculation of a parent ion, which is a precursor peptide ion before CID fragmentation, was performed by the following manner: first, *m/z* value of selected parent ion for CID fragmentation is found from the top left portion of tandem mass spectrum (Figure V-12B). Second, the number of charges (two) is multiplied by the detected *m/z* value (718.3^{2+}) and from this is subtracted one less than the number of charges. For example, if the *m/z* value of a parent ion with double charge is 718.3, then the mass of the parent ion with one proton is $[718.3 \times 2] - 1 = 1435.6^{+}$; thus, this is the deconvoluted *m/z* value (monoisotopic), which is designated as '**M**'. This final deconvoluted mass indicates the

parent peptide mass with single proton attached right before the CID defragmentation process.

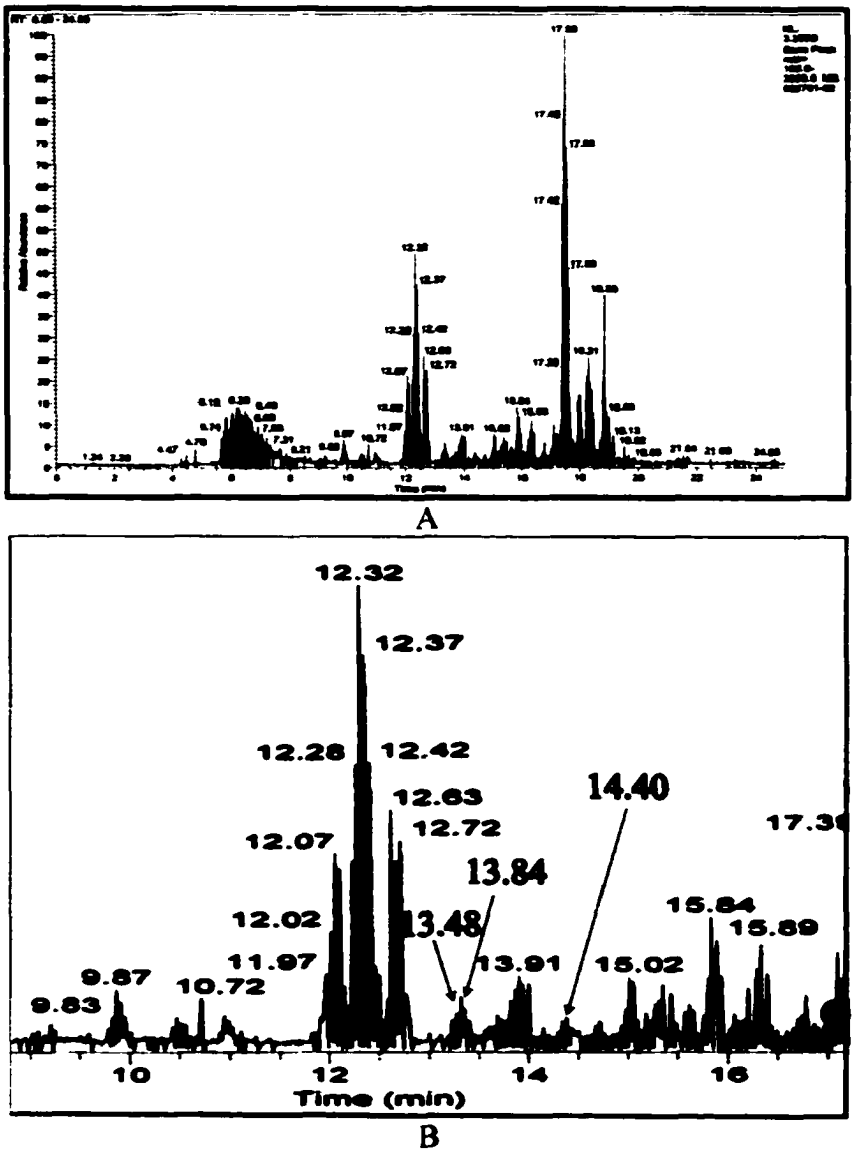

Figure V-11 (A) Peptide mass map acquired from the In-gel digest of Protein No 1. Since longer than 24 min of retention time was the end of gradient in a capillary HPLC column, acquisition after 24 min was truncated. (B) Enlarged spectrum image between the retention time 9 and 17 min. Peptide precursors for CID MS/MS are designated with arrows.

According to the general rule that most of daughter ions created from collision with collision gases (argon) are either y- or b-ions (35, 39, 41), different sizes of peptide fragments (daughter ions) are independently detected by the mass detector and the corresponding mass spectra are automatically acquired. The Xcalibur software then displays the relative intensities of ions over their *m/z* values along with relevant information (Figure V-12C). Two different approaches to manually determining peptide sequence were used: sequencing from either N- or C-terminus or sequencing from the middle of the tandem mass spectrum and connecting to both ends. By careful visual inspection of acquired tandem mass spectra, either method was used, but another method was also utilized to ensure the quality of the determined peptide sequence. Since low mass ions (< 300 *m/z*) are often not observed in an ion trap MS/MS spectrum for a doubly charged parent peptides (35), reading out the terminal ion series (y- or b-ions) could be difficult. Although a table for nominal residue masses of single amino acids and oligopeptides is available (47), it should be used only as a References.

Identification of both y- and b-ions was carried out using the concept that the sum of complementary *m/z* values for b- and y-ion is equal to the parent ion's *m/z* value. In the middle of a tandem mass spectrum, y-series ions appear with dominant intensity so that these predominant *m/z* peaks were a good starting point. The detailed sequence determination process for 1435.6^{-} is described in Figure V-12. Although the parent ion is not detected in the spectrum, the first amino acid residue at N-terminus is easily determined by subtracting 1306.6 from the *m/z* value of the parent ion (1435.6^{-}), which is 129 and corresponds to the monoisotopic mass of glutamic acid (E) (Table V-7). The

calculated *m/z* value of the b_1 ion is 129.0 by subtracting the complementary y_1 ion (1306.6) from the parent ion (1435.6), but it is not detected because the range of spectrum acquisition was 185 to 2000 (Figure V-12C). Although the corresponding b-ion was not detected, the identification of the first residue at N-terminus is always a good sign for the entire peptide sequencing process. From the y_{12} ion, the search for the next y-ion (y_{11}) started using the complementary concept described above. The difference of the *m/z* values between 1306.6 and 1234.6 matched with the monoisotopic *m/z* value of alanine (71.07), but its complementary b-ion (201.0) was still not observed. When the next y-ion (y_{10}) was found at an *m/z* value 1165.6 with the same procedure as before, the first complementary b-ion (b_4) was observed at an *m/z* value 400.4. It is acceptable for the tandem mass spectrum from an ion trap ESI MS/MS to have a variation of *m/z* value of 1/10 (35, 41). After finding the b_4 ion, identification of the rest of both b-ions ($b_4 - b_{11}$) and y-ions ($y_9 - y_2$) was straightforward and amino acid residues were easily determined. The determined sequence of the peptide fragment (1434.6) was (K/R)EAAE[L/I]G[L/I]EPFFX(K/R). Since a typical ESI-MS/MS is not able to discriminate less than 0.1 *m/z* difference, the amino acid residues such as leucine (113.1590) and isoleucine (113.1590), or glutamine (Gln, Q, 128.1304) and lysine (Lys, L, 128.1736) cannot be distinguished by an ESI-MS/MS method (34, 35, 39, 41, 44, 47). The possibility of lysine appearance in the middle of a *de novo* peptide sequencing by tandem mass spectrscopy could be relatively low under the assumption that no misscut by trypsin occurred. Therefore, it is relatively safe to assume it glutamine when the difference of *m/z* value between two consecutive ions is 128.1, but it should still be confirmed in protein identification process with sequence homology examination or

subsequent gene isolation and DNA sequencing. Often, determination of amino acid residues at both termini of a peptide is difficult because of the lack of ion detection (b_1 – b_3). In this case, the detection of the complementary y-ions (y_{12} – y_{10}) was used to determine the amino acid residues at N-terminus, but the residues at C-terminus were still undetermined due to missing y_1 ion (designated as X for the unknown amino acid residue). The sequences from other tryptic peptide fragments of Protein #1 are presented in Table V-9.

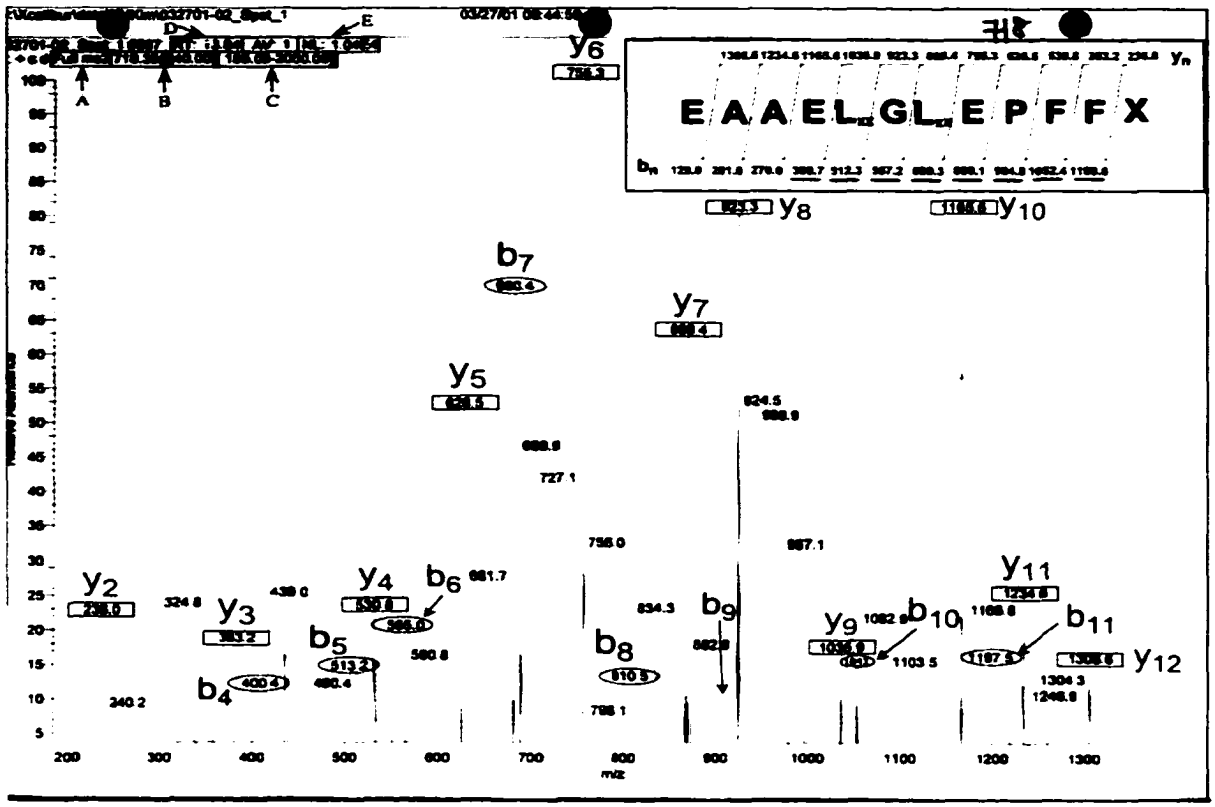

Figure V-12 The ESI-tandem mass spectrum of the $[M+2H]^{2+}$ ion from the Protein #1 fragment at *m/z* 718.3^{2+}. The masses of y-series ions are surrounded by rectangular boxes with corresponding numbered labels. The circles represent the masses of b-series ions. The determined peptide sequence is depicted at the right top corner within a box; with the observed b-series ion masses underlined. The capital letters in the top left corner represent the following; A: MS/MS operation mode. B: CID operation mode of *m/z* 718.3^{2+} at 40 eV CID energy. C: the acquisition range of tandem mass spectrum. D: retention time of the peptide introduced to the first mass analyzer. E: total intensity of daughter ions.

Table V-7 **Monoisotopic and average mass of amino acids (51).**

Amino Acid	Letter code		Mass. Da	
	Three	One	Monoisotopic	Average
Glycine	Gly	G	57.021	57.052
Alanine	Ala	A	71.037	71.079
Serine	Ser	S	87.032	87.078
Proline	Pro	P	97.053	97.117
Valine	Val	V	99.068	99.133
Threonine	Thr	T	101.048	101.105
Cystein	Cys	C	103.009	103.139
Isoleucine	**Ile**	**I**	**113.084**	**113.159**
Leucine	**Leu**	**L**	**113.084**	**113.159**
Asparagine	Asn	N	114.043	114.104
Aspartic acid	Asp	D	115.027	115.089
Glutamine	**Gln**	**Q**	**128.059**	**128.131**
Lysine	**Lys**	**K**	**128.095**	**128.174**
Glutamic acid	Glu	E	129.043	129.116
Methionine	Met	M	131.040	131.193
Histidine	His	H	137.059	137.141
Phenylalanine	Phe	F	147.068	147.177
Arginine	Arg	R	156.101	156.188
Tyrosine	Tyr	Y	163.063	163.176
Tryptophan	Trp	W	186.079	186.213

Table V-8 **Peptides sequenced from in-gel digestion of the Protein #1 by CID MS/MS spectra.**

Retention Time, min	m/z^{x-*}	Deduced Sequence	Parent ion, $[M+_xH]^{x+}$ (Monoisotopic, m/z^+)
13.48	466.6^{2+}	xxHPVAx(K/R)	932.2^+
13.84	718.3^{2+}	EAAE[L/I]G[L/I]EPFFx(K/R)	1435.6^+
14.40	654.4^{2+}	xxFEMRPTx(K/R)	1307.8^+

[L/I]: Leucine or Isoleucine

* the number of charges

V.2.2.5.4 Identification search with sequence homology search

With these partial sequences (Table V-8), sequence homology was examined in protein databases of NCBInr and SWISS-PROT. Mann *et al.* (23) developed an error-tolerant protein identification algorithm that uses the sequence tag to find the peptide in a sequence database with 1 million-fold more discrimination than the partial sequence information alone. PeptideSearch, which is available to the public on the Internet, was used to conduct protein database searches with the deduced sequence of the peptides as sequence tag (24, 28, 39, 42) (http://www.mann.embl-heidelberg.de/GroupPages/PageLink/peptidesearchpage.html).

The results of searching protein databases with PeptideSearch and SEQUEST did not show any significant matches with the peptide sequences in Table V-8. This non-matching result could be explained by the following possible reasons (26).

- The sequence of Protein #1 is completely unknown in the database.
- No significantly similar sequence exists in the database.
- No additional information (e.g. functional assignment, 3D structure) could be related to the similar sequences found in the available database.
- Low accuracy in the deduced peptide sequences.

Due to lack of genomic sequence data for *P. putida* F1, it is hard to decide which reason is correct. However, because the process for obtaining peptide sequences based on the interpretation of tandem mass spectra was relatively simple and straightforward,

unambiguous protein identification could be acquired or at least proper functional annotation could be made when the genomic sequence of *P. putida* species becomes available. The effort to sequence the genome of *P. putida* KT2441 and PRS is currently performed by The Institute for Genomic Research (TIGR, http://www.tigr.org/), and more protein identifications could be obtained in the near future.

V.3 Discussion

V.3.1 EDMAN SEQUENCING

Edman sequencing is certainly an attractive approach to identify unknown proteins because it can provide unambiguous *de novo* amino acid sequences for a peptide. The availability of N-terminal sequencers is also high due to their conventional use. However, identification of proteins with Edman degradation had several critical disadvantages. The first, it is useless when the amino terminus of a sample protein is blocked by various chemical or biological events, e.g. protection with acetylation or methylation on peptides or other posttranslational modifications). Several methods to remove the blocking chemicals have been developed, but those methods have had very limited success. Internal sequencing with the combination of proteolytic peptide digestion and HPLC separation could be a good alternative to overcome this disadvantage. However, it requires a much greater amount of valuable protein samples – the final concentration of a peptide prior to sequencing should be greater than 10 pmol, and would be more labor-intensive – all fractions were manually and carefully collected over a 1 hour period. Besides, this manual collection could be easily contaminated or disturbed by an operator. Recently a new Edman sequencer has been introduced, cLC Procise from Applied Biosystems (http://www.appliedbiosystems.com/). The vendor claims it can sequence less than one pmol of peptide, but it takes about twice as long to operate and more

importantly it was not available for this project. Furthermore, a price about twice that of a conventional sequencer would be another limitation.

After rapid advancement of mass spectrometric technology, especially tandem mass spectrometers, most protein sequencing is now performed with tandem mass spectroscopy. However, mass-based protein identification and sequencing technology is only valid when the genetic information for target proteins is available in databases. Because of this simple fundamental fact, Edman sequencing can flourish again, despite those crucial disadvantages for modern proteomics research that requires more rapid and reliable tools (5).

V.3.2 MASS SPECTROMETRY

Protein identification by mass fingerprint and relevant database searching has been significantly improved recently (5, 7, 17, 29, 32, 42, 49, 52, 55), and it has emerged as a fast and convenient method for identifying proteins. However, the vast majority of genomic sequences for both prokaryotic and eukaryotic cells are not completely sequenced and the lack of genomic sequences is the greatest obstacle in expediting the application of proteomics (42, 52).

For those organisms for which genomic sequences are unknown, *de novo* peptide sequencing based on tandem mass spectrmetry can be an alternative tool (1, 3, 8-10, 15,

20, 33, 35, 36, 39, 44, 57). In this section, the detailed procedure for the interpretation of tandem mass spectrum was presented using experimental data. It would be much more difficult to determine correct peptide sequences if the target proteins have high degree of modification, e.g. glycosylation, phosphorylation, chemical modifications during 2D PAGE and in-gel digestion procedure, etc. Therefore, *de novo* peptide sequencing by a tandem mass spectrometer depends highly on the sensitivity and quality of the mass spectrometer. A quadrapole/time-of-flight (Q/TOF) hybrid mass spectrometer has been introduced (25) and is considered the best MS for *de novo* peptide sequencing with extremel sensitivity: as low as femtomole level of proteins extracted from a silver stained 2-D PAGE gel (11, 54).

The mass spectrometer used for this study was an ion trap mass spectrometer, which yielded successful peptide sequencing in CID MS/MS operation, but in terms of sensitivity it required much more protein samples (about 5 ~ 15 large format 2-D PAGE gels per protein spot). More peptide sequencing could have been performed by the ion trap MS if a nano-flow HPLC was on-line connected to nano-electrospray ionization (ESI) source.

Although it has been known that the interpretation of tandem mass spectrum generated by any MS/MS can be difficult for non-experts, another excellent alternative method for peptide sequencing is available: incorporation of oxygen isotopes to every carboxylic terminus of proteolytic peptides with the same ratio of H_2O^{16} and H_2O^{18} during the in-gel digestion process (35, 39). This isotopic method ensures to identify every y-ion series by

specifically producing twin peaks of y-ions so that the interpretation of tandem mass spectra can be carried out without confusion. However, it can produce more complicated tandem mass spectra since a pair of oxygen isotopes creates many twin peaks that share an equal proportion of y-type ions (35, 39). Therefore, the best solution to overcome this difficulty is using a tandem mass spectrometer that can produce better tandem mass spectrum, e.g. Q/TOF hybrid MS/MS.

Another disadvantage of protein identification by mass spectrometers is artificial contamination or cross contamination among samples during in-gel digestion process (31). Contamination by a person during in-gel digestion is well expressed in Figure V-11B. Most of the predominant peaks were identified as human keratin, possibly from a person carrying out in-gel digestion process. The best solution to avoid this contamination can be using an automatic liquid handling robot that minimizes human interference.

Identification of specific proteins depends highly on the availability of genomic sequences for a particular organism. In particular, attempts to obtain protein identification with mass spectrometry depends highly on the availability of the protein and genome databases because the mass spectrometric approaches are based on the exact molecular weight of peptides or ion fragments. Without that sequence information, protein identification process requires much more effort and time.

V.3.3 STRATEGY FOR PROTEIN IDENTIFICATION BASED ON 2D PAGE

The mass spectrometric approach for protein identification is certainly superior to the conventional Edman degradation in terms of time and sensitivity. MALDI-TOF MS could provide the mass fingerprint of a protein with only a few femtomoles of starting protein. The mass information obtained by MALDI could be directed to a convenient identification search engine that conducts the comparison with the protein database via the Internet. Electrospray ionization-based tandem mass spectrometry can generate not only a full mass fingerprint after proteolytic digestion of an intact protein, but also makes it possible to obtain *de novo* peptide sequences. This sequence information can be used to find protein identifications with various search engines and protein databases. After careful examination of various tools in proteomic research, the following strategy has been developed in this study (Figure V-13).

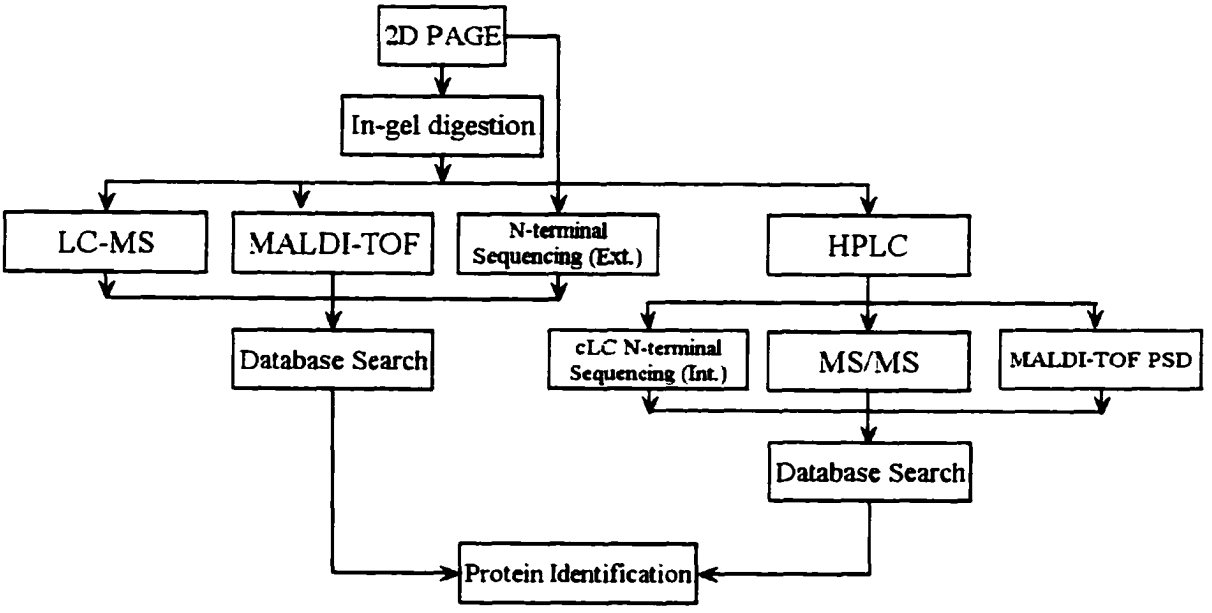

Figure V-13 Strategy for proteomics research. All methods were examined in this study but cLC N-terminal sequencing and MALDI-TOF PSD (post source decay).

Proteins that remained unidentified with the above procedure could be further studied using genomic techniques. Peptide sequence information obtained by the interpretation of tandem mass spectra is usually long enough to synthesize a primer for polymerase chain reaction (PCR) based gene cloning experiments. The typical length of primer in PCR-based cloning strategies is about 25 bases and eight to ten peptide sequences are good enough for the synthesis of a primer for PCR-based gene cloning. However, to obtain the synthesis of low-degeneracy primer, the longer peptide sequence information could provide better results for the gene cloning experiments (43).

Two unambiguous protein identifications and the partial sequence of a third protein associated with the degradation of toluene and phenol mixtures by *P. putida* F1 were

acquired in this study. The next step of research is to characterize the detailed functions of these proteins during the biodegradation phenomena of toluene-phenol mixtures in *P. putida* F1. Chapter VI presents this characterization for the identified proteins.

V.4 References

1. **Biemann, K.** 1990. Applications of tandem mass spectrometry to peptide and protein structure. p. 176-196. *In* A. L. Burlingame. McCloskey. J.A. (ed.). Biological Mass Spectrometry. Elsevier. Amsterdam.

2. **Biemann, K.** 1992. Mass spectrometry of peptides and proteins. Annu. Rev. Biochem. **61**:977-1010.

3. **Clauser, K. R., Peter Baker, and Alma L. Burlingame.** 1999. Role of Accurate Mass Measurement (± 10 ppm) in Protein Identification Strategies Employing MS or MS/MS and Database Searching. Anal. Chem. 7**1:2**871 -2882.

4. **Cohen, S. L., and B. T. Chait.** 1996. Influenece of matrix solution conditions on the MALDI-MS analysis of peptides and proteins. Anal. Chem. 6**8:3**1-37.

5. **Di Maro, A. Pasquale Ferranti, M. Mastronicola, L. Polito, A. Bolognesi, F. Stirpe, A. Malorni, and A. Parente.** 2001. Reliable sequence determination of ribosome- inactivating proteins by combining electrospray mass spectrometry and Edman degradation. J. Mass Spectrom. 3**6:38**-46.

6. **Ducret, A., Van Oostveen, I., Eng, J., Yates, J.R., Aebersold, R.** 1998. High throughput protein characterization by automated reverse-phase chromatography/electrospray tandem mass spectrometry. Protein Sci. 7:706-719.

7. **EMBL Bioinformatics Institute** 2001. posting date. FASTA searches a protein or DNA sequence data bank version 3.3t07 Nov. 2, 2000. [Online.]

8. **Eng, J. K., McCormack, A.L., Yates, J.R., III.** 1994. An Approach to Correlate Tandem Mass Spectral Data of Peptides with Amino Acid Sequences in a Protein Database. J. Am. Soc. Mass Spectrom 5:976-989.

9. **Fernandez-de-Cossio, J., and Y. S. Javier Gonzalez, Takaki Shima, Nobuaki Okumura, Vladimir Besada, Lazaro Betancourt, Gabriel Padron, Yasutsugu Shimonishi, Toshifumi Takao.** 2000. Automated interpretation of low-energy collision-induced dissociation spectra by SeqMS, a software aid for *de novo* sequencing by tandem mass spectrometry. Electrophoresis 21:1694-1699.

10. **Gatlin, C. L., J. K. Eng, S. T. Cross, J. C. Detter, and J. R. Yates III.** 2000. Automated Identification of Amino Acid Sequence Variations in Proteins by HPLC/Microspray Tandem Mass Spectrometry. Anal. Chem. 72:757-763.

11. **Gatlin, C. L., G. R. Kleemann, L. G. Hays, A. J. Link, and J. R. Yates III.** 1998. Protein Identification at the Low Femtomole Level from Silver-Stained Gels Using a New Fritless Electrospray Interface for Liquid Chromatography-Microspray and Nanospray Mass Spectrometry. Anal Biochem **263:9**3-101.

12. **Gobom, J., M. Schuerenberg, M. Mueller, D. Thesis, H. Lehrach, and E. Nordhoff.** 2001. a–cyano-4-hydroxycinnamic acid affinity sample preparation. A protocol for MALDI-MS peptide analysis in proteomics. Anal. Chem. **73:4**34-438.

13. **Hermodson, M. A., L. H. Ericsson, H. Neurath, and K. A. Walsh.** 1973. Determination of the amino acid sequence of porcine trypsin by sequenator analysis. Biochemistry **12:3**146-3153.

14. **Huang, G., L. Zhang and R. G. Birch.** 2000. Characterization of the acyl carrier protein gene and the fab gene locus in Xanthomonas albilineans. FEMS Microbiol. Lett. **193:1**29-136.

15. **Hunt, D. F., J.R. Yates III, J. Shabanowitz, S. Winton, and C.R. Hauer.** 1986. Protein sequencing by tandem mass spectrometry. Proc. Natl. Acad. Sci. **83:6**233-6237.

16. **Jensen, O. N., A. V. Podtelejnikov, and M. Mann.** 1997. Identification of the Components of Simple Protein Mixtures by High-Accuracy Peptide Mass Mapping and Database Searching. Anal. Chem. 69:4741 -4750.

17. **Jiang, Y., P.C. Wang, L. E. Locascio, and C. S. Lee.** 2001. Integrated plastic microfluidic devices with ESI-MS for drug screening and residue analysis. Anal Chem 73:2048-2053.

18. **Johnson, R. S., and K. A. Walsh.** 1992. Sequence analysis of peptide mixtures by automated integration of Edman and mass spectrometric data. Protein Sci. 1:1083-1091.

19. **Juhasz, P. M., L. Vestal, and S. A. Martin.** 1997. On the initial velocity of ions generated by matrix-assisted laser desorption ionization and its effects on the calibration of delayed extraction time-of-flight mass spectra. J.Am.Soc.Mass.Spectrom. 8:209-217.

20. **Keough, T., M. P. Lacey, A. M. Fieno, R. A. Grant, Y. Sun, M. D. Bauer, and K. B. Begley.** 2000. Tandem mass spectrometry methods for definitive protein identification in proteomics research. Electrophoresis 21:2252-2265.

21. **Kutchma, A. J., T. T. Hoang, and H. P. Schweizer.** 1999. Characterization of a *Pseudomonas aeruginosa* fatty acid biosynthetic gene cluster: Purification of acyl carrier protein (ACP) and malonyl-coenzyme A:ACP transacylase (FabD). J. Bacteriol. **181:**5498-5504.

22. **Lottspeich, F.** 2000. Identification of proteins by amino acid sequencing. p. 181-196. *In* T. Rabilloud (ed.). Proteome research: Two-Dimensional Gel Electrophoresis and Identification Methods. Springer Verlag. New York.

23. **Mann, M.** 1994. Sequence database searching by mass spectrometric data. p. 223-245. *In* R. Kellner. F. Lottspeich., H.E. Meyer. (ed.). Microcharacterization of proteins. VCH. Weinheim.

24. **Mann, M., and M. Wilm.** 1994. Error-tolerant database identification of peptides in sequence databses by peptide sequence tag. Anal. Chem. **66:**4390-4399.

25. **March, R. E.** 1997. An Introduction to Quadrupole Ion Trap Mass Spectrometry. J. Mass Spectrom. **32:**351-369.

26. **Mews, H.-W., and D. G. George.** 1994. Protein sequences and sequence databases. p. 209-222. In F. L. Kelleher. H.E. Meyer (ed.). Michrocharacterization of proteins. VCH. Weinheim.

27. **Morris, H. R., T.Paxton, and A. Dell.** 1996. High sensitivity collisionally activated decomposition tandem mass spectrometry on a novel quadrupole/orthogonal accerleration TOF mass spectrometer. Rapid Commun. Mass Spectrom. **10:8**89-896.

28. **Mortz, E., P. B. O'Connor, P. Roepstorff, N. L. Kelleher, T. D. Wood, F. W. McLafferty, and M. Mann.** 1996. Sequence tag identification of intact proteins by matching tandem mass spectral data against sequence data ases. PNAS 93:**826**4-8267.

29. **Okerberg, E., and J. B. Shear.** 2001. Attomole-level protein fingerprinting based on intrinsic peptide fluorescence. Anal. Chem. 73:**16**10 -1613.

30. **Pappin, D. J. C., P. Hojrup, and A. J. Bleasby.** 1993. Rapid identification of proteins by peptide-mass fingerprinting. Current Biology 3:**32**7-332.

31. **Parker, K. C., J. I. Garrels, W. Hines, E. M. Butler, A. H. McKee, D. Patterson, and S. Martin.** 1998. Identification of yeast proteins from two-dimensional gels: working out spot cross-contamination. Electrophoresis 19:**19**20-1932.

32. **Pevzner, P. A., Z. Mulyukov, V. Dancik, and C. L. Tang.** 2001. Efficiency of Database Search for Identification of Mutated and Modified Proteins via Mass Spectrometry. Genome Res 11:290-299.

33. **Price, W. D., P. D. Schnier, and E. R. Williams.** 1996. Tandem Mass Spectrometry of Large Biomolecule Ions by Blackbody Infrared Radiative Dissociation. Anal. Chem. 68:859-866.

34. **Qian, M. G., and D. M. Lubman.** 1996. Procedures for Tandem Mass Spectrometry on an Ion Trap Storage/Reflectron Time-of-flight Mass Spectrometer. Rapid Communications in Mass Spectrometry 10:1911-1920.

35. **Qin, J., C.J. Herring., and X. Zhang.** 1998. *De novo* peptide sequencing in an ion trap mass spectrometer with O18 labeling. Rapid Commun. Mass Spectrom. 12:209-216.

36. **Qin, J., D. Feny? Y. Zhao, W. W. Hall, D. M. Chao, C. J. Wilson, R. A. Young, and B. T. Chait.** 1997. A Strategy for Rapid, High-Confidence Protein Identification. Anal. Chem. 69:3995-4001.

37. **Rawlings, M., and J. Cronan, Jr. 1992.** The gene encoding Es*cherichia coli* *acyl* carrier protein lies within a cluster of fatty acid biosynthetic genes. J. Biol. Chem. 267:**5751**-5754.

38. **Rosenfeld, J., J. Capdevielle, J.C. Guillemot, and P. Ferrara. 1992.** In-gel digestion of proteins for internal sequence analysis after one- or two-dimensional gel electrophoresis. Anal. Biochem. 203:**173**-179.

39. **Shevchenko, A., I. Chernuchevich, and W. Ens. 1997.** Rapid *de novo* peptide sequencing by a combination of nanoelectrospray, isotope labeling and a quarrupole/time-of-flight mass spectrometer. Rapid Commun. Mass Spectrom. 11:**1015**-1024.

40. **Shevchenko, A., A. Loboda, A. Shevchenko, W. Ens, and K. G. Standing.** 2000. MALDI Quadrupole Time-of-Flight Mass Spectrometry: A Powerful Tool for Proteomic Research. Anal. Chem. 72:**2132**-2141.

41. **Shevchenko, A., M. Wilm, O. Vorm, and M. Mann. 1996.** Mass spectrometric sequencing of proteins from silver-stained polyacrylamide gels. Anal Chem 68:**850**-858.

42. **Shevchenko, A., S. Sunyaev, A. Loboda, A. Shevchenko, P. Bork, W. Ens, K. G. Standing.** 2001. Charting the proteomes of organisms woth unsequenced genomes by MALDI-quadrupole time-of-flight mass spectrometry and BLAST homology searching. Anal. Chem. ASAP **Web Release.**

43. **Shevchenko, A., M. Wilm, and M. Mann.** 1997. Peptide sequencing by mass spectrometry for homology searches and cloning of genes. J. Protein Chem. 16:**481**-490.

44. **Shukla, A. K., and J. H. Futrell.** 2000. Tandem mass spectrometry: dissociation of ions by collisional activation. J. Mass Spectrom. 35:**1069**-1090.

45. **Siggaard-Andersen, M., M. Wissenbach, J. Chuck, I. Svendsen, J. G. Olsen, and P. von Wettstein-Knowles.** 1994. The fabJ-Encoded b-Kεtoacyl-[acyl Carrier Protein] Synthase IV from Es*cherichia coli is* Sensitive to Cerulenin and Specific for Short-Chain Substrates. PNAS 91:**11027**-11031.

46. **Sinclair, B.** 1999. MALDI-TOF goes mainstream. The Scientist 13:**18**-20.

47. **Snyder, A. P.** 2000. Interpreting protein mass spectra - A comprehensive resource. Oxford University Press. Oxford.

48. **Tang, L., A. Weissborn, and E. Kennedy.** 1997. Domains of Esc*herichia coli* *acyl* carrier protein important for membrane- derived-oligosaccharide biosynthesis. J. Bacteriol. 179:3697-3705.

49. **Verhaert, P., S. Uttenweiler-Joseph, M. d. Vries, A. Loboda, W. R. Ens, and K. G. Standing.** 2001. Matrix-assisted laser desorption/ionization quadrupole Time-of-Flight Mass Spectrometry: An elegant tool for peptidomics. Proteomics 1:118-131.

50. **Vestling, M. M., C. M. Murphy, and C. Fenselau.** 1990. Recognition of trypsin autolysis products by high-performance liquid chromatography and mass spectrometry. Anal Chem 62:2391-2394.

51. **Weight, C., H.E. Meyer, and R. Kellner.** 1994. Sequence analysis of proteins and peptides by mass spectrometry. In *F.* L. Kelleher. H.E. Meyer (ed.). Microcharacterization of proteins. VCH. Weinheim.

52. **Wheeler, D. L., D. M. Church, A. E. Lash, D. D. Leipe, T. L. Madden, J. U. Pontius, G. D. Schuler, L. M. Schriml, T. A. Tatusova, L. Wagner, and B. A. Rapp.** 2001. Database resources of the National Center for Biotechnology Information. Nucl. Acids. Res. 29:11-16.

53. **Williams, K., U. Hellman, R. Kobayashi, W. Lane, S. Mische, and D. Speicher.** 1997. Internal protein sequencing of SDS PAGE-separated proteins: A collaborative ABRF study. p. 99-109. Techniques in Protein Chemistry. vol. VIII. The Association of Biomolecular Resource Facilities. ABRF. Academic Press.

54. **Wilm, M., A. Shevchenko, T, Houthaeve, S. Breit, L. Schweigerer, T. Fotsis, and M. Mann.** 1996. Femtomole sequencing of proteins from polyacrylamide gels by nano-electrospray mass spectrometry. Nature 379:466-469.

55. **Wilson, J. F.** 2001. New technology spurs on proteomics. The Scientist 15:12-13.

56. **Yates, J., S. Speicher, P. R. Griffin, and T. Hunkapiller.** 1993. Peptide mass maps: A highly informative approach to protein identification. Analytical Biochemistry 214:397-408.

57. **Yates, J. R. I.** 1998. Mass spectrometry and the age of the proteome. 33:1-19.

58. **Zhang, B., and B.T. Chait.** 2000. ProFound: An expert system for protein identification using mass spectrometric peptide mapping information. Anal. Chem. 72:2482-2489.

CHAPTER VI PHYSIOLOGICAL STUDIES OF THE IDENTIFIED PROTEINS

VI.1 Research Motivation and Goals

Two proteins of interest were identified in the research described Chapter V. Acyl carrier protein (ACP) was identified by Edman sequencing (external N-terminal sequencing) and β-ketoadipate:succinyl-CoA transferase was identified by mass fingerprint analysis followed by database searching. Neither those identified proteins are directly involved in the toluene/phenol metabolic pathway. Acyl carrier protein (ACP) is an essential substrate carrier protein in the biosynthesis of fatty acid (35) and β-ketoadipate:succinyl CoA transferase is known as a key enzyme in the biodegradation of benzoate through catechol to acetaldehyde and pyruvate for the tricarboxylic acid cycle (11). Their differential productions in the course of toluene-phenol degradation by *P. putida* F1 were observed in 2-D PAGE gels. To better understand their involvement in the degradation of toluene-phenol mixtures. their physiological functions in *Pseudomonas putida* F1 were studied.

VI.2 Acyl carrier protein

VI.2.1 BACKGROUND FOR ACYL CARRIER PROTEIN

As shown in the pathway of fatty acid biosynthesis in Figure VI-1, ACP is a substrate carrier (35, 58) in the *de novo* biosynthesis of fatty acids in the cytosol fraction of the cell (57, 58). Fatty acid biosynthesis falls into two separate processes: initiation and elongation (for comprehensive reviews of the fatty acid biosynthesis pathway, see References (5, 35). The precursors for fatty acid biosynthesis are derived from the acetyl coenzyme A (CoA) pool. Initiation requires malonyl CoA and malonyl-ACP. The ATP-dependent carboxylation of acetyl-CoA by acetyl-CoA carboxylase forms malonyl-CoA (C_n) and is the first-rate controlling step in fatty acid biosynthesis (12). The initial condensation of malonyl-ACP and acetyl-ACP is catalyzed by the 3-ketoacyl-ACP synthases (6, 20). The resulting β-ketoester is reduced to a β-hydroxyacyl-ACP by a β-ketoacyl-ACP reductase. The conversion of trans-2-enoyl-ACP to acyl-ACP (C_{n-2}) is catalyzed by a NADH-dependent enoyl-ACP reductase and the next cycle of elongation is driven by acetyl-CoA carboxylase until the final product of the fatty acid elongation becomes palmitic acid (C16:0, $CH_3(CH_2)_{14}COOH$) (12). The biosynthesis of unsaturated fatty acids from saturated fatty acids is catalyzed by a specific dehydroxydecanoyl-ACP dehydrase (57). ACP contains a phosphopantetheine group that forms thioesters with the acyl group. The intermediates of fatty acid biosynthesis are attached to the terminal sulfhydryl of the 4-phosphopantetheine prosthetic group, which is attached to the protein via a phosphodiester linkage to serine located in the N-terminus of an ACP (50).

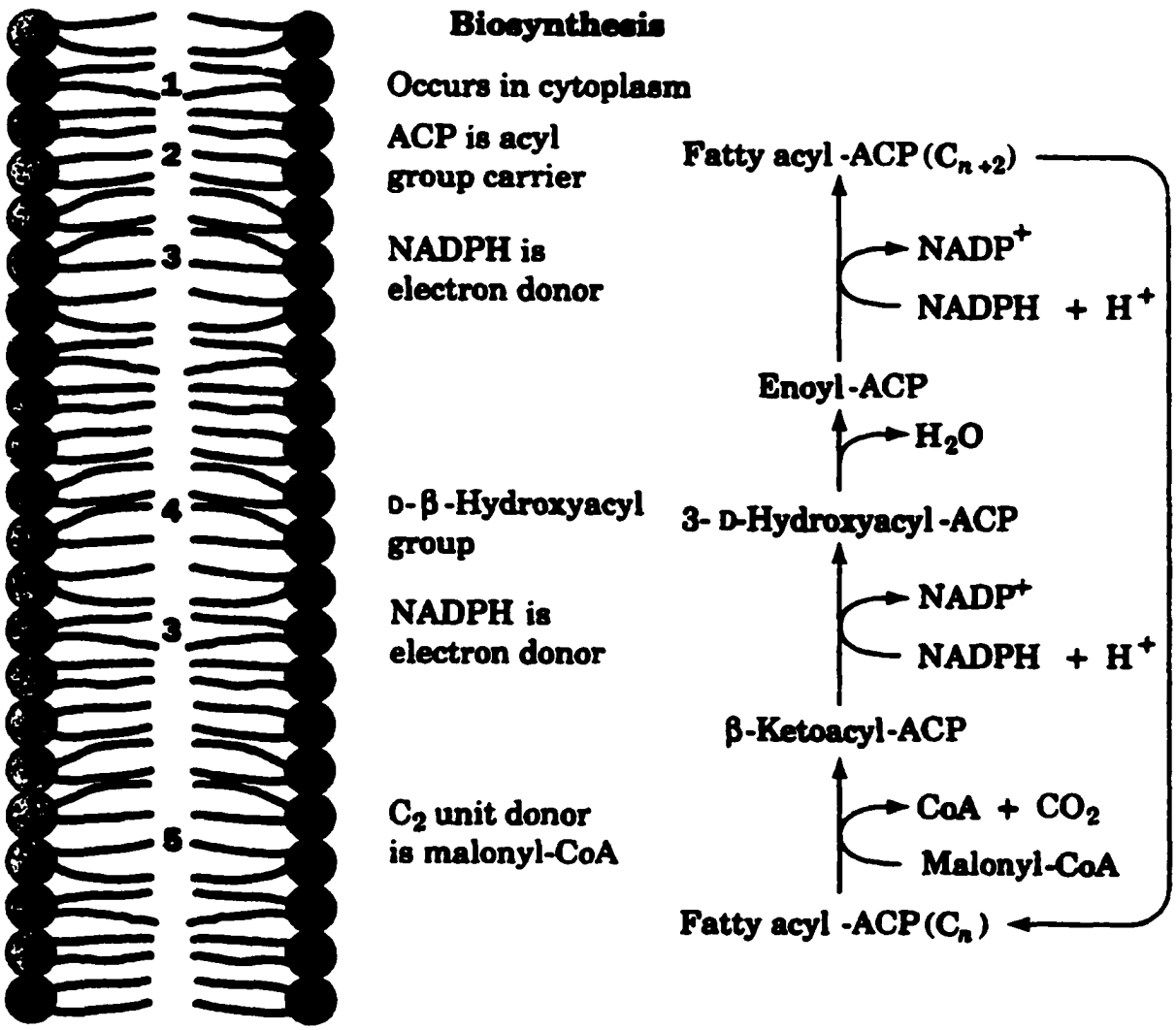

Figure VI-1 The detailed fatty acid biosynthesis pathway of *E. coli* (58). Acyl carrier protein is denoted as ACP. The numbers indicate the order of fatty acid synthesis reactions.

Ingram (21) found that the fatty acid and phospholipid composition of the cell membrane were altered when *E. coli* was cultured in the presence of sublethal concentrations of a variety of organic solvents and food additives. As this was relevant to environmental biotechnology, solvent tolerant microorganisms drew attention and a number of

investigations with solvent-degrading bacteria were performed. A comparison of the growth of free and immobilized *E. coli* on phenol was conducted by Heipieper *et al.* (15), who presented evidence that immobilized cells showed a greater tolerance than cells grown in suspension because the loss of outer membrane integrity was smaller in immobilized cells than in free cells. This study suggested that the cell membrane was an important cell component to resist the toxicity of phenol. In 1992, Heipieper *et al.* (14) proposed a possible protection mechanism against phenol in *Pseudomonas putida* P8: that conversion of *cis* to *trans* unsaturated fatty acids in both outer and inner-cell membrane led to change the membrane fluidity in the presence of phenols and to inhibit the permeation of the toxic solvent (phenol) into the cell. This *cis/trans* isomerization of fatty acids as a defense mechanism of several strains of *P. putida* to toxic concentrations of toluene was confirmed by Weber *et al.* (59) two years later. The *cti* gene encoding *cis-trans* isomerase was cloned and sequenced from *P. putida* P8 (18), and *P. putida* DOT-T1E (27). The 9-hexadecenoic acid *cis-trans* isomerase was purified and characterized from *Pseudomonas* sp. strain E-3 (38) and *Pseudomonas oleovorans* GPo12 (43). From the characterization of both purified *cti* isomerases, the location of *cti* isomerase was determined to be in the periplasmic fraction and thus *cti* isomerase did not have any enzymatic activities in the absence of the polar head group of the phospholipid (38, 43). Although a *cis/trans* isomerization as a defense system was accepted, investigation of the phenomenon has been limited to the initial adaptation of cells to toxic concentrations of toluene or phenol. Previous researchers used solvents for "pulse and chase" experiments (59) or additives (13, 34, 45) rather than as a sole carbon source for entire growth period.

Ramos *et al.* (46) proposed that the development of tolerance in *Pseudomonas putida* DOT-T1 to toluene and other toxic compounds involved short- and long-term responses. An increase of membrane fluidity by isomerization of unsaturated fatty acid from *cis* to *trans* was responsible for the short-term resistance to the toxic concentration of solvents. For the long-term responses, other ways to increase the rigidity of cell membranes by alteration of the level of the phospholipid polar head groups were proposed (46). For the long-term tolerance, a system to continuously remove toxic solvents from the outer membrane is also essential (60). The degree of toxicity of an organic solvent was found to correspond to its log P_{ow} value (the logarithm of the partition coefficient of the organic solvent between *n*-octanol and water) (22, 23). Organic solvents with a low log P_{ow} were more toxic to microorganisms (23). Hydrophobic solvents like toluene are partitioned and accumulated in the outer membrane, resulting in the loss of cell integrity by disrupting outer membrane (53, 54). An efflux system was found in *P. putida* S12 by an assay based on radiolabled toluene (25) and the corresponding gene (*srpABC*) was cloned, sequenced, and characterized to show the crucial role of an active efflux pump in the solvent resistance of *P. putida* S12 (29). Toluene tolerance in other *Pseudomonas* strains - *P. putida* DOT-T1E (47) and *P. fluorescens* LP6a (3)- was also related to the presence of an active efflux system.

An active efflux system can partly explain the long-term tolerance to the high concentration of solvents with lower log P_{ow} value, but much of the initial damage caused by aromatic hydrocarbons occurs by disruption of phospholipid membranes (52-54). Pinkart *et al.* (44) demonstrated the relationship between phospholipid biosynthesis and

solvent tolerance in *P. putida* strains. They found the ability to repair damaged membranes by efficient phospholipid turnover and increased phospholipid biosynthesis was responsible for the greater tolerance of *P. putida* Idaho relative to *P. putida* MW1200, a solvent-sensitive strain. In addition to this, Kim *et al.* (30) suggested that both an active efflux system and efficient repair of damaged membranes were important for toluene resistance based on their isolation and characterization of toluene-sensitive mutants of the toluene-tolerant *P. putida* GM73.

Although a number of the adaptation mechanisms of solvent-tolerant *Pseudomonas* strains have been studied in detail, not many studies have been made of (A) the effects of mixed solvents (toluene-phenol mixtures) on the compositional change of fatty acids in cell membrane and (B) the differential production of the proteins that are essential for the biosynthesis or/and biotransformation of fatty acid in the cytoplasm of *Pseudomonas putida* F1. In this study, differential production of ACP as a function of solvent consumption by *P. putida* F1 was presented. During the consumption of single and mixed form of toluene and phenol, the changes of fatty acid components were observed. Based on these analyses, a competitive transport mechanism across cell membrane for toluene and phenol mixtures is suggested and a fundamental information for the development of a mathematical model to predict the growth and biodegradation of toluene-phenol mixtures by *P. putida* F1.

VI.2.2 DIFFERENTIAL CONCENTRATION OF ACYL CARRIER PROTEIN

The intracellular concentration of acyl carrier protein (ACP) changed during the biodegradation of toluene-phenol mixtures. The qualitative and quantitative analysis of the ACP levels are presented in Figures VI-2 (A) and (B), respectively. However, ACP production was not observed when *P. putida* F1 grew on either toluene or phenol as a single substrate (see Figure IV-7, circle #28). Although a trace amount of ACP was observed in a silver-stained large format 2-D PAGE gel loaded with 400 μg of protein extracted from cells grown on phenol alone (data not shown), ACP was not observed in an analytical size 2-D PAGE gel due to the detection limit of silver staining.

The change in the ACP level paralled toluene degradation in the presence of phenol in the mixed substrate growth medium shown in Figure VI-2 but with a 5-10 hour lag. ACP was already observed at sample point A, when nearly 50% of the toluene was degraded but the phenol remained at its initial concentration in the growth medium. The highest level of ACP reached at sample point B, when the toluene was completely depleted and phenol consumption was beginning. The level of ACP decreased after sample point B, along with the concentration of phenol. Only 25% of the phenol remained the sample point C and the amount of ACP was left about 15% of that at the sample point B based on image quantification. No ACP was detectable on the gel from the sample point D, at which time the phenol was completely degraded (Figure IV-9).

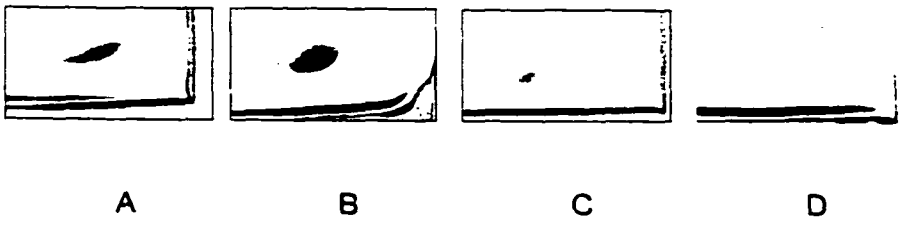

(A)

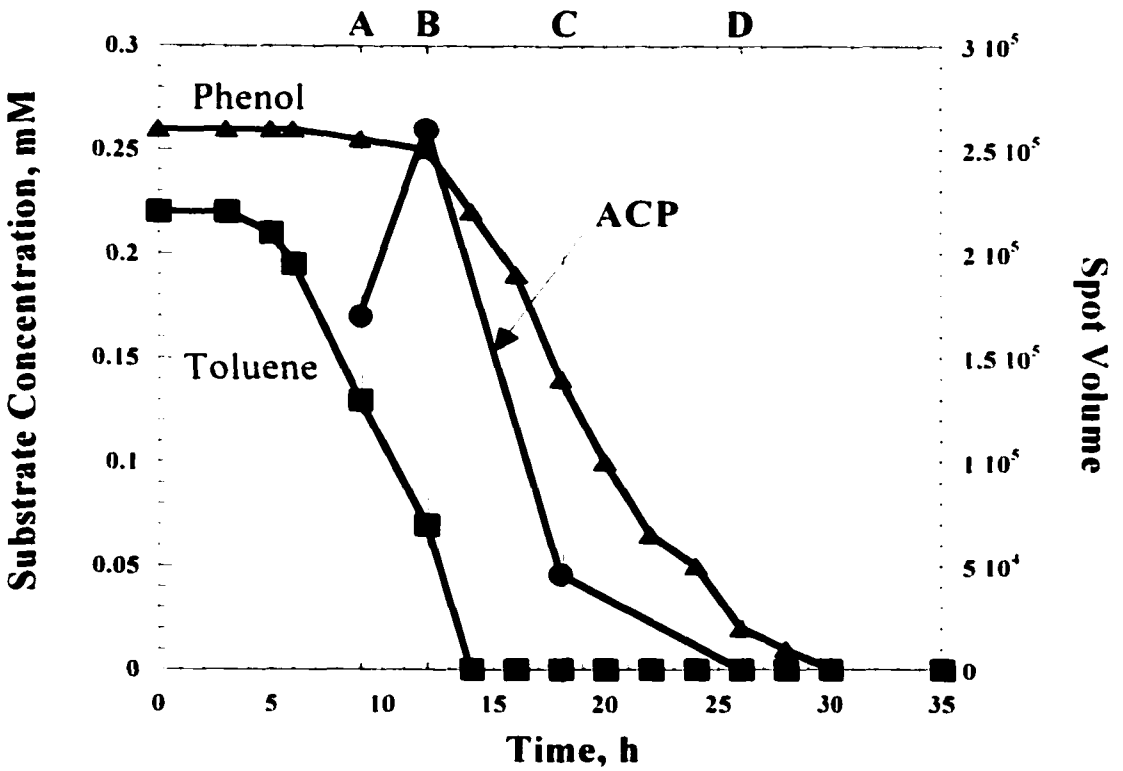

(B)

Figure VI-2 (A) The change of ACP level on 2-D PAGE gels during the biodegradation of toluene-phenol mixtures by *P. putida* F1. (B) The quantitative change of ACP level during degradation of toluene-phenol mixture is plotted in terms of spot volume (●) measured by a 2-DE gel image analysis software (Phoretix, TotalLab). The letters (A, B, C, and D) represent the sample points for proteome analysis, and toluene (■) and phenol (▲) concentration are presented, respectively.

VI.2.3 PLFA/FAME ANALYSIS

VI.2.3.1 PLFA/FAME analysis during growth on single substrates

Since ACP plays an essential role in the fatty acid biosynthesis and translocation to the cellular membrane (2, 58), a hypothesis was made: there is a correlation between the solvent transport and the change in membrane characteristics. The major component of cellular membrane is lipid that consists of three subcomponents such as fatty acid, hydrophilic head, and lipopolysaccarides (2). However, the compositional changes of the fatty acids were selected to study first. To analyze the compositional change of fatty acids in the cell membrane, the phospholipid fatty acid (PLFA) analysis was employed on samples taken at three points during exponential growth on toluene or phenol ad single substrates (Figure VI-3 and VI-5). The detailed species and quantification results of PLFA/FAME are presented in Figure VI-4 and 6, and Table VI-1 and 2.

When the toluene cell culture reached the exponential growth phase, the predominant phospholipid in the membranes of *P. putida* F1 (PpF1) cells growing on toluene was mono-unsaturated *cis*-hexadecenoic acid (16:1ω7c), Figure VI-4. The *trans*-monounsaturated hexadecenoic acid (16:1ω7t) was also observed while the cell was growing on toluene single substrate at levels less than 10 mole %. The ratio of *cis* to *trans* was also not substantially changed during the growth period (Figure VI-4). A slight increase of the *trans*- hexadecenoic acid (16:1ω7t) and decrease of the *cis*-hexadecenoic acid (16:1ω7c) were detected in the middle of exponential growth phase. Saturated cyclopropyl fatty acid (cy17:0) was also detected at the level of less than 5 mole % and

its quantity during the entire growth period was maintained at similar level. No further changes in the composition of fatty acids were observed after the middle of exponential growth phase of the cell.

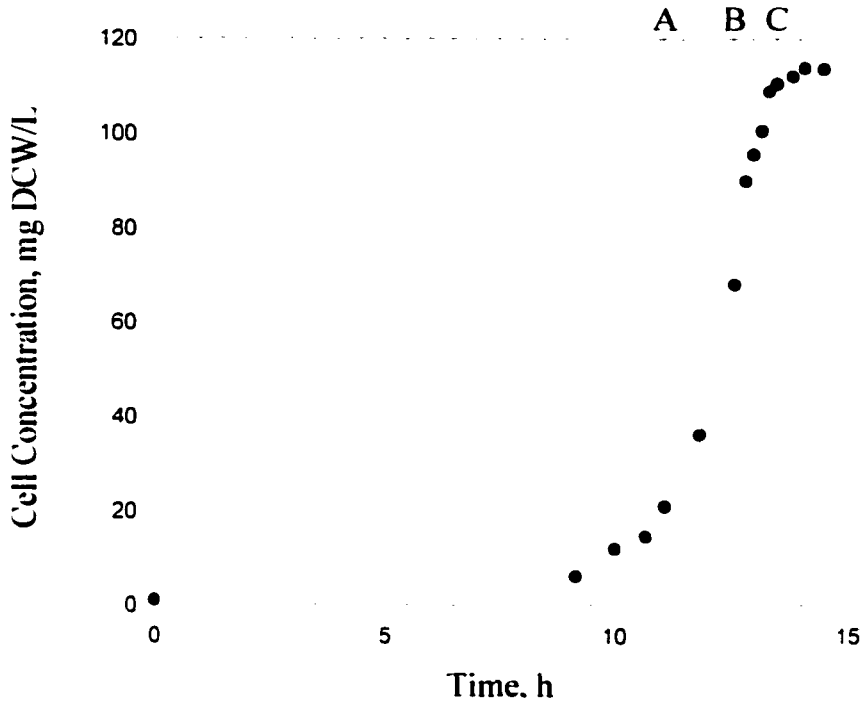

Figure VI-3 Sample points from the growth of *P. putida* F1 on toluene. The vertical lines and letters represent the times at which samples were removed for PLFA/FAME analysis. Each sample (4.5 mg dry cell weight) for PLFA/FAME taken from a batch culture was equally divided into three samples and independently subjected to PLFA/FAME analysis. • - cell concentrations. letters – sample points. X_o – 1.0 mg DCW/L. and S_o – 0.42 mM.

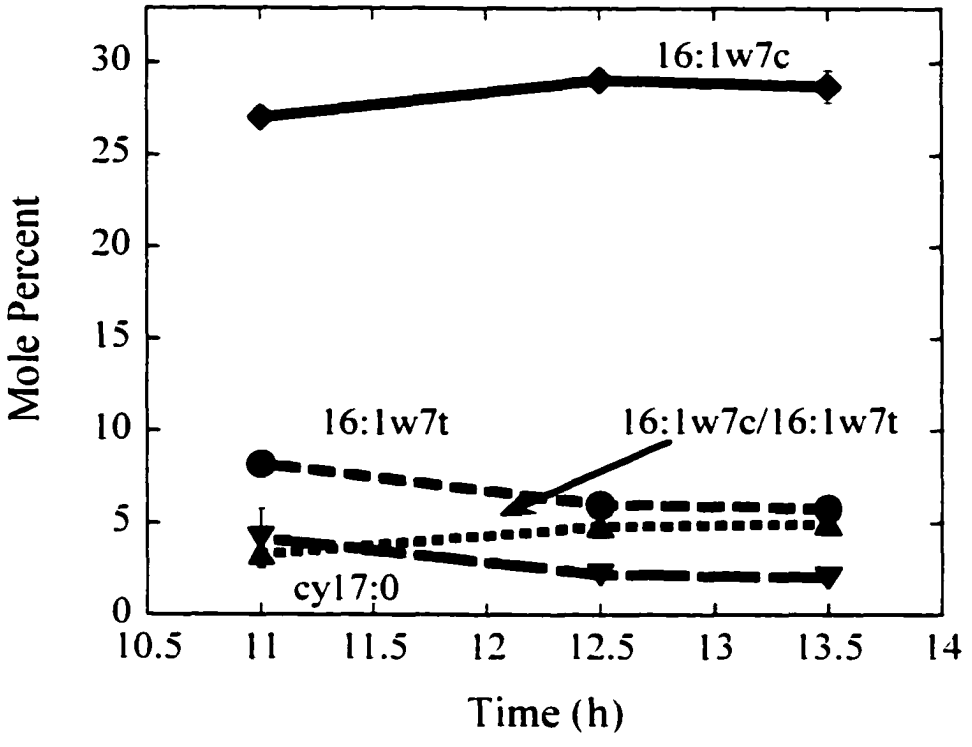

Figure VI-4 Analysis of phospholipids fatty acids in the membrane of *P. putida* F1 grown on toluene. Only the predominant fatty acids are depicted. PLFA/FAME analysis was performed by Dr. J. Bull Rogers and the detailed procedure was described elsewhere (51).

To examine the change of the phospholipids fatty acid composition in the cell membrane during growth on phenol, three samples were removed for PLFA/FAME from the early, middle, and late exponential growth (Figure VI-5). The PLFA/FAME analysis results are shown in Figure VI-6. The saturated cyclopropyl (cy17:0) was the most abundant species of fatty acid throughout the growth phase. Although the unsaturated *cis*- and *trans*-monounsaturated hexadecenoic were also detected, their total quantities were less than 8

mole % during the entire growth phase. The *cis/trans* ratio in the hexadecenoic acid (16:1ω7) also remained nearly constant during the course of cell growth on phenol.

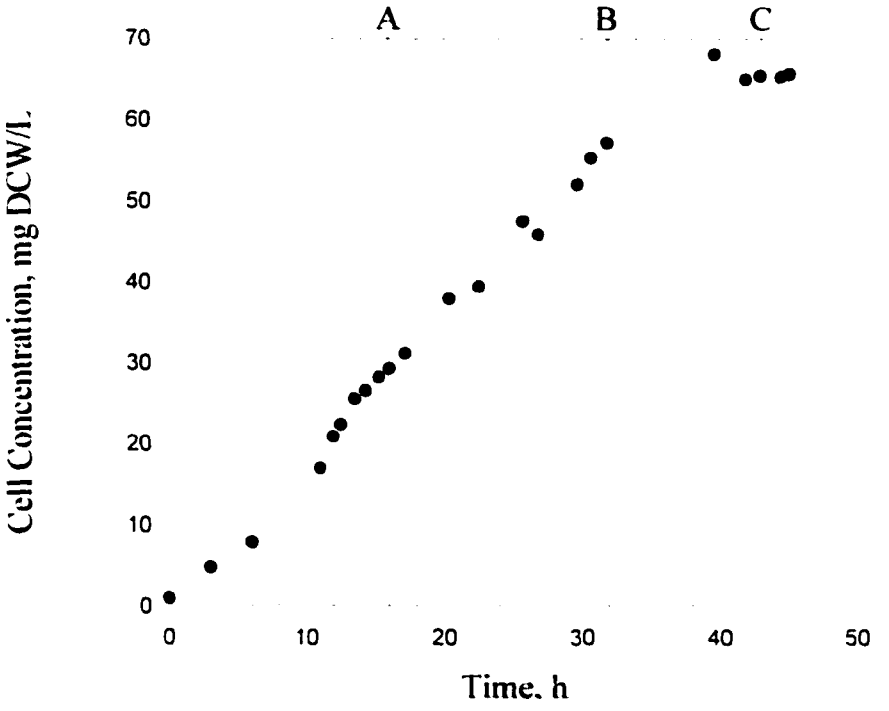

Figure VI-5 Sample points from the growth of *P. putida* F1 on phenol. The vertical lines and letters represent the times at which samples were removed for PLFA/FAME analysis. Each sample (4.5 mg dry cell weight) for PLFA/FAME taken from a batch culture was equally divided into three samples and independently subjected to PLFA/FAME analysis. • – cell concentrations, letters – sample points, X_o – 1.0 mg DCW/L, and S_o – 0.5 mM.

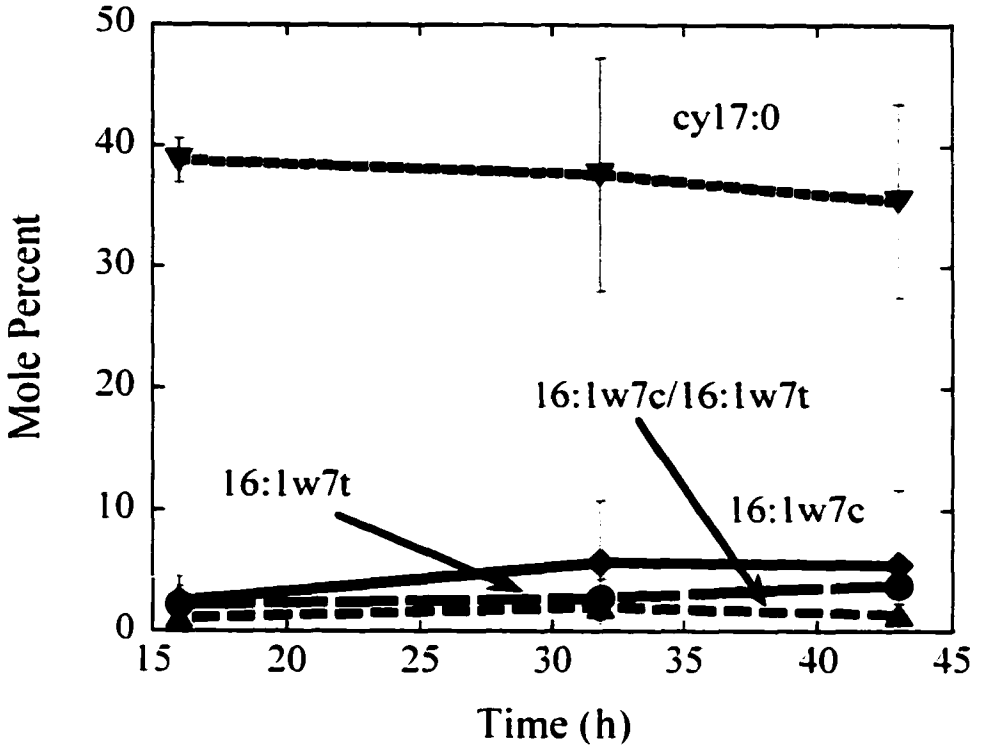

Figure VI-6 Analysis of phospholipids fatty acids in the membrane of *P. putida* F1 grown on phenol. Only the predominant fatty acids are depicted. PLFA/FAME analysis was performed by Dr. J. Bull Rogers and the detailed procedure was described elsewhere (51).

VI.2.3.2 PLFA/FAME analysis during growth on mixed substrates

The compositional change of the phospholipid fatty acids in the cell membrane was also examined during the course of *P. putida* F1 growth on toluene-phenol mixtures. Two samples for the PLFA/FAME analysis were taken from the first half of the exponential growth and two others were removed from the second half of the logarithmic growth phase for the PLFA/FAME analysis (Figure VI-7).

When *P. putida* F1 grew on the toluene-phenol mixture, a dramatic change of predominant fatty acids in the phospholipids of cell membrane occurred while *P. putida* F1 grew on the toluene in the mixture, the predominant species of fatty acid in the phospholipid was the monounsaturated *cis*-hexadecenoic acid (16:1ω7c) (Figure VI-8). This is the same PLFA observed in the toluene only growth. Another monounsaturated fatty acid (oleic acid, 18:1w7c) was observed in this period of cell growth. According to the toluene-phenol mixture biodegradation analysis in Chapter IV, the toluene was degraded first between the sample points A and B, while the phenol concentration in the growth medium was maintained at its initial value (0.25 mM). During this period of the growth, the saturated cyclopropyl (cy17:0) fatty acid was present in phospholipids of cell membrane at low levels, but a slight increase was detected at sample point B when the toluene was nearly depleted and the degradation of phenol began. The ratio of *cis* to *trans* based on the monounsaturated hexadecenoic acid (16:1) decreased.

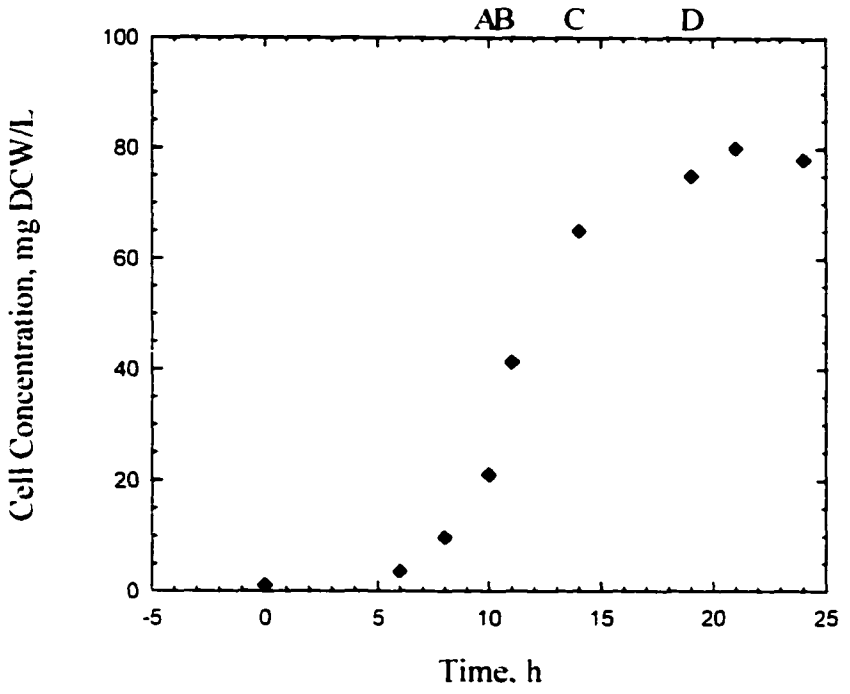

Figure VI-7 Sample points from the growth of *P. putida* F1 on toluene-phenol mixtures. The vertical lines and letters represent the times at which samples were removed for PLFA/FAME analysis. Each sample (4.5 mg dry cell weight) for PLFA/FAME taken from a batch culture was equally divided into three samples and independently subjected to PLFA/FAME analysis. • - cell concentrations, letters – sample points, X_o – 1.0 mg DCW/L, and S_o – 0.25 mM for toluene and phenol, respectively .

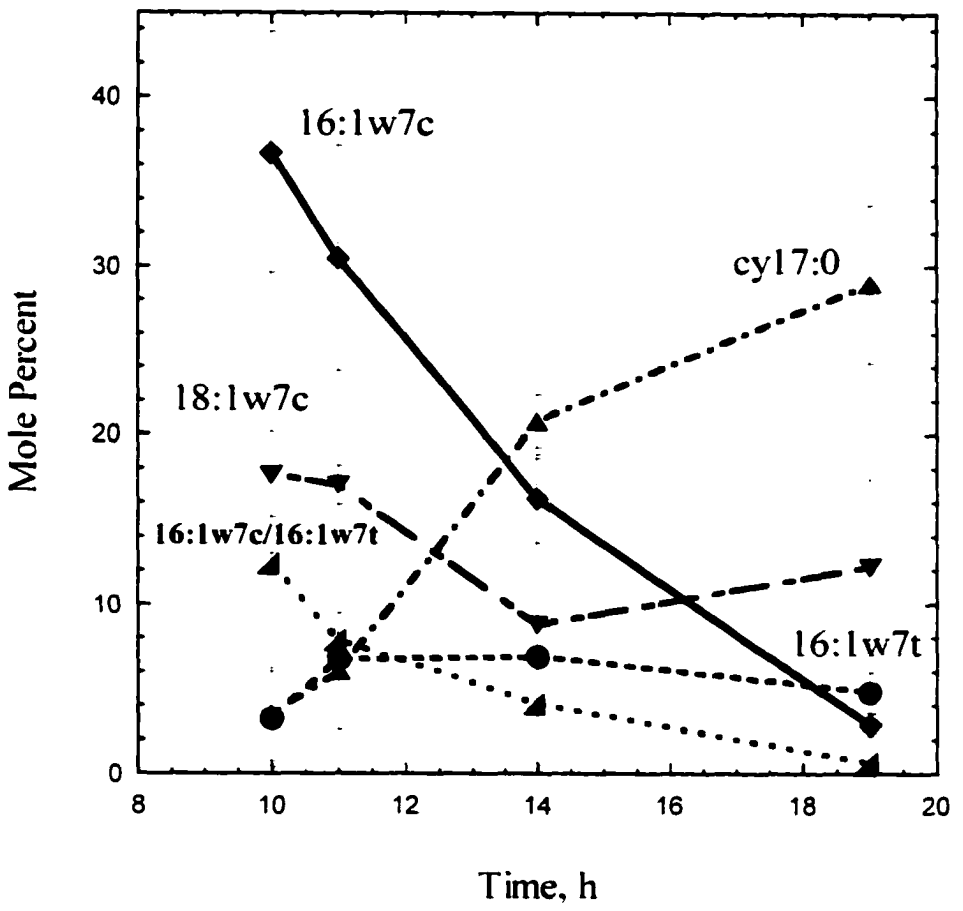

Figure VI-8 Analysis of phospholipids fatty acids in the membrane of *P. putida* F1 grown on toluene-phenol mixtures. Only the predominant fatty acids are depicted. PLFA/FAME analysis was performed by Dr. J. Bull Rogers and the detailed procedure was described elsewhere (51).

At the sample point C, when *P. putida* F1 used the phenol as the major growth substrate and the complete depletion of toluene was achieved, a shift of fatty acid compositions in phospholipids of the cell membrane was observed: the saturated cyclopropyl (cy17:0) became the primary species of fatty acid in the phospholipids of the cell membrane and a considerable decrease in the level of the *cis*-hexadecenoic acid (16:1ω7c) and *cis*-oleic

acid (18:1ω7c) was observed (Figure VI-8). The *cis/trans* ratio in the unsaturated hexadecenoic acid (16:1ω7) substantially decreased.

VI.2.3.3 PLFA/FAME analysis for the toluene spike experiment

A substantial shift in the fatty acid composition of the phospholipids in the cell membrane was observed during the biodegradation of the toluene-phenol mixture by *P. putida* F1 (Figure VI-8 and Table VI-1). This shift of the predominant species of fatty acids corresponded with the sequence of substrate consumption from toluene to phenol by the cells: in the presence of toluene, the predominant species of phospholipid fatty acid composition was the monounsaturated *cis*-hexadecenoic acid (16:1ω7c). When the toluene was completely depleted, the predominant component of phospholipid fatty acid was shifted to the saturated cyclopropyl (cy17:0) while the *cis*-hexadecenoic acid level considerably decreased.

To further investigate the relationship between the observed shifts in phospholipid fatty acid (PLFA) profiles and the growth substrates, a toluene spike experiment was conducted. An inoculum of 1.0 mg DCW/L of *P. putida* F1 was added to a batch bioreactor (1.0 L of MSB growth medium) that contained phenol (0.25 mM) as a sole carbon source. Once the cell concentration in the bioreactor reached about 14 mg DCW/L, toluene (0.25 mM) was added (sample point, Figure VI-9A). A cell sample (4.5 mg DCW) was removed before the toluene spike and equally divided into three separate

samples for PLFA/FAME analysis. After 12 hours of toluene spike, a second sample (4.5 mg DCW) was removed and also divided into three equal portions for PLFA/FAME analysis. Finally, when the cell growth reached in the end of exponential phase at which phenol was almost consumed, a third sample was removed and divided in the same manner (Figure VI-9).

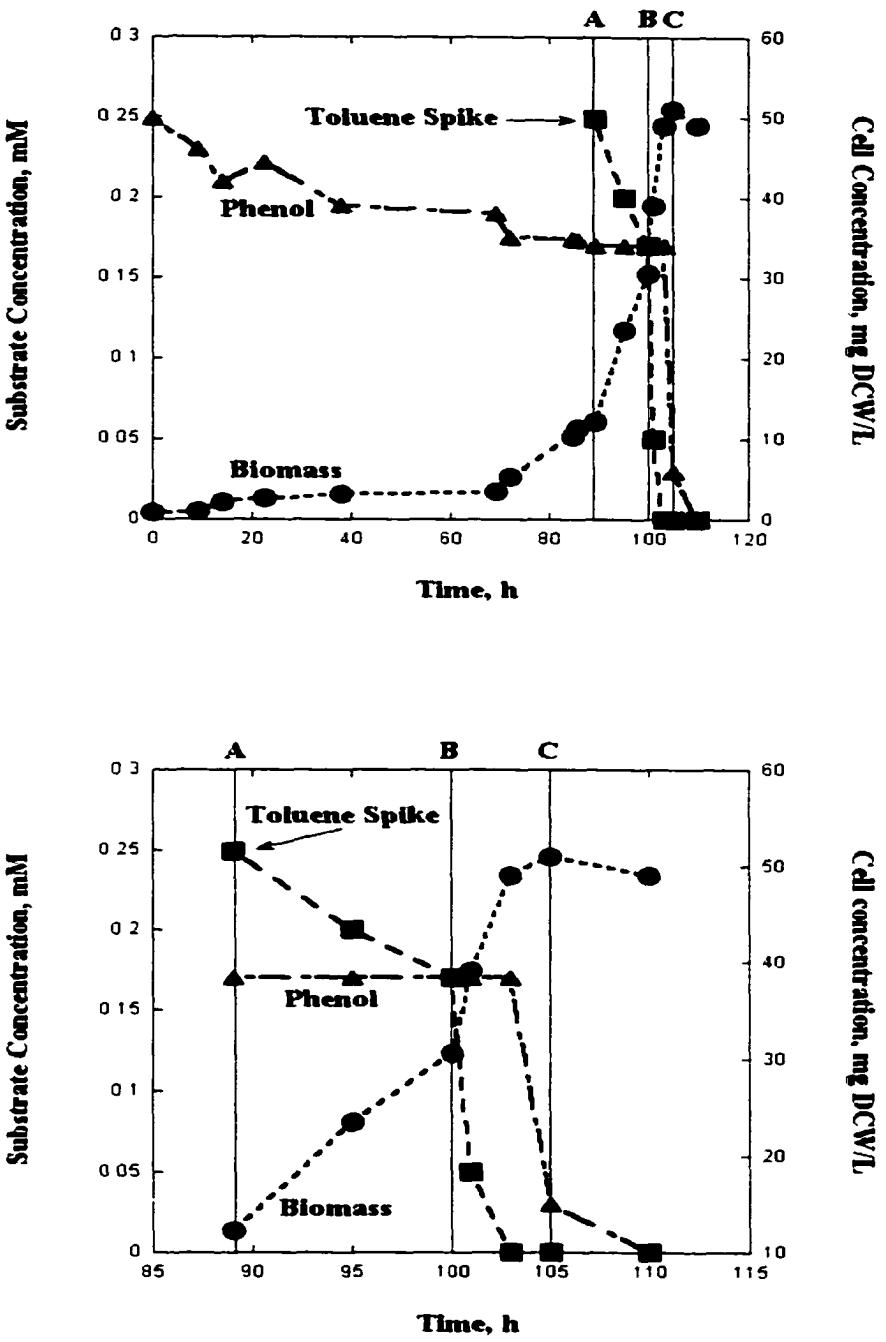

Figure VI-9 Data from a batch cultivation of *P. putida* F1 with a toluene spike. Symbols indicate measurements of liquid-phase toluene (■) phenol (▲) and cell (●) concentrations. The bottom figure depicts the detailed region between 85 and 110 hours of the growth. Vertical lines denote times at which samples were removed for PLFA/FAME. Initially, only phenol was present at 0.25 mM. Toluene (0.25 mM) was spiked after the first PLFA/FAME sample was removed.

The harvested cells were washed and the phospholipid fatty acid profiles were determined (Figure VI-10). When the phenol was the only substrate for the cell growth (before the toluene spike at the sample point A), the saturated cyclopropyl (cy17:0) was the predominant species of phospholipid fatty acid in the cell membrane (Figure VI-10). The unsaturated fatty acids (*cis*- and *trans*-hexadecenoic acid) were present at low levels.

As soon as the toluene was added (Figure VI-9), the degradation of toluene began and the growth rate of the cell was accelerated. The toluene was completely degraded within 10 h of the addition, while no degradation of the phenol was detected. The second sample was removed for the PLFA/FAME analysis as soon as the toluene disappeared. Rapid biodegradation of phenol was observed after the toluene was completely depleted and the complete degradation of the phenol required only 5 hours. The last sample for the PLFA/FAME analysis was taken at the point that the phenol was no longer detected in the growth medium.

The phospholipid fatty acid composition of the cell membrane revealed the significant changes after the toluene spike. The predominant fatty acid species in the phospholipid after the toluene spike (at the sample point B) was the monounsaturated *cis*-hexadecenoic acid (16:1ω7c), and the level of the previous predominant fatty acid (cy17:0) decreased. The *cis/trans* ratio of the hexadecenoic acids (16:1ω7c/16:1ω7t) increased.

At the final sample point C, where the consumption of the phenol was almost completed and the cell growth had reached the end of exponential phase, the saturated cyclopropyl (cy17:0) reached the lowest level of the three sample points and both *cis*- and *trans*-

hexadecenoic acids decreased and increased, respectively. The *cis/trans* ratio of the hexadecenoic acids decreased to about half of their previous values sample point B.

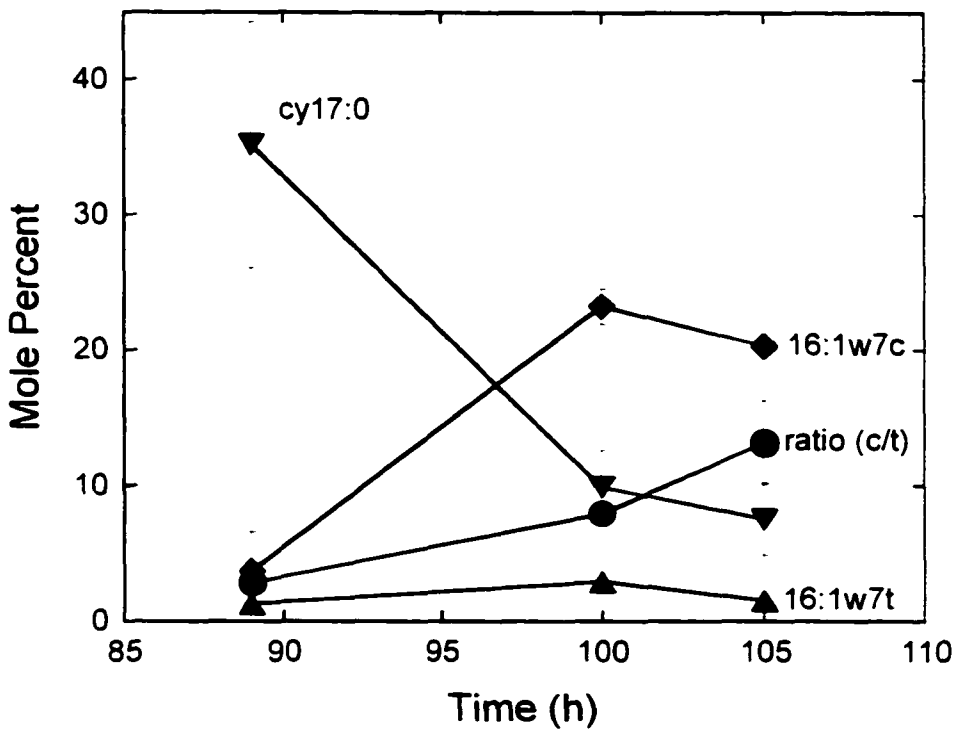

Figure VI-10 Analysis of phospholipids fatty acids in the membrane of *P. putida* F1 grown on phenol with toluene spike. The ratio of *cis*- to *trans*-fatty acids is denoted by ratio (c/t). Only the predominant fatty acids are depicted. PLFA/FAME analysis was performed by Dr. J. Bull Rogers and the detailed procedure was described elsewhere (51).

VI.2.4 DISCUSSIONS

The changes in the concentration of ACP during the biodegradation of toluene and phenol by *P. putida* F1 (Figure VI-2) indicates that the biosynthesis of fatty acids in the cytosol of *P. putida* F1 may be related to the solvent transport across cell membrane. Rawlings and Cronan (48) first isolated and sequenced ACP from *E. coli*. According to their findings, *acpP* encodes ACP and is located between *fabF* and *fabD*, which encode 3-ketoacyl-ACP synthase II and malonyl CoA-ACP transacylase, respectively. Thus, *acpP* is within a cluster of fatty acid biosynthetic genes (*fab* operon) that are regulated coordinately. Therefore, the differential concentration level of ACP during the biodegradation of toluene-phenol mixture could suggest the coordinative expression of *fabF* and *fabD* in *P. putida* F1, too. However, it is premature to conclude the coordinative expression of them in *P. putida* F1 without further identification and proteome analysis of both 3-ketoacyl-ACP synthase II (*fabF*) and malonyl CoA-ACP transacylase (*fabD*) during the biodegradation of toluene-phenol mixture.

ACP and other essential enzymes for *de novo* fatty acid biosynthesis in *Pseudomonas aeruginosa* were cloned, sequenced, and purified by Schweizer and collegues (16, 32). It is not surprising that the NH_2-terminal amino acid sequences of the *P. putida* ACP were highly matched to the ACP in *P. aeruginosa* (32) because ACPs are generally a well-conserved protein family (36) (Table V-2).

Because fatty acids are one of the three essential components of lipids that are the building blocks of the cell membranes, most fatty acids in bacteria are found in the membrane lipids (57). Changes of the phospholipid fatty acids in the bacterial cell membrane have been observed in response to the presence of several different organic solvents from a number of different *Pseudomonas* species (3, 7, 13, 17, 18, 20, 22, 24, 25, 27-31, 34, 37, 38, 43, 44, 47, 59, 61). Previous studies have reported changes in the phospholipid fatty acid composition of the membrane lipids when organic solvents were added. For example, cells were grown on sodium acetate (13, 59) or succinate (14, 34, 44, 45) as a major carbon source. Then, either toluene or phenol was introduced in the middle of logarithmic growth and the compositional changes of the phospholipid fatty acid in the cell membrane were studied for relatively short time (within 15 min of addition). Therefore, the changes of phospholipid fatty acid composition monitored by those studies could be considered as a short-term effect. In this study, *P. putida* F1 was grown on toluene or/and phenol as a sole carbon source for the entire growth period: the changes of the phospholipid fatty acid composition in the cell membrane under these conditions can be considered as a long-term adaptation to the single and mixture aromatic solvent(s).

Two major species of phospholipid fatty acid were observed during the growth of *P. putida* F1 on each single substrate. The monounsaturated *cis*-hexadecenoic acid (16:1ω7c) was the most abundant species during growth on toluene as a single substrate (Figure VI-4). The saturated cyclopropyl (cy17:0), however, was the most abundant species of phospholipid fatty acid in the cell membrane of *P. putida* F1 over the

exponential growth phase (Figure VI-6) when phenol was the sole growth substrate. In that case, the monounsaturated *cis*-hexadecenoic acid (16:1ω7c) was present at less than 5 mole %. This shifted predominance of fatty acid composition according to the structure of aromatic hydrocarbons suggests that the presence of toluene or phenol as a sole growth substrate for the entire growth, not for a short-term response, induces these changes in the cell membrane structure in *P. putida* F1 by altering phospholipid fatty acid composition. The isomeric conversion of *cis* to *trans* unsaturated fatty acids, as reported by Heipieper *et al.* (14) in the presence of 4-chlorophenol as the toxic substance, was not an important mechanism here. The *cis/trans* isomerization of fatty acids was also found in the presence of toluene as an additive (14, 59). In these previous investigations, the isomeric conversion of unsaturated fatty acids (especially the *cis/trans* ratio in the palmitoleic acid (16:1) and the oleic acid (18:1)) as a response to the presence of phenol (14) or toluene (13) was considered as an important initial adaptation for the cell protection. The results of this study did not show any substantial changes in the *cis/trans* ratio (Figure VI-4 and 6) and it is evident that (A) the *cis/trans* conversion can not be interpreted as a long-term protection mechanism for *P. putida* F1, (B) toluene and phenol induce different phospholipid structures in the cell membrane, and (C) this specificity of the cell membrane structure may be essential for the effective transport of toluene or phenol across the hydrophobic cell membrane.

In the studies of phospholipid fatty acid composition changes during the growth of *P. putida* F1 on toluene-phenol mixture, two predominant species of fatty acids were observed. Initially, while toluene was being consumed, the monounsaturated *cis*-

hexadecenoic acid (16:1ω7c) and *cis*-oleic acid (18:1ω7c) were the most abundant phospholipid fatty acids and the saturated cyclopropyl (cy17:0) was maintained at a low level (Figure VI-8). However, when toluene was completely depleted (sample point B) and the cell began consuming phenol as a growth substrate (sample point C), the saturated cyclopropyl (cy17:0) was detected as the most abundant phospholipid fatty acid (sample point C). At the sample point D, where phenol was nearly depleted, the cyclopropyl fatty acid reached its highest level (Figure VI-8).

Inoue and Horikoshi studied a number of Gram-positive and Gram-negative bacteria with regard to their tolerance to a number of toxic solvents with different log P_{ow} values (23). They reported that the polarity properties of solvents affect the characteristic of the cell surfaces and directly influenced the growth of the bacteria. Since toluene has a greater log P_{ow} value than phenol or benzene, it is reasonable to expect toluene can penetrate easier than either benzene or phenol by diffusion. Reardon *et al.* (49) reported the different kinetic parameters in the growth of *P. putida* F1 and the biodegradation rate on toluene, phenol, benzene, and their mixtures. The order of log P_{ow} values (toluene > benzene > phenol) for these three solvents corresponds to the order of the cell growth and biodegradation rates: i.e. the greater the log P_{ow} values, the faster the cell growth and biodegradation rate. These results support the hypothesis that the structure of the cell membrane during toluene transport may inhibit the transport of phenol when both toluene and phenol are present at the same time by changing the polarity of the cell membrane.

To examine the reversibility of the shift in fatty acid composition. the toluene spike experiment was performed. The compositional changes of the membrane fatty acids were exactly opposite of the mixture experiment in that: thus. the saturated cyclopropyl (cy17:0) was the predominant species while only phenol was present in the medium. but its predominance shifted to the unsaturated *cis*-hexadecenoic acid (16:1ω7c) (Figure VI-10) after toluene was spiked. The degradation of phenol also stopped while the spiked toluene was degraded (Figure VI-9). This reversibility of the predominant species of fatty acid composition suggests the inhibitory effect of toluene on phenol transport into the cell.

This study shows that (A) the cell membrane phospholipid fatty acid composition changes in response to the presence of toluene and phenol mixtures as a sole carbon source of *P. putida* F1 do not involve any substantial change of *cis/trans* conversion of the unsaturated fatty acids. (B) the shift of predominant species of fatty acid during the biodegradation of toluene-phenol mixtures is reversible. supporting the hypothesis that toluene inhibits phenol transport across the cell membrane. and (C) the differential production of ACP in the presence of toluene-phenol mixture provides a fundamental information to support the previous findings (30. 44-47) that the *de novo* biosynthesis of fatty acid is important to repair the damaged membrane caused by the partition of toxic solvents in the outer-membrane.

VI.3 β-ketoadipate:succinyl CoA transferase

The identification of protein No.18 as β-ketoadipate:succinyl-coenzyme A transferase (TR. β-ketoadipate:succinyl-CoA transferase. EC 2.8.3.6). Although no further characterization data is available from this research. the detection of this enzyme (a Group P protein) is interesting because it is one of two enzymes that complete the biodegradation of aromatic compounds through both catechol and protocatechuate in the β-ketadipate pathway of *Pseudomonas putida* (40). The β-ketadipate pathway has been widely observed among gram-positive (1. 4) and gram–negative bacteria (10. 26). Ornston reported comprehensive studies of the β-ketoadipate pathway in *Pseudomonas putida* PRS (39-42).

In the known toluene catabolic pathway of *P. putida*. toluene is first oxidized to cis-toluene dihydrodiol by toluene dioxygenase (8. 9. 62) and converted to 3-methyl catechol (63). Then. 3-methyl catechol is converted to acetaldehyde and pyruvate (33). Involvement of toluene dioxygenase (TDO) in the initial degradation of phenol was reported by Spain et al (55. 56). who found evidence that the conversion of phenol to catechol is initially oxidized by TDO in *P. putida* F1. Catechol. which is a product of oxidation by TDO. is not only the initial intermediate of phenol degradation through 2-hydroxy muconic semialdehyde (55. 56). but also one of two important phenolic intermediates that directly induce the β-ketoadipate pathway through *cis. cis*-muconic acid in *P. putida* (Figure VI-11) (19. 40. 42). The observation of the β-

ketoadipate:succinyl-coenzyme A transferase (TR) during the biodegradation of either phenol or toluene-phenol mixtures suggested the activation of β-ketoadipate pathways by *P. putida* F1. The production level of TR during the course of phenol degradation, however, was low (Figure IV-7), and also maintained at low level while *P. putida* F1 utilized phenol as a sole carbon source after the complete depletion of toluene (Figure IV-10 and V-5). This low level of the TR production suggests that there certainly exists a biodegradation activity through β-ketoadipate pathway at basal level in *P. putida* F1.

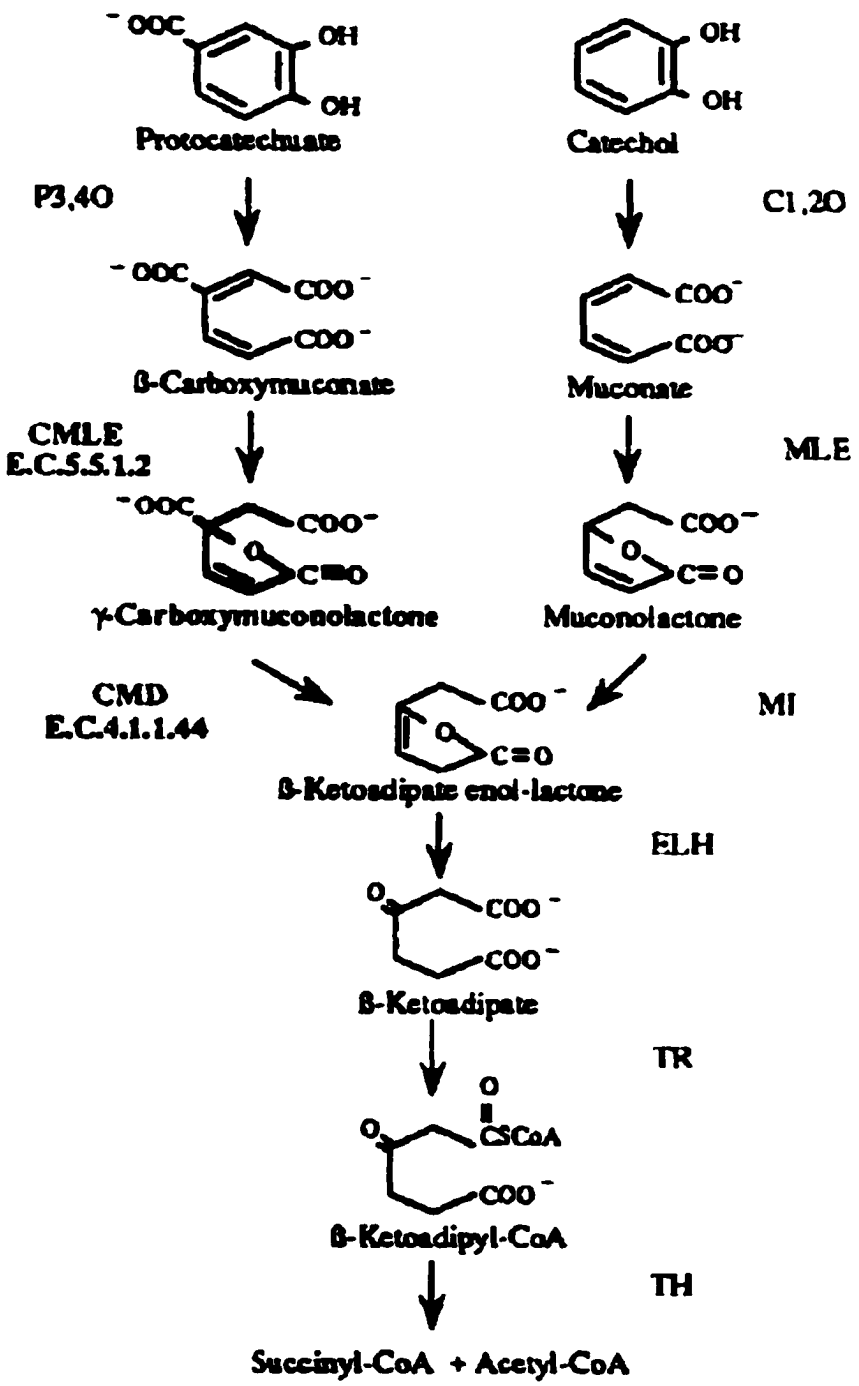

Figure VI-11 Bacterial β-ketoadipate pathway. Enzyme abbreviations: P3.O4 – protocatechuate 3.4-dioxygenase: CMLE – β-carboxy-*cis*, *cis*-muconate lactonizing enzyme: CMD – γ-carboxymuconolactone decarboxylase: C1.2O – catechol 1.2-dioxygenase: MLE -- *cis*, *cis* -muconate lactonizing enzyme: MI -- muconolactone isomerase: ELH -- enol-lactone hydrolase: TR -- β-ketoadipate:succinyl- CoA transferase: TH, β-ketoadipyl- CoA thiolase: CMH -- β -carboxymuconolactone hydrolase (11).

VI.4 References

1. **Blakley, E. R.** 1974. The microbial degradation of cyclohexanecarboxylic acid: a pathway involving aromatization to form p-hydroxybenzoic acid. Can. J. Microbiol. **20:**1297-1306.

2. **Boulton, C. A., and C. Ratledge.** 1985. Biosynthesis of fatty acids and lipids. p. 459-482. *In* M. moo-young (ed.), Comprehensive biotechnology, vol. 1. Pergamon Press. Oxford.

3. **Bugg, T., J. M. Foght, M. A. Pickard, and M. R. Gray.** 2000. Uptake and active efflux of polycyclic aromatic hydrocarbons by *Pseudomonas fluorescens* LP6a. Appl. Environ. Microbiol. **66:**5387-5392.

4. **Crawford, R. L.** 1976. Pathways of 4-hydroxybenzoate degradation among species of *Bacillus*. J. Bacteriol. **127:**204-10.

5. **Cronan Jr, J. E., and C.O. Rock.** 1996. Biosynthesis of membrane lipids.. p. 612-636. *In* F. Neidhardt, R. Curtiss III., J.L. Ingrahm, E.C.C. Lin., K.B. Low, B. Magasanik, W.S. Reznikoff, M. Riley, M. Schaechter, and H.E. Umbarger, (ed.), *Escherichia coli* and *Salmonella typhimurium* (Cellular and Molecular Biology). 2 ed. American Society of Microbiology, Washington, D.C.

6. **D'Agnolo, G. D., I.S. Rosenfeld, and P.R. Vagelos.** 1975. Multiple forms of b-ketoacyl-acyl carrier-protein synthetase in *Escherichia coli*. J. Biol. Chem. **250:**5289-5294.

7. **Diefenbach, R., and H. Keweloh.** 1994. Synthesis of trans unsaturated fatty acids in *Pseudomonas putida* P8 by direct isomerization of the double bond of lipids. Arch. Microbiol. **162:**120-125.

8. **Finette, B. A., V. Subramanian, and D. T. Gibson.** 1984. Isolation and characterization of *Pseudomonas putida* PpF1 mutants defective in the toluene dioxygenase enzyme system. J. Bacteriol. **160:**1003-1009.

9. **Gibson, D. T., G. J. Zylstra, and S. Chauhan.** 1990. Biotransformations catalyzed by toluene dioxygenase from *Pseudomonas putida* F1, p. 121-132. *In* I. S. Silver, A. M. Chakrabarty, B. Iglewski, and S. Kaplan (ed.), Pseudomonas: Biotransformations, Pathogenesis, and Evolving Biotechnology. American Society for Microbiology, Washington D.C.

10. **Hardisson, C., J. M. Sala-Trepat, and R. Y. Stanier.** 1969. Pathways for the oxidation of aromatic compounds by *Azotobacter*. J. Gen. Microbiol. **59:**1-11.

11. **Harwood, C. S., and R. E. Parales.** 1996. The β–ketoadipate pathway and the biology of self-identity. Annu. Rev. Microbiol. **50:**553-590.

12. **Heath, R. J., and C.O. Rock.** 1996. Roles of the FabA and FabZ. β-hydroxyacyl-acyl carrier protein dehydratase in *Escherichia coli* fatty acid biosynthesis. J. Biol. Chem. **271:**27795-27801.

13. **Heipieper, F., and J. A. M. deBont.** 1994. Adaptation of *Pseudomonas putida* S12 to ethanol and toluene at the level of fatty acid composition of membranes. Appl. Environ. Microbiol. **60:**4440-4444.

14. **Heipieper, H., R. Diefenbach, and H. Keweloh.** 1992. Conversion of *cis* unsaturated fatty acids to *trans*, a possible mechanism for the protection of

phenol-degrading *Pseudomonas putida* P8 from substrate toxicity. Appl. Environ. Microbiol. **58:**1847-1852.

15. **Heipieper, H. J., H. Keweloh, and H-J. Rehm.** 1991. Influence of phenols on growth and membrane permeability of free and immobilized *Escherichia coli.* Appl. Environ. Microbiol. **57:**1213-1217.

16. **Hoang, T. T., and H. P. Schweizer.** 1997. Fatty acid biosynthesis in *Pseudomonas aeruginosa*: cloning and characterization of the fabAB operon encoding b-hydroxyacyl-acyl carrier protein dehydratase (FabA) and b-ketoacyl-acyl carrier protein synthase I (FabB). J. Bacteriol. **179:**5326-5332.

17. **Holtwick, R., F. Meinhardt, and H. Keweloh.** 1997. *cis-trans* isomerization of unsaturated fatty acids: Cloning and sequencing of the *cti* gene from *Pseudomonas putida* P8. Appl. Environ. Microbiol. **63:**4292-4297.

18. **Holtwick, R., H. Keweloh, and F. Meinhardt.** 1999. *cis/trans* isomerase of unsaturated fatty acids of *Pseudomonas putida* P8: Evidence for a heme protein of the cytochrom c type. Appl. Environ. Microbiol. **65:**2644-2649.

19. **Houghton, J., T. Brown, A. Appel, E. Hughes, and L. Ornston.** 1995. Discontinuities in the evolution of *Pseudomonas putida* cat genes. J. Bacteriol. **177:**401-412.

20. **Huertas, M.-J., E. Duque, S. Marques, and J. L. Ramos.** 1998. Survival in soil of different toluene-degrading *Pseudomonas* strains after solvent shock. Appl. Environ. Microbiol. **64:**38-42.

21. **Ingram, L. O.** 1977. Changes in lipid composition of *Escherichia coli* resulting from growth with organic solvents and with food additives. Appl. Environ. Microbiol. **33:**1233-1236.

22. **Inoue, A., and K. Horikoshi.** 1989. A *Pseudomonas* thrives in high concentrations of toluene. Nature **338:**264-266.

23. **Inoue, A., and K. Horikoshi.** 1991. Estimation of solvent-tolerance of bacteria by the solvent parameter log P. J. Ferment. Bioeng. **71:**194-196.

24. **Isken, S., A. Derks, P. F. G. Wolffs, and J. A. M. de Bont.** 1999. Effect of organic solvents on the yield of solvent-tolerant *Pseudomonas putida* S12. Appl. Environ. Microbiol. **65:**2631-2635.

25. **Isken, S., and J. A. M. de Bont.** 1996. Active efflux of toluene in a solvent resistant bacterium. J. Bacteriol. **178:**6056-6058.

26. **Johnson, B. F., and R. Y. Stanier.** 1971. Dissimilation of aromatic compounds by *Alcali* genes *eutrophus*. J. Bacteriol. **107:**468-75.

27. **Junker, F., and J.L. Ramos.** 1999. Involvement of the *cis/trans* isomerase *Cti* in solvent resistance of *Pseudomonas putida* DOT-T1E. J. Bacteriol. **181:**5693-5700.

28. **Kieboom, J., and J. A. M. de Bont.** 2001. Identification and molecular characterization of an efflux system involved in *Pseudomonas putida* S12 multidrug resistance. Microbiology. **147:**43-51.

29. **Kieboom, J., J. J. Dennis, G. J. Zylstra, and J. A. M. de Bont.** 1998. Active efflux of organic solvents by *Pseudomonas putida* S12 is induced by solvents. J. Bacteriol. **180:**6769-6772.

30. **Kim, K., S. Lee, K. Lee, and D. Lim.** 1998. Isolation and characterization of toluene-sensitive mutants from the toluene-resistant bacterium *Pseudomonas putida* GM73. J. Bacteriol. **180:**3692-3696.

31. **Kobayashi, H., H. Takami, H. Hirayama, K. Kobata, R. Usami, and K. Horikoshi.** 1999. Outer membrane changes in a toluene-sensitive mutant of toluene-tolerant *Pseudomonas putida* IH-2000. J. Bacteriol. **181:**4493-4498.

32. **Kutchma, A. J., T. T. Hoang, and H. P. Schweizer.** 1999. Characterization of a *Pseudomonas aeruginosa* fatty acid biosynthetic gene cluster: Purification of acyl carrier protein (ACP) and malonyl-coenzyme A:ACP transacylase (FabD). J. Bacteriol. **181:**5498-5504.

33. **Lau, P. C. K., H. Bergeron, D. Labbe, Y. Wang, R. Brousseau, and D. T. Gibson.** 1994. Sequence and expression of the *todGIH* genes involved in the last three steps of toluene degradation by *Pseudomonas putida* F1. Gene **146:**7-13.

34. **Loffeld, B., and H. Keweloh.** 1996. *cis/trans* isomerization of unsaturated fatty acids as possible control mechanism of membrane fluidity in *Pseudomonas putida* P8. Lipids **31:**811-815.

35. **Magnuson, K., S. Jackowski, C.O. Rock, and J.E. Cronan Jr.** 1993. Regulation of fatty acid biosynthesis in *Escherichia coli.* Microbiol. Mol. Biolol. Rev. **57:**522-542.

36. **Morbidoni, H., D. de Mendoza, and J. Cronan, Jr.** 1996. *Bacillus subtilis* acyl carrier protein is encoded in a cluster of lipid biosynthesis genes. J. Bacteriol. **178:**4794-4800.

37. **Mosqueda, G., and J.-L. Ramos.** 2000. A set of genes encoding a second toluene efflux system in *Pseudomonas putida* DOT-T1E is linked to the *tod* genes for toluene metabolism. J. Bacteriol. **182:**937-943.

38. **Okuyama, H., A. Ueno, D. Enari, N. Morita, and T. Kusano.** 1998. Purification and characterization of 9-hexadecenoic acid *cis-trans* isomerase from *Pseudomonas* sp. strain E-3. Arch. Microbiol. **169:**29-35.

39. **Ornston, L. N.** 1966. The conversion of catechol and protocatechuate to β–ketoadipate by *Pseudomonas putida*. II. Enzymes of the protocatechuate pathway. J. Biol. Chem. **241:**3787-3794.

40. **Ornston, L. N.** 1966. The conversion of catechol and protocatechuate to β-ketoadipate by *Pseudomonas putida*. III. Enzymes of the catechol pathway. J. Biol. Chem. **241:**3795-99.

41. **Ornston, L. N.** 1966. The conversion of catechol and protocatechuate to β-ketoadipate by *Pseudomonas putida*. IV. Regulation. J. Biol. Chem. **241:**3800-10.

42. **Ornston, L. N., and R. Y. Stanier.** 1966. The conversion of catechol and protocatechuate to β-ketoadipate by *Pseudomonas putida*. I. Biochemistry. J. Biol. Chem. **241:**3776-86.

43. **Pedrotta, V., and B. Witholt.** 1999. Isolation and characterization of the *cis-trans*-unsaturated fatty acid isomerase of *Pseudomonas oleovorans* GPo12. J. Bacteriol. **181:**3256-3261.

44. **Pinkart, H., and D. White.** 1997. Phospholipid biosynthesis and solvent tolerance in *Pseudomonas putida* strains. J. Bacteriol. **179:**4219-4226.

45. **Pinkart, H., J. Wolfram, R. Rogers, and D. White.** 1996. Cell envelope changes in solvent-tolerant and solvent-sensitive *Pseudomonas putida* strains following exposure to *o*-xylene. Appl. Environ. Microbiol. **62:**1129-1132.

46. **Ramos, J. L., E. Duque, J.-J. Rodriguez-Herva, P. Godoy, A. Haidour, F. Reyes, and A. Fernandez-Barrero.** 1997. Mechanisms for solvent tolerance in bacteria. J. Biol. Chem. **272:**3887-3890.

47. **Ramos, J. L., E. Duque, P. Godoy, and A. Aegura.** 1998. Efflux pumps involved in toluene tolerance in *Pseudomonas putida* DOT-T1E. J. Bacteriol. **180:**3323-3329.

48. **Rawlings, M., and J. Cronan, Jr.** 1992. The gene encoding *Escherichia coli* acyl carrier protein lies within a cluster of fatty acid biosynthetic genes. J. Biol. Chem. **267:**5751-5754.

49. **Reardon, K. F., D. C. Mosteller, and J. D. Rogers.** 2000. Biodegradation kinetics of benzene, toluene, and phenol as single and mixed substrates for *Pseudomonas putida* F1. Biotechnol. Bioeng. **69:**385-400.

50. **Rock, C. O., and J. J. E. Cronan.** 1982. Regulation of bacterial membrane lipid synthesis. Curr. Top. Membr. Transp. **17:**209-233.

51. **Rogers, J.** 2000. Microbe-level investigation of sequential anaerobic/aerobic bioremediation of polychlorinated biphenyls in soil. Ph.D. dissertation. Colorado State University, Fort Collins.

52. **Sikkema, J., B. Poolman, W. N. Konings, and J.A.M. de Bont.** 1992. Effects of the membrane action of tetrralin on the functional and structural properties of artificial and bacterial membranes. J. Bacteriol. **174:**2986-2992.

53. **Sikkema, J., J. A. M. de Bont, and B. Poolman.** 1994. Interactions of cyclic hydrocarbons with biological membranes. J. Biol. Chem. **269:**8022-8028.

54. **Sikkema, J., J.A.M. de Bont, and B. Poolman.** 1995. Mechanism of membrane toxicity of hydrocarbons. Microbiol. Rev. **59:**201-222.

55. **Spain, J. C., and D. T. Gibson.** 1988. Oxidation of Substituted phenols by *Pseudomonas* putida F1 and *Pseudomonas* sp. strain JS6. Appl. Environ. Microbiol. **54:**1399-1404.

56. **Spain, J. C., G. J. Zylstra, C. K. Blake, and D. T. Gibson.** 1989. Monohydroxylation of phenol and 2,5-dichlorophenol by toluene dioxygenase in *Pseudomonas putida* F1. Appl. Environ. Microbiol. **55:**2648-2652.

57. **Stryer.** 1995. Fatty acid metabolism., p. 603-628. *In* L. Stryer (ed.). Biochemistry. W. H. Freeman and company., New York.

58. **Voet, D., and J.G. Voet.** 1990. Fatty acid biosynthesis., p. 634-641. Biochemistry. John Wiley & Sons, New York.

59. **Weber, F. J., S. Isken, and J A M de Bont.** 1994. *Cis/trans* isomerization of fatty acids as a defense mechanism of *Pseudomonas putida* strains to toxic concentrations of toluene. Microbiology **140:**2013-2017.

60. **Weber Jr, W. J., and J. A. M. de Bont.** 1996. Adaptation mechanisms of microorganisms to the toxic effects of organic solvents on membranes. Biochim. Biophys. Acta. **1286:**225-245.

61. **Wery, J., B. Hidayat, J. Kieboom, and J. A. M. de Bont.** 2001. An insertion sequence prepares *Pseudomonas putida* S12 for severe solvent stress. J. Biol. Chem. **276:**5700-5706.

62. **Yeh, W. K., D. T. Gibson, and T. N. Liu.** 1977. Toluene dioxygenase: A multicomponent enzyme system. Biochem. Biophy. Res. Comm. **78:**401-410.

63. **Zylstra, G. J., L. P. Wackett, and D. T. Gibson.** 1989. Trichloroethylene degradation by *Escherichia coli* containing the cloned *Pseudomonas putida* F1 toluene dioxygenase genes. Appl. Environ. Microbiol. **55:**3162-3166.

CHAPTER VII EFFECTS OF HEAVY METALS ON THE BIODEGRADATION OF TOLUENE-PHENOL MIXTURES BY *PSEUDOMONAS PUTIDA* F1

VII.1 Research Motivation and Goals

Metals are critical components of many biochemical systems as enzyme cofactors or as important components of ion pumps that help to maintain osmotic balance within cells (3, 13). However, high concentrations of metal ions can disrupt the osmotic conditions of cells or the electrochemical stability of cell membranes by forming nonspecific complexes, leading to toxic effects to cells (3, 12, 13). Extensive attention has been paid to the hazards arising from contamination of the environment by heavy metals (14). Decontamination of heavy metal-polluted soil and water (ground and surface) has been a difficult challenge for a long time. The high costs and the physical impracticality associated with physical and chemical treatments had led to research on alternative remediation technologies. Bioremediation approaches have been developed for the decontamination of heavy metal ions from many waste streams (5). Bioremediation of heavy metals can take the form of *in situ* bioremediation that can be achieved using intrinsic biological agents (e.g., bacteria, fungi, plants) of the contaminated sites. A

number of microbe-based bioremediation studies have been conducted on metal-contaminated soils (21, 26).

Through improper disposal or spillage of solvents, fuels, metal-cutting waste, or other mixtures, the soil and groundwater at these sites contain multiple pollutants. The National Research Council (1994) has recognized the frequency of metal and organic chemical co-contamination. This co-contamination may be a more serious threat than organic chemical contamination alone because the intrinsic toxic effects of heavy metals can severely inhibit the growth of microbial populations that are naturally able to metabolize the organic pollutants. Heavy metal ions can also affect the biochemical activities of the intrinsic microbial community and result in decreased biomass and diversity (7, 18, 21). However, very little is known about biotransformations within mixtures of organic chemicals and heavy metals.

The major goal of this study was to obtain information on the effects of heavy metals on both cell physiology and biodegradation kinetics of *P. putida* F1. Toluene and phenol were chosen as the carbon sources for the growth of the cell and two different heavy metals were chosen: cadmium and chromate.

Cadmium (Cd) ions have one valence (2+) and are thus not redox active. Cd^{2+} can form inorganic precipitates with sulfide and phosphate. It is toxic to aerobic and anaerobic cells (2). Although a tremendous amount of work on cadmium toxicity to microorganisms has been done, no defined mechanisms of toxic action have been

elucidated (for more complete review, see ref. (13)) and only few reports on the effects of Cd on pollutant biodegradation were found (8, 29). Toxic effects by cadmium can be generalized as thiol-binding and denaturation of proteins, interaction with calcium metabolism and membrane damage, or loss of a protective function by interaction with zinc metabolism (5). In *E. coli*, mutation of *dsbA*, encoding a product required for disulfide formation, leads to cadmium sensitivity (19). Thus, DsbA appears to be a target protein for cadmium in the periplasm of gram-negative bacteria. Feriance et al. (4) reported on the proteins induced by cadmium in *E. coli* K12, but the roles of these additional proteins are not understood. Cadmium efflux is mainly responsible for bacterial resistance except cyanobacteria, which contain metallothioneins (15).

Chromium (VI), found as chromate, can be used as an electron accepter by anaerobic bacteria (9, 10). Garbisu et al. (6) reported that aerobic bacteria can also reduce chromate (Cr(VI)). Cr(VI) is more toxic and mobile than its reduced form, Cr(III). Chromate reduction coupled with the oxidation of benzoic acid (24) and naphthalene (23) has been reported. At Department of Energy (DOE) sites, chromate is the second most common heavy metal contaminant, ranging in concentration between 0.008 and 173 μM in ground water and 98 nM to 76 mM in soil and sediments (20). Several bacteria have chromate reductase activity that can convert Cr(VI) to Cr(III); thus, reduction by chromate reductase affords a means of chromate bioremediation. Chromate reductase was purified from *P. putida* (16) and *P. ambigua* (27), and characterized. Chromate reductase was a target enzyme for protein engineering to increase the ability of the reduction capability in

the presence of other contaminants (28). However, once again very little is known about the effect of chromate (VI) on the biodegradation of aromatic hydrocarbon mixtures.

In this chapter, the effect of heavy metals (Cd or Cr(VI)) on the biodegradation and growth of *P. putida* F1 in the presence of toluene-phenol mixtures was studied. First, the tolerance of the cells to each heavy metal was examined in terms of viable cell counts. On the basis of those tolerance results, the inhibitory effect of cadmium on the cell growth on toluene or/and phenol was examined. The morphological changes of the cells in the presence of metals were then evaluated by a transmission electron microscopy (TEM).

VII.2 Results

VII.2.1 HEAVY METAL TOLERANCE

Tolerance tests were performed by counting the number of viable colonies on Petri dishes from samples removed from a serum bottle. Cells were grown on either single (toluene or phenol) or mixed (toluene and phenol) growth substrates with or without a heavy metal (Cd or Cr(VI)) in serum bottles. The culture in each serum bottle was allowed to grow for 7 days after inoculation with *P. putida* F1.

Two main objectives of this tolerance test with serum bottle cultivation were served: first, to determine the concentration of heavy metals that inhibit *P. putida* F1 growth, and second, to observe the inhibition patterns of heavy metal ions on the growth of the cell. These results were used to design the inhibition kinetics study with bioreactors in the following section.

VII.2.1.1 Cadmium

The results of the viable cell counts on Petri dishes are presented in Figure VII-1. In the absence of any heavy metal ions, the plate counts of toluene-grown cells were higher than any cases of colony counts in the presence of Cd or Cr(VI). This clearly indicates that the growth of *P. putida* F1 on toluene was inhibited by all tested levels of these metals. Although experimental variability prevents extensive quantitative analysis, some trends

can be observed. Apparent cell growth with 10 ppm Cd reached about 25% of the control growth (without Cd) after 4 days of incubation (Figure VII-1 (A)).

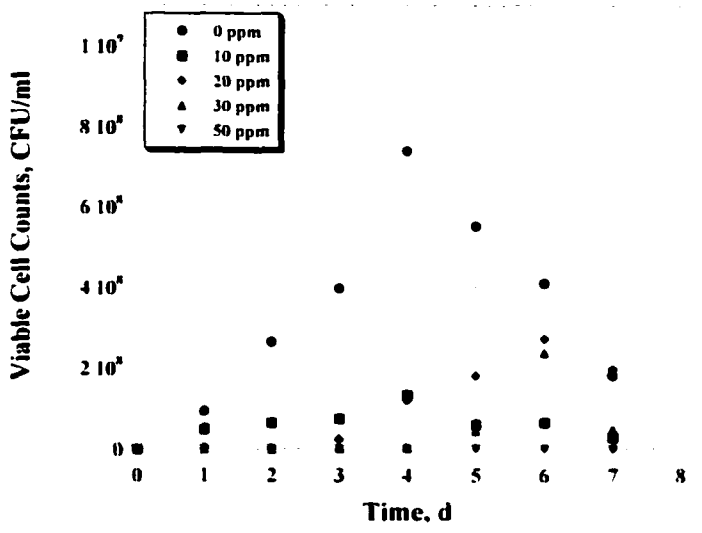

(A)

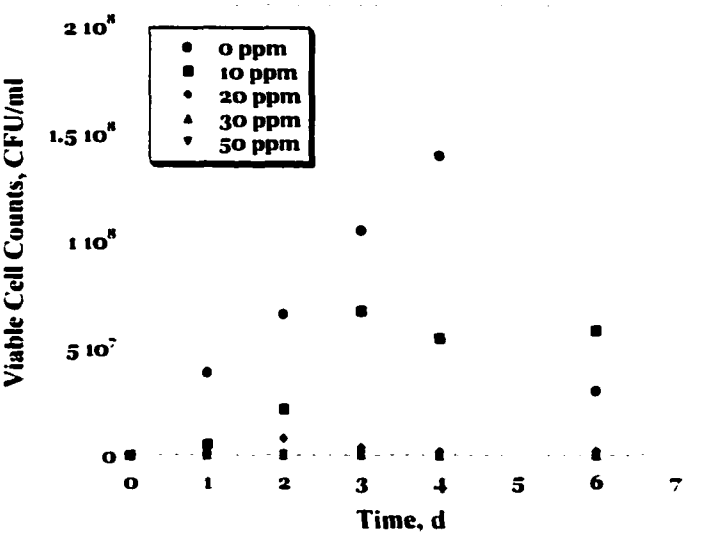

(1)

Figure VII-1 Cadmium (Cd) tolerance of *P. putida* F1 growing on toluene (A) and phenol (B) in a batch culture. The initial concentration of toluene and phenol were 0.45 and 0.5 mM, respectively. X_o = 1.0 mg/L.

Subsequently, the number of viable colonies with 10 ppm Cd suddenly dropped and remained at a low level. However, the number of viable cell counts with 20 ppm Cd outgrew the cells with 10 ppm Cd after 5 days of incubation and increased until 6^{th} days of growth. After 5 days of growth, the number of viable cell counts for all cultivations with Cd no longer increased. Based on this result, the Cd inhibition to the growth of *P. putida* F1 was apparently proportional to its concentration increase (Figure VII-1 (A)). Since ten parts per million of Cd inhibited cell growth, but allowed them grow about 25% of the control, this concentration of Cd was selected for the kinetics study in bioreactors.

The Cd tolerance of *P. putida* F1 grown on phenol was also examined in the same manner. In Figure VII-1 (B), the cells grown on phenol show higher Cd tolerance than those grown on toluene. For example, in the presence of 10 ppm Cd, the number of viable cell counts reached between 40 and 50 percent of the control after 3 days of incubation and this was maintained for 3 days. However, more than 20 ppm of Cd completely inhibited the growth of the cell on phenol.

VII.2.1.2 Chromate

Since chromate is known to be more toxic to bacterial growth than cadmium (21-24), much lower concentrations of chromate than cadmium were added to the growth medium. Cells grown on toluene with chromate (0.2 and 0.5 ppm) did not show differences in terms of viable cell counts compared to that of the control (Figure VII-2 (A)). This

tolerance of *P. putida* F1 to chromate (up to 1.0 ppm) might be due to the chromate reductase. A novel chromate resuctase was purified and characterized recently from a *P. putida* strain by Park et al. (16). However, in this study no evaluation of chromate reductase activity was performed. More than 1.0 ppm of chromate severely inhibited the cell growth (Figure VII-2 (A)).

In the case of the cell growth on phenol with Cr(VI), three concentrations (0.2, 0.5, and 1.0 ppm) of chromate did not inhibit the growth of the cells for the first two days of incubation. After three and four days, respectively, the numbers of viable cell counts with 0.2 and 0.5 ppm of Cr(VI) were higher than in the other cases, including the control cultivation (without chromate) (Figure VII-2 (B)). This result could be considered as a stimulatory effect of low concentrations of chromate, and it opens a possibility that there may be a synergistic interaction between phenol (or intermediates of phenol degradation) and chromate.

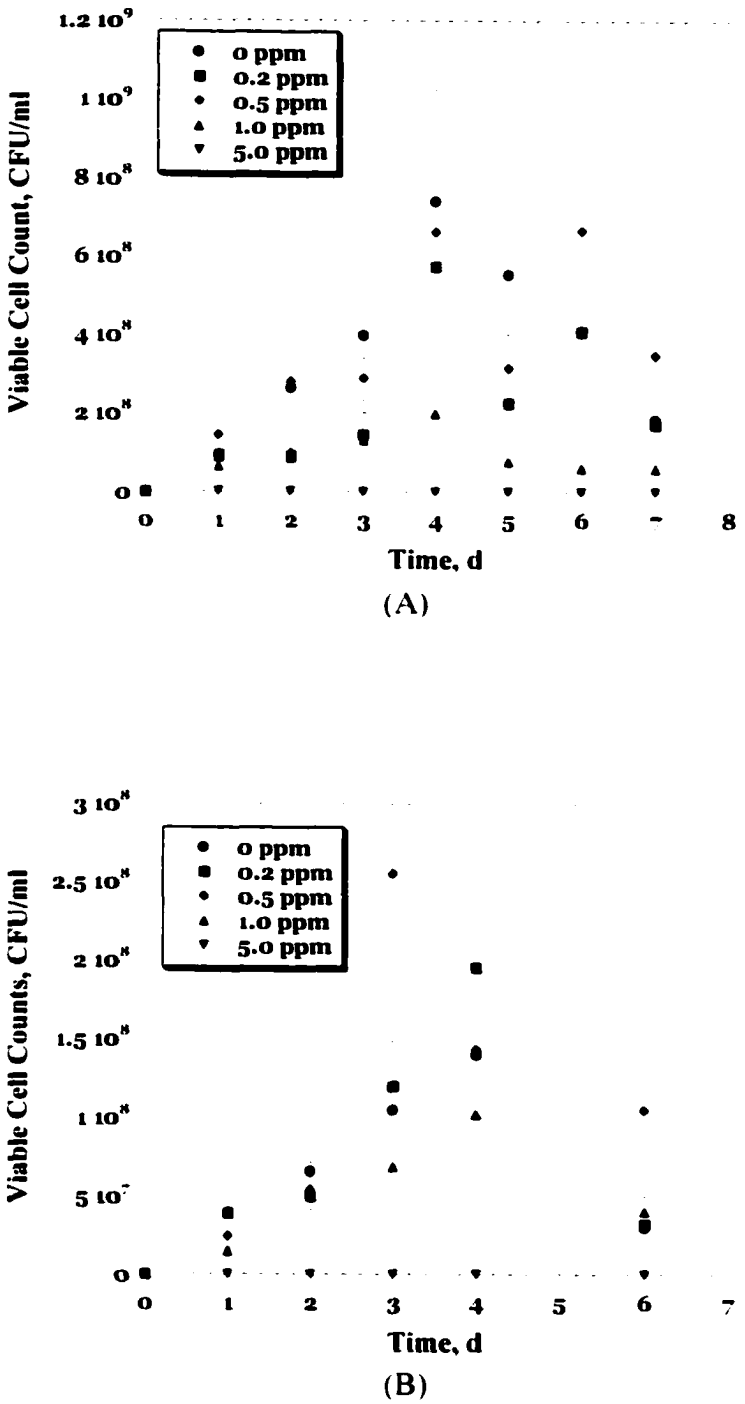

Figure VII-2 Chromate tolerance of *P. putida* F1 on toluene (A) and phenol (B) in a batch culture. The initial concentration of toluene and phenol were 0.45 and 0.5 mM. respectively. X_o = 1.0 mg/L.

VII.2.2 GROWTH AND BIODEGRADATION IN THE PRESENCE OF CADMIUM

VII.2.2.1 Toluene Biodegradation

Data from the toluene biodegradation experiment are presented in Figure VII-3. In the absence of 10 ppm Cd. growth was apparent after 5.5 h lag period and mirrored the toluene consumption. Toluene (initially 0.42 mM) was completely degraded in less than 13 h. which was earlier than that (15 h) in MSB medium. The calculated growth yield coefficient ($Y_{X/S}$) was 1.37 g/g. In the presence of 10 ppm Cd. growth was observed after a 17-h of lag period and was approximately mirrored by toluene consumption. The cell growth maintained its exponential phase until 27 h and the complete consumption of 0.42 mM toluene required 29 h. The growth yield coefficient ($Y_{X/S}$) in the presence of 10 ppm Cd was 0.81 g/g.

The inhibitory effect on the growth of *P. putida* F1 on toluene was evident. The presence of Cd caused a longer period of lag phase (17 h) than that without cadmium (5.5 h). However, *P. putida* F1 clearly showed its ability to grow on toluene in the presence of 10 ppm Cd. which is a fairly high concentration. In the presence of 10 ppm Cd. the growth inhibition was reflected on the decrease of growth yield coefficient from 1.37 to 0.81 g/g with Cd. The decrease of the yield coefficient in the presence of 10 ppm Cd indicates that the cells spend more energy for cell maintenance and thus less is available for growth.

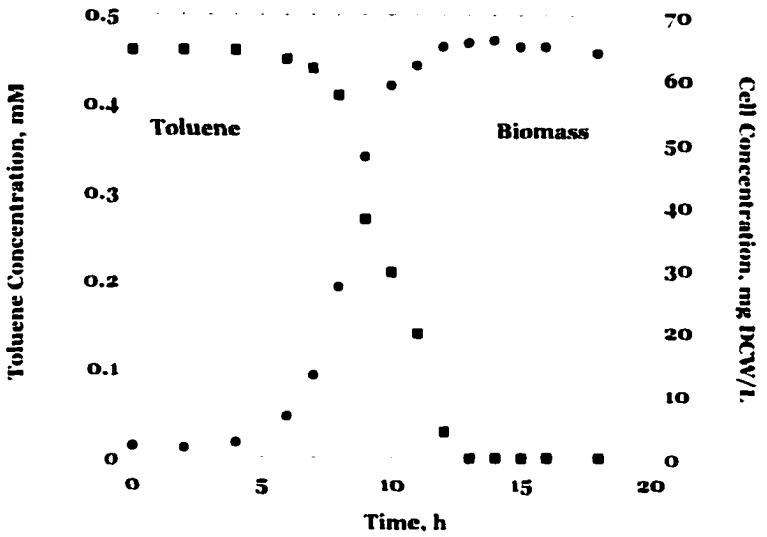

(A)

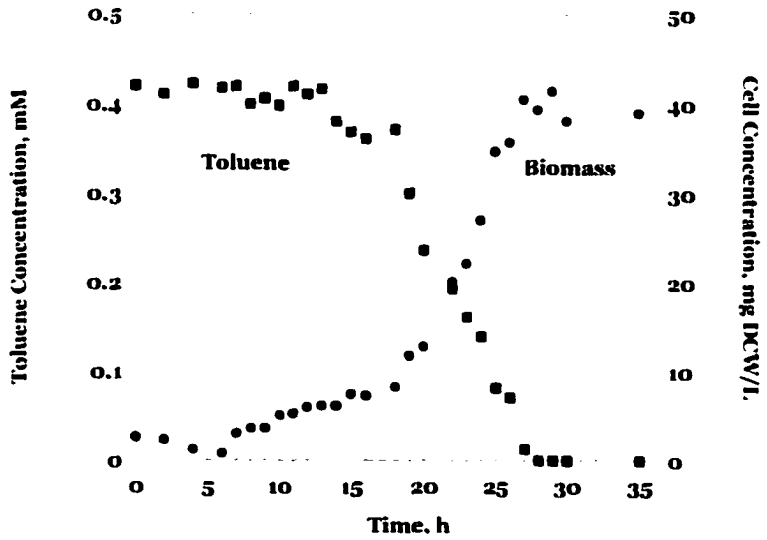

(B)

Figure VII-3 Growth of *P. putida* F1 on toluene in the absence (A) and the presence (B) of 10 ppm cadmium. Symbols indicate measurements of liquid-phase toluene (■) and biomass (●) concentrations. Cells were grown in PIPES medium (see Chapter III for the detailed growth conditions).

VII.2.2.2 Phenol

The experimental results of the phenol degradation and cell growth in the presence and absence of 10 ppm cadmium are shown in Figure VII-4. A longer lag period (14 h) than that of the toluene degradation (5.5 h) without Cd was expected from previous experiments with MSB medium (17). The complete consumption of 0.5 mM phenol by *P. putida* F1 required 49 h and the degradation of phenol again mirrored to the growth of the cells.

In contrast to toluene degradation with and without 10 ppm Cd, *P. putida* F1 did not display a difference in the length of the lag phase between the presence and absence of 10 ppm Cd. The period for the complete depletion of phenol in the presence of Cd was longer (56 h) than that without Cd (49 h). For unknown reasons, the consumption of phenol in the presence of 10 ppm Cd paused after 38 h of growth and then resumed at a higher rate after 46 h of growth. This pause in the middle of phenol degradation in the presence pf 10 ppm Cd was observed again in a duplicate experiment. The growth yield coefficient ($Y_{x/s}$) values decreased from 0.75 g/g (without Cd) to 0.53 g /g (with 10 ppm Cd). The presence of 10 ppm Cd forces again the cells to spend more energy for cell maintenance and it results in less available energy for the cell growth.

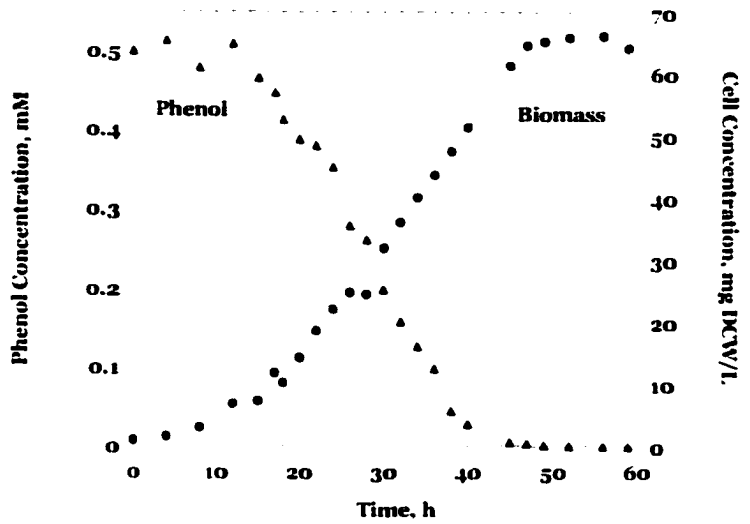

(A)

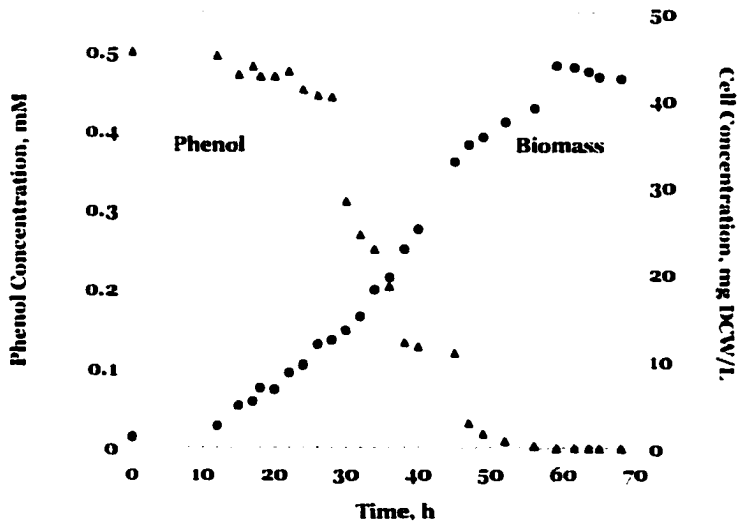

(B)

Figure VII-4 Growth of *P. putida* F1 on phenol in the absence (A) and the presence (B) of 10 ppm cadmium. Symbols indicate measurements of liquid-phase phenol (▲), and biomass (●) concentrations.

VII.2.2.3 Toluene-Phenol Mixture

The results of a biodegradation experiment with toluene-phenol mixtures in the absence and presence of 10 ppm Cd are shown in Figure VII-5. As the case of toluene-phenol mixture biodegradation in MSB (17), toluene was consumed first before phenol regardless the presence of Cd, and the phenol concentration remained essentially constant until toluene was consumed. The lag phase of the cell growth was monitored for 6 h without Cd and 10 h with 10 ppm Cd.

In the absence of Cd, no clear growth regions were correlated to the dominant growth substrate after the initial period of rapid cell growth. The complete consumption of toluene occurred after 11 hours of cultivation. Phenol degradation began around this time point (~11 h) and lasted until 26 hours post-inoculation. Although the growth pattern appears to be a typical example of diauxic growth, it is not; because Spain et al. (25) reported that *P. putida* F1 used the same enzyme to initiate metabolism of both toluene and phenol.

In the presence of 10 ppm Cd, the growth curve could be divided into two separate regions that correspond to the substrate consumed at that time. After 10 hours of lag phase, the cells began to degrade toluene until 17 hours of growth when toluene was nearly depleted and then phenol consumption started. Since complete consumption of toluene required 10 h without Cd and 20 h with 10 ppm Cd, the inhibition of cell growth was evident in the presence of 10 ppm Cd during this toluene degradation period. In the middle of phenol degradation, a pause period between 20 and 28 h, was observed again.

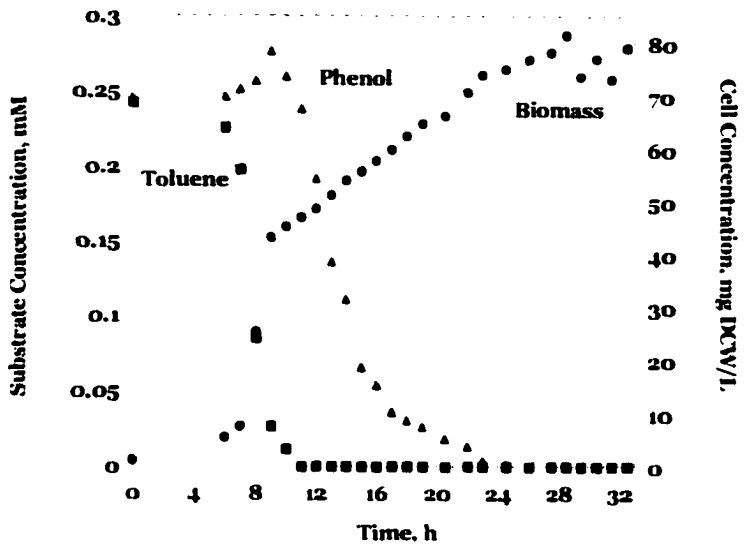

(A)

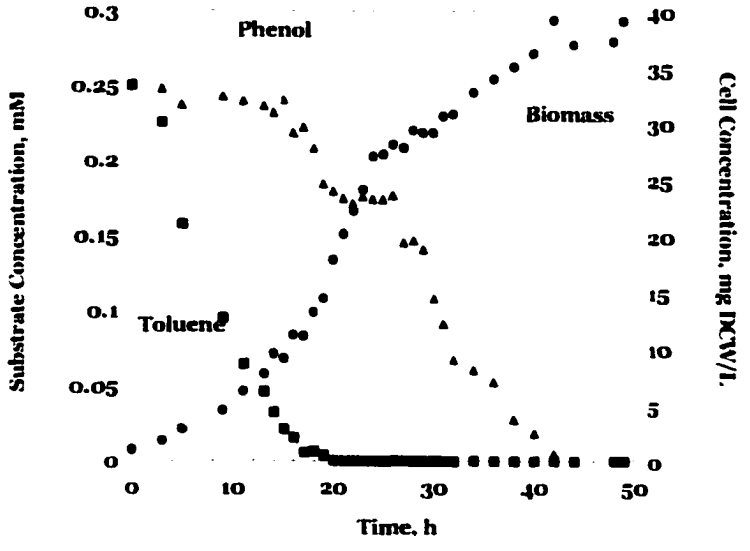

(B)

Figure VII-5 Growth of *P. putida* F1 on toluene-phenol mixtures in the absence (A) and the presence (B) of 10 ppm cadmium. Symbols indicate measurements of liquid-phase toluene (■), phenol (▲), and biomass (●) concentrations.

VII.2.3 BIOAVAILABILITY OF HEAVY METALS

Maintaining heavy metals in a soluble form in the growth medium is a critically important factor in a study on the metal effects on biodegradation. Metal ions can easily form a complex with salts and precipitate, significantly lowering the bioavailability of metal ions to the cells; thus, it should be avoided. Both cadmium and chromate precipitation were examined by an inductively coupled plasma mass spectrometer (ICP MS). The culture solution including cells was regularly removed from both bioreactors and serum bottles, and then they were filtered with a 0.2-μm syringe filter to remove cells. The soluble metal ions in the final supernatant were measured by an ICP MS after appropriate dilution with completely deionized water. Therefore, the ICP MS results could be considered as measurements of completely soluble metal ions.

ICP MS data from *P. putida* F1 calculations with Cd and Cr are presented in Figure VII-3. Up to 50 ppm of cadmium and 5.0 ppm of chromate in PIPES medium were examined (Figure VII-3). At 50 ppm Cd, some variation during the growth period in serum bottles was observed (Figure VII-3 (A)). Since the samples were extensively diluted before analysis, the apparent fluctuation in Cd levels at 50 ppm Cd might be caused by the successive dilution to less than 2 ppm. In other samples, the variation among ICP measurements was negligible. Chromate levels also did not change significantly over 7 days of cultivation (Figure VII-3 (B)). Therefore, no significant change of soluble cadmium or chromate concentrations for 7 days of growth in serum bottles was observed and the following is evident: (1) up to 50 ppm of Cd and 5.0 ppm of Cr were not

precipitated in PIPES medium. (2) *P. putida* F1 did not sequester either Cd or Cr inside the cell or absorb these metals on the cell wall.

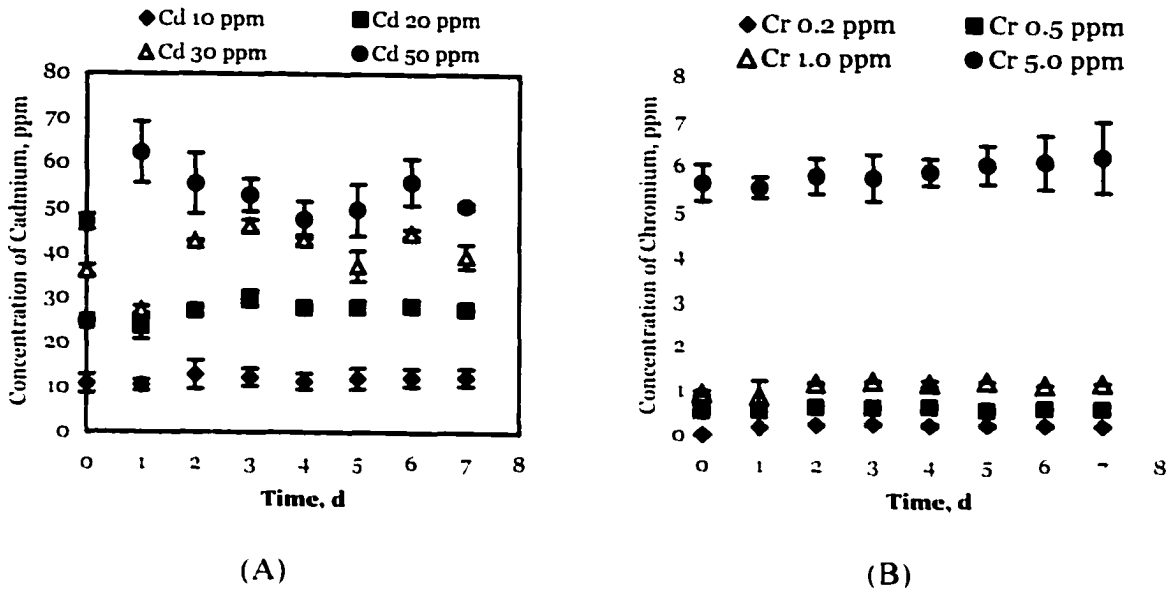

Figure VII-6 Heavy metal concentrations during the cultivation of *P. putida* F1 on toluene in serum bottles with various concentrations of cadmium (A) and chromate (B). All ICP MS samples were analyzed in triplicate (n = 3) and two standards of Cd and Cr were used for calibration.

Another experiment was performed to examine the metal solubility in the presence of phenol and in toluene-phenol mixtures. The results of this experiment are presented in Figure VII-4. The triplicate samples were removed from 1.0 L (working volume) bioreactors that were used to study the biodegradation kinetics in the presence of 10 ppm Cd. Three samples were taken from a reactor separately and analyzed independently. The samples were processed as described above to ensure the removal of any particles. All three sets of results showed nearly constant levels of cadmium during the cultivation period regardless of the growth substrate (Figure VII-4). From this series of metal solubility experiments with variable concentrations of metals and growth substrates, it is apparent that the PIPES medium could eliminate any variation of metal bioavailability to *P. putida* F1.

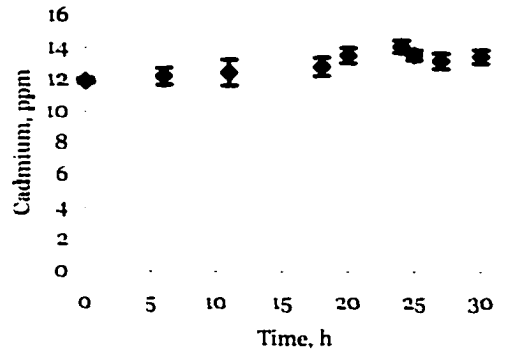

(A)

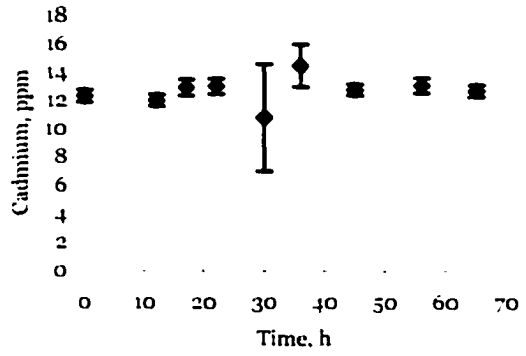

(B)

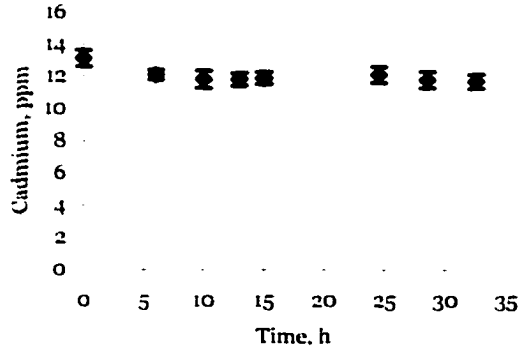

(C)

Figure VII-7 Variation of cadmium concentration during the cultivation of *P. putida* F1 on toluene (A), phenol (B), and a toluene-phenol mixture (C) in bioreactors. The initial cadmium concentration in the PIPES medium was 10 ppm. All ICP samples were triplicates (n = 3) and two standards of Cd were used for the calibration.

VII.2.4 TRANSMISSION ELECTRON MICROSCOPY

The morphological changes of *P. putida* F1 in the absence and presence of heavy metals were examined using transmission electron microscopy. The sample descriptions are presented in Table VII-1 and the TEM images are shown in Figure VII-8, 9, 10, and 11. Although each sample for TEM analysis had a different age (cultivation period), each represents its morphology in that growth environment.

Table VII-1 Descriptions of samples for TEM analysis.

Growth substrate	Heavy Metal (ppm)		Age (h)
	Cd	Cr(VI)	
Toluene[1]	-	-	18
Toluene[1]	10 ppm	-	30
Toluene[2]	-	1 ppm	168
Phenol[1]	10 ppm	-	26

[1] Samples were removed at the end of batch cultivation from bioreactors.
[2] Sample was removed from a serum bottle cultivation at the end of cultivation.

The images of cells in Figure VII-8 show that the presence of Cd or Cr(VI) apparently did not affect the overall shape of the cell. The shape of a cell was closely examined at 100.000 X magnification (Figure VII-9). The cell shape was round and smooth with an intact cell membrane in the absence of metals (Figure VII-9A) and in the presence of 10 ppm Cd (Figure VII-9B). The cell growth in the presence of 1.0 ppm Cr(VI), however, had a distorted in cellular membrane (Figure VII-9C). This distortion in the cell membrane with the presence of 1.0 ppm Cr(VI) was more obvious when the cell

membrane area was magnified (Figure VII-10). In Figure VII-10C, it is not clear whether the distortion of the cell membrane is limited to the outer membrane or inner membrane or both. However, the presence of Cr(VI) (1.0 ppm) in the PIPES medium clearly affected the morphology of the cellular membrane. Thus, in the presence of 1.0 ppm chromate, the cellular membrane may have become more fragile and resulted in the loss of some essential components of a cell (e.g., proteins and cellular fluids, etc.). Complete loss of membrane integrity would ultimately lead to the death of cells. Recently, Michel et al. (11) reported the leakage of some cytochrome *c* and periplasmic proteins out of sulfate-reducing bacteria (*Desulfovibrio* and *Desulfomicrobium*) in the presence of chromate. They observed the presence of cytochrome *c* only in the growth medium in the presence of Cr(VI). In the chromate toxicity experiment shown in Figure VII-2 (B), *P. putida* F1 could not survive at all in the presence of 5 ppm Cr(VI). This hypersensitivity of the cell to Cr(VI) could be explained by the loss of membrane integrity, and thus, 1.0 ppm of Cr(VI) could be the maximum concentration for the survival and growth of *P. putida* F1 on toluene.

As the Figure VII-11 shows, the presence of 10 ppm Cd did not affect at all the morphology of the cell grown on phenol. Thus, morphology of *P. putida* F1 with 10 ppm Cd appears the same whether grown on toluene or phenol.

Figure VII-8 Transmission electron microscope (TEM) images of *P. putida* F1 cells grown on toluene. (A) without metal, (B) in the presence of 10 ppm Cd, and (C) in the presence of 1.0 ppm Cr(VI). All images were 10,000 times magnified; the bar at the right side of each image is 1.0 μm.

Figure VII-9 Transmission electron microscope (TEM) images of a *P. putida* F1 cell grown on toluene, (A) without metal, (B) in the presence of 10 ppm Cd, and (C) in the presence of 1.0 ppm Cr(VI). All images were 100,000 times magnified; the bar at the right side of each image is 1.0 μm.

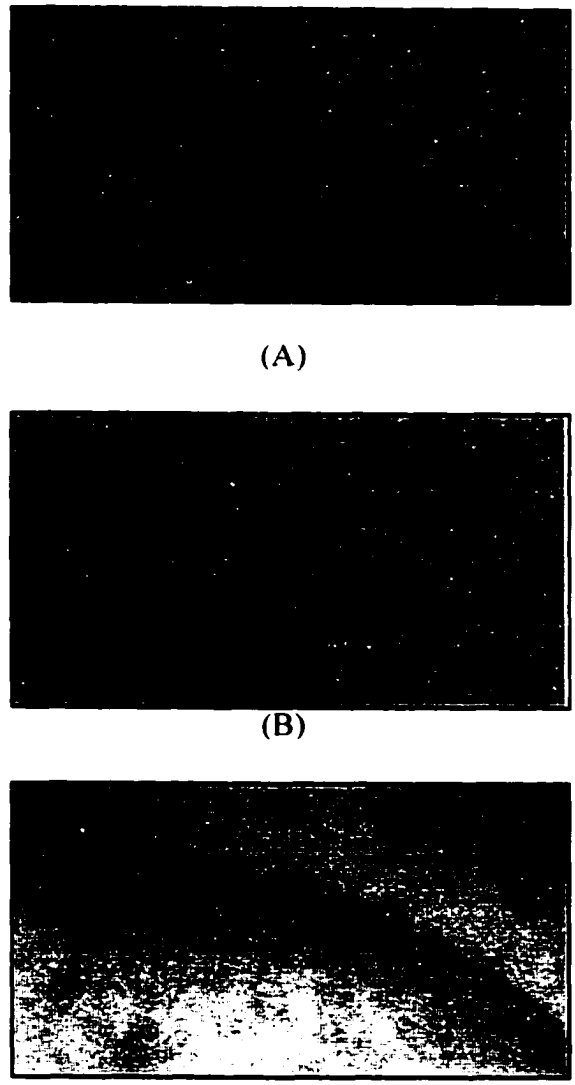

Figure VII-10 Magnified Transmission electron microscope (TEM) images of *P. putida* F1 cell membrane in the absence and presence of heavy metals. (A) *P. putida* F1 grown on toluene without metals. (B) *P. putida* F1 grown on toluene in the presence of 10 ppm Cd. (C) *P. putida* F1 on toluene in the presence of 1.0 ppm Cr (VI). All images were cropped out from 100,000 × magnified TEM images (shown in Figure VII-6); the bar at the right side of each image is 1.0 μm.

Figure VII-11 Transmission electron microscope (TEM) image of a *P. putida* F1 cell grown on phenol in the presence of 10 ppm Cd. The image was 100.000 times magnified: the bar at the right side of each image is 1.0 μm.

VII.3 Discussion

Growth of the cells on both single and mixed toluene and phenol in a new growth medium (PIPES), which did not contain any metal chelating reagents, was similar to growth in MSB medium. These similar characteristics between two different media (MSB and PIPES) are promising in that PIPES medium can be used for the growth medium of *P. putida* F1 for future studies.

Toxic effects of heavy metals on the growth of the cells on either toluene or phenol as single substrate was obvious. A longer period of each growth phase in the presence of heavy metals can be an initial evidence of inhibitory effects on the cell growth. Although the cell growth on phenol with 10 ppm Cd did not display a different lag period, the complete biodegradation of phenol with Cd required more time than without Cd. Besides these descriptive characteristics, the comparison of growth yield coefficients between the presence and absence of 10 ppm Cd directly indicates its inhibitory effect on the cell growth.

When the cells grew on the toluene-phenol mixtures, a pause in the cell growth was observed at the start of phenol degradation (Figure VII-5 (B), 20 – 27 h) in the presence of 10 ppm Cd immediately after the complete depletion of toluene. Although the reason of this pause is unclear at the moment, it is premature to conclude that it might be related to the alteration of membrane lipid alone, because this pause of phenol degradation was also observed when phenol was only growth substrate in the presence of 10 ppm Cd

(Figure VII-4 (B), 36-44 h). From the analysis of membrane fatty acids in the previous chapter (Chapter VI), alteration of the fatty acid composition in the cell membrane lipids in favor of toluene uptake was hypothesized. As an addition to the toluene-phenol mixtures, the existence of 10 ppm Cd in the growth medium might require more complicate and coordinate alteration in the cell membrane and cytoplasm of the cell than the biodegradation of toluene-phenol mixtures in the absence of metal ions.

Both the pause in the phenol degradation and the previous observation of fatty acid alteration in the cell membrane lead to the morphological analysis of cell membrane in the presence of 10 ppm Cd with a transmission electron microscopy. From the TEM results, the presence of 10 ppm Cd did not display obvious distortion of the cell membrane. However, severe distortion of the cell membrane was observed in the presence of 1.0 ppm Cr(VI). These image analyses can explain better tolerance of the cells to cadmium than to chromate. No obvious morphological changes of the cell membrane was observed between the cells grown either on toluene or phenol in the presence of 10 ppm Cd.

VII.4 Conclusions

Heavy metals can severely affect the physiological and biochemical activities of *P. putida* F1. In this portion of the study, I have shown that chromate is more toxic to *P. putida* F1 than cadmium: *P. putida* F1 could survive and grow in the presence of Cd at a maximum 30 ppm, but just 1.0 ppm of Cr(VI) could substantially inhibit the growth of the cell on either toluene or phenol. The inhibitory effect of Cr(VI) to the cell survival and growth on toluene was likely caused at least in part by the distortion of cell membrane structure and resulting loss of cell integrity based on TEM image analysis.

From the solubility experiments of heavy metals in the PIPES medium, I determined that this medium could be used to further investigate the effects of metals on the biodegradation of chemical mixtures. In the analysis of biodegradation parameters obtained from bioreactors, the presence of 10 ppm cadmium in the PIPES medium inhibited both cell growth and pollutant(s) degradation. Although it is obvious that the development of a mathematical expression to predict the biodegradation of toluene and phenol mixtures in the presence of metal ions (i.e. Cd) could be more complicated than in its absence, the observations made in this study could assist to understand the nature of the biodegradation of toluene-phenol mixture by *P. putida* F1 in the presence of either Cd or Cr(VI).

VII.5 References

1. **Bhattacharya, S. K., R. E. Leslie, and R. L. Madura.** 1995. Effects of bioavailable cadmium on aerobic systems. Water Environ. Res. **67:**1092-1095.

2. **Duxbury, T.** 1985. Ecology of heavy metal responses in microorganism. Adv. Microbiol. Ecol. **8:**185-235.

3. **Feriance, P., A. Farewell, and T. Nystrom.** 1998. The cadmium-stress stimulon of *Escherichia coli* K-12. Microbiology (Reading) **144:**1045-1050.

4. **Gadd, G. M.** 1992. Microbial control of heavy metal pollution.. p. 59-87. *In* J. C. Fry. Gadd. G.M.. Herbert. R.A.. Jones. C.W.. and Watson-Craik. I.A. (ed.). Microbial control of pollution. Cambridge University Press. Cambridge. United Kingdom.

5. **Garbisu, C. I., M.J. Alkorta, M.J. Llama, and J. L. Serra.** 1998. Aerobic chromate reduction by *Bacillus subtilis*. Biodegradation **9:**133-141.

6. **Ietswaart, G. J. H. and W. A. J. Ernst.** 1992. Seasonality of VAM infection in three populations of *Agrostis capillaris* (Gramineae) on soil with or without heavy metal enrichment. Plant. Soil. **139:**67-73.

7. **Kuo, C. and B.R. S. Genthner.** 1996. Effects of added heavy metal ions on biotransformation and biodegradation of 2-chlorophenol and 3-chlorobenzoate in anaerobic bacteria consortia. Appl. Environ. Microbiol. **62:**2317-2323.

8. **Lovely, D. R.** 1995. Microbial reduction of iron. manganase. and other metals. Adv. Agron. **54:**175-231.

9. **Lovley, D. R. and E. J. P. Phillips.** 1994. Reduction of chromate by Desulfovibrio vulgaris and its c3 cyochrome. Appl. Environ. Microbiol. **60:**726-728.

10. **Michel, C., M. Brugna, C. Aubert, A. Bernadac, M. Bruschi.** 2000. Enzymatic reduction of chromate: comparative studies using sulfate-reducing bacteria. JBIC **4:**95-100.

11. **Mills, A. L.** 1997. Metal requirements and tolerance.. p. 349-357. *In* C. J. Hurst. Knudsen. G.R.. McInerney. M.J.. Stetzenbach. and Walter. M.V. (ed.). Manual of Environmental Microbiology. American Society of Microbiology. Washington D.C.

12. **Nies, D. H.** 1999. Microbial heavy-metal resistance. Appl. Microbiol. Biotechnol. **51:**730-750.

13. **Nriagu, J. O. and J.M. Pacyna.** 1989. Quantitative assesment of worldwide cintamination of air. water and soils by trace metals. Nature **333:**134-139.

14. **Olafson, R. W., K. Abel, and R. S. Sim.** 1979. Prokaryotic metallothionein: preliminary characterization of a blue-green algae heavy-metal binding protein. Biochem. Biophys. Res. Commun. **89:**36-43.

15. **Park, C. H., M. Keyhan, B. Wielinga, S. Fendoef, and A. Matin.** 2000. Purification to homogeneity and characterization of a novel *Pseudomonas putida* chromate reductase. Appl. Environ. Microbiol. **66:**1788-1795.

16. **Reardon, K. F., D. C. Mosteller, and J. D. Rogers.** 2000. Biodegradation kinetics of benzene. toluene. and phenol as single and mixed substrates for *Pseudomonas putida* F1. Biotechnol. Bioeng. **69:**385-400.

17. **Reber, H.** 1992. Simultaneous estimates of the diversity and the degradative capability of heavy-metal-affected soil bacterial communities. Biol. Fert. Soils. **13:**181-186.

18. **Rensing, C., B. Mitra, and B. P. Rosen.** 1997. Insertional inactivation of dsbA produces sensitivity to cadmium and zinc in *Escherichia coli*. J. Bacteriol. **179:**2769-2771.

19. **Riley, R. G., J. M. Zachara, and F. J. Wobber.** 1992. Chemical contaminants on DOE lands and selection of contaminant mixtures for subsurface science research. DOE/ER-0547T. U.S. Department of Energy.

20. **Roane, T. M., and I. L. Pepper.** 2000. Microbial responses to environmentally toxic cadmium. Microb. Ecol. **38:**358-364.

21. **Roane, T. M., R.M. Miller, and I.L. Pepper.** 1996. Microbial remediation of metals.. p. 312-340. *In* R. L. Crawford, and Crawford, D.L. (ed.), Bioremediation: Principles and applications. Cambridge University Press, United Kingdom.

22. **Shen, H., P. H. Pritchard, and G. W. Sewell.** 1996a. Microbial reduction of Cr(VI) during anaerobic degradation of benzoate. Environ. Sci. Technol. **30:**1667-1674.

23. **Shen, H., P. H. Pritchard, and G. W. Sewell.** 1996b. Kinetics of chromate reduction during naphthalene degradation in a mixed culture. Biotechnol. Bioeng. **52:**357-363.

24. **Spain, J. C., G. J. Zylstra, C. K. Blake, and D. T. Gibson.** 1989. Monohydroxylation of phenol and 2,5-dichlorophenol by toluene dioxygenase in *Pseudomonas putida* F1. Appl. Environ. Microbiol. **55:**2648-2652.

25. **Summers, A. O.** 1992. The hard stuff: metals in bioremediation. Curr. Opin. Biotechnol. **3:**271-276.

26. **Suzuki, T., N. Miyata, H. Horitsu, K. Kawai, K. Takamizawa, Y. Tai, and M. Okazaki.** 1992. NAD(P)H-dependent chromium(VI) reductase to *Pseudomonas ambigua*

G-1: a Cr(VI) intermediate is formed during the reduction of Cr(VI) to Cr(III). J. Bacteriol. **174**:5340-5345.

27. **Timmis, K. N., R. J. Steffan, and R. Unterman.** 1994. Designning microorganisms for the treatment of toxic wastes. Annu. Rev. Microbiol. **48**:525-557.

28. **Ting, Y.-P., C. Fang, and H.-M. Tan.** 1999. Effect of heavy metals on the bioremediation of petroleum hydrocarbons. *In* B. C. Alleman and A. Leeson (ed.). In situ bioremediation of petroleum hydrocarbon and other organic compounds. Battielle Press. Columbus.

CHAPTER VIII CONCLUSIONS

VIII.1 Introduction

In this research, the biodegradation of toluene-phenol mixtures by *Pseudomonas putida* F1 were investigated in terms of dynamic protein production profiles. Two identifications of those proteins were obtained by a combination of N-terminal sequencing, mass spectrometry, and protein database searches. The function of one of the identified proteins was further characterized by PLFA/FAME method. Analysis of the fatty acid composition in the cellular membrane indicated that a shift of fatty acid composition might contribute to the mode of membrane adaptation as a response to the presence of toluene-phenol mixed substrates in the growth medium of *P. putida* F1. The growth of *P. putida* F1 was also examined in the presence of divalent heavy metal ions, cadmium and chromate.

VIII.2 Proteomic analysis

Since proteins are responsible for most biological activities in a life form, the proteomics approach to investigate the effect of physiological changes of *P. putida* F1 during the biodegradation of toluene-phenol mixtures was employed. Soluble proteins were separated by 2-D PAGE, and the protein production patterns of *P. putida* F1 grown on toluene or phenol were determined. Production of two different protein groups was observed by comparing 2-D PAGE gels. These groups of proteins (27 proteins) were

designated as Group T and Group P. In the subsequent analysis of proteins isolated from toluene-phenol mixture-grown cells, both groups of proteins (Group T and P) were found to have unique sequences of production patterns with respect to substrate consumption. One protein was only observed during the biodegradation of toluene-phenol mixtures and designated as Group M. Proteome analysis clearly indicated that biodegradation of toluene and phenol produced different proteins.

Acquiring identifications of those proteins (Group T, P, and M) was the next target. To obtain protein identifications, various procedures were utilized. Although the N-terminal sequence method was used first, four of five proteins submitted for analysis were found to be N-terminal blocked. With the Edman degradation method (N-terminal sequence), only the Group M protein was identified as acyl carrier protein (ACP). Mass spectrometry (MS) was utilized for the second procedure: a Matrix-Assisted Laser Desorption/Ionization Time-of-Flight (MALDI-TOF) mass spectrometer measured molecular weights of trypsin-digested peptide fragments. Those mass finger prints were subsequently compared with the theoretically possible molecular weights of peptide fragments compiled by computer software (ProFound or MS-Fit) based on genomic sequences of various prokaryotic microorganisms. Although mass finger print information did not provide many identifications due to the lack of the genomic sequence of *Pseudomonas putida*, one identification (β-ketoadipate:succinyl CoA transferase) of a Group P protein was unambiguously obtained. Without a complete genomic sequence, it was difficult to obtain more identifications with the mass finger print approach. A *de novo* sequencing of peptide fragments by a tandem mass spectrometer was the next

choice. Electrospray ionization (ESI) ion-trap mass spectrometer was utilized for *de novo* sequencing. It was successful in deducing several sets of *de novo* peptide sequences. However, no significant hits were obtained by searching protein databases, and the identifications of those proteins remain unknown at the moment.

Identification of proteins after 2-D PAGE plays an important role in proteomics (4, 6). Since identifications of interesting proteins provide basic information in understanding the series of biological events of the cells in response to treatments, they are valuable starting points to solve problems. In this research, I have shown that using the mass fingerprint method is very limited for acquiring protein identification unless the entire genomic sequence of a target microorganism is available. N-terminal sequencing could be a better method if a more sensitive sequencer than one used for this study is available and a low level of N-terminal blockage ratio occurs. Therefore, using *de novo* peptide sequences deduced from tandem mass spectra and homology searches could be the best approach to identify proteins, unless genomic sequences of a target microorganism are available (5, 7, 8).

VIII.3 Characterization

The identification of the Group M protein, acyl carrier protein (ACP), triggered the investigation of fatty acid compositional changes in the cellular membrane of *P. putida* F1 because ACP is known as an essential substrate carrier through the entire fatty acid biosynthesis pathway and most fatty acids found in the cellular membrane. Substantial changes in the fatty acid composition in the cellular membrane in the presence of the two different substrates were observed. These results led to the hypothesis that any amount of toluene in the presence of phenol could effectively inhibit the phenol transport across the cellular membrane by altering the fatty acid composition. This hypothesis is not extensively proved yet, but it would be reasonable based on experimental data provided in this study. However, there is one important factor that should be considered in the evaluation of the hypothesis: fatty acids are not solely responsible for the change of the polarity or hydrophobicity in the cellular membrane. Lipopolysaccarides (LPS) and the type of hydrophilic head of the lipids also play a significant role in determining total membrane polarity (2).

Differential production of β-ketoadipate:succinyl CoA transferase with respect to phenol degradation suggested that an intermediate of phenol degradation, catechol, induces the β-ketoadipate catabolic pathway and influences to the phenol degradation rate.

VIII.4 Effects of Heavy metals

A new optimized medium successfully retained essentially all heavy metal ions in soluble form and demonstrated its ability to provide an appropriate environment for cell growth. *P. putida* F1 could grow and metabolize single substrate and toluene-phenol mixtures in the presence of 10 ppm Cd in a batch mode bioreactor. Its tolerance to cadmium was up to 30 ppm, but that to chromate was only 1.0 ppm. Data from batch reactors clearly demonstrated the inhibitory effects of cadmium and chromate ions on the growth of *P. putida* F1 utilizing single and mixed pollutants. Their inhibition of cell growth was demonstrated by the comparison of the cell growth yields. The effect of metals on the cell morphology was examined by TEM images and a low concentration of chromate (1.0 ppm) was found to severely disrupt the cell membrane. Based on the TEM image analysis, the cells had better tolerance to cadmium than to chromate and the tolerance of the cells to metal ions was directly related to the integrity of cell membrane. Chromate toxicity was hypothesized to be due to its effect on the membrane, causing loss of cell membrane integrity and finally to disruption of the cells.

VIII.5 Significance

The increasing demand by the public for a clean environment at a reasonable cost has driven research on bioremediation technologies. Bioremediation technologies could be one of the best alternative tools other than simple incineration, land-filling, excavations, etc. because remediation processes could be successfully accomplished by microorganisms that could not only survive in such harsh chemical conditions, but also metabolize chemical pollutants.

An engineering approach to understanding the nature of cell growth and biodegradation kinetics with previously established or new models is limited when one faces problems that are difficult to explain without fundamental information on cellular activities. In this research, three important fundamental pieces of information were presented to aid in the understanding of the nature of the biodegradation of toluene-phenol and toluene-phenol-metal mixtures by *P. putida* F1:

1. Proteomic analysis of the cell during the biodegradation of single and mixed aromatic compound(s) revealed the dynamic physiological changes of the cell in terms of protein production profiles. The identifications of proteins were obtained with currently available technologies, such as N-terminal sequencing, mass spectrometry, and bioinformatics.

2. Identifications of some proteins led to the further analysis of cellular activities. The results of fatty acid composition changes in the cellular membrane provided the experimental foundation of a hypothesis related to the transport of toluene and phenol across the cellular membrane. Identification of specific proteins associated with the biodegradation of toluene and/or phenol will provide ways of understanding the biodegradation phenomena with wider and deeper insight.

3. Cadmium was found to impact *P. putida* F1 growth through a decrease in cell yield, suggesting higher maintenance energy requirements. However, the impact of Cd^{2+} on the toluene degradation rate was higher than the impact on phenol degradation, suggesting a concentration between Cd^{2+} toxicity/resistance and the nature of the growth substrate. Evidence was also found for the nature of Cr(VI) toxicity: cell membrane disruption.

VIII.6 Recommendations for future work

This research has demonstrated the importance of protein identification in understanding cellular activity while *P. putida* F1 utilizes the toluene-phenol mixtures. Protein identification is a starting point of further understanding the cell activity at molecular level. Based on the identification of the acyl carrier protein, fatty acid changes in the cell membrane were studied and the results provided a foundation to come up with a new biodegradation kinetics hypothesis. However, it is improper to promote a hypothesis based on only one protein identification. Therefore, more protein identification will be necessary. Using *de novo* sequencing of peptides and homology searches to existing databases could be the best approach until the entire genomic sequences of *P. putida* species are available and accessible to the public.

To evaluate the hypothesis that toluene inhibits phenol transport across cell membrane by changing the polarity of cell membrane, other parameters should be thoroughly examined: first, the hydrophilic heads of phospholipids, which can substantially contribute to the net polarity of cell membrane (3). Second, lipopolysaccharides (LPS) attached to the phospholipids could also alter the immediate polarity of the cell membrane (1). A way to examine the membrane polarity is using artificially synthesized lipid micelles: Using these, the transport coefficient of a target aromatic compound, labeled by isotope or fluorescent tag, across the micelle membrane in the presence of another aromatic compound could be measured.

Although an interesting pause in the course of phenol degradation during either the cell growth on the toluene-phenol mixtures or phenol single substrate was observed without clear reason at the moment, it could be related to transport of substrates cross cell membrane. Data for the change of the membrane fatty acid composition could provide more detailed information as well as the analysis of the phospholipids and LPS alteration.

VIII.7 Reference

1. **de Cock, H., K. Brandenburg, A. Wiese, O. Holst, and U. Seydel.** 1999. Non-lamellar structure and negative charges of lipopolysaccarides required for efficient folding of outer membrane protein PhoE of *Escherichia coli*. J Biol Chem **274:**5114-5119.

2. **Dowhan, W.** 1997. Molecular basis for membrane phospholipid diversity: Why are there so many lipids? Annu. Rev. Biochem. **66:**199-232.

3. **Huijbregts, R. P. H., A. I. P. M. de Kroon, and B. de Kruijff.** 1998. Rapid transmembrane movement of newly synthesized phosphatidylethanolamine across the inner membrane of *Escherichia coli*. J Biol Chem **273:**18936-42.

4. **Mann, M.** 1994. Sequence database searching by mass spectrometric data. p. 223-245. *In* R. Kellner, F. Lottspeich., H.E. Meyer. (ed.). Microcharacterization of proteins. VCH. Weinheim.

5. **Shevchenko, A., I. Chernuchevich, and W. Ens.** 1997. Rapid *de novo* peptide sequencing by a combination of nanoelectrospray, isotope labeling and a quarrupole/time-of-flight mass spectrometer. Rapid Commun. Mass Spectrom. **11:**1015-1024.

6. **Shevchenko, A., O. N. Jensen, A. V. Podtelejnikov, F. Sagliocco, M. Wilm, O. Vorm, P. Mortensen, A. Shevchenko, H. Boucherie, and M. Mann.** 1996. Linking genome and proteome by mass spectrometry: Large-scale identification of yeast proteins from two dimensional PAGE. PNAS **93:**14440-14445.

7. **Shevchenko, A., M. Wilm, O. Vorm, and M. Mann.** 1996. Mass spectrometric sequencing of proteins from silver-stained polyacrylamide gels. Anal Chem 68:850-858.

8. **Shevchenko, A., M. Wilm, and M. Mann.** 1997. Peptide sequencing by mass spectrometry for homology searches and cloning of genes. J. Protein Chem. 16:481-490.